Methods in Molecular Biology 1333

Springer Protocols

Jan Michiels
Maarten Fauvart *Editors*

Bacterial Persistence

Methods and Protocols

Humana Press

METHODS IN MOLECULAR BIOLOGY

Series Editor
John M. Walker
School of Life and Medical Sciences
University of Hertfordshire
Hatfield, Hertfordshire, UK

For further volumes:
http://www.springer.com/series/7651

Bacterial Persistence

Methods and Protocols

Edited by

Jan Michiels and Maarten Fauvart

Department of Microbial and Molecular Systems,
KU Leuven - University of Leuven,
Heverlee, Belgium

Humana Press

Editors
Jan Michiels
Department of Microbial and Molecular Systems
KU Leuven - University of Leuven
Heverlee, Belgium

Maarten Fauvart
Department of Microbial and Molecular Systems
KU Leuven - University of Leuven
Heverlee, Belgium

ISSN 1064-3745 ISSN 1940-6029 (electronic)
Methods in Molecular Biology
ISBN 978-1-4939-2853-8 ISBN 978-1-4939-2854-5 (eBook)
DOI 10.1007/978-1-4939-2854-5

Library of Congress Control Number: 2015945939

Springer New York Heidelberg Dordrecht London

Printed on acid-free paper

Humana Press is a brand of Springer
Springer Science+Business Media LLC New York is part of Springer Science+Business Media (www.springer.com)

Preface

Antibiotic treatment often fails to clear chronic infections, even in the absence of clinically detectable resistance. This is largely due to the so-called persister cells that can survive exposure to high concentrations of bactericidal antibiotics. It is generally accepted that persisters are responsible for the relapse of infections by notorious pathogens such as *Mycobacterium tuberculosis*, *Staphylococcus aureus*, *Pseudomonas aeruginosa*, *Salmonella* Typhimurium, and *Candida albicans*. Persisters typically make up only a small part of a cell population. They result from a temporary switch to a state that is insensitive to killing by antibiotics. Their rare and transient nature has long hampered the experimental study of persisters. This volume brings together the most respected researchers in the field of bacterial persistence. It presents a comprehensive collection of methods that have been instrumental to our current understanding of the topic and will likely remain so for years to come.

Heverlee, Belgium

Jan Michiels
Maarten Fauvart

Contents

Contributors

Ahalieyah Anantharajah • *Pharmacologie cellulaire et moléculaire, Louvain Drug Research Institute, Université catholique de Louvain, Brussels, Belgium*

Nathalie Q. Balaban • *The Racah Institute of Physics, The Hebrew University of Jerusalem, Jerusalem, Israel*

Mark P. Brynildsen • *Department of Chemical and Biological Engineering, Princeton University, Princeton, NJ, USA; Department of Molecular Biology, Princeton University, Princeton, NJ, USA*

Aaron T. Butt • *Department of Infection and Immunity, Medical School, University of Sheffield, Sheffield, UK*

Julien M. Buyck • *Pharmacologie cellulaire et moléculaire, Louvain Drug Research Institute, Université catholique de Louvain, Brussels, Belgium; Focal Area Infection Biology, Biozentrum, University of Basel, Basel, Switzerland*

Bruno P.A. Cammue • *Centre of Microbial and Plant Genetics (CMPG), KU Leuven – University of Leuven, Leuven, Belgium; Department of Plant Systems Biology, VIB, Ghent, Belgium*

Angela M. Cheverton • *Section of Microbiology, Medical Research Council Centre for Molecular Bacteriology and Infection, Imperial College London, London, UK*

Tom Coenye • *Laboratory of Pharmaceutical Microbiology, Ghent University, Ghent, Belgium*

Brian P. Conlon • *Antimicrobial Discovery Center, Department of Biology, Northeastern University, Boston, MA, USA*

Jan Danckaert • *Applied Physics Research Group (APHY), Vrije Universiteit Brussel, Brussels, Belgium*

Katrijn De Brucker • *Centre of Microbial and Plant Genetics (CMPG), KU Leuven – University of Leuven, Leuven, Belgium*

Kaat De Cremer • *Centre of Microbial and Plant Genetics (CMPG), KU Leuven – University of Leuven, Leuven, Belgium; Department of Plant Systems Biology, VIB, Ghent, Belgium*

Christina J. DeCoste • *Department of Molecular Biology, Princeton University, Princeton, NJ, USA*

Valerie Defraine • *Centre of Microbial and Plant Genetics (CMPG), Department of Microbial and Molecular Systems, KU Leuven – University of Leuven, Leuven, Belgium*

Maarten Fauvart • *Centre of Microbial and Plant Genetics (CMPG), Department of Microbial and Molecular Systems, KU Leuven – University of Leuven, Leuven, Belgium*

Robert A. Fisher • *Section of Microbiology, Medical Research Council Centre for Molecular Bacteriology and Infection, Imperial College London, London, UK*

Lendert Gelens • *Applied Physics Research Group (APHY), Vrije Universiteit Brussel, Brussels, Belgium; Department of Chemical and Systems Biology, Stanford University School of Medicine, Stanford, CA, USA*

F. Goormaghtigh • *Laboratoire de Génétique et Physiologie Bactérienne, IBMM, Faculté des Sciences, Université Libre de Bruxelles (ULB), Gosselies, Belgium*

Thomas J. Hannan • *Department of Pathology and Immunology, Washington University School of Medicine, St. Louis, MI, USA*
Wolf-Dietrich Hardt • *Institute of Microbiology, Eidgenössische Technische Hochschule ETH, Zurich, Switzerland*
Sophie Helaine • *Section of Microbiology, Medical Research Council Centre for Molecular Bacteriology and Infection, Imperial College London, London, UK*
Theresa C. Henry • *Department of Molecular Biology, Princeton University, Princeton, NJ, USA; Rutgers Robert Wood Johnson Medical School, Piscataway, NJ, USA*
David A. Hunstad • *Department of Pediatrics and Molecular Microbiology, Washington University School of Medicine, St. Louis, MI, USA*
Ryota Iino • *Okazaki Institute for Integrative Bioscience, Institute for Molecular science, National Institutes of Natural Science, Aichi, Japan; Department of Functional Molecular Science, School of Physical Science, The Graduate University of Advanced Studies (SOKENDAI), Kanagawa, Japan*
Henri Ingelman • *Institute of Technology, University of Tartu, Tartu, Estonia*
Arvi Jõers • *Institute of Technology, University of Tartu, Tartu, Estonia*
Patrick Kaiser • *Institute of Microbiology, Eidgenössische Technische Hochschule ETH, Zurich, Switzerland*
Niilo Kaldalu • *Institute of Technology, University of Tartu, Tartu, Estonia*
Iris Keren • *Antimicrobial Discovery Center, Department of Biology, Northeastern University, Boston, MA, USA*
Wouter Knapen • *Centre of Microbial and Plant Genetics (CMPG), Department of Microbial and Molecular Systems, KU Leuven – University of Leuven, Leuven, Belgium*
Sandrine Lemaire • *Pharmacologie cellulaire et moléculaire, Louvain Drug Research Institute, Université catholique de Louvain, Brussels, Belgium; GSK Biologicals, Rixensart, Belgium*
Irit Levin-Reisman • *The Racah Institute of Physics, The Hebrew University of Jerusalem, Jerusalem, Israel*
Kim Lewis • *Antimicrobial Discovery Center, Department of Biology, Northeastern University, Boston, MA, USA*
Veerle Liebens • *Centre of Microbial and Plant Genetics (CMPG), Department of Microbial and Molecular Systems, KU Leuven – University of Leuven, Leuven, Belgium*
Remy Loris • *Structural Biology Research Center, VIB, Brussels, Belgium; Structural Biology Brussels, Department of Biotechnology (DBIT), Vrije Universiteit Brussel, Brussels, Belgium*
Yoshimi Matsumoto • *Laboratory of Microbiology and Infectious Diseases, Institute of Scientific and Industrial Research, Osaka University, Osaka, Japan*
Jan Michiels • *Centre of Microbial and Plant Genetics (CMPG), Department of Microbial and Molecular Systems, KU Leuven – University of Leuven, Leuven, Belgium*
Joran E. Michiels • *Centre of Microbial and Plant Genetics (CMPG), KU Leuven – University of Leuven, Leuven, Belgium*
Kunihiko Nishino • *Laboratory of Microbiology and Infectious Diseases, Institute of Scientific and Industrial Research, Osaka University, Osaka, Japan*
Mehmet A. Orman • *Department of Chemical and Biological Engineering, Princeton University, Princeton, NJ, USA*

Frédéric Peyrusson • *Pharmacologie cellulaire et moléculaire, Louvain Drug Research Institute, Université catholique de Louvain, Brussels, Belgium*
Roland R. Regoes • *Institute of Integrative Biology, Eidgenössische Technische Hochschule ETH, Zurich, Switzerland*
Sarah E. Rowe • *Antimicrobial Discovery Center, Department of Biology, Northeastern University, Boston, MA, USA*
Shouichi Sakakihara • *Technical Division, Institute of Scientific and Industrial Research, Osaka University, Osaka, Japan*
Cristina Seral • *Pharmacologie cellulaire et moléculaire, Louvain Drug Research Institute, Université catholique de Louvain, Brussels, Belgium; Department of Microbiology, Hospital Clínico Universitario Lozano Blesa, Zaragoza, Spain*
Tanel Tenson • *Institute of Technology, University of Tartu, Tartu, Estonia*
Karin Thevissen • *Centre of Microbial and Plant Genetics (CMPG), KU Leuven – University of Leuven, Leuven, Belgium*
Richard W. Titball • *Biosciences, College of Life and Environmental Sciences, University of Exeter, Exeter, UK*
Paul M. Tulkens • *Pharmacologie cellulaire et moléculaire, Louvain Drug Research Institute, Université catholique de Louvain, Brussels, Belgium*
Heleen Van Acker • *Laboratory of Pharmaceutical Microbiology, Ghent University, Ghent, Belgium*
Françoise Van Bambeke • *Pharmacologie cellulaire et moléculaire, Louvain Drug Research Institute, Université catholique de Louvain, Brussels, Belgium*
Bram Van den Bergh • *Centre of Microbial and Plant Genetics (CMPG), KU Leuven – University of Leuven, Leuven, Belgium*
L. Van Melderen • *Laboratoire de Génétique et Physiologie Bactérienne, IBMM, Faculté des Sciences, Université Libre de Bruxelles (ULB), Gosselies, Belgium*
Ilse Vandecandelaere • *Laboratory of Pharmaceutical Microbiology, Ghent University, Ghent, Belgium*
Alexandra Vandervelde • *Structural Biology Research Center, VIB, Brussels, Belgium; Structural Biology Brussels, Department of Biotechnology (DBIT), Vrije Universiteit Brussel, Brussels, Belgium*
Natalie Verstraeten • *Centre of Microbial and Plant Genetics (CMPG), Department of Microbial and Molecular Systems, KU Leuven – University of Leuven, Leuven, Belgium*

Part I

Introduction

Chapter 1

A Historical Perspective on Bacterial Persistence

Natalie Verstraeten, Wouter Knapen, Maarten Fauvart, and Jan Michiels

Abstract

Bactericidal antibiotics quickly kill the majority of a bacterial population. However, a small fraction of cells typically survive through entering the so-called persister state. Persister cells are increasingly being viewed as a major cause of the recurrence of chronic infectious disease and could be an important factor in the emergence of antibiotic resistance. The phenomenon of persistence was first described in the 1940s, but remained poorly understood for decades afterwards. Only recently, a series of breakthrough discoveries has started to shed light on persister physiology and the molecular and genetic underpinnings of persister formation. We here provide an overview of the key studies that have paved the way for the current boom in persistence research, with a special focus on the technological and methodological advances that have enabled this progress.

Keywords: Persisters, Persistence, Antibiotic tolerance, Dormancy, Antibiotics, Review

1 The Early Days

The first report on the survival of a small fraction of streptococci cells following treatment with penicillin dates from 1942 [1]. Two years later, Joseph Bigger established that addition of penicillin to staphylococci does not result in complete sterilization of all cells in a clonal population. One out of a million cells survived even prolonged treatment with antibiotics. He appropriately named the surviving cells persisters [2]. More recently, it was shown that in most bacterial species, the majority of cells are efficiently killed by relatively low concentrations of bactericidal antibiotics. However, killing shows a biphasic pattern and beyond a certain threshold, further increasing the concentration of the antibacterial does not result in complete clearing of the culture (Fig. 1) [3].

For 40 years following its discovery, the persistence phenomenon was largely neglected, at least by molecular geneticists. This was partly due to the fact that the clinical relevance of persister

Jan Michiels and Maarten Fauvart (eds.), *Bacterial Persistence: Methods and Protocols*, Methods in Molecular Biology, vol. 1333, DOI 10.1007/978-1-4939-2854-5_1,

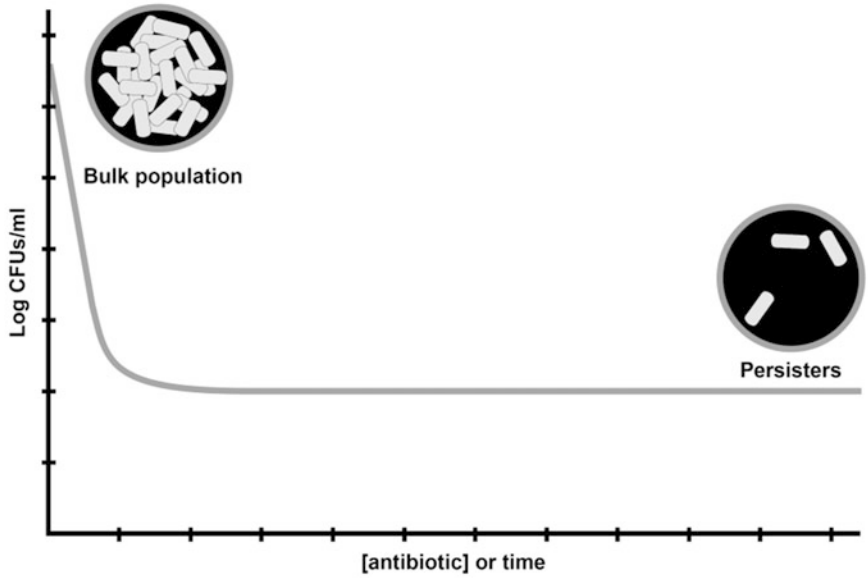

Fig. 1 Illustration of persistence: The majority of cells in a bacterial culture are efficiently killed by relatively low concentrations of antibiotics. However, beyond a certain threshold, a killing plateau is observed as only persister cells remain viable. When regrown in fresh medium, the surviving cells generate a population as sensitive to the antibiotic as the original population

cells was not clear. In contrast, the threat posed by inherited antibiotic resistance was generally recognized, adding incentives to resistance research. The problem was compounded by technical challenges that inevitably accompany the study of a transient phenotype that is associated with only a very small fraction of cells.

A breakthrough discovery came in the early 1980s, from research carried out by Harris Moyed during a sabbatical leave in the lab of Alexander Tomasz [4]. Mutagenesis of *Escherichia coli* populations with ethyl methanesulfonate (EMS) led to the identification of three highly persistent (*hip*) mutants exhibiting 10–10,000-fold increased persister fractions upon incubation with penicillin [4, 5]. Moyed's pioneering work led to the identification of two mutants hit in the *hipA* locus that up until now remains the best studied persister gene [6–10]. Furthermore, because of their increased persister fraction, *hipA* mutants have frequently been used as a tool in persistence research. Crucially and for the first time, *hipA* mutants enabled the direct observation of persister cells. Using a combination of microfluidics and live cell microscopy, Nathalie Balaban recorded how persisters survived killing by antibiotics through dormancy and subsequent resuscitation [11]. In addition, the *hipBA* locus is a representative for other toxin– antitoxin (TA) loci that are now intensively studied in relation to persistence. TA modules consist of a stable toxin, typically targeting essential cellular functions, and an unstable antitoxin,

which counteracts the activity of its cognate toxin [12, 13]. TA systems were originally identified on plasmids, where they play a role in plasmid maintenance; yet a significant number of TA loci are chromosomally encoded and these have been implicated in persistence [14]. Examples include RelE [6], MqsR [15–17], TisB [18, 19], MazF [20], and YafQ [21]. Interestingly, with the notable exception of *Salmonella* persisters residing within macrophage vacuoles [22], deletion of a single toxin generally does not affect persistence. This can partly be explained by redundancy of TA systems in most bacteria. Deletion of multiple TA systems, on the other hand, causes a decrease in *E. coli* persistence [23].

2 The Rise of Persistence Research

Following the discovery of *hipA*, persistence as a field of study steadily gained attention. This was partly due to the acknowledgement of its clinical significance (summarized by [24]). In 1944, Bigger already alluded to the role of persisters in the resuscitation of chronic infections [2]. Decades later, Kim Lewis postulated that persisters might contribute to the recalcitrance of biofilm infections [25, 26]. This is of particular interest as biofilms are known to withstand antibiotic treatment, thereby causing chronic infections [27]. Subsequently, mathematical modeling demonstrated that persistence could extend the duration of antibiotic treatment, thereby causing treatment failure and promoting the emergence of resistance [28]. Finally, two studies have unambiguously demonstrated that prolonged antimicrobial therapy selects for high-persistence strains of *Candida albicans* during candidiasis and of *Pseudomonas aeruginosa* during cystic fibrosis lung infections [29, 30]. In addition, the role of persister cells in the development of resistance is becoming increasingly clear [31]. Apart from providing incentives to further intensify persistence research, these findings also promoted the search for anti-persister therapies. At present, several strategies have been described, but their in vivo effectiveness remains to be investigated. Examples include the use of resonant activation [32], electrochemical currents [33], cadaverine [34], metabolites [35, 36], antimicrobial peptides [37], brominated furanones [38–41], and activated ClpP [42] (summarized by [43]).

Apart from increased interest due to the clinical importance of persistence, the development of novel techniques also caused persistence research to boom. An overview of these novel techniques is provided below.

2.1 Screening Approaches

Over the years, several screening procedures have been developed that led to the identification of persister genes. In a first approach, a non-redundant *E. coli* knockout library was screened for mutants

with altered persistence [44]. Persister cells of individual mutants were quantified by treating a stationary-phase culture with ofloxacin and plating the surviving cells on agar medium containing amdinocillin. As the number of spontaneous amdinocillin-resistant mutants is a fraction of the original number of cells, this obviates the need for dilution steps and greatly reduces the laborious task of screening several thousands of strains.

A second screening approach employed a *P. aeruginosa* plasposon knockout library. Individual mutants were grown until stationary phase and treated with either ofloxacin to kill non-persister cells or water, the latter serving as a control. Subsequently, samples were diluted and incubated in an automated plate reader (Bioscreen C, Oy Growth Curves Ab Ltd), allowing the optical density of 200 samples to be measured simultaneously as a function of time. Given the linear relationship between the number of cells in an inoculum and the lag phase, this allowed for the selection of mutants displaying altered persister levels [45].

Both screenings led to the identification of a number of interesting persister genes including some global regulators. In addition, not a single mutant lacking persisters was identified. As a general conclusion, these screenings therefore provided evidence pointing to the multiplicity of persister formation mechanisms.

In a final approach, a random overexpression library was generated in *E. coli*. Cells from the recombinant library were pooled and logarithmically growing cultures of library clones were exposed to multiple rounds of exposure to ampicillin. This led to the enrichment of mutants with increased probability of persister formation and ultimately to the identification of *glpD* as a genuine persister gene [46].

2.2 Single-Cell Studies

As persistence is a phenotypic trait expressed in only a subfraction of a population, advances in single-cell research signified an era of vast new possibilities. First used by the Balaban group [11], transparent microfluidic devices proved instrumental for microscopic examination of persister cells [47–49]. The strength of this technique lies in the possibility to monitor individual cells for prolonged periods of time while adapting growth conditions. For example, normal growth conditions can be alternated with antibiotic treatments in order to kill non-persister cells. This allows to pinpoint persister cells surviving treatment. Subsequently, the history of persister cells can be traced back through the recorded images. Several studies have used this technique to demonstrate preexisting heterogeneity in bacterial populations [11], to characterize the dormant state of single persister cells [47], to monitor persister formation following administration of indole [48], and to correlate high TA expression to cessation of growth [49].

Also developed by the Balaban group, a colony-appearance assay was elaborated to quantify single-cell persister lag phases [50].

Experiments demonstrated that a threshold concentration of toxin molecules is required for induction of persistence.

A major drawback of microfluidic devices, or more precisely of microscopy, is the limited number of cells that can be studied simultaneously. This can be circumvented by using flow cytometry, allowing thousands or even millions of cells to be evaluated in a high-throughput manner. A shortcoming of this technique is the inability to continuously monitor individual cells over time. Nonetheless, flow cytometry has been successfully used to study the kinetics of persister awakening [51]. In addition, while Bigger postulated that persisters are in a dormant, nondividing state [2], flow cytometry has been used to demonstrate that dormancy is not a requirement for entry into the persister state [52]. Finally, a recent study performed by the Holden group showed how to characterize the dynamics of intracellular bacterial replication at the single-cell level. They used a fluorescence dilution technique to quantify the number of replication cycles of internalized *Salmonella* [53]. This showed the existence of different *Salmonella* subpopulations in bone marrow-derived macrophages including a non-replicating but metabolically active subpopulation, comprising the persister cells, possibly capable of resuming growth and causing relapsing infections [22]. Similarly, the Bumann group exploited a DsRed variant called TIMER^{bac}, which spontaneously changes color from green to green/orange over time, as a dynamic growth rate reporter to identify persister cells in vivo [54].

2.3 Transcriptomics

Insight into global transcriptional changes in persister cells came from several elegant studies by the Lewis group. To enrich for persisters, all three approaches conveniently employed the metabolic inactivity of these cells. In the first report, logarithmically growing populations of the high-persistence *E. coli* mutant *hipA7* [4] were treated with ampicillin, thereby lysing non-persister cells. Isolated RNA was enriched for mRNA, labeled, and hybridized to *E. coli* GeneChips [6]. Similarly, gene expression profiling of persisters was performed after treating an exponentially growing population of *Mycobacterium tuberculosis* with D-cycloserine and collecting surviving persister cells by centrifugation. Transcriptome analysis was performed by microarray hybridization [55]. The third study followed a slightly different approach. It was based on the assumption that persisters are dormant cells with low levels of protein synthesis and corresponding low levels of rRNA transcription. *E. coli* persister cells were isolated by linking the *rrnB* promoter to a gene encoding an unstable fluorescent protein. In so doing, persister cells are dim as compared to normal cells in the population, which allows for the isolation of persisters using fluorescence-activated cell sorting (FACS). cDNA was prepared from purified RNA and hybridized to spotted *E. coli* DNA microarrays [56].

Based on the studies cited above, stress response pathways as well as TA loci were shown to be highly expressed in isolated persister cells. On the other hand, biosynthetic functions including energy production were downregulated [6, 55, 56].

2.4 Experimental Evolution

The use of experimental evolution for elucidating antibacterial resistance mechanisms is a widely used method. A recent study by the Balaban group used this technique for enriching a population with persisters by repeated exposure of a bacterial population to high concentrations of antibiotics. This resulted in evolved strains showing very high persister fractions caused by fixed specific genetic mutations. The increased survival appeared to be the result of an adjustment in the single-cell lag-time distribution, which was correlated with the extent of the antibiotic exposure interval [57]. They implemented the ScanLag method, which allows the simultaneous measurement of lag times of hundreds of cells [58]. These findings resulted in a new theory regarding persister cells and their ability to adapt to high doses of drugs called tolerance by lag.

2.5 Modeling

Apart from these wet lab techniques, mathematical modeling has provided interesting insights [28, 59–62] (summarized by [63]). Briefly, two main strategies can be discerned: the first one relies on estimating the switching rates between persister and non-persister growth states and assumes this process to take place continuously and stochastically (e.g., [11, 28, 59, 61, 64]). The balance between both switching rates provides a straightforward way to model a given persister level, although ignoring exactly what determines the switching rates. The second strategy focuses on the molecular mechanisms of persister formation by TA systems, with the ratio of (free) toxin over antitoxin ultimately determining, at the single-cell level, the decision to switch to the persister state (e.g., [50, 60, 65, 66]). A crucial factor in this type of models is the generation of phenotypic bistability at the population level, typically requiring noisy gene expression and noise amplification through positive feedback mechanisms [67]. Both modeling strategies have their merits, and until a more integrated approach is presented, the choice between both will depend on the goal and specific focus of the study at hand.

Mathematical modeling of persistence poses several advantages. Experiments that are not feasible in the lab can be simulated to predict the outcome. It also allows to explain empirically observed persister levels in terms of the parameters encompassed by the model, and why varying some parameters has more impact on persistence than others. Consequently, evolutionary forces that shape persister levels can be identified, which should help to devise strategies to avoid high persister levels emerging in the clinic.

3 State of the Art and Future Perspectives

Recently, the field of microbial persistence research has exploded, as evidenced by a host of publications in top-tier journals [10, 22, 23, 35, 48–50, 54, 68–70]. Currently, it is generally accepted that persister cells are present in a bacterial population preceding antibiotic treatment [71]. It is postulated that their formation results from noisy gene expression [72] as was first suggested by Kim Lewis [6]. However, over the years, several stimuli have been shown to induce persistence. For example, sub-inhibitory concentrations of fluoroquinolones are known to induce persistence via activation of the *tisAB/istR* TA locus [18, 19]. Other examples include quorum sensing molecules [73, 74], carbon source transitions [70], and nutrient deprivation leading to activation of the stringent response [75]. As was earlier described for HipA [76], a recent model ascribes TA-regulated persistence to stochastic fluctuations in cellular concentrations of the alarmone (p)ppGpp. High (p)ppGpp levels activate TA loci through a regulatory cascade requiring inorganic polyphosphate and Lon protease targeting protein toxins [49]. For an elaborate discussion on the role of these mechanisms in persistence, the reader is referred to some excellent reviews on the topic [3, 77–81].

Adding to the significance of these studies is the recent observation of a phenotypically distinct subpopulation of transiently drug-tolerant persisters in cancer cell populations. These cells are held responsible for "fractional killing" upon chemotherapy [82]. Cell-to-cell variations in protein levels were suggested to contribute to this phenomenon in which each round of therapy kills some but not all of the cells in a tumor [83]. There is a striking analogy between bacterial and cancer cell-derived persistence as both phenomena reflect a transiently phenotypic heterogeneity causing multidrug tolerance and recurrence of disease symptoms upon removal of treatment [84]. Added insight into bacterial persistence may therefore impact research areas far beyond infectious disease.

Acknowledgements

Research in the lab of JM is supported by grants from KU Leuven Research Council (PF/10/010; IDO/09/010; IDO/13/008), IAP-BELSPO, FWO, and IWT.

References

1. Hobby GL, Meyer K, Chaffee E (1942) Observations on the mechanism of action of penicillin. Exp Biol Med 50(2):281–285
2. Bigger JW (1944) Treatment of staphylococcal infections with penicillin. Lancet 244:497–500
3. Lewis K (2010) Persister cells. Annu Rev Microbiol 64:357–372
4. Moyed HS, Bertrand KP (1983) *hipA*, a newly recognized gene of *Escherichia coli* K-12 that affects frequency of persistence after

inhibition of murein synthesis. J Bacteriol 155 (2):768–775

5. Moyed HS, Broderick SH (1986) Molecular cloning and expression of *hipA*, a gene of *Escherichia coli* K-12 that affects frequency of persistence after inhibition of murein synthesis. J Bacteriol 166(2):399–403
6. Keren I, Shah D, Spoering A, Kaldalu N, Lewis K (2004) Specialized persister cells and the mechanism of multidrug tolerance in *Escherichia coli*. J Bacteriol 186(24):8172–8180
7. Correia FF, D'Onofrio A, Rejtar T, Li L, Karger BL, Makarova K, Koonin EV, Lewis K (2006) Kinase activity of overexpressed HipA is required for growth arrest and multidrug tolerance in *Escherichia coli*. J Bacteriol 188 (24):8360–8367
8. Hansen S, Vulic M, Min J, Yen TJ, Schumacher MA, Brennan RG, Lewis K (2012) Regulation of the *Escherichia coli* HipBA toxin-antitoxin system by proteolysis. PLoS One 7(6):e39185
9. Kaspy I, Rotem E, Weiss N, Ronin I, Balaban NQ, Glaser G (2013) HipA-mediated antibiotic persistence via phosphorylation of the glutamyl-tRNA-synthetase. Nat Commun 4:3001
10. Germain E, Castro-Roa D, Zenkin N, Gerdes K (2013) Molecular mechanism of bacterial persistence by HipA. Mol Cell 52(2):248–254
11. Balaban NQ, Merrin J, Chait R, Kowalik L, Leibler S (2004) Bacterial persistence as a phenotypic switch. Science 305(5690):1622–1625
12. Yamaguchi Y, Inouye M (2011) Regulation of growth and death in *Escherichia coli* by toxin-antitoxin systems. Nat Rev Microbiol 9(11): 779–790
13. Yamaguchi Y, Park JH, Inouye M (2011) Toxin-antitoxin systems in bacteria and archaea. Annu Rev Genet 45:61–79
14. Williams JJ, Hergenrother PJ (2012) Artificial activation of toxin-antitoxin systems as an antibacterial strategy. Trends Microbiol 20(6): 291–298
15. Kim Y, Wang X, Zhang XS, Grigoriu S, Page R, Peti W, Wood TK (2010) *Escherichia coli* toxin/antitoxin pair MqsR/MqsA regulate toxin CspD. Environ Microbiol 12(5): 1105–1121
16. Kim Y, Wood TK (2010) Toxins Hha and CspD and small RNA regulator Hfq are involved in persister cell formation through MqsR in *Escherichia coli*. Biochem Biophys Res Commun 391(1):209–213
17. Cheng HY, Soo VW, Islam S, McAnulty MJ, Benedik MJ, Wood TK (2013) Toxin GhoT of the GhoT/GhoS TA system damages the cell membrane to reduce ATP and to reduce growth under stress. Environ Microbiol 16 (6):1741–1754
18. Dörr T, Lewis K, Vulić M (2009) SOS response induces persistence to fluoroquinolones in *Escherichia coli*. PLoS Genet 5(12):e1000760
19. Dörr T, Vulić M, Lewis K (2010) Ciprofloxacin causes persister formation by inducing the TisB toxin in *Escherichia coli*. PLoS Biol 8(2): e1000317
20. Tripathi A, Dewan PC, Siddique SA, Varadarajan R (2014) MazF-induced growth inhibition and persister generation in *Escherichia coli*. J Biol Chem 289(7):4191–4205
21. Harrison JJ, Wade WD, Akierman S, Vacchi-Suzzi C, Stremick CA, Turner RJ, Ceri H (2009) The chromosomal toxin gene *yafQ* is a determinant of multidrug tolerance for *Escherichia coli* growing in a biofilm. Antimicrob Agents Chemother 53(6):2253–2258
22. Helaine S, Cheverton AM, Watson KG, Faure LM, Matthews SA, Holden DW (2014) Internalization of *Salmonella* by macrophages induces formation of nonreplicating persisters. Science 343(6167):204–208
23. Maisonneuve E, Shakespeare LJ, Jørgensen MG, Gerdes K (2011) Bacterial persistence by RNA endonucleases. Proc Natl Acad Sci U S A 108(32):13206–13211
24. Fauvart M, De Groote VN, Michiels J (2011) Role of persister cells in chronic infections: clinical relevance and perspectives on anti-persister therapies. J Med Microbiol 60(Pt 6): 699–709
25. Lewis K (2001) Riddle of biofilm resistance. Antimicrob Agents Chemother 45(4): 999–1007
26. Spoering AL, Lewis K (2001) Biofilms and planktonic cells of *Pseudomonas aeruginosa* have similar resistance to killing by antimicrobials. J Bacteriol 183(23):6746–6751
27. Costerton JW, Stewart PS, Greenberg EP (1999) Bacterial biofilms: a common cause of persistent infections. Science 284(5418): 1318–1322
28. Levin BR, Rozen DE (2006) Non-inherited antibiotic resistance. Nat Rev Microbiol 4(7): 556–562
29. LaFleur MD, Qi Q, Lewis K (2010) Patients with long-term oral carriage harbor high-persister mutants of *Candida albicans*. Antimicrob Agents Chemother 54(1):39–44
30. Mulcahy LR, Burns JL, Lory S, Lewis K (2010) Emergence of *Pseudomonas aeruginosa* strains producing high levels of persister cells in patients with cystic fibrosis. J Bacteriol 192 (23):6191–6199

31. Cohen NR, Lobritz MA, Collins JJ (2013) Microbial persistence and the road to drug resistance. Cell Host Microbe 13(6):632–642
32. Fu Y, Zhu M, Xing J (2010) Resonant activation: a strategy against bacterial persistence. Phys Biol 7(1):16013
33. Niepa TH, Gilbert JL, Ren D (2012) Controlling *Pseudomonas aeruginosa* persister cells by weak electrochemical currents and synergistic effects with tobramycin. Biomaterials 33(30):7356–7365
34. Manuel J, Zhanel GG, de Kievit T (2010) Cadaverine suppresses persistence to carboxypenicillins in *Pseudomonas aeruginosa* PAO1. Antimicrob Agents Chemother 54(12):5173–5179
35. Allison KR, Brynildsen MP, Collins JJ (2011) Metabolite-enabled eradication of bacterial persisters by aminoglycosides. Nature 473 (7346):216–220
36. Barraud N, Buson A, Jarolimek W, Rice SA (2013) Mannitol enhances antibiotic sensitivity of persister bacteria in *Pseudomonas aeruginosa* biofilms. PLoS One 8(12):e84220
37. Bahar AA, Ren D (2013) Antimicrobial peptides. Pharmaceuticals (Basel) 6(12): 1543–1575
38. Pan J, Bahar AA, Syed H, Ren D (2012) Reverting antibiotic tolerance of *Pseudomonas aeruginosa* PAO1 persister cells by (*Z*)-4-bromo-5-(bromomethylene)-3- methylfuran-2(5*H*)-one. PLoS One 7(9):e45778
39. Pan J, Ren D (2013) Structural effects on persister control by brominated furanones. Bioorg Med Chem Lett 23(24):6559–6562
40. Pan J, Song F, Ren D (2013) Controlling persister cells of *Pseudomonas aeruginosa* PDO300 by (*Z*)-4-bromo-5-(bromomethylene)-3-methylfuran-2(5*H*)-one. Bioorg Med Chem Lett 23(16):4648–4651
41. Pan J, Xie X, Tian W, Bahar AA, Lin N, Song F, An J, Ren D (2013) (*Z*)-4-bromo-5- (bromomethylene)-3-methylfuran-2(5*H*)-one sensitizes *Escherichia coli* persister cells to antibiotics. Appl Microbiol Biotechnol 97 (20):9145–9154
42. Conlon BP, Nakayasu ES, Fleck LE, LaFleur MD, Isabella VM, Coleman K, Leonard SN, Smith RD, Adkins JN, Lewis K (2013) Activated ClpP kills persisters and eradicates a chronic biofilm infection. Nature 503(7476): 365–370
43. Lewis K (2008) Multidrug tolerance of biofilms and persister cells. Curr Top Microbiol Immunol 322:107–131
44. Hansen S, Lewis K, Vulić M (2008) Role of global regulators and nucleotide metabolism in antibiotic tolerance in *Escherichia coli*. Antimicrob Agents Chemother 52(8):2718–2726
45. De Groote VN, Verstraeten N, Fauvart M, Kint CI, Cornelis P, Michiels J (2009) Identification of novel persistence genes in *Pseudomonas aeruginosa* in the combat against emerging antimicrobial resistance. Commun Agric Appl Biol Sci 74(4):51–56
46. Spoering AL, Vulić M, Lewis K (2006) GlpD and PlsB participate in persister cell formation in *Escherichia coli*. J Bacteriol 188(14): 5136–5144
47. Gefen O, Gabay C, Mumcuoglu M, Engel G, Balaban NQ (2008) Single-cell protein induction dynamics reveals a period of vulnerability to antibiotics in persister bacteria. Proc Natl Acad Sci U S A 105(16):6145–6149
48. Vega NM, Allison KR, Khalil AS, Collins JJ (2012) Signaling-mediated bacterial persister formation. Nat Chem Biol 8(5):431–433
49. Maisonneuve E, Castro-Camargo M, Gerdes K (2013) (p)ppGpp controls bacterial persistence by stochastic induction of toxin-antitoxin activity. Cell 154(5):1140–1150
50. Rotem E, Loinger A, Ronin I, Levin-Reisman I, Gabay C, Shoresh N, Biham O, Balaban NQ (2010) Regulation of phenotypic variability by a threshold-based mechanism underlies bacterial persistence. Proc Natl Acad Sci U S A 107 (28):12541–12546
51. Jõers A, Kaldalu N, Tenson T (2010) The frequency of persisters in *Escherichia coli* reflects the kinetics of wake-up from dormancy. J Bacteriol 192(13):3379–3384
52. Orman MA, Brynildsen MP (2013) Dormancy is not necessary or sufficient for bacterial persistence. Antimicrob Agents Chemother 57 (7):3230–3239
53. Helaine S, Thompson JA, Watson KG, Liu M, Boyle C, Holden DW (2010) Dynamics of intracellular bacterial replication at the single cell level. Proc Natl Acad Sci U S A 107 (8):3746–3751
54. Claudi B, Sprote P, Chirkova A, Personnic N, Zankl J, Schurmann N, Schmidt A, Bumann D (2014) Phenotypic variation of *Salmonella* in host tissues delays eradication by antimicrobial chemotherapy. Cell 158(4):722–733
55. Keren I, Minami S, Rubin E, Lewis K (2011) Characterization and transcriptome analysis of *Mycobacterium tuberculosis* persisters. MBio 2 (3):e00100–e00111
56. Shah D, Zhang Z, Khodursky A, Kaldalu N, Kurg K, Lewis K (2006) Persisters: a distinct physiological state of *E. coli*. BMC Microbiol 6:53

57. Fridman O, Goldberg A, Ronin I, Shoresh N, Balaban NQ (2014) Optimization of lag time underlies antibiotic tolerance in evolved bacterial populations. Nature 513(7518):418–421
58. Levin-Reisman I, Gefen O, Fridman O, Ronin I, Shwa D, Sheftel H, Balaban NQ (2010) Automated imaging with ScanLag reveals previously undetectable bacterial growth phenotypes. Nat Methods 7(9):737–739
59. Kussell E, Kishony R, Balaban NQ, Leibler S (2005) Bacterial persistence: a model of survival in changing environments. Genetics 169 (4):1807–1814
60. Cogan NG (2007) Incorporating toxin hypothesis into a mathematical model of persister formation and dynamics. J Theor Biol 248(2):340–349
61. Gardner A, West SA, Griffin AS (2007) Is bacterial persistence a social trait? PLoS One 2(8): e752
62. Klapper I, Gilbert P, Ayati BP, Dockery J, Stewart PS (2007) Senescence can explain microbial persistence. Microbiology 153(Pt 11): 3623–3630
63. Gefen O, Balaban NQ (2009) The importance of being persistent: heterogeneity of bacterial populations under antibiotic stress. FEMS Microbiol Rev 33(4):704–717
64. Hemsley CM, Luo JX, Andreae CA, Butler CS, Soyer OS, Titball RW (2014) Bacterial drug tolerance under clinical conditions is governed by anaerobic adaptation but not anaerobic respiration. Antimicrob Agents Chemother 58 (10):5775–5783
65. Gelens L, Hill L, Vandervelde A, Danckaert J, Loris R (2013) A general model for toxin-antitoxin module dynamics can explain persister cell formation in E. coli. PLoS Comput Biol 9 (8):e1003190
66. Lou C, Li Z, Ouyang Q (2008) A molecular model for persister in E. coli. J Theor Biol 255 (2):205–209
67. Veening JW, Smits WK, Kuipers OP (2008) Bistability, epigenetics, and bet-hedging in bacteria. Annu Rev Microbiol 62:193–210
68. Nguyen D, Joshi-Datar A, Lepine F, Bauerle E, Olakanmi O, Beer K, McKay G, Siehnel R, Schafhauser J, Wang Y, Britigan BE, Singh PK (2011) Active starvation responses mediate antibiotic tolerance in biofilms and nutrient-limited bacteria. Science 334(6058):982–986
69. Wakamoto Y, Dhar N, Chait R, Schneider K, Signorino-Gelo F, Leibler S, McKinney JD (2013) Dynamic persistence of antibiotic-stressed mycobacteria. Science 339(6115): 91–95
70. Amato SM, Orman MA, Brynildsen MP (2013) Metabolic control of persister formation in *Escherichia coli*. Mol Cell 50(4): 475–487
71. Keren I, Kaldalu N, Spoering A, Wang Y, Lewis K (2004) Persister cells and tolerance to antimicrobials. FEMS Microbiol Lett 230(1): 13–18
72. Fraser D, Kærn M (2009) A chance at survival: gene expression noise and phenotypic diversification strategies. Mol Microbiol 71(6): 1333–1340
73. Möker N, Dean CR, Tao J (2010) *Pseudomonas aeruginosa* increases formation of multidrug-tolerant persister cells in response to quorum-sensing signaling molecules. J Bacteriol 192(7):1946–1955
74. Leung V, Levesque CM (2012) A stress-inducible quorum-sensing peptide mediates the formation of persister cells with noninherited multidrug tolerance. J Bacteriol 194(9): 2265–2274
75. Gao W, Chua K, Davies JK, Newton HJ, Seemann T, Harrison PF, Holmes NE, Rhee HW, Hong JI, Hartland EL, Stinear TP, Howden BP (2010) Two novel point mutations in clinical *Staphylococcus aureus* reduce linezolid susceptibility and switch on the stringent response to promote persistent infection. PLoS Pathog 6 (6):e1000944
76. Korch SB, Henderson TA, Hill TM (2003) Characterization of the *hipA7* allele of *Escherichia coli* and evidence that high persistence is governed by (p)ppGpp synthesis. Mol Microbiol 50(4):1199–1213
77. Helaine S, Kugelberg E (2014) Bacterial persisters: formation, eradication, and experimental systems. Trends Microbiol 22(7):417–424
78. Maisonneuve E, Gerdes K (2014) Molecular mechanisms underlying bacterial persisters. Cell 157(3):539–548
79. Amato SM, Fazen CH, Henry TC, Mok WW, Orman MA, Sandvik EL, Volzing KG, Brynildsen MP (2014) The role of metabolism in bacterial persistence. Front Microbiol 5:70
80. Prax M, Bertram R (2014) Metabolic aspects of bacterial persisters. Front Cell Infect Microbiol 4:148
81. Kint CI, Verstraeten N, Fauvart M, Michiels J (2012) New-found fundamentals of bacterial persistence. Trends Microbiol 20(12): 577–585
82. Sharma SV, Lee DY, Li B, Quinlan MP, Takahashi F, Maheswaran S, McDermott U, Azizian N, Zou L, Fischbach MA, Wong KK, Brandstetter K, Wittner B, Ramaswamy S, Classon M,

Settleman J (2010) A chromatin-mediated reversible drug-tolerant state in cancer cell subpopulations. Cell 141(1):69–80

83. Spencer SL, Gaudet S, Albeck JG, Burke JM, Sorger PK (2009) Non-genetic origins of cell-to-cell variability in TRAIL-induced apoptosis. Nature 459(7245):428–432
84. Glickman MS, Sawyers CL (2012) Converting cancer therapies into cures: lessons from infectious diseases. Cell 148(6):1089–1098

Part II

Quantification of Persistence

Chapter 2

Persisters: Methods for Isolation and Identifying Contributing Factors—A Review

Sarah E. Rowe, Brian P. Conlon, Iris Keren, and Kim Lewis

Abstract

Persister cells are phenotypic variants surviving a lethal dose of antibiotic, sufficient to kill the bulk of an exponential phase population. In this chapter we summarize current techniques to isolate persisters and discuss limitations associated with identifying mechanisms of persister formation.

Keywords: Hip mutant, Toxin-antitoxin (TA) modules, Antibiotic, Biofilm

1 Introduction

Persisters were first described in 1944 by Joseph Bigger, a medical doctor from Trinity College Dublin [1]. Bigger reported that addition of a lethal dose of penicillin to a population of *Staphylococcus aureus* yielded a small subpopulation of surviving cells. Upon reinoculation, these colonies grew into a culture that once again lysed in the presence of penicillin and again yielded a subpopulation of survivors. Bigger referred to these surviving cells as persisters [1].

These cells are contrary to resistant cells as they cannot grow in the presence of the antibiotic. The proportion of persisters in a population varies dramatically depending on growth phase and environmental conditions [2, 3]. Specifically, persister numbers are greatly increased in stationary phase and biofilms [4, 5].

Persisters can be enumerated by adding a lethal concentration of a bactericidal antibiotic to a population of cells. The bulk of the population dies rapidly and the surviving persister cells either die much more slowly or do not die during the experiment (Fig. 1). The persister fraction can be enumerated at various time intervals by removing an aliquot, washing with 1 % NaCl, and plating serial dilutions for colony counting. The surviving persister fraction emerges in a clear biphasic curve in response to the antibiotic.

Jan Michiels and Maarten Fauvart (eds.), *Bacterial Persistence: Methods and Protocols*,
Methods in Molecular Biology, vol. 1333, DOI 10.1007/978-1-4939-2854-5_2,

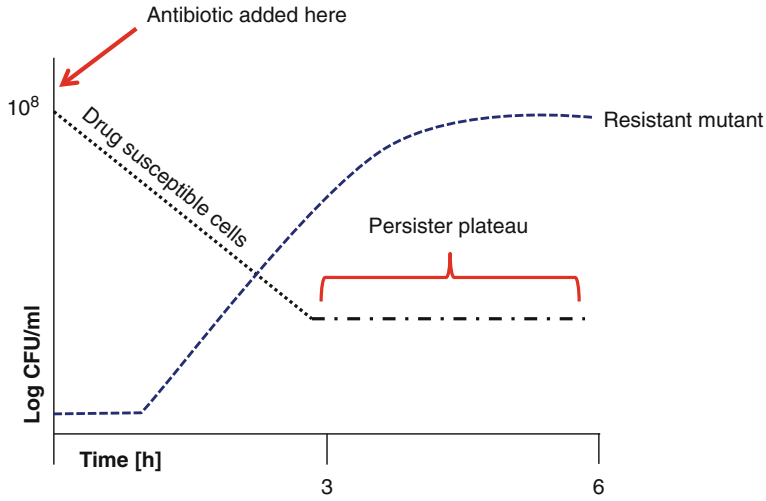

Fig. 1 Typical biphasic kill curve of a bacterial population in exponential phase of growth: A culture of *E. coli* grown to mid-exponential phase is challenged with 10× MIC of a bactericidal antibiotic (such as ciprofloxacin). The majority of cells die rapidly. The persister fraction is enumerated by removing an aliquot of cells after 3 and 6 h of exposure to the antibiotic. Cells are washed with 1 % NaCl and serial dilutions are plated for counting. Persister cells differ from resistant cells as they can tolerate the antibiotic but cannot grow in its presence

The time period where the persister fraction remains constant is referred to as the "persister plateau" (Fig. 1).

The majority of research has concentrated on persisters in *Escherichia coli* but persisters have been shown to be produced by many other bacterial species including *Pseudomonas aeruginosa*, *Mycobacterium tuberculosis*, *Salmonella enterica serovar typhimurium*, *Staphylococcus aureus*, and *Streptococcus mutans Burkholderia cepacia* and even in the fungal pathogen *Candida albicans* [6–13].

2 High-Persister (hip) Mutants

Although persisters were discovered in the 1940s, they were largely ignored until the early 1980s when Harris Moyed and co-workers isolated high-persistence (hip) mutants [14, 15]. They identified the gene *hipA*, which was the first gene known to contribute to persister formation; this gene was later identified as the toxin of an antitoxin/toxin (TA) module. The *hipA7* allele of the gene produced 1000 times more persisters to two classes of antibiotics: beta-lactams and fluoroquinolones [16]. This was the first indication that some persisters are multidrug tolerant. Importantly the *hipA7* mutant has the same minimal inhibitory concentration (MIC) as the parent strain [16], indicating that the increased level of persisters is not due to acquisition of resistance.

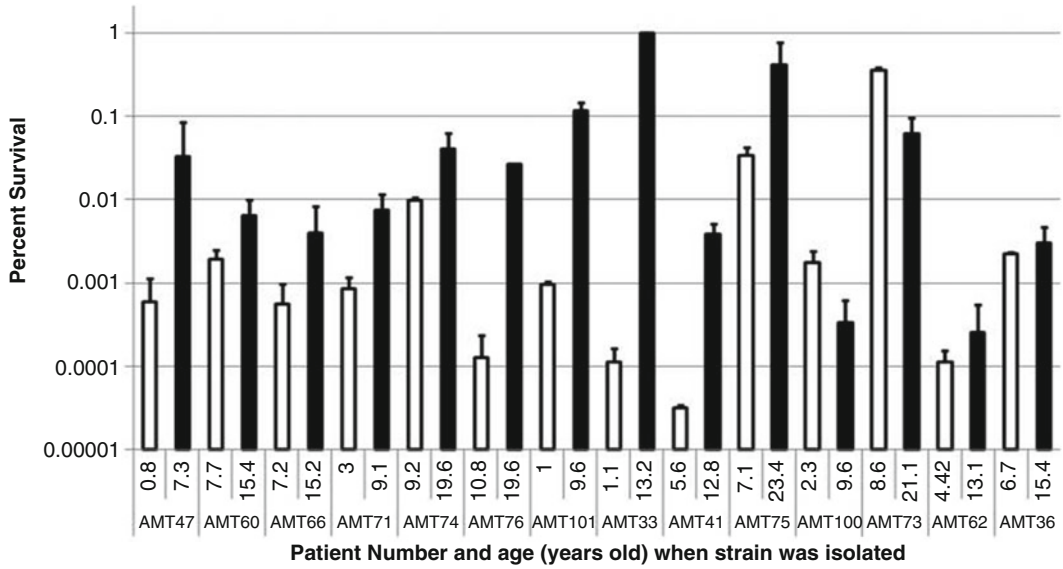

Fig. 2 A screen of *P. aeruginosa* clinical isolates for hip mutants: Stationary-phase cultures of clonal early/late isolate pairs from 14 patients were exposed to ofloxacin (50× MIC) for 8 h, and the surviving cells were determined by colony count and expressed as percent survival ($n = 4$). Early isolates are indicated with *white bars*, while late isolates are indicated with *black bars*. The patient number and age at which the tested isolates were obtained are displayed on the *x*-axis. A hip mutant emerged in 10 of the 14 patients. A hip mutant did not emerge in the isolates from the last four patients displayed on the right side of the graph. Taken from Mulcahy et al. 2010

Hip mutants can be identified in vitro by generating a mutant library and exposing it to several rounds of a lethal dose of an antibiotic [17]. The bacterial mutant library can be obtained either by chemical mutagenesis (ethyl methanesulfonate) [18] or by transposon mutagenesis [19]. Following several rounds of antibiotic challenge, the genetic basis for hip mutant phenotypes is identified by subjecting surviving cells to whole-genome sequencing or micro-array-based genetic footprinting [17].

Persisters represent transient phenotypic variants that are genetically identical to their drug-susceptible kin. Such traits have proved taxing for in vivo investigations as these persisters tend to resuscitate. Mulcahy et al. took a different approach [20]. They hypothesized that if hip mutants had an advantage then they will be selected for in vivo during infection or in response to antibiotic treatment. Longitudinal isolates of *Pseudomonas aeruginosa* were obtained from patients throughout the course of a cystic fibrosis infection. The study demonstrated that strains developed a hip phenotype over the course of the infection (Fig. 2). A similar finding was observed in *Candida albicans* with patients suffering from chronic oral thrush [21]. These studies indicate that persisters are clinically relevant and may contribute to treatment failures.

3 Pre-existing and Induced Persisters

The frequency of persisters in hip strains is much higher than in the wild-type *E. coli* which facilitates research into the mechanism of persister formation. The *hipA7* mutant was used for single-cell time-lapse microscopy, which showed that persisters are slow or non-growing cells, stochastically formed and pre-existing in the population [22].

In order to distinguish between growing and non-growing cells, Shah et al. used an unstable GFP variant driven from a ribosomal promoter [23]. Cells expressing this plasmid were grown to mid-exponential phase and analyzed by fluorescent-activated cell sorting (FACS) (Fig. 3). Two distinct populations were visualized using forward light scatter, one that fluoresced brightly and one that did not. Cells from both populations were sorted and visualized by epifluorescent microscopy and challenged with ofloxacin. The cells that did not express GFP were much more likely to survive antibiotic challenge. This study described a new mechanism for identifying persisters and demonstrated that non-growing cells exist in an untreated *E. coli* population [23]. These results suggest that there is a population of persisters that are pre-existing in the population and are not formed in a response to antibiotic treatment.

In support of this, it has been demonstrated that an *E. coli* culture, if diluted several times and challenged with either ampicillin or ofloxacin, displays a gradual decline and eventual elimination

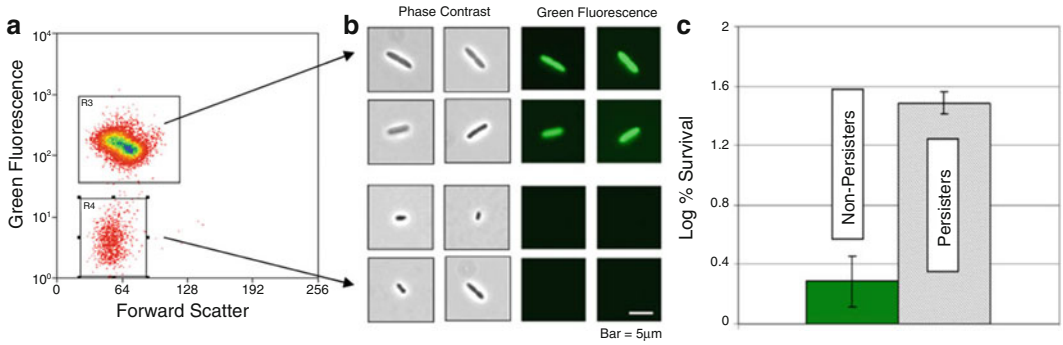

Fig. 3 Isolation of persister cells from an exponentially growing culture. *E. coli* cells containing a degradable GFP reporter cassette were grown in LB medium to mid-exponential phase (~1 × 10^8 cells/ml) at 37 °C with aeration and sorted using a high-speed cell sorter equipped with a standard GFP filter set. (**a**) Two populations were detected using forward light scatter, one that fluoresced brightly (R3), and another that did not (R4). (**b**) The sorted populations were visualized by epifluorescent microscopy (bar, 5 μm). (**c**) Cells were sorted as described in (**a**–**b**). Once sorted both populations were treated with ofloxacin (5 μg/ml) for 3 h, diluted, and spotted onto LB agar plates for colony counts. Taken from Shah et al. 2006

of persisters, even though the initial population size is kept constant [2]. This indicates that persisters are formed later in the growth phase, accumulate in stationary phase, and can be diluted out with serial reinoculation.

Johnson et al. showed that pretreatment of *S. aureus* with sub-MIC concentrations of a particular antibiotic significantly increases the level of multidrug-tolerant persisters [24]. From these results, the authors conclude that persister formation is the product of various errors during cell replication. These errors result in transient periods of slowed metabolism and/or non-replication by individual cells in growing populations [24].

Although there is mounting evidence to suggest that persisters are pre-existing and formed stochastically throughout growth, there is also data to support that persisters can be induced in response to antibiotics [24, 25] and environmental stress [26]. Dorr et al. demonstrated that pretreatment of *E. coli* with low levels of ciprofloxacin induced the formation of persisters to higher doses of ciprofloxacin (Fig. 4). This study shows that the majority of persisters to ciprofloxacin are induced in response to that antibiotic and this is dependent on a functional SOS response [25]. Later work has demonstrated that persisters can also be formed as a response to an environmental stress such as DNA damage or oxidative stress [26] and the stringent response [3, 27, 28].

4 Toxin Antitoxins (TA) Modules

The first transcriptome of persisters was generated by taking advantage of the fact that β-lactam antibiotics such as ampicillin are bacteriolytic, causing lysis of dying cells [29]. An *E. coli* culture was treated with a high concentration of ampicillin. A simple centrifugation step was used to collect the surviving persisters and expression profiles were determined using a microarray. Several TA modules were among the genes induced in persisters.

TA genes were first identified as addiction modules that play a role in plasmid maintenance [30]. The toxin and antitoxin genes make up an operon that is transcribed from the same promoter. In the case of type II TA systems, the toxin and antitoxins are proteins which bind together and often repress transcription of the operon [31]. The antitoxin is less stable and is degraded by cellular proteases; if a daughter cell loses the plasmid, the antitoxin is rapidly degraded and the toxin prevents cell growth [30]. TAs were subsequently discovered on bacterial chromosomes. Many studies have implicated chromosomal TAs to have a role in persistence which will be discussed in this section [14, 16, 32–35].

The *hipA* gene of the *hipBA* operon is the probably the most widely studied persister gene. It encodes the toxin HipA which is neutralized by its cognate antitoxin HipB. Under cellular stress, the

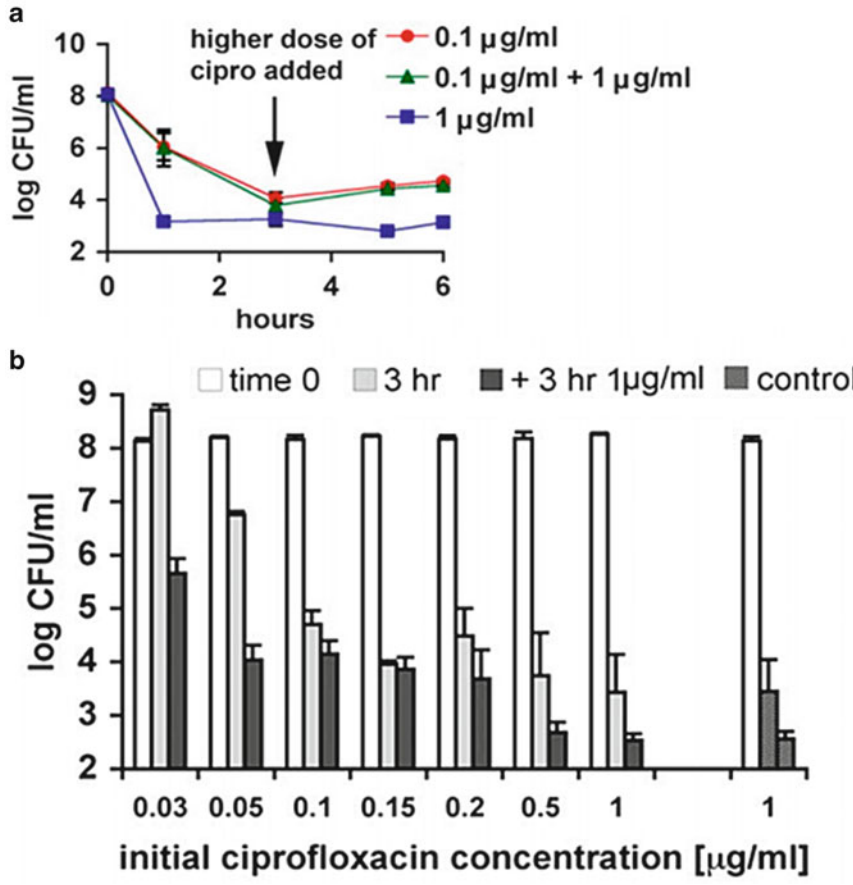

Fig. 4 Ciprofloxacin-induced persistence: (**a**) Survival of wild-type cells in exponential phase under different ciprofloxacin regimes. Two cultures were treated with 0.1 and 1 μg/ml, respectively, for 6 h. Third culture was treated with 0.1 μg/ml for 3 h after which 1 μg/ml was added (indicated by an *arrow*). The data are averages of three independent experiments and error bars indicate standard error. (**b**) Wild-type cells in exponential phase were treated for 3 h with increasing concentrations of ciprofloxacin indicated on *x*-axis. After the initial treatment, an additional 1 μg/ml of ciprofloxacin was added to the cultures and incubated for another 3 h as in (**a**). (Ciprofloxacin MIC is 0.05 μg/ml.) As a control, a parallel culture was exposed to 1 μg/ml for the duration of the experiment. *Bars* represent the viability at 0, 3, and 6 h of time course equivalents shown in (**a**). *Open bars*: The initial viability count. *Grey bars*: The viability after 3-h incubation with ciprofloxacin concentration indicated on the *x*-axis. *Full bars*: The final viability count after additional 3-h incubation with 1 μg/ml ciprofloxacin. *Dashed bars*: Viability of the control culture at 3 and 6 h. The data are averages of three independent experiments and error bars indicate standard error. Taken from Dorr et al. 2009

Lon protease degrades HipB, releasing HipA and allowing it to exert its toxic effects on the cell [35]. A recent study revealed that HipA is a kinase that phosphorylates an aminoacyl-tRNA synthetase, halts protein synthesis, and induces persister formation [36].

There are 11 TA mRNA interferases in *E. coli* K12, which are induced under various cellular stresses [3, 37–41]. Upon overexpression, these toxins have been shown to cleave

cellular mRNA and induce persister formation. However, single mutations of these TA modules did not result in a reduction of persister levels [34]. Redundancy could explain the lack of a persister phenotype but nevertheless this led to some debate as to their role in persister formation.

Kenn Gerdes and co-workers serially deleted up to ten of the recognized type II TA modules (Δ10) in *E. coli* [34]. They reported that at least five modules need to be deleted before a significant reduction in persister levels is observed. A progressive reduction in persister levels was observed when more TA modules were deleted, and the Δ10 strain displayed a 100-fold reduction in persister formation. These results demonstrate the importance of TA modules in persister formation and their high degree of redundancy for one another.

It is also a possibility that an individual TA locus may play a role in persister formation in a specific strain or under specific environmental conditions. Norton et al. reported that a single knockout of the TA module PasTI had no phenotype when deleted in *E. coli* lab strain MG1655 but displayed a 100-fold reduction in persisters when deleted in a clinical isolate CFT073 [42]. This study highlights the limitations of studying the mechanisms of persister formation in lab strains under lab conditions [42].

Similarly, Helaine et al. reported that internalization of *Salmonella* by macrophages induced persister formation over 100-fold [43]. Importantly, the group identified two stress conditions encountered in vivo, vacuolar acidification and nutritional deprivation, which induce persister formation through the 14 TA modules. Together these studies emphasize the need to study persistence in an environment that closely resembles in vivo conditions.

5 Genetic Determinants of Persisters

The standard approach for identifying genes which contribute to a function is to avail of a mutant library and generate a screen. This does not work well when redundant genes contribute to the same function, as is the case of the TA modules. An alternative method is to create an over-expression library and screen for gain-of-function phenotypes. In this case, even a mild contributor to the phenotype can be identified. However, this method can be problematic for persisters as overproduction of many proteins, particular membrane proteins, can result in toxic protein aggregates. This can cause growth cessation and artificially emulate an antibiotic tolerant state. Spoering et al. overexpressed a library in a low-copy vector, using native promoters for expression and challenged with a lethal dose of ampicillin [44]. In an attempt to exclude false positives the authors introduced a growth step in between rounds of antibiotic selection. Any strains that grew considerably slower than the wild

type would be selected against. A particular clone, with elevated levels of persisters tolerant to ampicillin, carried the gene *glpD*, involved in glycerol metabolism. Interestingly, overexpression of *glpD* also induced persisters tolerant to ofloxacin suggesting that these persisters are multidrug tolerant. Deletion of the *glpD* gene in a wild-type background reduced levels of persisters to ciprofloxacin in stationary phase. Recent work has suggested a mechanism by which the *glpD* mutant has increased levels of methylglyoxal, a bacteriostatic metabolite [17].

A screen for novel persister genes utilized the Keio collection [45], an ordered deletion library of all 3985 nonessential genes in *E. coli*. Strains were grown to stationary phase in 96-well plates and exposed to lethal concentration of ofloxacin [46]. This screen identified 150 mutants with decreased levels of persisters. Ten mutants were confirmed to display a decreased level of persisters to ofloxacin with an unchanged MIC. Most of these genes had mutations in global regulators, all of which had modest effects on persister levels [46].

Global regulators RpoS and RelA were also identified to have a role in *P. aeruginosa* persistence [6, 28, 47]. An additional nine genes were identified by a high-throughput screen of an incomplete *P. aeruginosa* transposon mutant library [48].

Despite these many screens, a mutant with a complete lack of persisters has not been identified. The mutants identified to date can display altered levels of persisters to one or more class of drugs. This strongly suggests that there is not a central mechanism for persister formation and persisters surviving different antibiotic treatments are not identical. It is more likely that persisters can be formed through different mechanisms and there is a degree of cross talk between these mechanisms that can lead multidrug-tolerant persisters.

6 The Importance of Persisters

Many bacteria form biofilms in response to environmental stress [49]. Biofilms are a surface-attached agglomeration of cells encased in an exopolymeric and proteinaceous matrix. While most antibiotics can penetrate through this matrix, biofilms do protect the cells from the immune response and can therefore complicate treatment of an infection leading to persistent and chronic infection [50]. It was demonstrated that biofilms of *P. aeruginosa* harbor persister cells tolerant to antibiotics [7, 27] and there is evidence to suggest that this complicates treatment for cystic fibrosis patients [20]. A similar role was recently suggested for the granuloma in MTB infection, acting as a physical barrier protecting persisters from the immune system [8]. Kim Lewis suggested a model (Fig. 5) explaining the recalcitrant nature of biofilm infection [51]. When

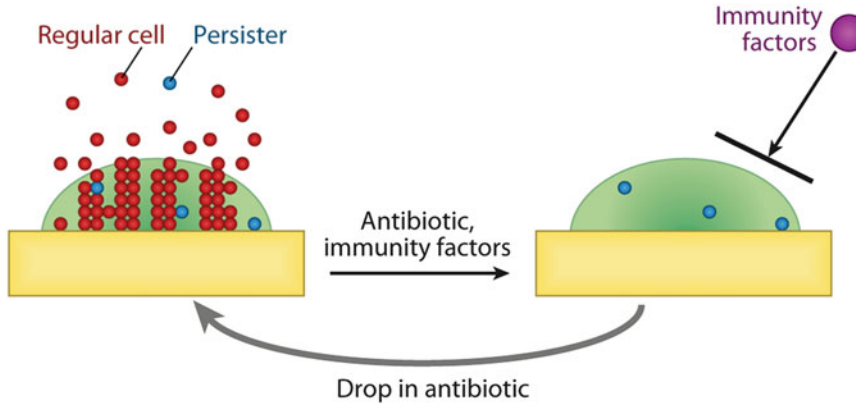

Fig. 5 A model of a relapsing biofilm infections. Regular cells and persister cells form in the biofilm and are shed off into surrounding tissue and the bloodstream. Antibiotics kill regular cells, and the immune system eliminates escaping persister cells. The matrix protects persister cells from the immune system, and when the concentration of the antibiotic drops, they repopulate the biofilm, causing a relapse. Taken from Lewis et al. 2010

a biofilm infection is treated with antibiotics, the majority of the bacterial cells die and only persisters survive. In the biofilm, persisters are protected from the immune system, and upon removal of the antibiotic pressure they can repopulate the biofilm matrix. The combination of persisters and biofilm is the likely culprit of relapsing chronic infections, with persister cells providing protection from antibiotics while the biofilm provides protection from the immune system.

Antibiotic resistance represents a huge problem, particularly with gram-negative bacteria [52, 53]. However, many bacterial strains isolated from chronic infections are susceptible to the antibiotics they were treated with [5, 20]. This indicates that persistence rather than resistance may be a key contributor to the recalcitrance of some infections. With this in mind, a search for novel antibiotics which target dormant or stationary cells rather than fast-growing cells could dramatically reduce treatment failures.

Bactericidal antibiotics target and corrupt active processes in cells which are inactive in persister cells, allowing them to survive the antibiotic treatment. Acyldepsipeptides (ADEPs) are a new class of antibiotics discovered by Eli Lily in 1985. Brotz-Oesterhelt et al. found that ADEP targets the ClpP protease, opening the proteolytic core resulting in ATP-independent proteolysis [54]. Despite impressive efficacy in a variety of animal models of acute infection, development of the drug was not pursued due to high frequency of resistance (1×10^{-6}) due to null mutation of the nonessential *clpP* gene.

Importantly, ADEP activates and dysregulates ClpP in an ATP-independent manner [54]. This suggested that ADEP could potentially target cells in a low-energy state and may be active against non-growing cells. Conlon et al. recognized the unique ability of the drug to target persister cells [5]. They reported that although a stationary population of *S. aureus* is highly tolerant to a range of antibiotics in vitro it remains susceptible to ADEP. However, following an initial death phase, the high frequency of resistant mutants allowed the culture to rebound and repopulate. ADEP paired with rifampicin resulted in eradication of the population due to increased antibiotic susceptibility of the ADEP4-resistant *clpP* null mutants. Importantly, the authors were able to sterilize a deep-seated murine thigh infection model of *S. aureus*. This study highlights the importance of discovering new antimicrobials that specifically target persister cells.

References

1. Bigger JW (1944) Treatment of staphylococcal infections with penicillin. Lancet ii:497–500
2. Keren I, Kaldalu N, Spoering A, Wang Y, Lewis K (2004) Persister cells and tolerance to antimicrobials. FEMS Microbiol Lett 230 (1):13–18
3. Maisonneuve E, Castro-Camargo M, Gerdes K (2013) (p)ppGpp controls bacterial persistence by stochastic induction of toxin-antitoxin activity. Cell 154(5):1140–1150. doi:10.1016/j.cell.2013.07.048
4. Amato SM, Brynildsen MP (2014) Nutrient transitions are a source of persisters in *Escherichia coli* biofilms. PLoS One 9(3), e93110. doi:10.1371/journal.pone.0093110
5. Conlon BP, Nakayasu ES, Fleck LE, LaFleur MD, Isabella VM, Coleman K, Leonard SN, Smith RD, Adkins JN, Lewis K (2013) Activated ClpP kills persisters and eradicates a chronic biofilm infection. Nature 503(7476):365–370. doi:10.1038/nature12790
6. Moker N, Dean CR, Tao J (2010) *Pseudomonas aeruginosa* increases formation of multidrug-tolerant persister cells in response to quorum-sensing signaling molecules. J Bacteriol 192(7):1946–1955. doi:10.1128/JB.01231-09
7. Spoering AL, Lewis K (2001) Biofilms and planktonic cells of *Pseudomonas aeruginosa* have similar resistance to killing by antimicrobials. J Bacteriol 183(23):6746–6751. doi:10.1128/JB.183.23.6746-6751.2001
8. Keren I, Minami S, Rubin E, Lewis K (2011) Characterization and transcriptome analysis of *Mycobacterium tuberculosis* persisters. MBio 2 (3):e00100–e00111. doi:10.1128/mBio.00100-11
9. Slattery A, Victorsen AH, Brown A, Hillman K, Phillips GJ (2013) Isolation of highly persistent mutants of *Salmonella enterica* serovar Typhimurium reveals a new toxin-antitoxin module. J Bacteriol 195(4):647–657. doi:10.1128/JB.01397-12
10. Lechner S, Lewis K, Bertram R (2012) *Staphylococcus aureus* persisters tolerant to bactericidal antibiotics. J Mol Microbiol Biotechnol 22(4):235–244. doi:10.1159/000342449
11. Leung V, Levesque CM (2012) A stress-inducible quorum-sensing peptide mediates the formation of persister cells with noninherited multidrug tolerance. J Bacteriol 194 (9):2265–2274. doi:10.1128/JB.06707-11
12. LaFleur MD, Kumamoto CA, Lewis K (2006) *Candida albicans* biofilms produce antifungal-tolerant persister cells. Antimicrob Agents Chemother 50(11):3839–3846
13. Van Acker H, Sass A, Bazzini S, De Roy K, Udine C, Messiaen T, Riccardi G, Boon N, Nelis HJ, Mahenthiralingam E, Coenye T (2013) Biofilm-grown *Burkholderia cepacia* complex cells survive antibiotic treatment by avoiding production of reactive oxygen species. PLoS One 8(3), e58943. doi:10.1371/journal.pone.0058943
14. Moyed HS, Bertrand KP (1983) *hipA*, a newly recognized gene of *Escherichia coli* K-12 that affects frequency of persistence after inhibition of murein synthesis. J Bacteriol 155 (2):768–775

15. Moyed HS, Broderick SH (1986) Molecular cloning and expression of *hipA*, a gene of *Escherichia coli* K-12 that affects frequency of persistence after inhibition of murein synthesis. J Bacteriol 166(2):399–403
16. Falla TJ, Chopra I (1998) Joint tolerance to beta-lactam and fluoroquinolone antibiotics in *Escherichia coli* results from overexpression of *hipA*. Antimicrob Agents Chemother 42 (12):3282–3284
17. Girgis HS, Harris K, Tavazoie S (2012) Large mutational target size for rapid emergence of bacterial persistence. Proc Natl Acad Sci U S A 109(31):12740–12745. doi:10.1073/pnas.1205124109
18. Bokel C (2008) EMS screens: from mutagenesis to screening and mapping. Methods Mol Biol 420:119–138. doi:10.1007/978-1-59745-583-1_7
19. Hayes F (2003) Transposon-based strategies for microbial functional genomics and proteomics. Annu Rev Genet 37:3–29. doi:10.1146/annurev.genet.37.110801.142807
20. Mulcahy LR, Burns JL, Lory S, Lewis K (2010) Emergence of *Pseudomonas aeruginosa* strains producing high levels of persister cells in patients with cystic fibrosis. J Bacteriol 192 (23):6191–6199. doi:10.1128/JB.01651-09
21. LaFleur MD, Qi Q, Lewis K (2010) Patients with long-term oral carriage harbor high-persister mutants of *Candida albicans*. Antimicrob Agents Chemother 54(1):39–44
22. Balaban NQ, Merrin J, Chait R, Kowalik L, Leibler S (2004) Bacterial persistence as a phenotypic switch. Science 305 (5690):1622–1625. doi:10.1126/science.1099390
23. Shah D, Zhang Z, Khodursky A, Kaldalu N, Kurg K, Lewis K (2006) Persisters: A distinct physiological state of *E. coli*. BMC Microbiol 6 (1):53–61
24. Johnson PJ, Levin BR (2013) Pharmacodynamics, population dynamics, and the evolution of persistence in *Staphylococcus aureus*. PLoS Genet 9(1), e1003123. doi:10.1371/journal.pgen.1003123
25. Dorr T, Lewis K, Vulic M (2009) SOS response induces persistence to fluoroquinolones in *Escherichia coli*. PLoS Genet 5(12), e1000760. doi:10.1371/journal.pgen.1000760
26. Wu Y, Vulic M, Keren I, Lewis K (2012) Role of oxidative stress in persister tolerance. Antimicrob Agents Chemother 56(9):4922–4926. doi:10.1128/AAC.00921-12
27. Nguyen D, Joshi-Datar A, Lepine F, Bauerle E, Olakanmi O, Beer K, McKay G, Siehnel R, Schafhauser J, Wang Y, Britigan BE, Singh PK (2011) Active starvation responses mediate antibiotic tolerance in biofilms and nutrient-limited bacteria. Science 334(6058):982–986. doi:10.1126/science.1211037
28. Viducic D, Ono T, Murakami K, Susilowati H, Kayama S, Hirota K, Miyake Y (2006) Functional analysis of *spoT*, *relA* and *dksA* genes on quinolone tolerance in *Pseudomonas aeruginosa* under nongrowing condition. Microbiol Immunol 50(4):349–357
29. Keren I, Shah D, Spoering A, Kaldalu N, Lewis K (2004) Specialized persister cells and the mechanism of multidrug tolerance in *Escherichia coli*. J Bacteriol 186(24):8172–8180
30. Ogura T, Hiraga S (1983) Mini-F plasmid genes that couple host cell division to plasmid proliferation. Proc Natl Acad Sci U S A 80 (15):4784–4788
31. Hayes F, Van Melderen L (2011) Toxins-antitoxins: diversity, evolution and function. Crit Rev Biochem Mol Biol 46(5):386–408. doi:10.3109/10409238.2011.600437
32. Dorr T, Vulic M, Lewis K (2010) Ciprofloxacin causes persister formation by inducing the TisB toxin in *Escherichia coli*. PLoS Biol 8(2): e1000317. doi:10.1371/journal.pbio.1000317
33. Kim Y, Wood TK (2010) Toxins Hha and CspD and small RNA regulator Hfq are involved in persister cell formation through MqsR in *Escherichia coli*. Biochem Biophys Res Commun 391(1):209–213. doi:10.1016/j.bbrc.2009.11.033
34. Maisonneuve E, Shakespeare LJ, Jorgensen MG, Gerdes K (2011) Bacterial persistence by RNA endonucleases. Proc Natl Acad Sci U S A 108(32):13206–13211. doi:10.1073/pnas.1100186108
35. Hansen S, Vulic M, Min J, Yen TJ, Schumacher MA, Brennan RG, Lewis K (2012) Regulation of the *Escherichia coli* HipBA toxin-antitoxin system by proteolysis. PLoS One 7(6), e39185. doi:10.1371/journal.pone.0039185
36. Germain E, Castro-Roa D, Zenkin N, Gerdes K (2013) Molecular mechanism of bacterial persistence by HipA. Mol Cell 52 (2):248–254. doi:10.1016/j.molcel.2013.08.045
37. Christensen SK, Mikkelsen M, Pedersen K, Gerdes K (2001) RelE, a global inhibitor of translation, is activated during nutritional stress. Proc Natl Acad Sci U S A 98 (25):14328–14333
38. Christensen SK, Pedersen K, Hansen FG, Gerdes K (2003) Toxin-antitoxin loci as stress-response-elements: ChpAK/MazF and

ChpBK cleave translated RNAs and are counteracted by tmRNA. J Mol Biol 332 (4):809–819

39. Christensen SK, Gerdes K (2004) Delayed-relaxed response explained by hyperactivation of RelE. Mol Microbiol 53(2):587–597
40. Gonzalez Barrios AF, Zuo R, Hashimoto Y, Yang L, Bentley WE, Wood TK (2006) Autoinducer 2 controls biofilm formation in *Escherichia coli* through a novel motility quorum-sensing regulator (MqsR, B3022). J Bacteriol 188(1):305–316
41. Yamaguchi Y, Inouye M (2011) Regulation of growth and death in *Escherichia coli* by toxin-antitoxin systems. Nat Rev Microbiol 9 (11):779–790. doi:10.1038/nrmicro2651
42. Norton JP, Mulvey MA (2012) Toxin-antitoxin systems are important for niche-specific colonization and stress resistance of uropathogenic *Escherichia coli*. PLoS Pathog 8 (10), e1002954. doi:10.1371/journal.ppat.1002954
43. Helaine S, Cheverton AM, Watson KG, Faure LM, Matthews SA, Holden DW (2014) Internalization of *Salmonella* by macrophages induces formation of nonreplicating persisters. Science 343(6167):204–208. doi:10.1126/science.1244705
44. Spoering AL, Vulic M, Lewis K (2006) GlpD and PlsB participate in persister cell formation in *Escherichia coli*. J Bacteriol 188 (14):5136–5144
45. Baba T, Ara T, Hasegawa M, Takai Y, Okumura Y, Baba M, Datsenko KA, Tomita M, Wanner BL, Mori H (2006) Construction of *Escherichia coli* K-12 in-frame, single-gene knockout mutants: the Keio collection. Mol Syst Biol 2:2006.0008
46. Hansen S, Lewis K, Vulić M (2008) The role of global regulators and nucleotide metabolism in antibiotic tolerance in *Escherichia coli*. Antimicrob Agents Chemother 8:2718–2726
47. Murakami K, Ono T, Viducic D, Kayama S, Mori M, Hirota K, Nemoto K, Miyake Y (2005) Role for *rpoS* gene of *Pseudomonas aeruginosa* in antibiotic tolerance. FEMS Microbiol Lett 242(1):161–167
48. De Groote VN, Verstraeten N, Fauvart M, Kint CI, Verbeeck AM, Beullens S, Cornelis P, Michiels J (2009) Novel persistence genes in *Pseudomonas aeruginosa* identified by high-throughput screening. FEMS Microbiol Lett 297(1):73–79. doi:10.1111/j.1574-6968.2009.01657.x
49. Costerton JW, Cheng KJ, Geesey GG, Ladd TI, Nickel JC, Dasgupta M, Marrie TJ (1987) Bacterial biofilms in nature and disease. Annu Rev Microbiol 41:435–464. doi:10.1146/annurev.mi.41.100187.002251
50. Lewis K (2010) Persister cells. Annu Rev Microbiol 64:357–372. doi:10.1146/annurev.micro.112408.134306
51. Lewis K (2005) Persister cells and the riddle of biofilm survival. Biochemistry (Mosc) 70 (2):267–274
52. Levy SB (2001) Antibiotic resistance: consequences of inaction. Clin Infect Dis 33(Suppl 3):S124–129. doi:10.1086/321837
53. Levy S (2005) Antibiotic resistance – the problem intensifies. Adv Drug Deliv Rev 57 (10):1446–1450. doi:10.1016/j.addr.2005.04.001
54. Brotz-Oesterhelt H, Beyer D, Kroll HP, Endermann R, Ladel C, Schroeder W, Hinzen B, Raddatz S, Paulsen H, Henninger K, Bandow JE, Sahl HG, Labischinski H (2005) Dysregulation of bacterial proteolytic machinery by a new class of antibiotics. Nat Med 11(10):1082–1087. doi:10.1038/nm1306

Chapter 3

A General Method for Measuring Persister Levels in *Escherichia coli* Cultures

Niilo Kaldalu, Arvi Jõers, Henri Ingelman, and Tanel Tenson

Abstract

Genetically homogeneous bacterial cultures contain persisters, cells that are not killed by bactericidal antibiotics. These cells are suggested to be involved in the establishment of chronic infections. Persister levels depend on growth conditions. Here, we discuss the parameters that have to be considered when measuring persister levels and provide a sample protocol to do it.

Keywords: Antibiotic, Persister, Antibiotic tolerance, Ampicillin, Fluoroquinolones

1 Introduction

In 1944, Joseph Bigger studied bactericidal action of penicillin on staphylococcal cultures. He found that some bacteria are able to evade killing and regrow after the treatment. Dr. Bigger called these cells persisters and either described or predicted several basic features that define such surviving minority. Besides, he concluded that persisters must be in part responsible for the limited success of antibiotic treatment against infections [1]. Seventy years later, the main conclusions of his research have been confirmed and elaborated by many laboratories using several different bacterial species. It is amazing how many of Bigger's early observations hold true, including the complaint that "irregularities and inconsistencies occurred in almost all experiments of this type" [1]. Below, we review principal concepts of persister research and try to look how much some of the researchers' findings depend on experimental setup.

1.1 Phenotypic Tolerance vs. Phenotypic Resistance

Persisters are defined as bacteria that are tolerant to bactericidal antibiotics; they are able to survive the drug treatment but are not able to grow in the presence of the drug [1, 2]. If bacteria grow in the presence of the drug, they are called resistant.

Jan Michiels and Maarten Fauvart (eds.), *Bacterial Persistence: Methods and Protocols*, Methods in Molecular Biology, vol. 1333, DOI 10.1007/978-1-4939-2854-5_3,

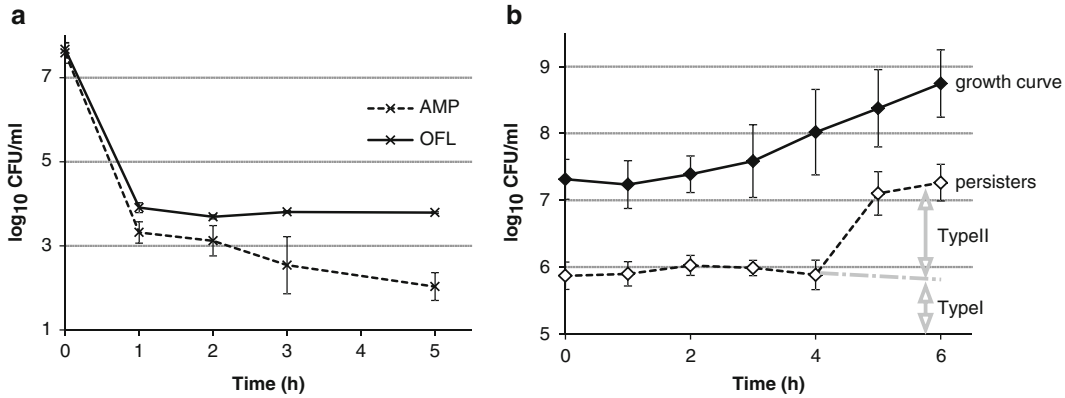

Fig. 1 Graphic presentation of results from persister experiments. (**a**). Typical killing curves of cultures treated with antibiotics. Killing curves represent kinetics of killing of bacteria during a bactericidal treatment. Cultures of *E. coli* MG1655 were grown and treated as described in this chapter. Briefly, both the overnight culture and the test culture were grown in filter-sterilized LB broth. At the beginning of the experiment, overnight culture was diluted 1000× and incubated on a shaker at 37 °C for 3 h. Then, ampicillin, 100 μg/mL (AMP; *dashed line*) or ofloxacin, 5 μg/mL (OFL; *solid line*) was added and incubation was continued. Killing curves show that the number of living microbes decreased more than 1000× during the first hour of antibiotic treatment. That drop is caused by killing of the bulk of phenotypically sensitive bacteria. Starting from the 1-h time point, CFU numbers decrease more slowly and indicate the number of persisters in the culture. The values represent the means of five independent AMP treatments and three independent OFL treatments. The error bars indicate the standard deviation. (**b**). The number of persisters increases when a growing culture approaches stationary phase. An overnight culture of *E. coli* BW25113 was diluted 1:100 and cultured with aeration at 37 °C. At the designated time points, samples were taken and treated with ciprofloxacin (1 μg/mL) for 5 h. Closed symbols, cell count before the treatment (growth curve); open symbols, cell count after the ciprofloxacin treatment (persister count). During the first 4 h, the number of persisters does not increase. In this stage, persisters are the cells that have been in the non-proliferating state since inoculation (type I persisters). After the 4-h time point, the number of persister increases rapidly and newly formed (type II) persisters make up the majority of surviving cells. The values are averages of three replicates and the error bars indicate the standard deviation

The phenomenon of persistence is phenotypic, a culture that was started from clonal descendants of a persister cell contains persisters at the same frequency as the original parental culture [1, 3]. Over several years, persister cells have been considered as non-replicating cells [2]. According to a central concept of the field, the non-growing, i.e., nondividing, state is crucial to persistence. Bacterial cultures contain individual cells that stay non-replicating in conditions enabling growth [4–6]. These cells can survive treatment with antibiotics and, if they resume growth after the removal of the drug, these bacteria are called persisters (Fig. 1a). It is a matter of debate if such heterogeneity of the population is a survival strategy [7–9] or reflects different extent of unavoidable damage to the cells [10].

Recently, it has been reported that some persisters might be actively proliferating: in *Mycobacterium*, the surviving subset of bacteria can have highly active efflux pumps [11] or express

catalase-peroxidase, which is necessary for killing by isoniazid, in stochastic pulses [12]. In these instances, surviving cells are replicating, not quiescent. It has also been suggested that some of the persisters in *E. coli* are actively dividing [6]. The concept of actively growing persisters raises terminological discrepancies. Resistance is usually determined genetically but still, the genetic component is not part of the definition. Mechanisms of phenotypic antibiotic resistance have been described recently [13, 14] and occurrence of noncanonical, phenotypic resistance due to the growth conditions and metabolic state of bacteria is well known to the microbiological community [15]. The mycobacterial "dynamic persistence" [11, 12] would fall under phenotypic resistance as well.

Replicative dormancy of persisters does not necessarily mean the lack of metabolic activity. It is intuitively reasonable to suggest, that "shutdown of a target function" (i.e., cell wall synthesis, protein synthesis, or DNA replication) "will prevent the lethal action" of the drug [16]. However in dormant cells not all the targets are equally inactive. For example, the same persister cells of *E. coli* log-phase cultures that are tolerant to fluoroquinolones and cell-wall synthesis inhibitors are killed effectively by aminoglycosides, a group of antibiotics that targets protein synthesis and causes mistranslation [5, 17, 18]. Such killing is dependent on the membrane potential of these cells, which is required for the uptake of aminoglycosides. Membrane potential is created due to the active metabolism and depends on the nutrients provided. Therefore, whether the non-growing subset of bacteria is killed by aminoglycosides, depends on the carbon source of the growth medium [18]. Consequently, persisters may have at least limited activity of protein synthesis, metabolism, and membrane transport [19].

1.2 Type I and Type II Persisters

Joseph Bigger acknowledged that some bacteria "are in the persister phase when inoculated into fresh medium, but the condition is induced in others by their new environment" [1]. Such distinction defines two groups of persisters that either retain dormancy acquired in the stationary phase (type I) or fall into dormancy during growth (type II) [4]. If antibiotic is supplied at the very moment of inoculation of the culture [5], in the lag phase, or in the early logarithmic phase then the surviving persisters belong to type I. At early stages of growth, the number of persisters does not increase (Fig. 1b). Type I persisters are lost in the course of repeated cycles of dilution and growth into early log phase [3].

Type II persisters are formed when a growing culture starts approaching to the stationary phase. When nutrients are depleting and growth conditions deteriorate, their number is progressively increasing and they make up a great majority of the persister fraction [3] (Fig. 1b). In this state, functional stress response circuits (e.g., ppGpp synthesis) are important for type II persister formation but lack of these stress responses still does not fully stop

formation of new persister cells [20, 21]. In addition to the nutrient depletion, new persister cells are generated in response to many different stress conditions (see below), including low concentrations of antibiotics [22–24].

1.3 Visualizing and Isolating Persisters

The cells with different growth rates can be labeled with various fluorescent reporters. The reporter can either manifest the physiological activity of the cell [25] or cell division rate that dilutes the fluorescent protein [26, 27]. Cell division and potential dormancy can be observed directly in a microfluidics system under the microscope [4, 28]. Alternatively, the cell population can be analyzed either by flow cytometry [5, 25, 27, 29] or by monitoring growth of plated cells [30]. For *Mycobacterium* it has been reported that cell divisions can be followed from the loss of a very unstable plasmid [11, 31].

For analyzing the macromolecular content of persisters it is important to physically isolate this fraction of the population. Lysis with antibiotics [3, 16, 32] or with alternative agents [33] has been suggested in the literature as a method to eliminate growing cells. However, it has to be noted that these methods pool the cells fulfilling the persister definition with the cells that will never be able to grow again (*see* Subheading 1.4). The nonrecovering population can be considerably higher than the persister population [5, 6, 27]. Alternatively, cell sorting can be used for isolating bacteria in different physiological states [6, 25]. Here three complications arise. First, the amount of material that can be isolated is much smaller compared to the methods based on cell lysis. Second, and more importantly, the physiological state of the bacteria might be altered by the sorting procedure. Bacteria are exposed to high pressure during sorting and carefully planned experiments are needed to control for dormancy induction by the sorting procedure. Finally, separation of persisters from permanently nondividing cells remains unresolved. Density gradient centrifugation has been used for fractionating an *E. coli* culture into subpopulations [34, 35]. Although more than 15 fractions have been described, the connection with the phenomenon of persisters has not been demonstrated [35].

1.4 Persisters and VBNC

It has to be noted that not all nondividing cells resume growth in the usual detection window of 1 or 2 days. In many cases, the cells preserve membrane integrity and are called viable but nonculturable (VBNC) [27, 36]. It is currently not clear how many of these cells might finally resume growth as slow wakeup over several months has been described [37].

1.5 Stationary-Phase Persisters

Most of the bactericidal antibiotics are ineffective against stationary-phase cultures. Certain fluoroquinolones, e.g., ofloxacin, ciprofloxacin, and gatifloxacin against *E. coli*, are an exception.

If the stationary-phase cells are diluted into the fresh growth medium and antibiotic is supplied at the same moment, it must be noted that most of the cells resume growth and become antibiotic sensitive soon after dilution. Type I persisters, not stationary-phase persisters, are assayed in such experiments [5]. For counting stationary-phase persisters, antibiotics have to be supplied directly to undiluted non-growing (i.e., stationary phase) cultures, which are in fact much less sensitive to antibiotic treatment [24, 38].

1.6 Are Persisters Tolerant to Different Antibiotics?

High-persistence (*hip*) mutants were isolated from the original screens for *E. coli* mutants with altered persister frequency [39]. Later, it was found that although the screens were made with ampicillin, increased persister frequency was observed also against fluoroquinolone antibiotics and vice versa [40]. This suggested that persisters are equally tolerant to many or all antibiotics. Current results suggest that the mechanism of antibiotic action considerably influences the persister levels and different (but probably overlapping) populations survive different antibiotics [24, 41, 42].

1.7 Growth Inhibition Induces Persistence

Bigger already showed that growth inhibition, either by suboptimal temperature, nutrient limitation, or bacteriostatic agents, induces persister formation [1]. In the pioneering work for finding out the molecular mechanisms of persister formation, Moyed was looking for mutants with altered persister levels. For avoiding indirect effects, attempts were made to find mutants with no changes in minimum inhibitory concentration (MIC) and growth parameters [39]. Indeed, it was demonstrated later that overexpression of various toxic proteins can induce increased persister levels [43]. This calls for cautious interpretation of several results where the growth of bacteria is inhibited or the culture is stressed, as these might not reveal the biologically relevant mechanisms of persister formation. The examples include screening for mutants with altered persister levels, expression of toxins from toxin-antitoxin systems [11, 44–47], manipulations with ppGpp levels [44], treating the bacteria with sub MIC antibiotic concentrations [24], etc. In addition, all strains and mutants with increased MIC values should be compared with care [38]. Even cell sorting by flow cytometry [6, 25, 27] might induce persisters from actively growing cells.

1.8 Introduction to the Current Protocol

As discussed above, different labs often use different protocols for the measurement of persister levels. Because the measurement output is sensitive to conditions, there are several parameters that are important to control. Here we have assembled a protocol that contains the most commonly used steps and have highlighted the essential parameters.

2 Materials

Prepare all media using deionized water. Store liquid media at room temperature and agar plates at 4 °C, agar side up, in closed bags.

1. LB medium: Dissolve premixed powder for LB broth in water according to the manufacturer's instructions (*see* **Note 1**). Filter-sterilize (*see* **Note 2**). Prepare fresh and use within 1 week.
2. LB agar plates: Prepare LB medium as described in **step 1**, and add agar to a final concentration of 1.5 % (w/v). Pour powder on the top of water in a beaker, stir to dissolve the soluble components, bring to boil in a microwave oven, and boil for 1 min to dissolve agar. Transfer by 200 mL into 250 mL flasks; autoclave at 121 °C for 15 min. Allow to cool to ~55 °C and pour plates. Pour ~20 mL of LB agar per 10 cm polystyrene Petri dish (*see* **Note 3**).
3. Phosphate-buffered saline (PBS): For 1 L of 10× PBS, dissolve 2 g KCl, 2.4 g KH_2PO_4, 80 g NaCl, and 11.45 g Na_2HPO_4 (*see* **Note 4**) in 800 mL water, and fill up to 1000 mL. Dilute 10× in water to prepare 1× PBS. Autoclave and store at room temperature.
4. Stock solutions of antibiotics (*see* **Note 5**).
   (a) Ampicillin: Dissolve ampicillin sodium salt in water at a concentration of 100 mg/mL. Do not freeze and melt. Store at 4 °C for up to 1 week (*see* **Note 6**).
   (b) Ciprofloxacin, norfloxacin, gatifloxacin, ofloxacin: All these fluoroquinolone antibiotics are soluble in 0.1 M NaOH. Dissolve, dilute with water to a concentration of 5 mg/mL, aliquot, and freeze. Store at −20 °C for up to 3 months.
5. Dimethyl sulfoxide (DMSO).

3 Methods

We provide a procedure for characterization of persistence of *E. coli*, which is suitable for comparison of different isolates and strains. Altering incubation times and temperatures, media for growth of the inoculum and the test culture, aeration regimens, and other experimental details have an impact on persister formation and must explicitly stated when publishing results.

3.1 Preparation of E. coli Culture DMSO Stocks

We recommend starting overnight cultures from frozen DMSO stocks. This helps to standardize cultures and reduce variability between individual experiments (*see* **Note 7**).

1. Inoculate a test tube containing 3 mL LB medium with cells from a freshly grown colony on an LB agar plate. Grow on a shaker at 37 °C overnight (*see* **Note 8**).
2. Make a 100× dilution of the overnight culture into 20 mL of LB medium. Incubate on a shaker at 37 °C. Sample over time to measure the optical density at $\lambda = 600$ nm.
3. When the OD_{600} of the culture has reached ~0.6, add DMSO to 8 % (v/v) by mixing 9.2 mL of the culture with 0.8 mL of DMSO. Dispense in 100 μl aliquots in cluster tubes and store frozen at −80 °C. DMSO stocks can be stored for up to 3 months.

3.2 Growing Overnight Cultures for Inoculum

A standardized procedure for preparation of inocula makes experiments reproducible and is required for consistent results (*see* **Note 9**).

1. Transfer 3 mL of filter-sterilized LB medium into a sterile test tube.
2. Melt an aliquot of the DMSO stock and use 50 μL for starting a culture. DMSO stocks should not be refrozen and reused.
3. Grow on a shaker at 220 rpm and 37 °C for 16 h.

3.3 Growing Experimental Cultures and Performing Antibiotic Treatments

1. Transfer 20 mL of filter-sterilized LB medium into a sterile 100 mL Erlenmeyer flask.
2. Inoculate with 20 μL of overnight culture (1000× dilution). Put on a shaker at 220 rpm and 37 °C.
3. Incubate for 3 h, and then take a 100 μL pretreatment sample of the culture to determine the number of culturable bacteria at the start of the antibiotic treatment.
4. Add antibiotic solution to the culture. Use ampicillin at a concentration of 100 μg/mL, ciprofloxacin, gatifloxacin, norfloxacin, and ofloxacin at concentrations of 5 μg/mL (*see* **Note 10**). If using antibiotic stock solutions listed in Subheading 2, add 20 μL of an antibiotic solution. Continue incubation on a shaker at 220 rpm and 37 °C (*see* **Note 11**).
5. Make serial dilutions of the pretreatment sample. Use LB medium for dilution. Alternatively, serial dilutions can be made using sterile PBS or 0.9 % solution of NaCl (*see* **Note 12**).
6. Plate dilutions onto LB agar plates (*see* **Note 13**). Bacteria can be either spot plated or spread plated (*see* **Note 14**).
7. Place plates at 37 °C for overnight incubation (*see* **Note 15**).
8. If you treat your cultures with ampicillin (Amp) or any other cell-wall synthesis inhibitor, take 100 μL samples 1, 2, 3, and 5 h after addition of the drug. Make serial dilutions just like you did of the pretreatment sample and plate. Incubate at 37 °C for 24 h (*see* **Note 15**) and count colonies.

9. If you treat your cultures with fluoroquinolones (ciprofloxacin, ofloxacin, norfloxacin, gatifloxacin), take 1 mL samples 1, 2, 3, and 5 h after addition of the drug. Spin down the cells in a 1.5 mL test tube for 5 min at 5000 × *g* and room temperature. Remove supernatant and resuspend bacteria in 1 mL LB medium. Repeat centrifugation, remove supernatant, and resuspend cells in 1 mL of fresh PBS. Continue with serial dilutions and plating as in the case of the non-treated and ampicillin-treated samples (*see* **Note 16**). Example results of the persister measurement are shown in Fig. 1. Alternatively, the results of antibiotic treatment and growth resumption can be analyzed by flow cytometry (*see* **Note 17**).

4 Notes

1. Let the powdered medium hydrate by pouring it slowly on the surface of the water. This avoids clumping.
2. We strongly recommend using filter-sterilized rich media or defined minimal media. Autoclaving causes degradation of the components of rich media and alters the content in an unpredictable way. This contributes to inconsistency of results [29, 48]. If you use autoclaved media, minimizing experimental error would require using always the same model of autoclave, aliquoting identical volumes, loading the same amount of material to autoclave, and sterilizing your media for the same time at the same temperature.
3. LB agar can be allowed to solidify and stored at room temperature. It can be remelted in a microwave oven, allowed to cool to ~55 °C, and used for pouring plates. The autoclaved, melted LB agar should not be stored at 55 °C for more than a few hours.
4. If using $Na_2HPO_4{\cdot}7H_2O$, take 21.6 g; for $Na_2HPO_4{\cdot}12H_2O$, use 28.8 g.
5. Comprehensive guidelines for preparation and storage of antibiotic solutions are provided in [49].
6. Ampicillin solution can be routinely frozen and thawed without any bad consequences if this drug is used for selection of resistant organisms. However, we have seen that repeated freezing and thawing cycles of ampicillin solution can change bactericidal activity [50].
7. Typically, a clonal culture is started from a single fresh colony. This routine is fully acceptable in the study of persisters. However, it is practically inevitable that such cultures are started from an uncertain number of bacteria of uncertain age. If grown overnight, these cultures may have different physiology at the moment when they are used for inoculation

of the test cultures. We have seen that persister frequency depends considerably on exact physiological parameters of the inoculum [29]. DMSO stocks allow starting all overnight cultures from a similar number of bacteria, which are in a controlled physiological condition, and decrease inconsistency.

8. Regular, autoclaved LB medium may be used for preparation of DMSO stocks.
9. Besides the strain's genotype, persister frequency depends on the growth medium and temperature, aeration, the fold of dilution of the inoculum, the growth phase of both the test culture, and the culture that was the source of inoculum [5, 29, 51]. Even minor details of the procedure such as the volume of the culture, shape of the culture vessel, angle of the test tube, and the radius of gyration of the rotary shaker have an effect on bacterial physiology [52] and may affect the outcome. We recommend to record and publish these details to enhance reproducibility of experiments.
10. Bactericidal activity of antibiotics is concentration dependent, which is manifested by minimum bactericidal activity (MBC) values and concentration-dependent killing curves. By definition, persisters can survive high concentrations of antibiotics for prolonged times. Therefore, high concentrations of antibiotics, at least 10× above the MIC, must be used to quantify the persister fraction [17]. Applying antibiotics at low concentrations, those close to MIC, characterizes antibiotic tolerance of the bulk of sensitive cells in a population, which should not be confused with the high-level antibiotic tolerance of persisters [53]. The antibiotic concentrations listed in this protocol have been routinely used in numerous papers in the field.
11. Aeration has a strong effect on bacterial physiology and survival of bacterial cells [52]. In this protocol, cultures are shaken during the antibiotic treatment, while typical MBC measurements are carried out in standing liquid cultures. If antibiotics are added to smaller aliquots taken from a culture, it is important whether these samples are further aerated or not.
12. Serial dilutions can be made into individual test tubes but it is convenient and common to use 96-well microtiter plates. 96-Well plates allow dilution of cultures using either a multichannel pipette or a slot pin replicator. In our lab, we routinely use a 5 μL slot 12-pin replicator strip (VP 451S5; V&P Scientific, Inc., San Diego, CA, USA) for making serial dilutions in the following setup.
    (a) 100 μL samples of culture are transferred to the wells of the first (A) row of a microtiter plate.
    (b) All wells of the other rows are filled with 95 μL of the culture medium.

(c) Samples of 5 μL are transferred from wells of row A to row B using the replicator strip.

(d) Pins of the replicator strip are decontaminated by immersing into bleach and rinsed twice with water. Between each step, the excess liquid is absorbed into paper towels. Finally, the pins are immersed into ethanol and flame sterilized.

(e) Transfer of 5 μL aliquots from the wells of the previous row to the next row is repeated. The replicator is bleached/flame sterilized between each round of dilution.

If using a multichannel pipette for making serial dilutions, we recommend 10× dilutions instead of 20× to reduce error.

13. Colony formation after bactericidal treatment is a result of regrowth of individual persister cells. We know that the rate and efficiency of such regrowth depend on the growth medium [5] and that many dormant cells remain nondividing and do not form colonies after plating [5, 6, 27]. Thus, the solid medium used for plating and the time of incubation before colony counting might supposedly affect persister count. Plating of the samples from the same antibiotic-treated culture onto several different solid media shows that unexpected effects are possible but generally, choice of the plating medium does not produce significant differences in persister count (*see* Fig. 2).

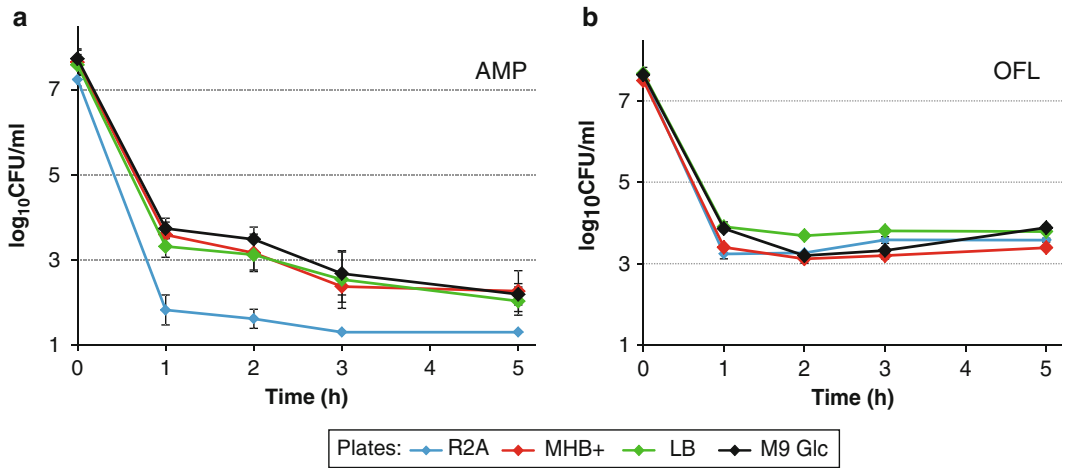

Fig. 2 Effect of the plating medium on persister count. Cultures of *E. coli* BW25113 were grown on a shaker at 37 °C. After 3 h of growth (time point 0 h), ampicillin, 100 μg/mL (AMP; **a**) or ofloxacin, 5 μg/mL (OFL; **b**) was added and incubation was continued. Samples of the same culture were plated on different solid media: LB agar (*green*), MHB+ agar (*red*), M9 agar supplemented with 0.2 % glucose (*black*) and R2A agar [55] (*blue*). Lower CFU counts on R2A agar after the treatment with ampicillin indicate less efficient cell recovery after plating compared to the other media. The values are averages of five AMP treatments and three OFL treatments. The error bars indicate the standard deviation

14. The exact number of viable cells in a sample is often hard to predict and, therefore, it is easier to spot plate all serial dilutions using a multichannel pipette. Colonies are counted from the largest dilution. If this spot contains only 1–2 colonies, counting colonies from the previous dilution may reduce error. The experimental error of this method is significant and we recommend plating serial dilutions of one sample in several repetitions. Five microliter volumes are suitable for spot plating and the agar surface must be dry to avoid merging of spots. To achieve better accuracy, results of spot plating can be used as preliminary data for spread plating an appropriate amount of a suitable dilution.
15. Individual persister cells resume growth over time [5]. That is equally true when regrowth happens on plates and colonies appear during a time period of several hours [4, 30]. Moreover, antibiotic treatment causes the delay of regrowth called post-antibiotic effect [54]. Thus, longer incubation of plates is expected to increase persister count. However, tests in our lab have shown that keeping LB agar plates at 37 °C for additional 24 h does not increase the number of colonies by more than 10 % and usually by much less (Hannes Luidalepp, unpublished).
16. Washing fluoroquinolone-treated bacteria before plating is required to avoid the carry-over of the drug. Fluoroquinolones bind to the bacterial outer surface and would interfere with accurate counting of viable bacteria. Bulk of the drug is removed with the culture medium and washing with PBS allows to get rid of the growth-inhibiting residue. Spinning down and washing the bacteria is not necessary nor recommend after incubation with Amp and other cell wall synthesis inhibitors, which promote bacterial lysis because the remaining tiny cell pellet could be easily lost. The residual Amp is diluted below MIC upon plating and has no effect on regrowth of colonies.
17. Flow cytometry is a powerful method for identification of different subpopulations of bacteria that coexist in the same culture. It can be used to discriminate between the nongrowing subpopulation, including persisters, and the growing cells. That is possible using inducible expression and subsequent dilution of GFP (or some other fluorescent protein). Cells are grown in the presence of inducer so that GFP accumulates in the cells. At the desired time, cells are transferred into a growth medium lacking the inducer. GFP content of dividing cells decreases twofold by dilution at every cell division. Nondividing cells will keep their initial (high) GFP content and can be distinguished from dividing cells using flow cytometry [27]. Persisters belong to this nondividing,

label retaining subpopulation of cells. However, also dead and VBNC cells fall into this category and it is impossible to distinguish between these groups using flow cytometry alone. For example, after a relatively long stationary phase in LB medium, only a small fraction of cells resume growth following the transfer into fresh medium [29]. Most of the label retaining cells never produce a colony on agar plates and thus do not meet the definition of persisters.

Acknowledgements

This work was supported by the European Regional Development Fund through the Center of Excellence in Chemical Biology and Estonian Science Foundation grant 8822.

References

1. Bigger JW (1944) Treatment of staphylococcal infections with penicillin by intermittent sterilization. Lancet 244(6320):497–500
2. Lewis K (2010) Persister cells. Annu Rev Microbiol 64:357–372
3. Keren I, Kaldalu N, Spoering A, Wang Y, Lewis K (2004) Persister cells and tolerance to antimicrobials. FEMS Microbiol Lett 230 (1):13–18
4. Balaban NQ, Merrin J, Chait R, Kowalik L, Leibler S (2004) Bacterial persistence as a phenotypic switch. Science 305(5690):1622–1625
5. Joers A, Kaldalu N, Tenson T (2010) The frequency of persisters in Escherichia coli reflects the kinetics of awakening from dormancy. J Bacteriol 192(13):3379–3384
6. Orman MA, Brynildsen MP (2013) Dormancy is not necessary or sufficient for bacterial persistence. Antimicrob Agents Chemother 57 (7):3230–3239
7. Epstein SS (2009) Microbial awakenings. Nature 457(7233):1083
8. Kussell E, Kishony R, Balaban NQ, Leibler S (2005) Bacterial persistence: a model of survival in changing environments. Genetics 169 (4):1807–1814
9. Ratcliff WC, Denison RF (2011) Bacterial persistence and bet hedging in Sinorhizobium meliloti. Commun Integr Biol 4(1):98–100
10. Fredriksson A, Nystrom T (2006) Conditional and replicative senescence in Escherichia coli. Curr Opin Microbiol 9(6):612–618
11. Adams KN, Takaki K, Connolly LE, Wiedenhoft H, Winglee K, Humbert O, Edelstein PH, Cosma CL, Ramakrishnan L (2011) Drug tolerance in replicating mycobacteria mediated by a macrophage-induced efflux mechanism. Cell 145(1):39–53
12. Wakamoto Y, Dhar N, Chait R, Schneider K, Signorino-Gelo F, Leibler S, McKinney JD (2013) Dynamic persistence of antibiotic-stressed mycobacteria. Science 339 (6115):91–95
13. Ezraty B, Vergnes A, Banzhaf M, Duverger Y, Huguenot A, Brochado AR, Su SY, Espinosa L, Loiseau L, Py B, Typas A, Barras F (2013) Fe-S cluster biosynthesis controls uptake of aminoglycosides in a ROS-less death pathway. Science 340(6140):1583–1587
14. Javid B, Sorrentino F, Toosky M, Zheng W, Pinkham JT, Jain N, Pan M, Deighan P, Rubin EJ (2014) Mycobacterial mistranslation is necessary and sufficient for rifampicin phenotypic resistance. Proc Natl Acad Sci U S A 111 (3):1132–1137
15. Martinez JL, Blazquez J, Baquero F (1994) Non-canonical mechanisms of antibiotic resistance. Eur J Clin Microbiol Infect Dis 13 (12):1015–1022
16. Keren I, Shah D, Spoering A, Kaldalu N, Lewis K (2004) Specialized persister cells and the mechanism of multidrug tolerance in Escherichia coli. J Bacteriol 186(24):8172–8180
17. Spoering AL, Lewis K (2001) Biofilms and planktonic cells of Pseudomonas aeruginosa

have similar resistance to killing by antimicrobials. J Bacteriol 183(23):6746–6751

18. Allison KR, Brynildsen MP, Collins JJ (2011) Metabolite-enabled eradication of bacterial persisters by aminoglycosides. Nature 473 (7346):216–220
19. Orman MA, Brynildsen MP (2013) Establishment of a method to rapidly assay bacterial persister metabolism. Antimicrob Agents Chemother 57(9):4398–4409
20. Maisonneuve E, Castro-Camargo M, Gerdes K (2013) (p)ppGpp controls bacterial persistence by stochastic induction of toxin-antitoxin activity. Cell 154(5):1140–1150
21. Nguyen D, Joshi-Datar A, Lepine F, Bauerle E, Olakanmi O, Beer K, McKay G, Siehnel R, Schafhauser J, Wang Y, Britigan BE, Singh PK (2011) Active starvation responses mediate antibiotic tolerance in biofilms and nutrient-limited bacteria. Science 334(6058):982–986
22. Dorr T, Lewis K, Vulic M (2009) SOS response induces persistence to fluoroquinolones in Escherichia coli. PLoS Genet 5(12):e1000760
23. Dorr T, Vulic M, Lewis K (2010) Ciprofloxacin causes persister formation by inducing the TisB toxin in Escherichia coli. PLoS Biol 8(2): e1000317
24. Goneau LW, Yeoh NS, Macdonald KW, Cadieux PA, Burton JP, Razvi H, Reid G (2014) Selective target inactivation rather than global metabolic dormancy causes antibiotic tolerance in uropathogens. Antimicrob Agents Chemother 58(4):2089–2097
25. Shah D, Zhang Z, Khodursky A, Kaldalu N, Kurg K, Lewis K (2006) Persisters: a distinct physiological state of *E. coli*. BMC Microbiol 6:53
26. Helaine S, Thompson JA, Watson KG, Liu M, Boyle C, Holden DW (2010) Dynamics of intracellular bacterial replication at the single cell level. Proc Natl Acad Sci U S A 107 (8):3746–3751
27. Roostalu J, Joers A, Luidalepp H, Kaldalu N, Tenson T (2008) Cell division in Escherichia coli cultures monitored at single cell resolution. BMC Microbiol 8:68
28. Gefen O, Gabay C, Mumcuoglu M, Engel G, Balaban NQ (2008) Single-cell protein induction dynamics reveals a period of vulnerability to antibiotics in persister bacteria. Proc Natl Acad Sci U S A 105(16):6145–6149
29. Luidalepp H, Joers A, Kaldalu N, Tenson T (2011) Age of inoculum strongly influences persister frequency and can mask effects of mutations implicated in altered persistence. J Bacteriol 193(14):3598–3605
30. Levin-Reisman I, Gefen O, Fridman O, Ronin I, Shwa D, Sheftel H, Balaban NQ (2010) Automated imaging with ScanLag reveals previously undetectable bacterial growth phenotypes. Nat Methods 7(9):737–739
31. Gill WP, Harik NS, Whiddon MR, Liao RP, Mittler JE, Sherman DR (2009) A replication clock for mycobacterium tuberculosis. Nat Med 15(2):211–214
32. Keren I, Minami S, Rubin E, Lewis K (2011) Characterization and transcriptome analysis of Mycobacterium tuberculosis persisters. MBio 2 (3):e00100–e00111
33. Canas-Duarte SJ, Restrepo S, Pedraza JM (2014) Novel protocol for persister cells isolation. PLoS One 9(2):e88660
34. Cuny C, Dukan L, Fraysse L, Ballesteros M, Dukan S (2005) Investigation of the first events leading to loss of culturability during *Escherichia coli* starvation: future nonculturable bacteria form a subpopulation. J Bacteriol 187 (7):2244–2248
35. Makinoshima H, Nishimura A, Ishihama A (2002) Fractionation of *Escherichia coli* cell populations at different stages during growth transition to stationary phase. Mol Microbiol 43(2):269–279
36. Oliver JD (2005) The viable but nonculturable state in bacteria. J Microbiol 43 Spec No:93–100
37. Buerger S, Spoering A, Gavrish E, Leslin C, Ling L, Epstein SS (2012) Microbial scout hypothesis, stochastic exit from dormancy, and the nature of slow growers. Appl Environ Microbiol 78(9):3221–3228
38. Ma C, Sim S, Shi W, Du L, Xing D, Zhang Y (2010) Energy production genes sucB and ubiF are involved in persister survival and tolerance to multiple antibiotics and stresses in *Escherichia coli*. FEMS Microbiol Lett 303 (1):33–40
39. Moyed HS, Bertrand KP (1983) hipA, a newly recognized gene of *Escherichia coli* K-12 that affects frequency of persistence after inhibition of murein synthesis. J Bacteriol 155 (2):768–775
40. Wolfson JS, Hooper DC, McHugh GL, Bozza MA, Swartz MN (1990) Mutants of *Escherichia coli* K-12 exhibiting reduced killing by both quinolone and beta-lactam antimicrobial agents. Antimicrob Agents Chemother 34 (10):1938–1943
41. Hofsteenge N, van Nimwegen E, Silander OK (2013) Quantitative analysis of persister fractions suggests different mechanisms of formation among environmental isolates of *E. coli*. BMC Microbiol 13:25
42. Wiuff C, Andersson DI (2007) Antibiotic treatment in vitro of phenotypically tolerant

bacterial populations. J Antimicrob Chemother 59(2):254–263

43. Vazquez-Laslop N, Lee H, Neyfakh AA (2006) Increased persistence in *Escherichia coli* caused by controlled expression of toxins or other unrelated proteins. J Bacteriol 188 (10):3494–3497
44. Lioy VS, Machon C, Tabone M, Gonzalez-Pastor JE, Daugelavicius R, Ayora S, Alonso JC (2012) The zeta toxin induces a set of protective responses and dormancy. PLoS One 7 (1):e30282
45. Tabone M, Lioy VS, Ayora S, Machon C, Alonso JC (2014) Role of toxin zeta and starvation responses in the sensitivity to antimicrobials. PLoS One 9(1):e86615
46. Tripathi A, Dewan PC, Barua B, Varadarajan R (2012) Additional role for the ccd operon of F-plasmid as a transmissible persistence factor. Proc Natl Acad Sci U S A 109 (31):12497–12502
47. Tripathi A, Dewan PC, Siddique SA, Varadarajan R (2014) MazF-induced growth inhibition and persister generation in *Escherichia coli*. J Biol Chem 289(7):4191–4205
48. Madar D, Dekel E, Bren A, Zimmer A, Porat Z, Alon U (2013) Promoter activity dynamics in the lag phase of *Escherichia coli*. BMC Syst Biol 7(1):136
49. Andrews JM (2001) Determination of minimum inhibitory concentrations. J Antimicrob Chemother 48(Suppl 1):5–16
50. Luidalepp H, Hallier M, Felden B, Tenson T (2005) tmRNA decreases the bactericidal activity of aminoglycosides and the susceptibility to inhibitors of cell wall synthesis. RNA Biol 2 (2):70–74
51. Udekwu KI, Parrish N, Ankomah P, Baquero F, Levin BR (2009) Functional relationship between bacterial cell density and the efficacy of antibiotics. J Antimicrob Chemother 63 (4):745–757
52. Kram KE, Finkel SE (2014) Culture volume and vessel affect long-term survival, mutation frequency, and oxidative stress of *Escherichia coli*. Appl Environ Microbiol 80 (5):1732–1738
53. Keren I, Wu Y, Inocencio J, Mulcahy LR, Lewis K (2013) Killing by bactericidal antibiotics does not depend on reactive oxygen species. Science 339(6124):1213–1216
54. MacKenzie FM, Gould IM (1993) The post-antibiotic effect. J Antimicrob Chemother 32 (4):519–537
55. Reasoner DJ, Geldreich EE (1985) A new medium for the enumeration and subculture of bacteria from potable water. Appl Environ Microbiol 49(1):1–7

Chapter 4

Optimized Method for Measuring Persistence in *Escherichia coli* with Improved Reproducibility

F. Goormaghtigh and L. Van Melderen

Abstract

Monitoring persister cells can be extremely difficult due to their transient and stochastic nature, their low abundance, and their resemblance to Viable But Non-Culturable Cells (VBNCs). To date, the predominant method consists of determining the survival rate of a bacterial population after antibiotic treatment as a function of time or antibiotic concentration. Unfortunately, this method is limited, as it shows high levels of dispersion of the data around the mean, making interpretation difficult. Furthermore, additional reproducibility problems arise from the lack of a standard method, different research groups using different protocols. Here, we describe a standard and optimized method for monitoring *E. coli* persister cells at the population level allowing for maximal reproducibility.

Keywords: Persister cells, Persistence assay, Biphasic killing curve

1 Introduction

One of the first and most widely used approaches to study persistence is to quantify the persistence fraction, through survival rate calculations, in different bacterial populations so as to compare, for instance, the effect of gene overexpression or mutation, or that of a specific antibiotic treatment [1–3]. Survival fractions are calculated by measuring the bacterial concentration (CFU/mL) after different periods of exposure to antibiotics and dividing them by the initial bacterial concentration prior to antibiotic treatment. This results in a biphasic killing curve, showing the survival fraction of bacteria as a function of time of exposure to antibiotics (Fig. 1). On the one hand, this method frees the process up from the various issues inherent in the instability of the persistence phenotype and in the resemblance of persistent cells to Viable But Non-Culturable Cells (VBNCs). VBNCs are cells that survive antibiotic treatment, stain as live in LIVE/DEAD assays, but are not capable of forming a colony on standard media after removal of the antibiotic. It has

Jan Michiels and Maarten Fauvart (eds.), *Bacterial Persistence: Methods and Protocols*,
Methods in Molecular Biology, vol. 1333, DOI 10.1007/978-1-4939-2854-5_4,

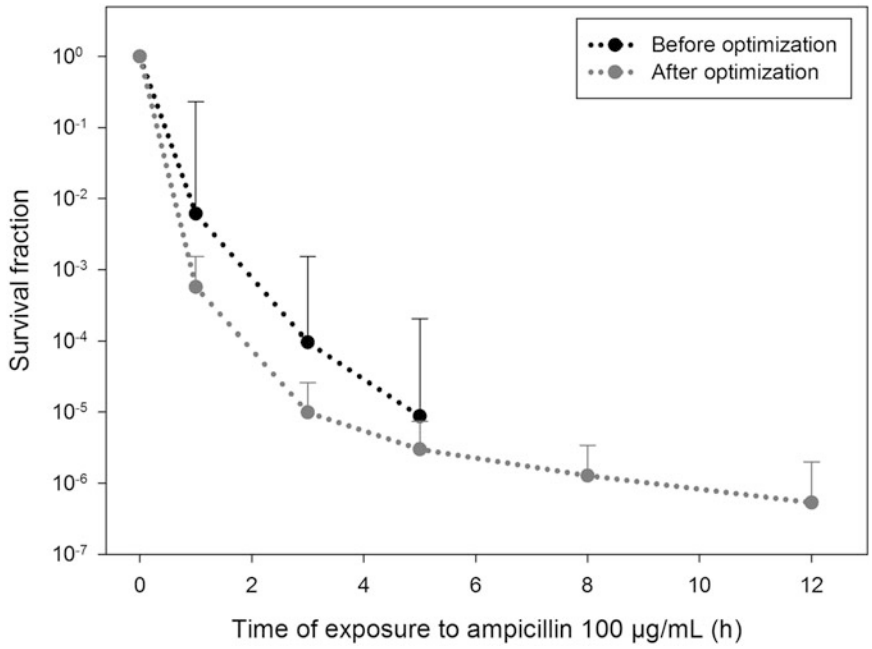

Fig. 1 Typical biphasic killing curve of *E. coli* MG1655 using a non-optimized method (*black* symbols) and the optimized method (*grey* symbols). Ampicillin (100 µg/mL) was added to the culture at time 0 h. *Black* symbols are calculated as the geometric mean of seven independent replicates. *Grey* symbols are calculated as the geometric mean of 18 independent replicates. Error bars are geometric standard deviations and are represented above the mean due to the asymmetry of the *Y*-axis logarithmic scale. The non-optimized method (*black* symbols) differs from the optimized method for different parameters. Bacteria are grown in LB Lennox Broth (Invitrogen) complex medium (vs. MOPS balanced medium), pre-cultures are performed for 16 $\pm$ 1 h and culture treatment occurs directly after dilution of the pre-culture to OD_{600} 0.1 in fresh medium (vs. treatment occurring at OD_{600} 0.3)

been shown that exponential phase cultures of *E. coli* MG1655 treated with ampicillin contain 100-fold more VBNCs than persisters [4]. On the other hand, reproducibility problems are detected using this method as shown by the large standard deviations (Fig. 1, black curve), making it difficult to interpret the data and even more difficult to compare data collected from different research groups [5, 6].

In light of these issues, experiments were carried out to identify the main parameters affecting reproducibility of persistence measurements. These parameters were then optimized by minimizing variability of persistence measurements. The key issues of the optimization procedure are to provide bacteria with an optimally balanced medium, ensuring that metabolic energy requirements are met at any time of the culture (while in exponential growth phase). Moreover, treatment should be carried out in cultures reaching mid-exponential phase, ensuring steady-state growth in the bacterial culture at treatment time. The main advantage of cultures in steady-state growth is the high reproducibility of this

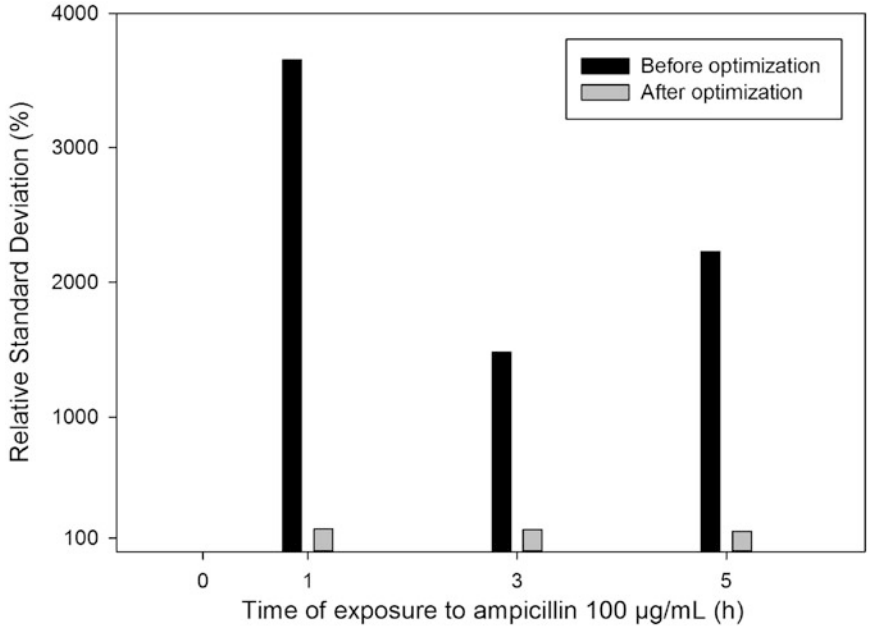

Fig. 2 Measurement of variability of a typical killing curve of *E. coli* MG1655 strain after ampicillin treatment using a non-optimized method and the optimized method for persistence assays. The relative standard deviation (geometric standard deviation divided by the geometric mean) is plotted as a function of time of exposure to ampicillin. The non-optimized method (*black* symbols) differs from the optimized method for different parameters. Bacteria are grown in LB Lennox Broth (Invitrogen) complex medium (vs. MOPS balanced medium), pre-cultures are performed for 16 ± 1 h and culture treatment occurs directly after dilution of the pre-culture to OD_{600} 0.1 in fresh medium (vs. treatment occurring at OD_{600} 0.3)

physiological state [7]. As shown in Fig. 2, the method optimization led to a 10- to 25-fold decrease in variability for *E. coli* MG1655 treated with ampicillin at a concentration of 100 µg/mL.

To confirm this method, it has been used to study persistence for *E. coli* MG1655 to ofloxacin treatment at a concentration of 5 µg/mL. In this case, the method optimization led to a 3- to 12-fold decrease in the measurement variability (Fig. 3).

2 Materials

1. 10× MOPS salt solution: 400 mL of 1.0 M potassium morpholinopropane sulfonate (MOPS) pH 7.4, 40 mL of 1.0 M *N*-Tris(hydroxymethyl)-methyl glycine (Tricine) pH 7.4, 10 mL of 0.01 M $FeSO_4$, 50 mL of 1.90 M NH_4Cl, 10 mL of 0.276 M K_2S0_4, 10 mL of 5.0×10^{-4} M $CaCl_2$, 10 mL of 0.528 M $MgCl_2$, 100 mL of 5.0 M NaCl, 10 mL Micronutrients solution, 360 mL glass-distilled water. Prepare MOPS, Tricine and $FeSO_4$ solutions freshly. Adjust MOPS and

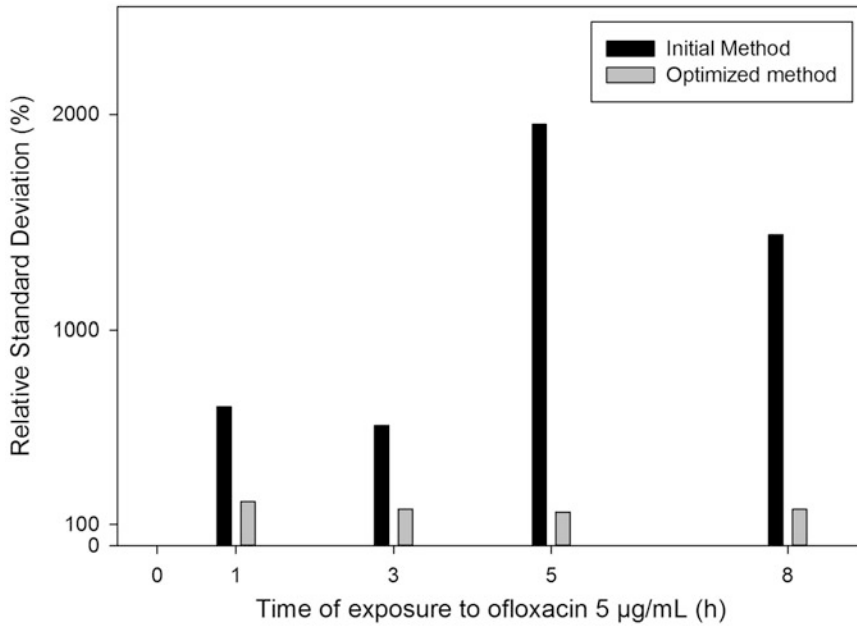

Fig. 3 Measurement of variability of a typical killing curve of *E. coli* MG1655 strain after ofloxacin treatment using a non-optimized method and the optimized method for persistence assays. The relative standard deviation (geometric standard deviation divided by the geometric mean) is plotted as a function of time of exposure to ofloxacin. The non-optimized method (*black* symbols) differs from the optimized method for different parameters. Bacteria are grown in LB Lennox Broth (Invitrogen) complex medium (vs. MOPS balanced medium), pre-cultures are performed for 16 ± 1 h and culture treatment occurs directly after dilution of the pre-culture to OD_{600} 0.1 in fresh medium (vs. treatment occurring at OD_{600} 0.3)

Tricine solutions to pH 7.4. Mix the different solutions in the given order to prevent precipitation of various salts. The composition of the final medium is shown in Tables 1 and 2. For further information, see [8]. Filter sterilize (disposable filter units, 0.20 µm) this solution, using a filter pre-rinsed with a small volume (10 mL) of the solution. This sterile 10× medium concentrate lacks a carbon source and phosphate (which would precipitate at this concentration), it may be stored for long periods (at least 2 years) at −20 °C.

2. Micronutrients solution: 3×10^{-6} M $(NH_4)_6(MO_7)_{24}$, 4×10^{-4} M H_3BO_3, 3×10^{-5} M $CoCl_2$, 10^{-5} M $CuSO_4$, 8×10^{-5} M $MnCl_2$, 10^{-5} M $ZnSO_4$.
3. MOPS-based culture medium 100 mL: 10 mL 10× MOPS salt solution, 1 mL 0.132 M KH_2PO_4, 10 mL 10× carbon source, 79 mL autoclaved distilled water. Aseptically mix the different solutions (*see* **Note 1**). Add 70 mL water first to prevent phosphate from precipitating in contact with the 10× MOPS salt solution. The final pH of the medium should be close to 7.2. Store at 4 °C.

Table 1
Composition of the 10× MOPS-based salt solution

	Stock solution (M)	Volume (mL)	Final concentration (M)
Potassium MOPS	1 (pH 7.4)	400	0.4
Tricine	1 (pH 7.4)	40	4×10^{-2}
$FeSO_4$	0.01	10	1×10^{-4}
NH_4Cl	1.9	50	9.5×10^{-2}
K_2SO_4	0.276	10	2.76×10^{-3}
$CaCl_2$	5×10^{-4}	10	5×10^{-6}
$MgCl_2$	0.528	10	5.28×10^{-3}
NaCl	5	100	0.5
Micronutrients	*See* Table 2	10	*See* Table 2
Distilled water		360	

First column represents the chemical species present in the medium. Second column represents the concentration of stock solutions. Third column represents the volume of stock solution necessary for 1 L of 10× MOPS-based salt solution. Last column represents the final concentration of these chemical species in 10× MOPS-based salt solution

Table 2
Composition of the micronutrient solution

	Stock solution (M)	Final concentration in MOPS-based salt solution (M)
$(NH_4)_6Mo_7O_{24}$	3×10^{-6}	3×10^{-8}
H_3BO_3	4×10^{-4}	4×10^{-6}
$CoCl_2$	3×10^{-5}	3×10^{-7}
$CuSO_4$	1×10^{-5}	1×10^{-7}
$MnCl_2$	8×10^{-5}	8×10^{-7}
$ZnSO_4$	1×10^{-5}	1×10^{-7}

First column represents the chemical species present in the micronutrient solution. Second column represents concentration in the micronutrient solution. Third column represents the final concentration of these chemical species in 10× MOPS-based salt solution

4. 10× Carbon source solution: prepare a tenfold concentrated carbon source solution. A common example would be a 4 % glucose solution. In this case, dissolve 4 g glucose in 100 mL deionized water, and filter sterilize using disposable filter units with a 0.20 μm pore size.

5. LB medium: dissolve 10 g tryptone, 5 g yeast extract and 10 g NaCl in 1 L deionized water, and autoclave for 30 min at 121 °C.
6. LB agar plates: Dissolve 15 g agar in 1 L LB medium. Autoclave for 30 min at 121 °C. Allow the medium to cool to 50–60 °C before pouring in Petri dishes. Finally, add 5–6 glass beads (±5 mm diameter) to each plate.
7. Antibiotic stock solutions: 100 mg/mL ampicillin, 5 mg/mL ofloxacin, 1 mg/mL ciprofloxacin, and 25 mg/mL tobramycin. Dissolve 1 mg ciprofloxacin, 100 mg ampicillin and 25 mg tobramycin in 1 mL deionized water, or 5 mg ofloxacin in 1 mL acid water (pH 2–5) and filter sterilize the solutions. Antibiotics should be kept at 4 °C and, regarding ampicillin, no longer than 7 days. Moreover, when using ampicillin in persistence assays, it should be kept in mind that a possible regrowth after a long-term incubation at 37 °C (24–48 h) can occur due to ampicillin degradation.
8. Dilution tubes: add 900 μL of $MgSO_4$ 10^{-2} M to each dilution tube.
9. Bacterial strain: *E. coli* MG1655 (*F⁻ λ⁻ ilvG-rfb-50 rph-1*) [9] was used in all experiments.

3 Methods

3.1 Day I: Preparation of Medium and Cultures

1. Calculate the number of Petri dishes needed and pour melted LB agar into the appropriate number of Petri dishes. Dry the plates for 20–40 min and add 5–6 glass beads in LB agar plates. Store at 4 °C.
2. Prepare fresh MOPS-based culture medium with the appropriate carbon source.
3. Prepare an appropriate number of dilution tubes containing 900 μL of $MgSO_4$ 10^{-2} M.
4. Pick an isolated bacterial colony and inoculate 15 mL MOPS-based culture medium in a 100 mL flask. Consider making three independent overnight cultures for each strain and treatment of interest. Incubate pre-culture for 16 ± 1 h (*see* **Note 2**) at 37 °C with shaking (0.36 × *g*) (*see* **Note 3**).

3.2 Day II: Persistence Assay

1. 100 mL Culture flasks containing 15 mL fresh MOPS-based culture medium are pre-warmed at 37 °C for 30 min.
2. The OD_{600} of the pre-cultures is measured and dilutions are made in pre-warmed medium to obtain an initial OD_{600} of 0.01 (corresponding to around 3×10^7 bacteria/mL). Cultures are incubated at 37 °C with shaking (0.36 × *g*)

(*see* **Note 3**). Each pre-culture should be used to inoculate two culture flasks (with and without antibiotic).

3. When reaching an OD_{600} of 0.5 (around $1.5–2 \times 10^8$ bacteria/mL) (typically after 4 h30 of incubation), antibiotic is added to the culture flasks (except for the control flasks) (*see* **Note 4**).
4. To determine CFU/mL, 250 µL aliquots are withdrawn from the cultures at different time points, typically 0 (before addition of the antibiotic), 1, 3, 5, 8, 12, and 24 h. It is important to withdraw small volumes compared to the total volume so as to ensure a constant aeration rate (*see* **Note 3**). Samples are serially diluted in $MgSO_4$ 10^{-2} M (tenfold dilutions by transferring 100 µL in 900 µL). One hundred µL of diluted sample is plated and plates are incubated for 16 h at 37 °C (*see* **Note 5**).

3.3 Day III: CFU Counting

Count the number of colonies on plates containing between 10 and 600 colonies (*see* **Note 6**). In the presence of multiple colony morphologies, different morphology types should be counted separately and a few colonies of each morphology type should be streaked and tested on antibiotic plates to ensure that these colonies are formed of viable bacteria that are still sensitive to the given antibiotic.

4 Mathematical Analysis

4.1 Counting the Survival Fraction

Persistence is measured as the survival fraction of the population after at least 5 h of exposure to antibiotics (*see* **Note 7**). The survival fraction is calculated by dividing the number of CFU/mL at a given time by the number of CFU at time 0 (before antibiotic treatment). If multiple morphologies exists, the survival fraction is calculated with the total number of bacteria able to regrow on LB agar and unable to grow on LB antibiotic.

4.2 Graphical Representation: The Biphasic Killing Curve

1. Biphasic killing curves are often used to represent data collected from persistence assays. A biphasic killing curve consists of plotting the survival fraction of a bacterial population as a function of time of exposure to a given antibiotic (*see* Fig. 1). It is important to note that different time points should not be joined by solid lines, but by dotted lines, given that the curve profile might not be linear between two data points.
2. The Y-axis of a biphasic killing curve is plotted on a logarithmic scale, because of the exponential killing rate during the first hours of antibiotic treatment (corresponding to the killing of the bulk of the population). Therefore, each set of replicates (A_1, A_2, …, A_n) should be represented by means of its

geometric mean (μ_g) and its geometric standard deviation (σ_g) which are calculated as follows:

$$\mu_g = \sqrt[n]{\prod_{i=1}^{n} A_i}$$

$$\sigma_g = \exp\left(\sqrt{\frac{\sum_{i=1}^{n}\left(\ln A_i - \ln \mu_g\right)^2}{n}}\right)$$

To simplify calculations, the data are often transformed by extracting their logarithm. Geometric mean and geometric standard deviation are then calculated, based on the arithmetic mean and arithmetic standard deviation of the transformed data, as follows:

$$\mu_g = \exp(\text{arithmetic.mean}\{\ln A_{i\to n}\})$$

$$\sigma_g = \exp(\text{arithmetic.standard.deviation}\{\ln A_{i\to n}\} + \text{arithmetic.mean}\{\ln A_{i\to n}\})$$

It is important to note that, due to the asymmetry of the Y-axis log-scale, standard deviation will not have the same length above and under the mean. One could choose to only represent the standard deviation above the mean and mention it in the legend.

4.3 Statistical Analysis

Comparison of different persister fractions should be done using statistic tests on the geometric mean of the survival fraction after at least 5 h of antibiotic exposure (*see* **Note 7**). Parametric tests (e.g. Student's test or ANOVA) should be used if the replicates follow a Gaussian distribution and if the samples have similar variances. Otherwise, non-parametric tests (e.g. Mann–Whitney test or Kruskal–Wallis test) should be used to increase the power of the tests.

5 Notes

1. The benefits of using a chemically defined and balanced medium (MOPS culture medium) instead of a complex medium (e.g. Lennox Broth or Mueller-Hinton) are primarily due to the steady-state growth it allows, ensuring that metabolic energy requirements are met at any time of the culture, which is far from being the case with Lennox Broth medium for instance. In the particular case of Lennox Broth medium, steady-state growth ceases at an OD_{600} of 0.3, when the growth rate slows down and cell mass decreases due to a lack of utilizable carbon source [7].

2. The age of the pre-culture is of great importance. It has been shown that the frequency of persistence is highly dependent on the age of the inoculum. For instance, increasing the length of the pre-culture stationary phase from 4 to 12 h leads to a 1000-fold increase of the persistence frequency in *E. coli* K-12 MG1655 [10]. Persistence assays using different pre-culture growth times should therefore be compared carefully, knowing there is an unknown bias between the sets of data. Moreover, when working with cultures with different growth rates, the time of pre-culture should be adapted so as to ensure identical stationary phase lengths for every culture.
3. The aeration rate has been shown to influence significantly the persistence frequency [5]. Maintaining a constant aeration could therefore substantially lower the measurement variability in persistence assays.
4. Cultures should be treated in mid-exponential phase, so as to ensure treating bacteria in steady-state growth. Treating at higher bacterial concentrations (OD_{600} 0.5–0.8) will significantly improve the sensitivity of the assay. With an initial number of bacteria of the order of 10^8, the number of CFU plated with 100 μL culture sample is of approximately 10, knowing that the persistence frequency is of about $1{:}10^6$. Therefore, treating at higher bacterial concentrations will improve the accuracy and reduce the measurement variability in persistence assays.
5. Some protocols recommend that culture samples should be washed and resuspended in $MgSO_4$ 10^{-2} M prior performing serial tenfold dilutions and plating the samples, in order to eliminate the antibiotic [11]. We compared persistence frequency obtained with and without a wash/resuspension step for *E. coli* MG1655 strain treated with ampicillin 100 μg/mL. For dilutions equal or greater than 10^{-1}, no differences between both methods were observed. However, when plating non-diluted samples, significant differences between both methods were detected. Therefore the wash/resuspension step can be omitted only for diluted samples.
6. Persistence being a low frequency phenomenon, in some cases, the number of CFU per plate can be very low, even in non-diluted samples. Therefore, it is necessary to count even low numbers of CFU per plate. When doing so, the measurement variability will substantially raise, reinforcing the importance of making multiple independent replicates and performing the appropriate statistical analysis, notably by establishing the variance of the data.
7. Upon antibiotic treatment, the bulk of the population is killed within a few hours. After 3–5 h, killing rate decreases and

surviving bacteria are considered as persisters. Therefore, the survival fraction of bacteria after 5 h of exposure to antibiotics represents an accurate estimate of the persistence frequency of this population.

Acknowledgement

Research in Van Melderen's lab was funded by FNRS (FRSM 3.4621.12), the Interuniversity Attraction Poles Programme initiated by the Belgian Science Policy Office (MICRODEV), the Fonds Jean Brachet and the Fondation David and Alice Van Buuren. F.G. was supported by the FRIA.

References

1. Keren I, Kaldalu N, Spoering A, Wang Y, Lewis K (2004) Persister cells and tolerance to antimicrobials. FEMS Microbiol Lett 230 (1):13–18
2. Balaban NQ, Merrin J, Chait R, Kowalik L, Leibler S (2004) Bacterial persistence as a phenotypic switch. Science 305 (5690):1622–1625. doi:10.1126/science.1099390
3. Joers A, Kaldalu N, Tenson T (2010) The frequency of persisters in Escherichia coli reflects the kinetics of awakening from dormancy. J Bacteriol 192(13):3379–3384. doi:10.1128/JB.00056-10
4. Orman MA, Brynildsen MP (2013) Establishment of a method to rapidly assay bacterial persister metabolism. Antimicrob Agents Chemother 57(9):4398–4409. doi:10.1128/AAC.00372-13
5. Korch SB, Henderson TA, Hill TM (2003) Characterization of the hipA7 allele of Escherichia coli and evidence that high persistence is governed by (p)ppGpp synthesis. Mol Microbiol 50(4):1199–1213
6. Hansen S, Lewis K, Vulic M (2008) Role of global regulators and nucleotide metabolism in antibiotic tolerance in Escherichia coli. Antimicrob Agents Chemother 52 (8):2718–2726. doi:10.1128/AAC.00144-08
7. Sezonov G, Joseleau-Petit D, D'Ari R (2007) Escherichia coli physiology in Luria-Bertani broth. J Bacteriol 189(23):8746–8749. doi:10.1128/JB.01368-07
8. Neidhardt FC, Bloch PL, Smith DF (1974) Culture medium for enterobacteria. J Bacteriol 119(3):736–747
9. Blattner FR, Plunkett G 3rd, Bloch CA, Perna NT, Burland V, Riley M, Collado-Vides J, Glasner JD, Rode CK, Mayhew GF, Gregor J, Davis NW, Kirkpatrick HA, Goeden MA, Rose DJ, Mau B, Shao Y (1997) The complete genome sequence of Escherichia coli K-12. Science 277(5331):1453–1462
10. Luidalepp H, Joers A, Kaldalu N, Tenson T (2011) Age of inoculum strongly influences persister frequency and can mask effects of mutations implicated in altered persistence. J Bacteriol 193(14):3598–3605. doi:10.1128/JB.00085-11
11. Maisonneuve E, Shakespeare LJ, Jorgensen MG, Gerdes K (2011) Bacterial persistence by RNA endonucleases. Proc Natl Acad Sci U S A 108(32):13206–13211. doi:10.1073/pnas.1100186108

Chapter 5

A Microplate-Based System as In Vitro Model of Biofilm Growth and Quantification

Ilse Vandecandelaere, Heleen Van Acker, and Tom Coenye

Abstract

We describe a 96-well microtiter plate-based system as an in vitro model for biofilm formation and quantification. Although in vitro assays are artificial systems and thus significantly differ from in vivo conditions, they represent an important tool to evaluate biofilm formation and the effect of compounds on biofilms. Stainings to evaluate the amount of biomass (crystal violet staining) and the number of metabolically active cells (resazurin assay) are discussed and specific attention is paid to the use of this model to quantify persisters in sessile populations.

Keywords: Biofilms, In vitro model system, Microtiter plate, Crystal violet staining, Resazurin assay, Persisters

1 Introduction

Biofilms are often unwanted and cause severe problems in industrial and biomedical settings [1, 2]. It has been estimated that up to 80 % of all infections worldwide are biofilm-related and antibiotic treatments often fail due to the presence of biofilms [3, 4]. One of the mechanisms thought to contribute to treatment failure is the presence of a small subpopulation of hypertolerant persister cells [5]. Despite their clinical importance, the mechanisms involved in persistence in biofilms are still largely unknown. In vitro biofilm model systems are indispensable to better understand the mechanisms of biofilm formation and resistance [6]. Growing biofilms in microtiter plates (MTP) is a widely used system which has some major advantages. Firstly, it is a user-friendly method which can be used in most (if not all) microbiology laboratories [7, 8]. Secondly, the MTP-based system is cheap as only small volumes of growth media and/or test substances are required. Thirdly, the effect of several substances (e.g. antibiotics) on biofilms can be determined in a high-throughput fashion [6]. Finally, the system is very flexible as

Jan Michiels and Maarten Fauvart (eds.), *Bacterial Persistence: Methods and Protocols*, Methods in Molecular Biology, vol. 1333, DOI 10.1007/978-1-4939-2854-5_5,

parameters such as growth media and growth temperature can be easily modified [6].

As MTP-based assays are closed systems, the environment in the well (e.g. nutrients, waste products) will change during biofilm formation and growth [9], and this closed system does not generally reflect the in vivo conditions (e.g. shear stress under flow conditions) [10]. Importantly, the techniques used to grow biofilms in MTP require thorough standardization as, for instance, an air bubble can already cause serious artifacts in the biofilm [6, 11]. Although culturing biofilms in a 96-well MTP has some disadvantages, this technique has provided a tremendous increase in our knowledge about biofilm formation [6, 12, 13].

The amount of biofilm formed can be evaluated by several methods. The number of cells can be determined by conventional plate counts [8]. However, this method is labor-intensive and fails in recovering viable but nonculturable cells [6]. The total biofilm biomass and the number of metabolically active biofilm cells can be determined by specific stainings. Crystal violet (CV) is a basic dye which binds to negatively charged cell surface molecules and polysaccharides in the extracellular matrix [13]. Since both dead and living cells as well as parts of the extracellular matrix, are stained, the total biofilm biomass is measured [12]. Other assays can be used to determine the number of metabolically active cells in a biofilm. For instance, 2,3-bis (2-methoxy-4-nitro-5-sulfophenyl)-5-[(phenylamino)carbonyl]-2H-tetrazolium hydroxide (XTT) and fluorescein diacetate (FDA) are converted, by metabolically active cells, to formazan and fluorescein, respectively. The absorbance or fluorescence generated in this way is proportional to the number of metabolically active cells [12, 13]. Another viability assay is based on the reduction of resazurin to resofurin. The latter is fluorescent and the fluorescence can be measured by a MTP reader [13, 14].

In this protocol, the formation of biofilms in 96-well MTP is described. It is also possible to grow biofilms in 6-well, 12-well or 24-well plates on, e.g. silicon disks [6, 15–19] but the description of these protocols is beyond the scope of the current chapter. We also describe CV and resazurin assays to measure biofilm formation and metabolic activity, respectively. Moreover, the quantification of persister cells in biofilms is discussed.

2 Materials

2.1 General Equipment

1. Sterile 96-well MTP (round-bottomed) (*see* **Notes 1** and **2**).
2. Pipette (sterile tips of 100 and 1000 µl), automatic pipette (set at a dispensing volume of 100 µl; sterile tips of 5 ml), and/or multichannel pipette (sterile tips of 100 µl). Sterile pipette of 10 ml (*see* **Note 2**).

3. Sterile Petri dishes (with a diameter of 90 mm) (*see* **Note 2**).
4. Sterile MilliQ water (*see* **Note 3**). Store at room temperature.
5. Sterile physiological saline (PS): 9 g NaCl per liter MilliQ (*see* **Note 3**). Store at room temperature.
6. Centrifuge set at 4000 × *g*, at room temperature.

2.2 Biofilm Formation

1. Spectrophotometer to measure absorbance (λ: 590 nm).
2. Sterile liquid culture medium: bottle of 40 ml (to grow starting culture) and tubes of 10 ml (to prepare the working suspension for biofilm inoculation) (*see* **Note 3**). Store at 4 °C.

2.3 Crystal Violet and Resazurin Staining

1. MTP reader to measure absorbance (λ: 590 nm) and fluorescence (λ_{ex}: 560 nm; λ_{em}: 590 nm).
2. Sterile (*see* **Note 2**) falcon tubes to store the stock solutions of resazurin and CV, and sterile glass bottles to store methanol and acetic acid.
3. Centrifuge set at 500 × *g*, at room temperature.
4. 99 % Methanol. Store at room temperature.
5. Crystal Violet (CV) solution. Concentration of stock solution can vary depending on the manufacturer, e.g. the concentration of CV (ProLab Diagnostics, Richmond Hill, ON, Canada), is 0.5 %. Store at room temperature.
6. 33 % Acetic acid: 33 ml 100 % acetic acid, 66 ml MilliQ water. Prepare in a sterile glass bottle and store at room temperature.
7. Resazurin stock solution (commercially available as ready-to-use solution): Prepare aliquots of 2.1 ml in sterile falcon tubes and protect from light (e.g. using aluminum foil). Store at −20 °C.

2.4 Biofilm Removal

1. Sonicator bath, set at 40 kHz.
2. Vortex with 96-well MTP adapter or rotator.
3. Sterile falcon tubes to collect sessile cells.
4. Sterile sealing tape.

2.5 Plate Counting

1. Warm water bath, temperature set at 48 °C to store the growth medium (*see* **Note 4**).
2. Sterile tubes filled with 9 ml PS.
3. Growth medium (*see* **Note 5**).

3 Methods

Carry out all procedures at room temperature in a sterile environment (*see* **Note 6**). The protocol below is suited for the growth of most aerobic bacteria (*see* **Note 7**).

3.1 Biofilm Formation

1. Culture the bacterial cells in liquid medium in a shaking warm water bath (200 rpm) for 24 h at optimal growth temperature (*see* **Note 8**).
2. After 24 h, dilute the cell suspension to 10^7–10^8 CFU/ml (*see* **Note 9**).
3. Fill row A (top) and row H (bottom) of the 96-well MTP with sterile medium (*see* **Note 10**).
4. Add 100 μl of the diluted cell suspension to all wells of row B to G (*see* **Note 11**).
5. Incubate the MTP for 4 h at the optimal growth temperature to allow cell adhesion (*see* **Note 12**).
6. Remove the supernatant (containing nonadherent cells) (*see* **Note 13**).
7. Add 100 μl of sterile PS to each well.
8. Remove the PS (Fig. 1).
9. Add 100 μl of fresh sterile medium to each well and incubate for an additional 20 h at the optimal growth temperature (*see* **Note 14**).
10. Most procedures to evaluate biofilm formation start with a rinsing step (*see* **Note 15a**, **b**). The supernatant is removed, 100 μl of PS is added to each well and the PS is subsequently removed.

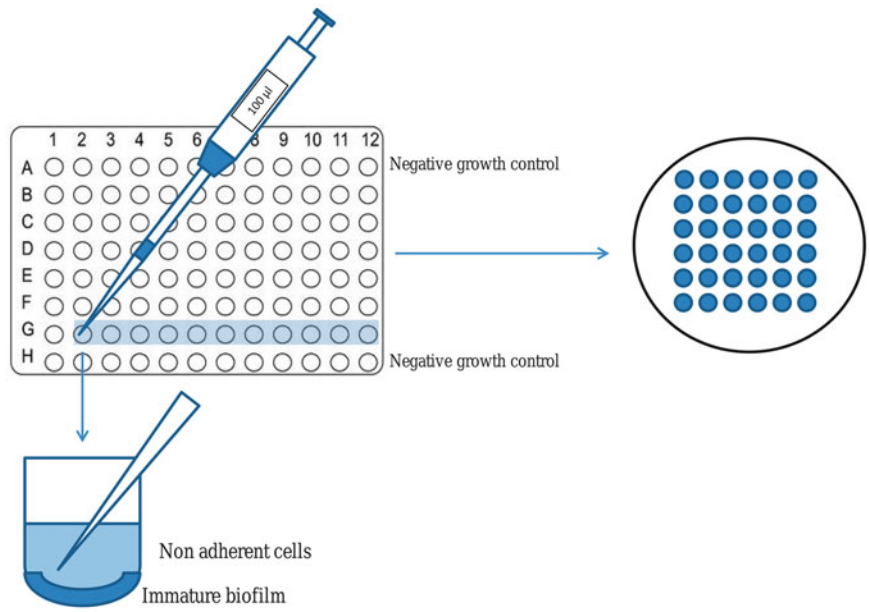

Fig. 1 The supernatant (containing nonadherent cells) is removed after the adhesion phase. Thereby, it is important not to touch or to disrupt the immature biofilm

3.2 Crystal Violet Staining

1. Add 100 µl of 99 % methanol to each well to fix the biofilms.
2. Incubate the MTP at room temperature for 15 min.
3. Remove the methanol (*see* **Note 16**).
4. Incubate the MTP without lid at room temperature to allow complete evaporation of the methanol (*see* **Note 17**).
5. Add 100 µl of the CV solution to each well and incubate the MTP at room temperature for 20 min (*see* **Note 18**).
6. Remove the CV by extensive washing under running tap water (*see* **Note 19**).
7. Add 150 µl of 33 % acetic acid to each well in order to release bound CV.
8. Incubate the MTP on a rotator (500 × *g*) for at least 20 min (*see* **Note 20**).
9. Measure the absorbance of all wells at $\lambda = 590$ nm (Fig. 2) (*see* **Notes 21** and **22**).

3.3 Resazurin Assay

1. Thaw a falcon tube containing the resazurin stock solution (2.1 ml) (*see* **Note 23**).
2. Dilute this solution 1/6 with sterile PS (*see* **Note 24**).
3. Add 120 µl to each well of a 96-well MTP.
4. Incubate the MTP (protected from light) at optimal incubation temperature for an appropriate period of time (*see* **Note 25**).

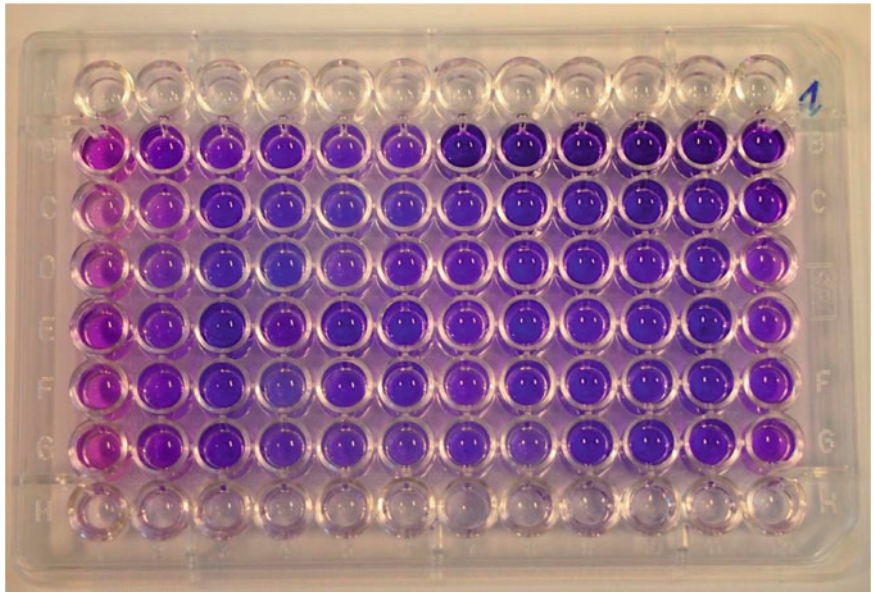

Fig. 2 Photograph of a 96-well MTP in which biofilms were stained by crystal violet. Top and bottom rows represent negative growth controls

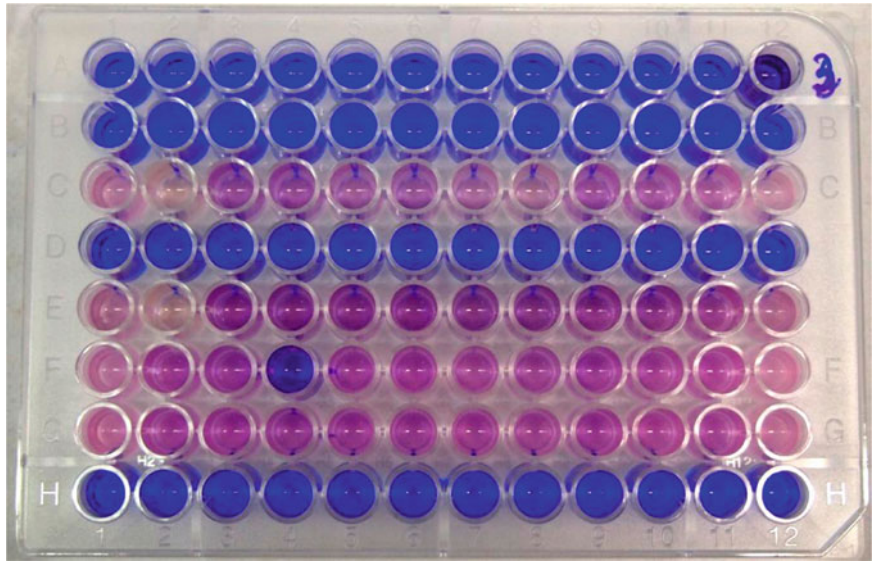

Fig. 3 Photograph of a 96-well MTP in which the metabolically activity of the biofilm cells was evaluated using a resazurin assay. Top and bottom rows represent negative growth controls

5. Measure the fluorescence (λ_{ex}: 560 nm and λ_{em}: 590 nm) (*see* **Note 26**) (Fig. 3).
6. Calculate the net average fluorescent values (*see* **Note 27**).

3.4 Biofilm Removal

1. To quantify persisters (*see* **Note 28**), remove the supernatant of mature biofilms.
2. Treat the biofilms by adding 120 μl of an antibiotic solution (*see* **Notes 29–31**).
3. After an appropriate amount of time, remove the antibiotic solution and wash the biofilms with sterile PS.
4. Add 100 μl of PS to each well and cover the MTP using sealing tape.
5. Put the MTP on the vortex for 5 min at a shaking speed of 900 rpm (*see* **Note 32**).
6. Afterwards, put the MTP into the sonicator bath for an additional 5 min (*see* **Notes 33** and **34**).
7. Remove the tape from the MTP and quantitatively transfer the cells to a sterile falcon tube using a sterile pipette.
8. Add 100 μl of PS to the wells and repeat sonication and vortexing (**steps 5** and **6**).
9. Transfer the cell suspensions from the wells to the falcon tube. To ensure complete removal of the biofilms, pipette up and down before transferring the suspensions to the falcon tube (*see* **Note 35**).

10. Centrifuge the falcons at 4000 × *g* for 5–10 min (*see* **Note 36**).
11. Remove the supernatant and add 10 ml of PS.

3.5 Plate Counting

1. Resuspend the pellet (*see* **Note 37**) and make 1/10 dilutions by adding 1 ml of the suspension to 9 ml of PS. Transfer 1 ml of each dilution to an empty sterile Petri dish and add melted sterile growth medium (Fig. 4) (*see* **Notes 38**, **39** and **40**).
2. Allow solidification of the growth medium. Subsequently, turn the plates upside down and put them in an incubator set at the optimal growth temperature.
3. Select the countable plates (i.e. between 10 and 350 colonies) and count the colonies (*see* **Note 41**).
4. Calculate the number of colony forming units (CFU) (*see* **Note 42**).

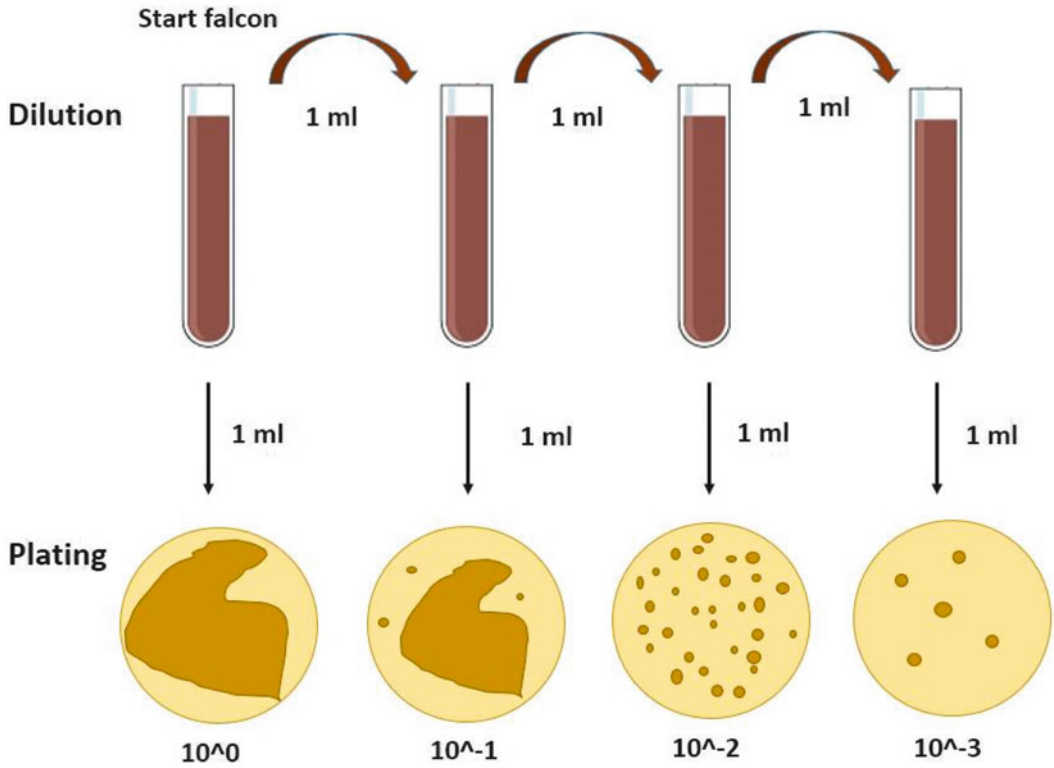

Fig. 4 Plate counting. Resulting colonies reflect the number of viable and cultivable microbes present in a biofilm. This technique assumes that each bacterium grows into a single colony. However, this is not necessary always the case (for example due to cell clumps), therefore plate counts are reported as the number of colony forming units instead of the number of cells. If the concentration of bacteria is too high, colonies will grow into each other and the plate will be uncountable

4 Notes

1. The choice between round-bottomed and flat-bottomed MTP depends on the protocols routinely used in a particular laboratory. Both types of MTP can be used for biofilm formation: [1, 13, 20, 21]. We prefer to use round-bottomed MTP for biofilm growth and quantification.
2. Sterile MTP, tips and Petri dishes are purchased. Sterilization by γ-radiation was performed by the manufacturer.
3. PS, MilliQ water and liquid medium are sterilized by autoclaving.
4. Solid growth medium is prepared by adding agar (e.g. 1.5 %) to the growth medium. Agar is liquid at high temperatures, but solidifies at lower temperatures. After autoclaving, the agar will be liquid and has to be placed in a warm water bath, set at 48 °C. This way, the agar will remain liquid until poured into the Petri dishes.
5. Different growth media can be used depending on the organisms working with. To quantify single species biofilms, nonselective growth media are used, whereas selective growth media can be used to distinguish between species when grown in a mixed species biofilm.
6. All experiments need to be carried out in a sterile environment, unless indicated otherwise. A sterile environment can be achieved by either working in a fume hood or near to a Bunsen flame. All materials used for the experiments need to be sterilized (*see* **Notes 2** and **3**).
7. Anaerobic biofilms can also be cultured. Therefore, adaptations to culture media and conditions are required [19]. Also, biofilms of yeast cells can be grown in a 96-well MTP [16, 22, 23].
8. Liquid cultures are incubated at the appropriate growth temperature depending on the strain. For instance, staphylococci are grown at 37 °C [20]. In addition, the incubation time depends on the strain studied. For instance, slow-growing bacteria (e.g. *Mycobacterium* spp.) require up to 1 week of incubation in order to obtain log-phase bacteria [24].
9. In some experiments, it is necessary to get rid of the "original" growth medium. Therefore, the cell cultures are pelleted (by centrifuging at 4000 × *g* for at least 5 min), washed (by adding PS) and resuspended in PS [15]. The optical density of the bacterial cultures (either in the original growth medium or in PS) is measured at 590 nm. Thereafter, the cell suspension is diluted; most biofilm studies start with cell densities ranging between 10^6 and 10^8 CFU/ml [13, 15, 22, 23]. However, cell densities of only 10^4 CFU/ml were already used to

grow biofilms [17]. In general, the inoculum size depends on the aim of the study and on the protocols routinely used in a particular laboratory. Importantly, the same inoculum size must be used in all experiments in order to be able to compare the results.

10. Row A and row H are filled with sterile medium; these rows serve as negative growth controls [13]. If growth is observed in these rows after incubation, the MTP is not included in further experiments.
11. An automatic pipette can be used in order to fill all wells. Different microorganisms can be cultured in one MTP, e.g. every row can contain a different microorganism.
12. A number of protocols include an adhesion phase of 4 h [13, 20, 25]. Also, 1 h [16] or 2 h of adhesion [17] were already described. In other protocols, no adhesion phase is described and thus, the nonadherent cells are removed when the biofilm is mature [1, 18, 22, 26].
13. Removing nonadherent cells can be performed by using a pipette of 100 µl or a multichannel pipette. Firstly, the supernatant of the negative growth controls is removed. It is important to keep the lid as long as possible on the inoculated wells in order to avoid contamination. The supernatant of every well can be transferred to sterile Petri dishes (Fig. 1). It is recommended to use a new sterile tip for every six wells. The removal of the supernatant, containing nonadherent cells, is a delicate step as the immature biofilm should not be touched or disrupted by the tip of the pipette. Adding PS can be performed by using a (multichannel) pipette or an automatic pipette. Thereby, it is important not to touch or disrupt the biofilm. Therefore, the dispensing speed of the automatic pipette must be quite low and the PS cannot be added perpendicularly to the biofilm.
14. The total incubation time can vary and depends on the organism and on the experiment. For instance, the additional incubation time can vary from 20 or 24 h [1, 20, 25] to 5 weeks [18].
15. (a) After incubation, biofilms are rinsed in order to remove nonadherent cells. Most protocols include a PS rinsing step [13, 20]. Other substances can also be used to rinse the biofilm; for instance, sterile water [1], phosphate-buffered saline [27] or 3-(*N*-morphino)propanesulfonic acid [13] were already used. (b) In order to study the degree of dispersal in biofilms, the number of CFU in the supernatant (containing the nonadherent cells after incubation) can be determined by, e.g. plate countings [27, 28].

16. Once the biofilm is fixed, it is no longer necessary to work in a sterile environment.
17. It is important that all methanol is removed. The methanol cannot be poured away in the sink and must be put in an appropriate closed barrel. The MTP can be air-dried or alternatively, the MTP (without lid) can be placed in an incubator at 37 °C to ensure complete evaporation.
18. Optimal CV concentrations need to be determined for the strains studied and this can be done by plotting the absorbance values (at 590 nm) as a function of different CV concentrations. The highest CV concentration, which resulted in absorbance values still within the dynamic range of the MTP reader, can be used in the assay.
19. It is important to remove all unbound CV. The MTP can be vigorously washed under running tap water. The CV waste must be collected in an appropriate closed barrel. The MTP can be air-dried or alternatively, placed in an incubator at 37 °C.
20. The addition of 33 % acetic acid results in the release of bound CV. It is possible that 20 min is too short to completely dissolve bound CV. Therefore, additional incubation time may be necessary.
21. Average absorbances at $\lambda = 590$ nm are calculated and the net absorbances are determined by taking into account the absorbance values of the negative growth controls.
22. Variants of the current protocol were already described in literature. For instance, the methanol-fixation step was replaced by a simple air-drying step [19, 22] or by an (96 %) ethanol-fixation step [29]. Also, the CV incubation time varied from 1 to 20 min [1, 12, 13, 18, 21, 22]. Ethanol (>70 %) [12, 18, 22] or methanol [19] instead of acetic acid can be used to elute the bound CV from the biofilms. The absorbance can be measured at $\lambda = 540$ nm [12], 570 nm [1, 19, 21, 29], 590 nm [13, 22] or 600 nm [18] using a MTP reader.
23. Stock solutions of resazurin (aliquots of 2.1 ml) are stored at −20 °C. The falcon tubes must be protected from light (e.g. aluminum foil).
24. 10.5 ml of sterile PS is added to the resazurin stock solution in order to prepare a 1/6 dilution. Again, the tubes must be protected from light. Also, the 1/6 resazurin working solution must be vigorously mixed before use.
25. In fact, the appropriate incubation temperature for the resazurin assay is the optimal growth temperature of the organism studied. The appropriate incubation time for the resazurin assay needs to be determined. This can be done by plotting the fluorescence in function of time and the longest incubation

time, which is still within the dynamic range of the MTP reader, will be used in the assay. The incubation time, just as the incubation temperature, depends on the organism studied. During incubation, the MTP must be protected from light.

26. A MTP reader can be used to measure fluorescence.
27. The net fluorescence values can be calculated by taking into account the fluorescence values of the negative growth controls.
28. Persisters form a subpopulation that is able to survive a lethal antibiotic treatment (i.e. that kills most of the population) [5]. This protocol is useful to determine the number of surviving persisters whereas the use of staining methods to quantify persisters is limited, since the small fraction of surviving persisters usually generates a signal that is below the detection limit. Since persistence is highly dependent on the experimental conditions [30, 31], it is important to standardize the different steps in biofilm formation.
29. In this protocol, the formation and quantification of biofilms in 96-well MTP is described. When determining the number of persisters, 96-well MTP may be preferred since the total number of harvested cells is high and volumes are smaller, which reduces the amount of antimicrobials needed. Also, more conditions can be tested on the same MTP, avoiding plate-to-plate variation.
30. To differentiate between persisters and normally growing cells, biofilms first have to be treated with increasing concentrations of antibacterial agents (relative to the MIC) or for prolonged periods of time, depending on whether the antibacterial agent has a concentration- or time-dependent activity. Antibacterial solutions are made in PS or in growth medium depending on the protocols routinely used in a particular laboratory. Each row can represent a different condition. For example, row B: untreated control (PS), row C = treated with antibiotics in a concentration of $1\times$ MIC, row $D = 2\times$ MIC, etc. Survival curves of biofilm cells show a biphasic pattern: an initial rapid killing and a plateau of surviving persisters. The concentration of the antibacterial agent or incubation time where the number of surviving cells does not change anymore, has to be used in the further experiments (Fig. 5).
31. The method has already been successfully used to quantify and characterize persisters [32, 33].
32. A row containing positive growth controls must be included (120 μl PS is added instead of the antibiotic solution), in order to be able to calculate the fraction of surviving cells. 120 μl is used to be sure that the entire biofilm is covered.

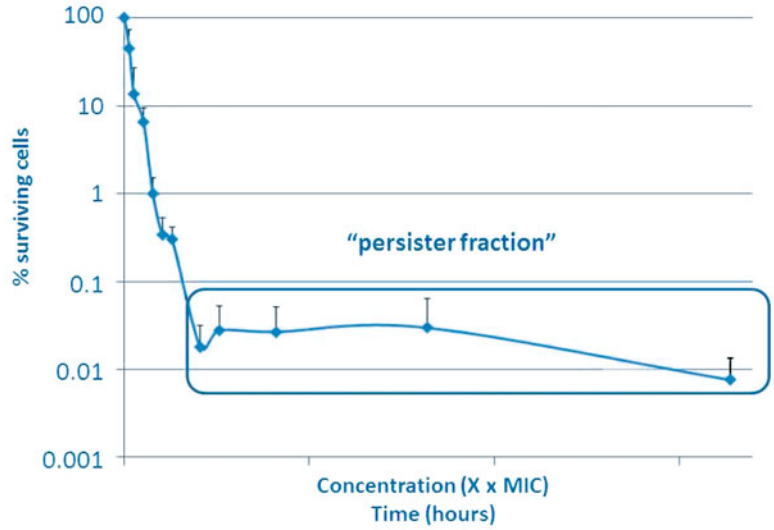

Fig. 5 Survival curve indicating the presence of persister cells

33. A vortex or shaking incubator can be used, but make sure not to spill cells onto the sealing tape.
34. Weight must be put on top of the MTP to avoid floating of the MTP; make sure that all wells are under water, but avoid that the tape becomes wet.
35. To correct for well-to-well variability, it is recommended to collect the biofilm cell suspensions of 12 wells of the same condition in one sterile falcon tube and to calculate the mean CFU of these 12 wells.
36. For most bacteria, two rounds of sonication and vortexing should be sufficient. However, this process may be repeated if necessary. When using this technique for the first time, the resulting MTP can be stained with CV to determine the remaining biomass and to optimize the protocol. The combination of vortexing and sonication has already been used in different studies to efficiently remove biofilms from a surface [34, 35]. The duration times indicated in this protocol were proven not to influence viability of *Pseudomonas aeruginosa* PAO1, *Staphylococcus aureus* Mu50, *Escherichia coli* K-12, *Candida albicans* SC5314, and *Burkholderia cenocepacia* J2315 (unpublished results).
37. Because of possible differences in the final cell suspension volume in the falcon and to remove residual antibiotics, cells are centrifuged and resuspended in a defined volume, e.g. 10 ml of PS.
38. Make sure to vortex well to avoid cell clumps.

39. It is recommended to make these dilutions in duplicate in order to correct for technical variation.
40. Generally, dilutions up to 10^{-9} should be sufficient.
41. A plate count can be done using the pour plate method as described above or using the spread plate method. In the spread plate method, a smaller volume (usually 0.1 ml) is added to a plate containing solid growth medium and evenly spread over the surface using a Drigalski spatel. This way, colonies will only grow on the surface.
42. Depending on the treatment and on the organism(s), colonies can be counted within 24–72 h. The number of colony forming units (CFU) per biofilm can be calculated as follows:
CFU/ml per falcon:

$$N = \frac{c\, x\, 10^{x}}{(n1 + 0.1\ n2)}$$

c = sum countable data
$n1$ = number of countable colonies in the lowest dilution
$n2$ = number of countable colonies in the highest dilution
10^{x} = dilution factor of the lowest dilution
CFU/biofilm = $N \times 10/12$

References

1. Gomes LC, Moreira JM, Miranda JM et al (2013) Macroscale versus microscale methods for physiological analysis of biofilms formed in 96-well microtiter plates. J Microbiol Methods 95:342–349
2. Flemming HC (2002) Biofouling in water systems – cases, causes and countermeasures. Appl Microbiol Biot 59:629–640
3. Costerton JW (1999) Introduction to biofilm. Int J Antimicrob Ag 11:217–221
4. Hall-Stoodley L, Stoodley P (2005) Biofilm formation and dispersal and the transmission of human pathogens. Trends Microbiol 13:7–10
5. Lewis K (2001) Riddle of biofilm resistance. Antimicrob Agents Chemother 45:999–1007
6. Coenye T, Nelis HJ (2010) In vitro and in vivo model systems to study microbial biofilm formation. J Microbiol Methods 83:89–105
7. Christensen GD, Simpson WA, Younger JJ et al (1985) Adherence of coagulase-negative staphylococci to plastic tissue culture plates: a quantitative model for the adherence of staphylococci to medical devices. J Clin Microbiol 22:996–1006
8. Heersink J (2003) Basic biofilm analytical methods. In: Hamilton M, Heersink J, Buckingham-Meyer J, Goeres D (eds) The biofilm laboratory: step-by-step protocols for experimental design, analysis, and data interpretation. Cytergy Publishing, Bozeman, pp 16–23
9. Heersink J, Goeres D (2003) Reactor design considerations. In: Hamilton M, Heersink J, Buckingham-Meyer J, Goeres D (eds) The biofilm laboratory: step-by-step protocols for experimental design, analysis, and data interpretation. Cytergy Publishing, Bozeman, pp 13–15
10. Waters EM, McCarthy H, Hogan S et al (2014) Rapid quantitative and qualitative analysis of biofilm production by *Staphylococcus epidermidis* under static growth conditions. Methods Mol Biol 1106:157–166
11. Gomez-Suarez C, Busscher HJ, van der Mei HC (2001) Analysis of bacterial detachment from substratum surfaces by the passage of air-liquid interfaces. Appl Environ Microbiol 67:2531–2537
12. Pitts B, Hamilton MA, Zelver N et al (2003) A microtiter-plate screening method for biofilm

disinfection and removal. J Microbiol Methods 54:269–276
13. Peeters E, Nelis HJ, Coenye T (2008) Comparison of multiple methods for quantification of microbial biofilms grown in microtiter plates. J Microbiol Methods 72:157–165
14. O'Brien J, Wilson I, Orton T et al (2000) Investigation of the Alamar Blue (resazurin) fluorescent dye for the assessment of mammalian cell cytotoxicity. Eur J Biochem 267:5421–5426
15. Brackman G, De Meyer L, Nelis HJ et al (2013) Biofilm inhibitory and eradicating activity of wound care products against *Staphylococcus aureus* and *Staphylococcus epidermidis* biofilms in an in vitro chronic wound model. J Appl Microbiol 114:1833–1842
16. Vandenbosch D, Braeckmans K, Nelis HJ et al (2010) Fungicidal activity of miconazole against *Candida* spp. biofilms. J Antimicrob Chemother 65:694–700
17. Braem A, Van Mellaert L, Mattheys T et al (2013) Staphylococcal biofilm growth on smooth and porous titanium coatings for biomedical applications. J Biomed Mater Res A 102A:215–224
18. Ramsugit S, Guma S, Pillay B et al (2013) Pili contribute to biofilm formation in vitro in *Mycobacterium tuberculosis*. Antonie Van Leeuwenhoek 104:725–735
19. Dapa T, Unnikrishnan M (2013) Biofilm formation by *Clostridium difficile*. Gut Microbes 4:397–402
20. Vandecandelaere I, Depuydt P, Nelis HJ et al (2014) Protease production by Staphylococcus epidermidis and its effect on *Staphylococcus aureus* biofilms. Pathog Dis 70:321–331
21. Stepanovic S, Vukovic D, Dakic I et al (2000) A modified microtiter-plate test for quantification of staphylococcal biofilm formation. J Microbiol Methods 40:175–179
22. Herczegh A, Gyurkovics M, Agababyan H et al (2013) Comparing the efficacy of hyper-pure chlorine-dioxide with other oral antiseptics on oral pathogen microorganisms and biofilm in vitro. Acta Microbiol Immunol Hung 60:359–373
23. Delattin N, De Brucker K, Vandamme K et al (2013) Repurposing as a means to increase the activity of amphotericin B and caspofungin against Candida albicans biofilms. J Antimicrob Chemother. doi:10.1093/jac/dkt1449
24. Sosunov V, Mischenko V, Eruslanov B et al (2007) Antimycobacterial activity of bacteriocins and their complexes with liposomes. J Antimicrob Chemother 59:919–925
25. Messiaen AS, Nelis H, Coenye T (2013) Investigating the role of matrix components in protection of *Burkholderia cepacia* complex biofilms against tobramycin. J Cyst Fibros 13:56–62
26. Martinez LR, Ibom DC, Casadevall A et al (2008) Characterization of phenotypic switching in *Cryptococcus neoformans* biofilms. Mycopathologia 166:175–180
27. Brackman G, Hillaert U, Van Calenbergh S et al (2009) Use of quorum sensing inhibitors to interfere with biofilm formation and development in *Burkholderia multivorans* and *Burkholderia cenocepacia*. Res Microbiol 160:144–151
28. Ahiwale S, Tamboli N, Thorat K et al (2011) In vitro management of hospital *Pseudomonas aeruginosa* biofilm using indigenous T7-like lytic phage. Curr Microbiol 62:335–340
29. Moreira JM, Gomes LC, Araujo JDP et al (2013) The effect of glucose concentration and shaking conditions on *Escherichia coli* biofilm formation in microtiter plates. Chem Eng Sci 94:192–199
30. Luidalepp H, Joers A, Kaldalu N et al (2011) Age of inoculum strongly influences persister frequency and can mask effects of mutations implicated in altered persistence. J Bacteriol 193:3598–3605
31. Fung DK, Chan EW, Chin ML et al (2010) Delineation of a bacterial starvation stress response network which can mediate antibiotic tolerance development. Antimicrob Agents Chemother 54:1082–1093
32. Van Acker H, Sass A, Bazzini S et al (2013) Biofilm-grown *Burkholderia cepacia* complex cells survive antibiotic treatment by avoiding production of reactive oxygen species. PLoS One 8, e58943
33. Keren I, Minami S, Rubin E et al (2011) Characterization and transcriptome analysis of *Mycobacterium tuberculosis* persisters. MBio 2: e00100-00111
34. Bjerkan G, Witso E, Bergh K (2009) Sonication is superior to scraping for retrieval of bacteria in biofilm on titanium and steel surfaces in vitro. Acta Orthop 80:245–250
35. Kobayashi H, Oethinger M, Tuohy MJ et al (2009) Improved detection of biofilm-formative bacteria by vortexing and sonication: a pilot study. Clin Orthop Relat Res 467:1360–1364

Chapter 6

Protocol for Determination of the Persister Subpopulation in *Candida Albicans* Biofilms

Katrijn De Brucker, Kaat De Cremer, Bruno P.A. Cammue, and Karin Thevissen

Abstract

In contrast to planktonic cultures of the human fungal pathogen *Candida albicans*, *C. albicans* biofilms can contain a persister subpopulation that is tolerant to high concentrations of currently used antifungals. In this chapter, the method to determine the persister fraction in a *C. albicans* biofilm treated with an antifungal compound is described. To this end, a mature biofilm is developed and subsequently treated with a concentration series of the antifungal compound of interest. Upon incubation, the fraction of surviving biofilm cells is determined by plating and plotted versus the used concentrations of the antifungal compound. If a persister subpopulation in the biofilm is present, the dose-dependent killing of the biofilm cells results in a biphasic killing pattern.

Keywords: *Candida albicans*, Biofilm, Persisters, Antifungal compound

1 Introduction

Persisters are subpopulations of cells that are transiently tolerant to multiple drugs [1]. Biofilms of the human fungal pathogen *C. albicans* contain a small fraction of persisters that are completely tolerant to currently used antifungals [2]. Interestingly, attachment rather than biofilm formation itself seems to initiate persister formation. Upon reinoculation of the surviving cells, a similar fraction of persisters is formed in the biofilm, suggesting that these cells are phenotypic variants of the wild type rather than mutants. Remarkably, so far no persister fraction has been detected in *C. albicans* planktonic cultures [2, 3]. This is in contrast to bacteria, which produce persisters in both planktonic and biofilm populations. Periodic application of antimicrobial agents in patients selects for *C. albicans* strains with increased persister levels, indicating the clinical relevance of persisters [4]. However, not all *C. albicans* strains have a biofilm persister fraction [3]. Whereas molecular

Jan Michiels and Maarten Fauvart (eds.), *Bacterial Persistence: Methods and Protocols*, Methods in Molecular Biology, vol. 1333, DOI 10.1007/978-1-4939-2854-5_6,

insights into *C. albicans* persistence are scarce, the occurrence of miconazole-tolerant persisters in *C. albicans* biofilms has been linked to the ROS (reactive oxygen species) detoxifying activity of different superoxide dismutases (Sod), as a *sod4Dsod5D* biofilm contains threefold less miconazole-tolerant persisters compared to a biofilm formed by the wild type. In addition, Sod inhibitors can be used to reduce the fraction of miconazole-tolerant persisters [5]. A persister fraction is also present in biofilms of other *Candida* species, such as *C. krusei* and *C. parapsilosis* [3]. As persisters might be the main reason of recalcitrance of chronic infectious diseases to antimicrobial therapy [6], insights into the molecular basis of persistence in *C. albicans* biofilms can certainly contribute to the rational design of antibiofilm agents that also target the persister fraction.

Here, the protocol to determine the fraction of *C. albicans* persister cells in mature biofilms upon treatment with an antifungal compound is described. This protocol is based on protocols of LaFleur and coworkers [2, 4] and Bink and coworkers [5] and consists of three consecutive steps: development of a mature biofilm, treatment of the mature biofilm with an antifungal compound, and quantification of the surviving biofilm cells.

2 Materials

1. Yeast-extract Peptone Dextrose (YPD) liquid medium: 10 g yeast extract, 20 g peptone, 20 g glucose, 1 L distilled water. Dissolve 10 g yeast extract powder and 20 g peptone in 950 mL distilled water. Prepare a 40 % glucose stock solution (w/v) in distilled water in a separate bottle (*see* **Note 1**). Sterilize both liquids. After autoclaving, add 50 mL of 40 % glucose to 950 mL YP medium to obtain YPD liquid medium. YPD liquid medium can be stored at room temperature.
2. Phosphate-buffered saline (PBS): 8 g NaCl, 0.291 g KCl, 1.44 g Na_2HPO_4, 0.24 g KH_2PO_4, 1 L distilled water. Stir the solution until all salts are completely dissolved. Adjust the pH to pH 7.4. PBS can be stored at room temperature.
3. Roswell Park Memorial Institute (RPMI) 1640 medium: 10.4 g RPMI 1640, 34.52 g 3-[*N*-morpholino] propanesulfonic acid (MOPS), 1 L distilled water, pH 7.0. RPMI 1640 medium with L-glutamine and without sodium bicarbonate was purchased from Sigma-Aldrich. Dissolve 10.4 g RPMI 1640 in 900 mL distilled water and add 34.52 g 3-[*N*-morpholino] propanesulfonic acid (MOPS). Stir until dissolved. Afterwards, adjust the pH to 7.0 using 1 M NaOH. Add additional distilled water to obtain a final volume of 1 L. Sterilize immediately by filtration using a membrane with a porosity

of 0.22 μm. Do not sterilize by autoclaving. Store RPMI 1640 at 4 °C in the dark.

4. Yeast-extract Peptone Dextrose (YPD) solid medium: 10 g yeast extract, 20 g peptone, 20 g glucose, 15 g agar, 1 L distilled water. Dissolve 10 g yeast extract powder, 20 g peptone and 15 g agar in 950 mL distilled water. Prepare a 40 % glucose stock solution (w/v) in distilled water in a separate bottle (*see* **Note 1**). Sterilize both liquids by autoclaving. After sterilization, add 50 mL of 40 % glucose to 950 mL YP medium to obtain YPD agar medium. YPD plates can be stored for several weeks at 4 °C if evaporation is prevented.
5. Round-bottomed polystyrene 96-well microtiter plates.
6. Flat-bottomed polystyrene 96-well microtiter plates.
7. Sterilized glass beads (4 mm diameter).

3 Methods

3.1 Development of a Mature Biofilm

1. Inoculate one colony of *C. albicans* overnight in a test tube containing 3–5 mL YPD liquid medium at 30 °C in shaking conditions (133 g) (*see* **Note 2**).
2. Centrifuge 1 mL of the overnight culture (845 g in a microfuge, 3 min) and wash twice using 1 mL PBS. Measure the OD (at 600 nm) of the washed overnight culture.
3. Dilute the optical density of the washed overnight culture to 0.1 (approximately 1.10^6 cells/mL) in RPMI 1640.
4. Add 100 μL of the diluted culture to wells of a round-bottomed microtiter plate (*see* **Note 3**). Cover the microtiter plate with the lid.
5. Incubate for 1 h at 37 °C in static conditions (adhesion phase).
6. Rinse the wells: dispose the inoculated RPMI 1640 medium to remove non-adherent cells. Wash the wells by gently adding 100 μL PBS/well (*see* **Note 4**).
7. Remove PBS and add 100 μL fresh RPMI 1640 medium to each well (*see* **Note 4**). Cover the microtiter plate with the lid.
8. Incubate the microtiter plate for 24 h at 37 °C under static conditions to allow development of a mature biofilm.

3.2 Treatment of the Mature Biofilm with an Antifungal Compound

1. Make twofold serial dilutions of the antifungal compound in RPMI 1640 in a flat-bottomed microtiter plate (*see* **Note 5**). To this end, first a twofold dilution series of the antifungal compound should be prepared at 100 times final strength in the appropriate solvent, for example in 100 % dimethyl sulfoxide (DMSO). Afterwards, dilute this dilution series tenfold in RMPI 1640. As such these working concentrations are ten

times more concentrated (resulting in a 10 % solvent background) than the desired final concentration series (in 1 % solvent background). Note that in some cases, more diluted solvent backgrounds are necessary—the solvent itself should not affect the biofilm cells. If so, the above concentration series should be adapted.

2. Rinse the wells of the biofilm microtiter plate: remove the RPMI 1640 medium and gently add 100 μL PBS to each well. Remove the PBS (*see* **Note 4**).
3. Add 90 μL of fresh RPMI 1640 and 10 μL of the working concentrations of the antifungal compound (*see* Subheading 3.2, **step 1**) to the wells. This results in the desired final concentrations of the antifungal compound and a 1 % background concentration of the solvent. Use the 1 % background concentration of the solvent as negative control.
4. Incubate the biofilms for 24 h at 37 °C under static conditions.

3.3 Quantification of the Surviving Biofilm Cells

1. Wash the wells gently with 100 μL PBS (*see* **Note 4**).
2. Add 100 μL PBS to each well and resuspend biofilms by scraping and pipetting up and down vigorously.
3. Check visually if biofilms are completely resuspended (*see* **Note 6**).
4. Tape the lid carefully to the microtiter plate using parafilm and sonicate for 10 min (*see* **Note 7**).
5. Make tenfold dilution series in PBS: add 180 μL PBS to each well of a new flat-bottomed microtiter plate. Subsequently, transfer 20 μL of the resuspended biofilm or previous dilution to the next well and mix well before transferring 20 μL to the following well. Continue until the required dilution is reached (*see* **Note 8**).
6. Plate 100 μL of each dilution on YPD agar plates. Use sterilized glass beads to spread the liquid uniformly over the entire plate.
7. Incubate YPD agar plates for 48 h at 30 °C.
8. Count the colony forming units for each treatment.
9. Determine the percentage survival relatively to the control treatment.
10. Plot the percentage survival versus the used antifungal concentrations (Fig. 1). If persisters are present, the dose-dependent killing will result in a biphasic killing pattern. Whereas the majority of cells are killed at low concentrations of the antifungal, a persister fraction is present when a certain percentage of the cells remains unaffected by treatment with increasing concentrations of the antifungal, resulting in a distinct plateau of surviving persistors (Fig. 1).

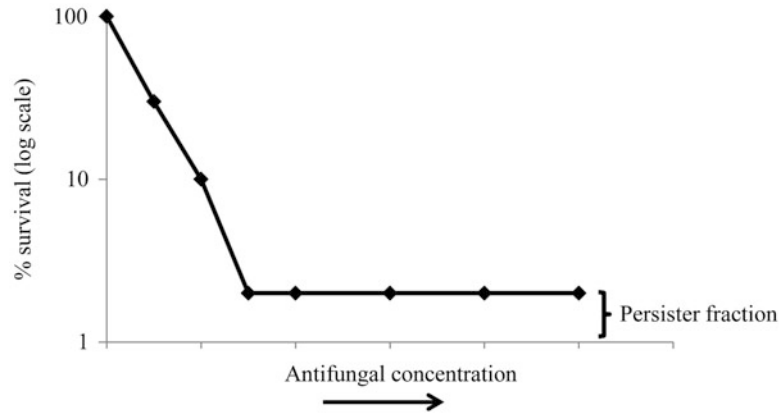

Fig. 1 Dose-dependent killing with an antifungal compound reveals the persister fraction of a *C. albicans* biofilm

4 Notes

1. Glucose stock solution has to be prepared in a separate bottle to prevent caramelization of the YPD medium during autoclaving.
2. Refresh your plate containing *C. albicans* colonies at least every 2 weeks, using a *C. albicans* stock stored at −80 °C.
3. Avoid growing biofilms in the outer wells of the microtiter plate as these wells are more susceptible to evaporation, which can affect your results. Instead, fill these wells with 100 μL PBS to prevent evaporation in the inner wells.
4. Carefully rinse the wells to avoid disruption of the adhered cells or biofilm: place tips to the sides of the wells and avoid touching the bottom of the wells. Keep the microtiter plates in an angle to remove or add the liquid. Liquid should be removed and added very slowly.
5. Use concentrated stock solutions of your antifungal compounds such that the solvent background of your dilution series in RPMI 1640 is not affecting biofilm cells. For example, if the compound is dissolved in dimethyl sulfoxide (DMSO), the final DMSO background in RPMI 1640 should be maximally 2 % but preferably 1 % or lower to prevent toxic side-effects. In the protocol, 100 times concentrated stock solutions are used as an example, resulting in a solvent background of 1 %.
6. In particular, parts of the biofilm at the sides of the wells are more difficult to resuspend. Therefore, scrape and pipette up and down until the complete biofilm is resuspended and no remains of biofilms can be visually detected.

7. Check that the bottom of the microtiter plate is in contact with the water.
8. Before transferring 20 μL of the dilution to the next well, make sure that your dilutions are very well mixed by pipetting up and down thoroughly. Upon growth on YPD agar plates, the accuracy of the different dilutions can be verified as each subsequent dilution should result in an approximately tenfold reduced number of colonies.

Acknowledgements

The research leading to these results has received funding from the European Commission's Seventh Framework Programme (FP7/2007-2013) under the grant agreement COATIM (project n° 278425).

References

1. Fauvart M, De Groote VN, Michiels J (2011) Role of persister cells in chronic infections: clinical relevance and perspectives on anti-persister therapies. J Med Microbiol 60:699–709
2. LaFleur MD, Kumamoto CA, Lewis K (2006) *Candida albicans* biofilms produce antifungal-tolerant persister cells. Antimicrob Agents Chemother 50:3839–3846
3. Al-Dhaheri RS, Douglas LJ (2008) Absence of amphotericin B-tolerant persister cells in biofilms of some *Candida* species. Antimicrob Agents Chemother 52:1884–1887
4. LaFleur MD, Qi Q, Lewis K (2010) Patients with long-term oral carriage harbor high-persister mutants of *Candida albicans*. Antimicrob Agents Chemother 54:39–44
5. Bink A, Vandenbosch D, Coenye T et al (2011) Superoxide dismutases are involved in *Candida albicans* biofilm persistence against miconazole. Antimicrob Agents Chemother 55:4033–4037
6. Lewis K (2012) Persister cells: molecular mechanisms related to antibiotic tolerance. In: Handb. Exp. Pharmacol. Springer, Heidelberg, Berlin, pp 121–133

Part III

Single Cell Analysis of Persister Cells

Chapter 7

Quantitative Measurements of Type I and Type II Persisters Using ScanLag

Irit Levin-Reisman and Nathalie Q. Balaban

Abstract

The present method quantifies the number of slow-growing bacteria leading to antibiotic persistence in a clonal population. First, it enables discriminating between slow growers that are generated by exposure to a stress signal (Type I persisters) and slow growers that are continuously generated during exponential growth (Type II persisters). Second, the method enables determining the amount of slow growers in a culture.

Keywords: Persisters, Type I persistence, Type II persistence, ScanLag, Automatic imaging, Bacterial growth, Lag, High-throughput measurements, Stationary phase

1 Introduction

Persisters are a small fraction of a genetically uniform population that survives antibiotic stress [1, 2]. The survival of the persister cells is traditionally explained by their transient non-growing state [3, 4]. However, it has been shown that transient growth arrest may be achieved through two distinct mechanisms: either the bacteria encounter a stress signal, e.g. starvation that result in a long lag phase before growth resumes (Type I persistence), or they stochastically enter a non-growing state in the absence of external signals (Type II persistence) [5]. Whereas Type I persistence vanishes when bacteria are maintained at exponential growth, Type II persisters are continuously generated at exponential phase.

Typically, the level of persistence is measured by monitoring the biphasic killing curve of the culture exposed to antibiotics. In order to measure the Type I persistence level, the culture should be diluted directly into antibiotics after the stress signal that generates persistence, whereas Type II persistence should be measured at strictly exponential growth (Fig. 1). Therefore, it is imperative to determine first which type of persistence is observed before its level can be

Jan Michiels and Maarten Fauvart (eds.), *Bacterial Persistence: Methods and Protocols*,
Methods in Molecular Biology, vol. 1333, DOI 10.1007/978-1-4939-2854-5_7,

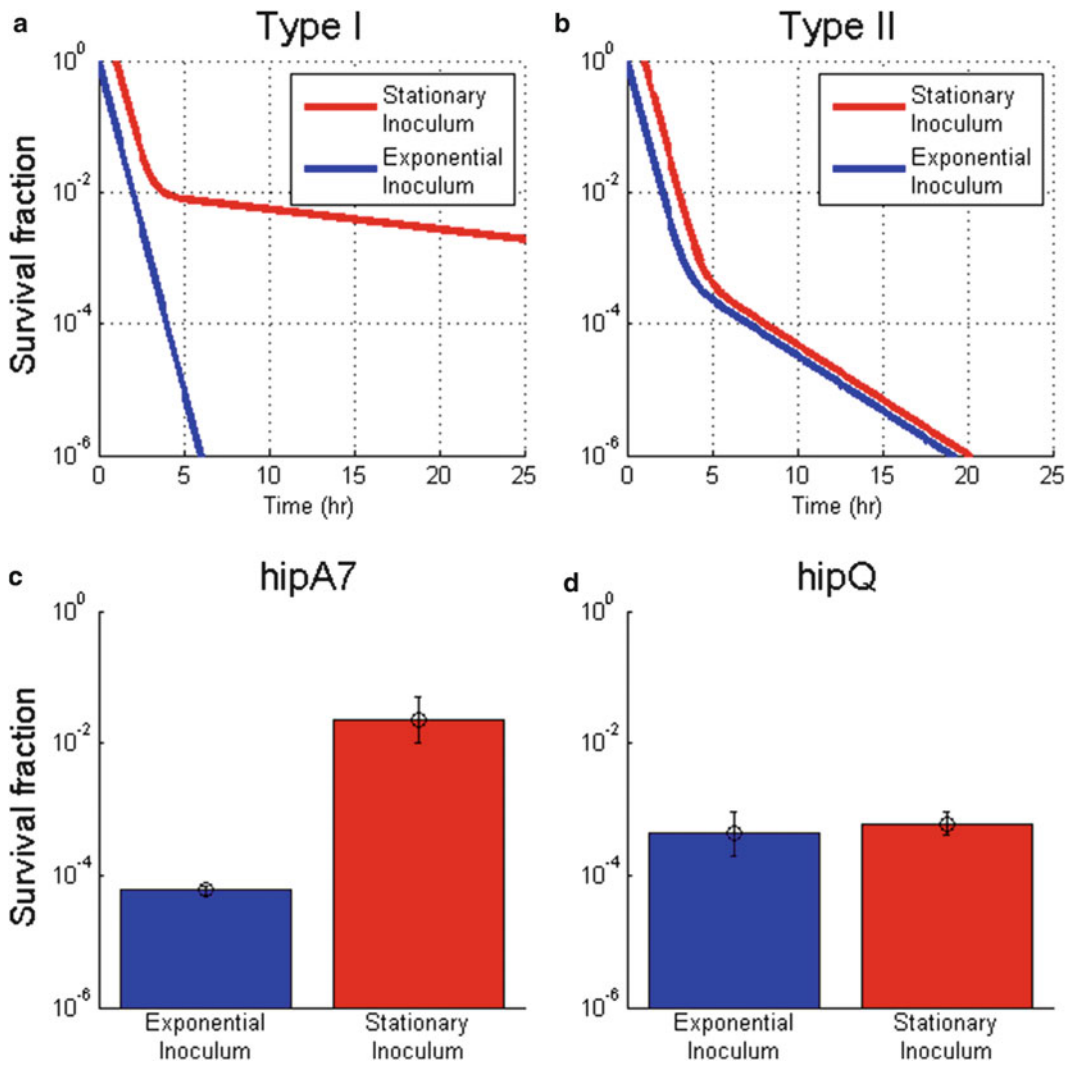

Fig. 1 Kill curve of Type I and Type II persisters. (**a**, **b**) A schematic solution of the killing curves of Type I and Type II persisters during stationary (*red*) and exponential (*blue*) phase. (**c**, **d**) The fractions of persisters of stationary inoculum (*red*) and of exponential inoculum (*blue*) of Type I (*hipA7 E. coli* mutant) and Type II (*hipQ E. coli* mutant) persisters were measured experimentally after 5 h in ampicillin [5]. The comparison of survival between culture of exponential inoculum and stationary inoculum enables the distinction between Type I and Type II persistence: Type II persistence is observed irrespective of the inoculum history whereas Type I persistence requires a past exposure to stress, here stationary phase

quantified. Discriminating whether a persistent pathogenic strain is characterized by Type I or Type II persistence is important for finding ways to target persistence, as well as for the mathematical modeling of the phenomenon [6]. Unfortunately, many experiments are performed in a way that does not allow determining which type of persistence is measured. This reduces the reproducibility of the measurements and impedes on comparing results from different labs.

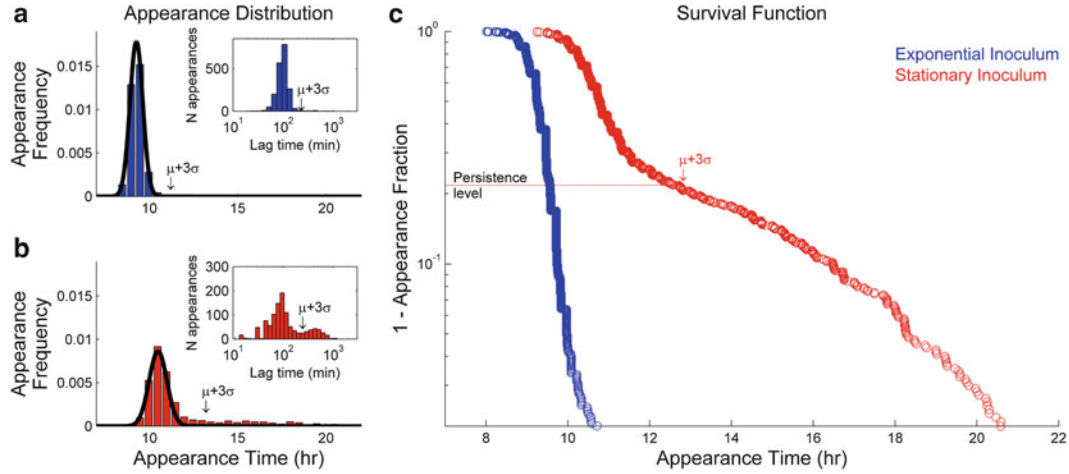

Fig. 2 Estimation of the persisters fraction. (**a**, **b**) A stationary phase bacteria (*red*, total of 1102 colonies) and an exponential phase bacteria (*blue*, total of 1947 colonies) of *hipA7* (Type I persisters) was scanned using ScanLag. Note that only the stationary phase bacteria appearance has a long tail of late appearing colonies which constitute the persister population. Inset of (**b**): same data plotted on a log scale shows more clearly the bimodal distribution of lag time in this high persistence mutant. A Gaussian was fitted to the main peak (*black line*) and the persistence level defined as the fraction of colonies that appeared later than three standard deviations away from the median, namely after 12.6 h (marked by *arrow*). Here, the fraction of persistence is found to be 0.2 in the stationary inoculum and 0.01 in the exponential inoculum. (**c**) Same data as in (**a**, **b**) presented as 1-the Cumulative Distribution Function (1-CDF). CDF of the exponential inoculum (*blue*) and of the stationary inoculum (*red*). When the persistence level is low, the representation as 1-CDF on a logarithmic scale allows visualizing the persistence fraction, marked by the intersection with the line three standard away from the median

In this chapter, we focus on persistence due to slower growth, and determine the persistence level by measuring the number of slow-growing cells in the population. Our goals are (a) to present a methodology to discriminate between Type I and Type II persistence, and (b) to reproducibly measure the amount of slow-growing cells in the population. The first goal is achieved by comparing persistence levels of cultures at the exponential growth phase and after the stress signal that induces Type I persistence. We illustrate the method on the well-studied induction of Type I persistence by starvation, and compare two cultures: one inoculated from an exponential culture, and the other one inoculated from a stationary phase culture. The second goal requires the quantitative measurement of the number of single cells having a delay in growth, using the ScanLag setup [7]. The ScanLag method was developed to detect delayed growth of colonies in a high-throughput manner. It uses standard office scanners [8, 9] to image automatically thousands of colonies on solid medium Petri dishes [10], and extracts, by automated image analysis, the colonies appearance distribution. When bacteria are plated on regular Petri dishes with rich nutrient agar, colonies typically appear within a few hours (about 9 h for *E. coli*) and their appearance time distribution

is narrow (Fig. 2). A colony originating from a persister bacterium will start growing at a later time and will be in the tail of the appearance time distribution. Therefore, the distribution of appearance time of colonies on Petri dishes allows measuring the number of persister present in the original culture, as well as their typical time for switching to active growth. Thus the appearance time distribution provides a robust quantitative measurement of the number of growth arrested bacteria in the population that does not depend on the specifics of the antibiotic used to reveal the slow-growing population.

The protocol described below enables to determine the type of persistence and its level in a given strain. First, two different cultures of the strain are grown; one strictly exponentially growing culture and one culture exposed to the stress inducing persistence, here stationary phase. Second, each culture is serially diluted to approximately 200 CFU/mL and plated on Petri dishes with nutrient agar. Finally, the appearance time distributions of the two cultures are measured using ScanLag for extracting the type of persistence and its level.

2 Materials

2.1 ScanLag Setup

1. Flatbed scanners with Hardware resolution: 4800 × 9600 dpi; color bit depth: 48 bit; and optical resolution: 4800 dpi, that can operate at the relevant temperature and humidity levels (*see* **Note 1**).
2. Custom-made white plate holders, the size of the flatbed scanner surface with six holes the size of a Petri dish (Fig. 3b).
3. Sterile squares of black felt cloth ~100 × 100 cm, to cover the lid of the plate (Fig. 3b) (*see* **Note 2**).

2.2 Media and Reagents

1. Nutrient Petri dishes or Luria-Bertani Lennox (LBL) agar: Mix 10 g Tryptone, 5 g Yeast extract, 5 g sodium chloride, 15 g agar and 1 L distilled water and autoclave (*see* **Note 3**).
2. Liquid growth medium: The bacterial culture can be grown in any growth medium. Here, we use LBL supplemented with appropriate antibiotics.

3 Methods

3.1 Building the Setup

1. Connect number of flatbed scanners to a computer (Fig. 3a) (*see* **Note 1**).
2. Install the automatic scanning application, "ScanningManager."

3.2 Stationary Culture Growth

1. Inoculate bacterial culture into fresh medium, and grow the culture to stationary phase with the appropriate environmental

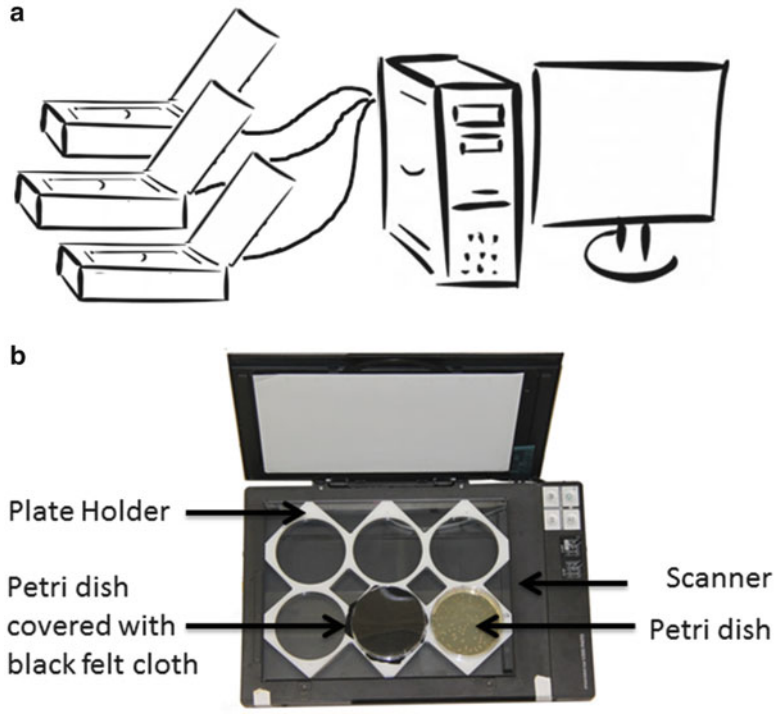

Fig. 3 (**a**) A schematic illustration ScanLag setup: an array of scanners attached to a computer. (**b**) An image of the scanner, with plate holder, and two Petri dishes on it—one covered with black Felt cloth

conditions (*see* **Note 4**). Here, we grow *E. coli* in LBL at 37 °C with shaking (300 rpm).

3.3 Exponential Culture Growth

1. Dilute a stationary culture into fresh medium (1:1000) and grow the culture in appropriate conditions. When the culture is at exponential phase, dilute again (1:1000) and regrow the culture while following its growth rate with an OD reader.
2. Take a sample of this culture when the culture is still at exponential phase (typically $OD_{630} < 0.2$), and evaluate the number of bacteria in the culture using its current OD value (*see* **Note 5**).

3.4 Scanning Colonies

1. Dilute the stationary phase culture and the exponential phase culture to approximately 2000 CFU per mL (*see* **Note 6**).
2. Plate 100 μL on properly dried plate (*see* **Note 7**).
3. Cover the plate with sterile black felt cloth (*see* **Note 2**).
4. Place the plates in the plate holder on top of the scanners.
5. Scan the Petri dishes periodically: Start the automatic scan using the application "ScanningManager."

3.5 Image Analysis

1. The image analysis requires very basic knowledge of Matlab. The functions used to analyze the images are explained in the ScanLag manual.
2. Using Matlab, preprocess the images to align the images taken by the same scanner at different time points and to crop each plate (*see* **Note 8**).
3. Find the appearance time of each colony on the Petri dishes using the script "TLAllPlates."
4. Generate the appearance distribution using the script "AddHistograms."

3.6 Determine the Type of Persistence

1. Plot the appearance distributions of both the stationary culture and the exponential culture (*see* **Note 9**).
2. If both distributions are bimodal, Type II persistence is observed. If the exponential culture is uni-modal whereas the stationary culture is bimodal, then Type I persistence is observed (Fig. 2).
3. When the fraction of persisters is low, it is recommended to use survival function presentation (1-Cumulative Distribution Function), which enables to visualize the fraction of bacteria that are still lagging (Fig. 2). Here persistence will appear as a biphasic curve. If both the exponential and stationary cultures curves are biphasic, Type II persistence is observed. If only the stationary culture curve is biphasic, Type I persistence is observed (*see* **Note 10**).

3.7 Estimation of Persistence Level

1. To estimate the persistence level fit a Gaussian to the main distribution of appearance.
2. Find the Gaussian's mean and standard deviation.
3. Sum up the amount of colonies that appeared later than three standard deviations away from the mean (Fig. 2).

4 Notes

1. We use Epson Perfection V37 that allows controlling multiple scanners under the same computer. Note that some scanner brands do not allow more than one scanner on the same computer.
2. The black felt cloth is used to gain good contrast, and also to prevent condensation on the lid.
3. Other types of nutrient agar dishes might need calibration when using the ScanLag image analysis software.
4. Note that persistence level can be very sensitive to exact growth conditions such as aeration and pH, and those should be appropriately controlled.

5. It is recommended to create calibration curve of the measured OD to the number of CFU beforehand.
6. The number of optimal CFU per plate was checked for *E. coli*. The control experiment determining this number is described in detail in [7].
7. The plates must be well dried so that the CFU will not smear.
8. Read the help file for further explanation about the Matlab functions.
9. When the fraction of persisters is low, it is recommended to use survival function presentation (1-Cumulative Distribution Function), which describes what fraction of bacteria are still lagging (Fig. 2).
10. In order to evaluate the type of persistence, without a precise measurement of its level, the survival fraction of a stationary inoculum culture may be compared to the survival fraction of an exponential inoculum culture. Type I persistence will be characterized as a difference in those survival levels (Fig. 1c, d).

Acknowledgments

The work was supported by the European Research Council (Starting Grant no. 260871) and the Israel Science Foundation (no. 592/10). I.L.R. acknowledges support from the Maydan Foundation.

References

1. Bigger J (1944) The bactericidal action of penicillin on staphylococcus pyogenes. Ir J Med Sci 19(12):585–595
2. Hobby GL, Meyer K, Chaffee E (1942) Observations on the mechanism of action of penicillin. Exp Biol Med 50(2):281–285
3. Lewis K (2007) Persister cells, dormancy and infectious disease. Nat Rev Microbiol 5 (1):48–56
4. Fridman O, Goldberg A, Ronin I et al (2014) Optimization of lag time underlies antibiotic tolerance in evolved bacterial populations. Nature 513(7518):418–421. doi:10.1038/nature13469
5. Balaban NQ, Merrin J, Chait R et al (2004) Bacterial persistence as a phenotypic switch. Science 305(5690):1622–1625. doi:10.1126/science.1099390
6. Gefen O, Balaban NQ (2009) The importance of being persistent: heterogeneity of bacterial populations under antibiotic stress. FEMS Microbiol Rev 33(4):704–717, doi: FMR156 [pii] 10.1111/j.1574-6976.2008.00156.x
7. Levin-Reisman I, Gefen O, Fridman O et al (2010) Automated imaging with ScanLag reveals previously undetectable bacterial growth phenotypes. Nat Methods 7 (9):737–739. doi:10.1038/nmeth.1485
8. Michel JB, Yeh PJ, Chait R et al (2008) Drug interactions modulate the potential for evolution of resistance. Proc Natl Acad Sci U S A 105(39):14918–14923
9. Levin-Reisman I, Fridman O, Balaban NQ (2014) ScanLag: high-throughput quantification of colony growth and lag time. J Vis Exp (89). doi: 10.3791/51456
10. Guillier L, Pardon P, Augustin JC (2006) Automated image analysis of bacterial colony growth as a tool to study individual lag time distributions of immobilized cells. J Microbiol Methods 65(2):324–334

Chapter 8

Analyzing Persister Physiology with Fluorescence-Activated Cell Sorting

Mehmet A. Orman, Theresa C. Henry, Christina J. DeCoste, and Mark P. Brynildsen

Abstract

Bacterial persisters are phenotypic variants that exhibit an impressive ability to tolerate antibiotics. Persisters are hypothesized to cause relapse infections, and therefore, understanding their physiology may lead to novel therapeutics to treat recalcitrant infections. However, persisters have yet to be isolated due to their low abundance, transient nature, and similarity to the more highly abundant viable but non-culturable cells (VBNCs), resulting in limited knowledge of their phenotypic state. This technical hurdle has been addressed through the use of fluorescence-activated cell sorting (FACS) and quantification of persister levels in the resulting sorted fractions. These assays provide persister phenotype distributions, which can be compared to the phenotype distributions of the entire population, and can also be used to examine persister heterogeneity. Here, we describe two detailed protocols for analysis of persister physiology with FACS. One protocol assays the metabolic state of persisters using a fluorescent metabolic stain, whereas the other assays the growth state of persisters with use of a fluorescent protein.

Keywords: Persister, Antibiotic, Fluorescence-activated cell sorting (FACS), Phenotypic heterogeneity, Viable but non-culturable cell (VBNC), Redox sensor green (RSG)

1 Introduction

Bacterial cultures treated with high concentrations of bactericidal antibiotics often exhibit two regimes of killing (Fig. 1). The first regime is characterized by a rapid killing rate, depicting the death of normal cells, whereas the second regime, characterized by a much slower or non-existent killing rate, indicates the presence of a separate subpopulation of cells [1, 2]. When these "persisters" are subsequently cultured, they give rise to a population with antibiotic sensitivity identical to that of the original culture, demonstrating that they are not antibiotic-resistant mutants. Rather, persisters are phenotypic variants that tolerate extraordinary levels of antibiotics due to their physiological state at the time of treatment [3, 4].

Jan Michiels and Maarten Fauvart (eds.), *Bacterial Persistence: Methods and Protocols*, Methods in Molecular Biology, vol. 1333, DOI 10.1007/978-1-4939-2854-5_8,

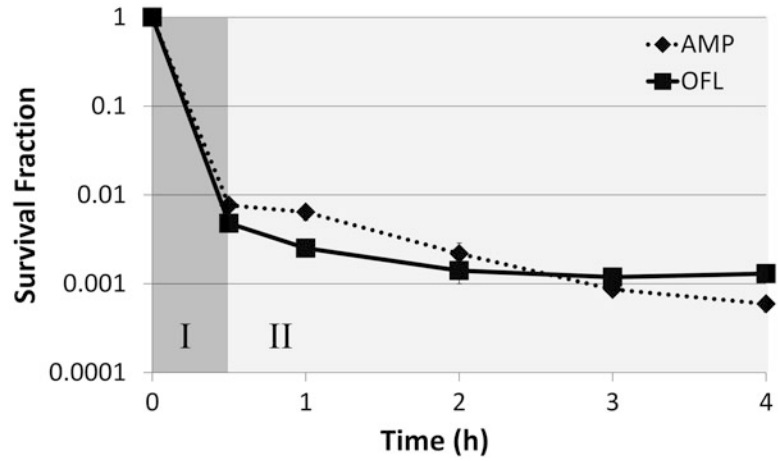

Fig. 1 Biphasic killing of *E. coli* treated with antibiotics. Survival fraction of exponential phase *E. coli* treated with 200 μg/mL ampicillin (AMP) or 5 μg/mL ofloxacin (OFL) as measured by CFU. Initial phase of killing (I: *dark gray*) corresponds to death of normal cells, whereas the second phase of killing (II: *light gray*) represents colonies derived from persisters

Persisters have been hypothesized to underlie the propensity of biofilm infections to relapse, and strategies to eliminate them have the potential to impact over half of infections treated in hospitals [5, 6]. To facilitate the identification of such potential therapeutics, a greater understanding of persister physiology is desirable. However, persisters are rare, generally 1 in 10^2–10^6, transient, and by all measures to date, extremely similar to another more highly abundant subpopulation in bacterial cultures known as viable but non-culturable cells (VBNCs) [7–10]. Both persisters and VBNCs exclude propidium iodide (PI) (which stains dead cells), harbor metabolic activity, and do not grow (though exceptions exist [10, 11]). Indeed, the only known differentiating characteristic between VBNCs and persisters is that persisters can divide and produce colonies after antibiotic treatment on standard medium, whereas VBNCs cannot (though some non-standard media can revive some VBNCS [12]). Unfortunately, those resulting colonies are no longer persisters, because the cells had exited the persistent state and initiated cell division once again. These technical challenges necessitate that persisters be studied while in their transient, antibiotic-tolerant state, surrounded by other, more highly abundant cell types, such as VBNCs. The difficulties posed by VBNCs for the interrogation of persister physiology have only recently been recognized [7–10], and this revelation suggests that two previous methods for "isolating" persisters [13, 14] actually provided only persister-enriched samples that contained many more other cell types. A recent attempt at isolating persisters was published by Canas-Duarte and colleagues, where *Escherichia coli* were treated

with lysis solutions and biphasic killing was observed [15]. Unfortunately, the authors did not test the surviving bacteria for antibiotic tolerance, which is the defining characteristic of persistence. Further, the VBNC levels of the resulting cell suspensions were not quantified, which is of particular concern, since a previous lysis-based technique [13] was found to yield far more VBNCs than persisters [9]. Without these controls it is not possible to ascertain whether the method of Canas-Duarte and colleagues was able to segregate persisters from other cell types. Therefore, at present, isolation of persisters has yet to be realized, and biomarkers able to distinguish persisters from VBNCs have yet to be found. In the absence of techniques to separate persisters from other cell types, fluorescence-activated cell sorting (FACS) has become the gold standard technique to examine persister physiology [8–10, 16, 17]. In essence, bacterial populations are segregated into groups (quantiles) based on a quantitative characteristic (e.g., expression of a fluorescent protein), and although the existence of persisters within those distributions are unknown at the time of sorting, persistence assays can be performed on the resulting quantiles to quantify the abundance of persisters (Fig. 2). In this manner, a persister phenotype distribution is obtained, which can differ quite significantly from that of the total bacterial population [10]. Beyond providing one of the only means to quantify persister physiology to date, FACS approaches quantify persister heterogeneity, which has become a topic of increasing interest due to the challenges it poses for eradicating chronic, relapsing infections [18].

Here, we describe FACS procedures to assay both the metabolic and cell division states of exponential phase *E. coli* persisters [10]. These cellular qualities were chosen as model characteristics because they involve the use of both a fluorescent stain and protein, and therefore can serve as templates for the interrogation of cellular properties that can be fluorescently labeled by either means.

2 Materials

2.1 Bacterial Strains

The methods described here have been used to examine metabolic activity and cell division in persisters of *E. coli* MG1655 [10]. To monitor cell division, the methods described here make use of MO001, which is an MG1655 strain with a chromosomally integrated *lacI*^{q} promoter in place of the *lacI* promoter, and a chromosomally integrated *T5p-mCherry* in place of *lacZYA* [10].

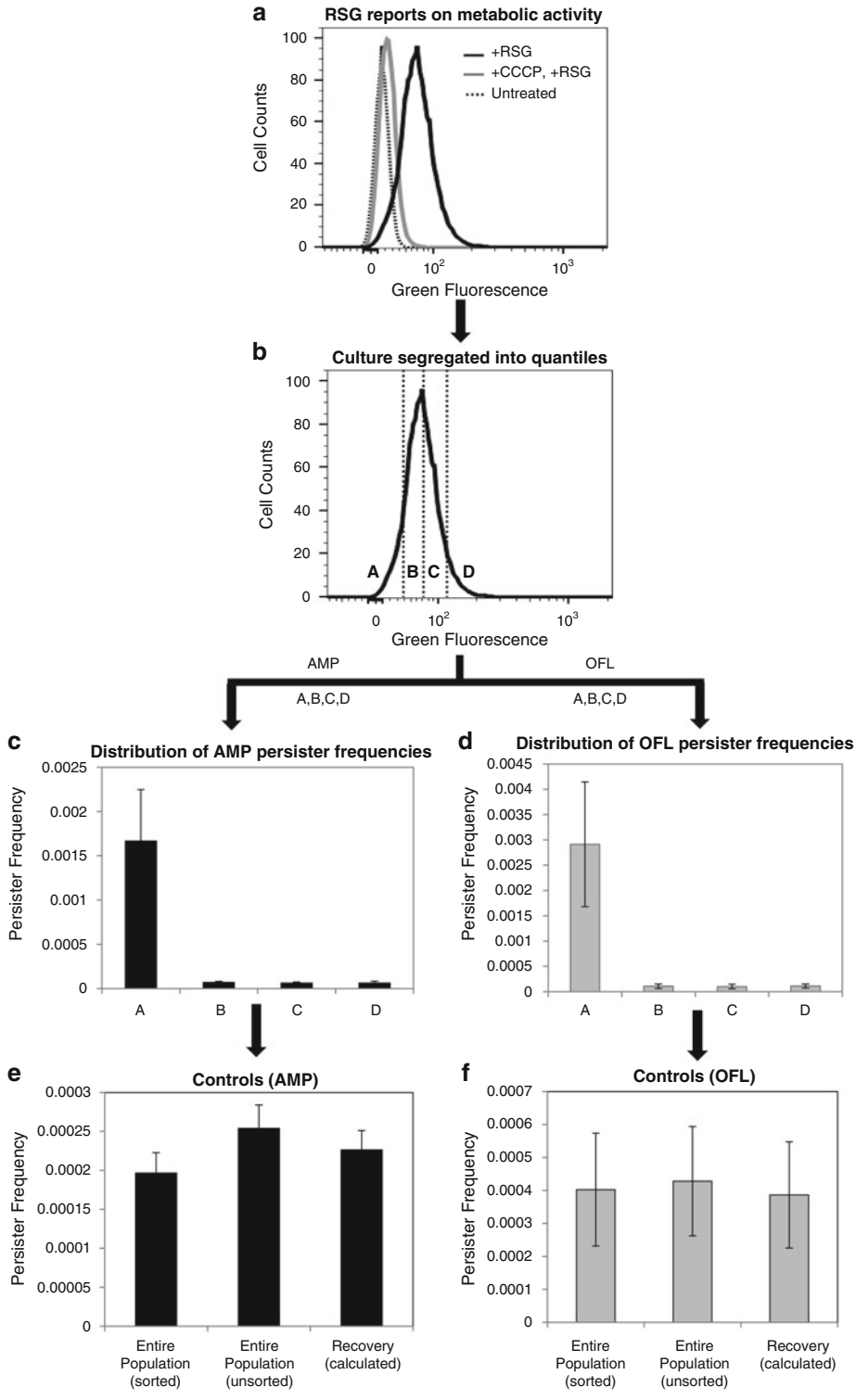

Fig. 2 FACS method to study persister metabolism. (**a**) Exponential phase cells (*E. coli* MG1655::Δ*cyoA*) were stained with RSG. RSG produces a stable green fluorescent signal when reduced by bacterial reductases. Staining was diminished when cells were pre-treated with CCCP, which depletes proton motive force.

2.2 Media

1. LB medium: Dissolve 10 g tryptone, 5 g yeast extract and 10 g NaCl in 1 L deionized (dI) water, and autoclave for 30 min at 121 °C.
2. 2×-Concentrated LB medium: Dissolve 20 g tryptone, 10 g yeast extract and 10 g NaCl in 1 L dI water, and autoclave for 30 min at 121 °C. Only 1× NaCl is included in this medium, as the 2×-concentrated LB is mixed with PBS, which contains NaCl.
3. LB agar plates: Add 15 g pure agar powder to 1 L LB medium. Autoclave 30 min at 121 °C and allow the medium to cool to 50–60 °C. Pour approximately 30 mL LB agar into each square Petri dish.

2.3 Persister Assay

1. Antibiotics: 5 μg/mL Ofloxacin (OFL) [19] or 200 μg/mL Ampicillin (AMP) [7]. To generate a 5 mg/mL OFL stock solution, the solution was titrated with sodium hydroxide (1 M, dissolved in sterile dI H_2O) to fully dissolve the OFL, and then filter-sterilized and stored at 4 °C. The day of the experiment, a working solution of 500 microgram/mL OFL was generated by diluting the stock solution in sterile dI water. Sterile 20 mg/mL AMP solution in dI water was prepared freshly on each experimental day.
2. Phosphate-buffered saline (PBS): Dissolve 8 g of NaCl, 0.2 g of KCl, 1.44 g of Na_2HPO_4, 0.24 g of KH_2PO_4 in 800 mL of distilled water, adjust the pH to 7.4 with HCl, and then add distilled water to a total volume of 1 L. Filter sterilize and store at room temperature.
3. 96-Well round-bottom plates.
4. Tubes: test tubes (glass and/or polypropylene), microcentrifuge tubes (1.5 mL), 5 mL polystyrene round-bottom tubes, BD Falcon 35 μm cell strainer capped tubes.
5. 0.22 μm filter units.

Fig. 2 (continued) (**b**) RSG-stained cells were sorted from the indicated regions (gates) in order to quantify the persister distribution within the quantiles. Gates A, B, C, and D compromise 10, 40, 40, and 10 %, respectively, of the entire population. (**c**, **d**) Persister frequencies were quantified after 5 h antibiotic treatment of FACS sorted cells from regions A, B, C, and D. The frequency is the ratio of persisters to initial number of FACS sorted cells. (**e**, **f**) Persister frequencies in control samples were similarly quantified after 5 h antibiotic treatment. "Entire population (sorted)" corresponds to samples that were sorted without gating, "Entire population (unsorted)" corresponds to samples that did not enter the sorter, and "Recovery (calculated)" is the frequency of persisters one would expect from the total population, as calculated from the persister frequencies measured from the segregated quantiles (A, B, C, D). We note that these three quantities should be indistinguishable from one another. Genetic deletion for MG1655::*ΔcyoA* strain was transduced from the Keio collection using the standard P1 phage method [33] and the mutation was confirmed with PCR

3 Methods

3.1 Fluorophore Selection

Here we describe the use of two fluorophores to study persister physiology: Redox sensor green (RSG), which is a metabolic stain, and mCherry, a fluorescent protein (FP). RSG is a fluorogenic redox indicator that yields green fluorescence when reduced by bacterial reductases. Unlike tetrazolium salts, such as 5-cyano-2,3-ditolyl tetrazolium chloride (CTC), that are reduced to an insoluble, fluorescent formazan product, RSG is nontoxic and does not suppress cellular metabolism [10, 20–22]. FPs can be used to monitor numerous cellular properties including promoter activity (transcriptional fusion), protein abundance (translational fusion), and cell division (FP dilution due to growth) [8, 10, 14, 16, 17]. Here we describe the use of mCherry as a cell division reporter, where its expression is controlled by a synthetic, chromosomally integrated expression system that is induced by isopropyl β-D-1-thiogalactopyranoside (IPTG) [10]. Cell division is monitored by fully inducing the expression system and then transferring cells to an inducer-free environment. mCherry is stable in *E. coli* during the time course of experiments, and therefore, a reduction in fluorescence would be accomplished by dilution through cell division. In general, fluorophores used to study persister physiology should have negligible impact on culturability or persister levels. Below are template protocols to determine whether a fluorescent stain or protein can be used in persistence studies. We note that persisters are enumerated by measuring CFUs within the second regime of a biphasic kill curve [4, 19]. To illustrate, Fig. 1 depicts biphasic kill curves of *E. coli* cultures treated with either OFL or AMP. The first, rapid-killing regime depicts normal cell dying (I), whereas the second phase of killing demonstrates the presence of persisters (II). Therefore, to measure persisters it is important to establish that antibiotic treatments yield biphasic killing, otherwise the CFUs counted may not reflect the abundance of persisters in a population. It is also important to note that the killing rate of persisters need not be zero, it must only deviate significantly from that of normal cells (first regime of biphasic kill curve).

3.1.1 Determination of the Impact of a Fluorescent Stain on Culturability and Persistence

1. Prepare an overnight (O/N) culture by inoculating cells from a 25 % glycerol, −80 °C stock into 2 mL medium in a test tube, and then incubate the culture at 37 °C with shaking (250 rpm). We generally use 16 or 24 h O/N.
2. Dilute O/N cultures in fresh medium to desired optical density (OD_{600}), we suggest ≤ 0.01, and grow until desired OD_{600} is reached (we prefer $OD_{600} \sim 0.1$).

3. Place a 1 mL aliquot of the exponential phase culture into a test tube (*see* **Note 1**).
4. Remove 10 μL of the sample and serially dilute into 90 μL PBS. Plate tenfold dilutions of this untreated sample onto LB agar plates (*see* **Note 2**). CFUs from this sample will enumerate the number of cells in the culture before RSG treatment. For ease of serial dilutions, we recommend using a 96-well round-bottom plate, with each well containing 90 μL PBS.
5. Add 1 μL of 1 mM RSG into 1 mL of cell culture in 5 mL polystyrene tubes and incubate in the dark at room temperature for approximately 30 min. For an unstained cell culture control, incubate 1 mL of diluted culture in the dark at room temperature for 30 min without staining.
6. Remove 10 μL of the samples from both stained and unstained cultures, serially dilute into 90 μL PBS, and plate onto LB agar. CFUs from these samples will enumerate the number of cells in the cultures after RSG treatment. This determines the impact of RSG staining on culturability.
7. Add 10 μL of a freshly prepared stock solution of antibiotic at 100× the treatment concentration (*see* **Note 3**) into both stained and unstained cell cultures. Be sure to add antibiotic directly to liquid, and gently shake the tube several times so that the antibiotic is evenly dispersed and any cells that may be on the side of the tube are washed into the liquid sample.
8. Incubate the sample at 37 °C with shaking at 250 rpm.
9. At desired time points during the treatment, transfer the 1 mL aliquot from one test tube to a microcentrifuge tube.
10. Centrifuge at 21,130 × *g* for 3 min in a microcentrifuge.
11. Remove 900 μL of supernatant.
12. Add 900 μL of PBS.
13. Repeat **steps 10–12** until the antibiotic concentration is below the MIC. Do not add PBS to the last wash. Rather, resuspend the pellet in the remaining 100 μL PBS (*see* **Note 4**), resulting in a 10×-concentrated sample, and then serially dilute 10 μL of this cell suspension into 90 μL PBS.
14. Plate 10 μL of serial dilutions of the 10×-concentrated sample on LB agar plates.
15. In order to increase the limit of detection, plate the remaining 80 μL of the 10×-concentrated sample onto another LB agar plate.
16. Incubate plates at 37 °C for 16 h.
17. Count CFUs in both the treated and untreated samples (*see* **Note 5**). Account for the 10× concentration of the treated samples and the dilution of the untreated sample. Biphasic kill curves are generated by plotting the CFU values in logarithmic scale with respect to duration of antibiotic treatment.

3.1.2 Determination of the Impact of a FP Cell Division Reporter on Culturability and Persistence

Perform the following protocol on both FP-expressing cells and cells not expressing FP (wild-type cells):

1. Prepare an O/N culture by inoculating cells from a 25 % glycerol, −80 °C stock into 2 mL medium in a test tube with an inducer (1 mM IPTG), and then incubate the culture at 37 °C with shaking (250 rpm) for the desired O/N duration.
2. Remove the inducer by centrifuging 1 mL of O/N culture for 3 min at 21,130 × *g*, and then removing the supernatant. Resuspend the cell pellet in 1 mL of fresh medium.
3. Dilute the resuspended cells in fresh medium ($OD_{600} \leq 0.01$) and culture at 37 °C with shaking (250 rpm).
4. Take 1 mL samples at desired time points from the exponential phase cultures.
5. Remove 10 μL of the samples from both cultures, serially dilute into 90 μL PBS, and plate onto LB agar. CFUs from these samples will enumerate the number of cells in the cultures before antibiotic treatment. This also determines the impact of an FP on culturability.
6. Follow **steps 7–17** in Subheading 3.1.1 to determine the persister levels in cultures of both the FP expressing and wild-type strains.

An additional fluorophore characteristic to be mindful of is whether its fluorescence can exceed that of bacterial autofluorescence; fluorescence approaching that of autofluorescence would not reflect a physiological property. The fluorophore must also be compatible with the excitation and emission capabilities of the intended FACS system. Also, for two-color or higher-dimensional sorting experiments, the fluorophore should be chosen to minimize overlap of emission spectra, and appropriate single color control samples should be used to compensate for any fluorescence spillover caused by spectral overlap. For example, it is well known that fluorescein isothiocyanate (FITC) and R-phycoerythrin (PE) produce fluorescence that can be detected by photomultiplier tubes receiving emitted fluorescence through 525 nm (green) and 575 nm (orange) bandpass filters, respectively. Single-stained samples can be used to determine the percentages of total FITC or PE fluorescence signals that spillover into the opposite detection channel and then can be appropriately subtracted out of subsequent double-stained samples.

3.2 Initial Estimate of the Number of Cells Needed to Be Sorted to Quantify Persister Physiology

The fraction of persisters in a bacterial population can vary, often between 1 in 10^2 and 10^6, depending on the strain and environment of interest. To ensure that sufficient cells will be sorted to draw conclusions on the physiology of the persister subpopulation, persister levels under conditions identical to those that will be used on the sorted samples should be measured. Our experience has shown that >100 persisters in the entire sorted population are desirable and can yield statistical significance between sorted fractions. A general protocol to perform this experiment is outlined below.

3.2.1 Preliminary Experiment to Identify the Number of Cells Needed to Study Persister Physiology with Sorting

1. Follow **steps 1–17** in Subheading 3.1.1 to determine the number of persisters in both RSG-stained and unstained cultures (*see* **Note 6**).
2. Follow **steps 1–6** in Subheading 3.1.2 to determine the number of persisters in both wild-type and FP-expressing strain cultures (*see* **Note 6**).
3. Determine the persister fractions in the cultures by taking into account the CFUs at $t = 0$ h and $t = 5$ h during the antibiotic treatment (in our studies, 5 h treatment is sufficient to reach the second killing regime within biphasic kill curves of exponential *E. coli* cultures).

3.3 Sample Preparation for FACS

3.3.1 RSG Staining

1. Prepare O/N and exponential phase cultures as indicated in **steps 1**, **2** in Subheading 3.1.1.
2. If necessary, dilute the cells at desired growth stage in filter-sterilized spent medium from the same culture, i.e., medium in which the cells have been previously grown, to obtain a cell density of approximately 10^7 cells/mL. The cell density should not exceed this value to prevent clogging of the cell sorter.
3. Add 1 μL of 1 mM RSG into 1 mL of diluted cell cultures in 5 mL polystyrene tubes and incubate in the dark at room temperature for approximately 30 min before sorting. This sample can also be used as a positive control. Keep 1 mL of unstained cell culture as a negative control for FACS analysis.
4. As controls, add 2 μL of 5 mM carbonyl cyanide m-chlorophenyl hydrazine (CCCP) or 1 μL of 1 mM potassium cyanide (KCN) into 1 mL of diluted cell cultures for 5 min prior to addition of RSG. The final concentrations of CCCP and KCN in the cultures should be 10 μM and 1 mM, respectively. KCN blocks respiration, and CCCP depletes proton motive force; therefore, pretreatment of cells with these inhibitors should reduce green fluorescence.

3.3.2 Cell Division Assay Using FP

1. Prepare O/N and exponential phase cultures as indicated in **steps 1–3** in Subheading 3.1.2.
2. Take 1 mL samples at desired time points from the exponential phase culture to sort population based on cell division. If necessary, dilute the cells in filter-sterilized spent medium to obtain a cell density of approximately 10^7 cells/mL.

3. For a positive control, dilute fully induced O/N culture (*see* **step 1** in Subheading 3.1.2) in filter-sterilized spent medium to reach a desired cell density for flow cytometric analysis (~10^7 cells/mL). This control is used to determine the gating for non-growing subpopulations.
4. For a negative control, incubate the cells without IPTG during the O/N growth, and inoculate in fresh medium without inducer as described above.
5. To verify that the FP is not degraded during the timeframe of the experiment, dilute the washed O/N culture from **step 1** in fresh medium with 50 μg/mL Chloramphenicol (CAM) (to inhibit protein synthesis) and culture at desired conditions, and then analyze 1 mL samples with FACS.

3.4 FACS

We note that a basic working knowledge of flow cytometry and cell sorting is recommended prior to setting up and conducting FACS experiments [23–26]. Prior to execution of the experiment, the internal tubing of the FACS instrument should be cleaned to ensure it is free from contaminating bacteria or particulate matter. Refer to manufacturer guidelines for proper system sterilization for your instrument (*see* **Note 7**). Additionally, consideration must be given to the risk factor group and biosafety level designation of the organisms to be sorted. Cell sorting creates aerosols through droplet formation causing the potential risk for inhalation exposure, and the system can be under high pressure increasing the risk of splash exposure to liquids [27–29]. Biosafety professionals should be consulted and proper precautions should be in place prior to conducting any FACS experiments.

When studying *E. coli* with FACS, care must be taken during system setup and alignment to ensure the proper differentiation between actual particles (*E. coli*) and electronic noise, since the size of *E. coli* approaches the limit of detection of many commercially available FACS systems. Electronic noise is seen as background signal present without cellular material running on the instrument (e.g., 0.22 μm-filtered PBS) at a given set of conditions and can be affected by many factors. Photomultiplier tube (PMT) voltage and system threshold settings must be optimized to eliminate and/or minimize any signal contribution from electronic noise.

3.4.1 FACS Method

1. Start up FACS system and give proper time for lasers to warm up and the stream to stabilize according to the manufacturer's recommendations (*see* **Note 8**). A 488 nm laser and ~530 nm detection filter are required for RSG detection, whereas a 561 nm laser and ~600 nm detection filter are required for mCherry detection. Consult references or a flow cytometry specialist for proper setup choices for other dyes or FPs.

2. Align laser(s) and determine the proper droplet breakoff as per manufacturer's recommendations for your system. Consult vendor or professional cytometrist as needed.
3. Set forward scatter (FSC), side scatter (SSC), and appropriate fluorescence parameters to log scale (*see* **Note 9**).
4. Create FSC-A versus SSC-A and desired fluorescence parameter plots in acquisition software (*see* **Note 10**).
5. Place a tube of clean, particle-free PBS (0.22 μm-filtered) on the system as a sample and run.
6. Adjust FSC PMT voltage, SSC PMT voltage, and SSC threshold values while PBS is running to minimize electronic noise signal detected (*see* **Note 11**).
7. Remove PBS tube and rinse the sample uptake line with clean dI water.
8. Place a tube of live, non-fluorescent, exponential phase *E. coli* cells (e.g., unstained, non-FP expressing) on the system and adjust FSC and SSC PMT voltage settings so that cells are on scale and electronic noise remains low (*see* **Notes 12** and **13**) (Fig. 3). Make sure that the sample concentration is optimized for your FACS system setup. We have found that cell concentrations ~10^7/mL or less work well (*see* **Note 14**).

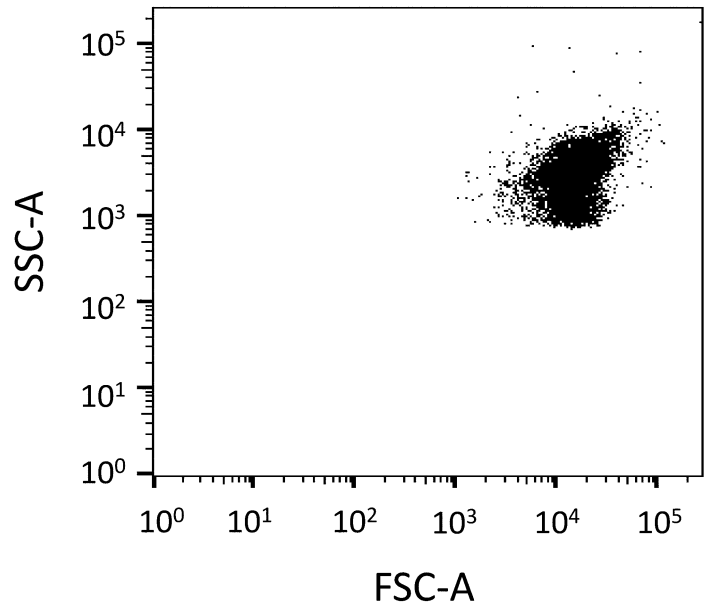

Fig. 3 SSC-A versus FSC-A dot-plot. FSC and SSC PMT voltage settings are adjusted so that exponential phase *E. coli* cells (unstained, non-FP expressing) are on SSC-A and FSC-A scales. Each dot represents a cell

9. Rinse the sample uptake line with clean dI water and re-sample the PBS. Confirm that there is little (normally less than 100 events/s) signal contribution from electronic noise.
10. Remove the PBS tube and run non-fluorescent *E. coli* cells (negative control: unstained, non-FP expressing) to evaluate cellular autofluorescence. Adjust fluorescence parameter PMT voltage setting(s) to place the signal from this negative control sample toward the lower end of the scale for each fluorescent signal to be detected.
11. Run positive controls (*see* Subheading 3.3) to check if sorter can detect the fluorescence signals. Adjust the fluorescence parameter PMT voltage settings if the positive signal is off scale (too bright). Rerun the negative control sample at the new PMT voltage setting.
12. Run additional controls to verify that RSG reports on metabolic activity (*see* Subheading 3.3.1) (Fig. 2a), or FP is not degraded during the time frame of the experiment (*see* Subheading 3.3.2) (representative images of this control can be found in Fig. S2 of ref. [10]).
13. Run test samples to be sorted (*see* **Note 15**). Assign sort gates via acquisition software, insert clean collection tubes, and begin sorting (*see* **Note 16**).
14. To evaluate the purity of post-sort fractions, rinse the sample lines well with clean dI water or PBS after sorting and then run a small amount of each quantile. To ensure proper analysis, be sure to rinse well between each sample (*see* **Note 17**).

3.5 Culturability and Persistence Assays on Sorted Samples

Following sorting, bacterial cells from their respective quantiles are suspended in sheath fluid, which is usually PBS, and these cell suspensions will be used to measure both culturability and the abundance of persisters within the quantiles (*see* **Note 18**).

3.5.1 Persistence and Culturability Assays on Sorted Fractions

1. After the total number of cells (T) have been isolated from each quantile, mix the collected sample with an equal volume of 2×-concentrated fresh LB medium in a test tube (*see* **Notes 19** and **20**). If the total volume (V) will be >2 mL, we recommend using a 50 mL Falcon tube for treatment to ensure proper aeration of the sample.

   For Controls

   - Dilute approximately T number of cells from the culture (without sorting) into V volume of a 2×-concentrated LB medium/PBS mixture (mixed at equal volumes) to analyze the effects of flow through the sorter on persister levels.
   - Dilute approximately T number of cells from the culture (without sorting) into V volume of fresh 1× LB medium to

examine the effects of the medium/PBS mixture when compared to medium only on persister levels.

- Collect T number of cells using FACS (from the entire population without segregating) and mix the collected sample at equal volume with 2×-concentrated LB medium to analyze the effects of segregation on persister levels (*see* **Note 21**).

2. Remove 10 μL from the samples and serially dilute into 90 μL PBS. Plate serial tenfold dilutions of these untreated samples onto LB agar plates. CFUs from this sample will enumerate the number of cells in the cultures before treatment ($t = 0$ h).
3. Add the appropriate volume of freshly prepared 100×-concentrated antibiotic to the samples (*see* **Note 3**).
4. Incubate the samples at 37 °C with shaking at 250 rpm.
5. Remove the samples from the shaker at desired time points.
6. If the volume of sample is less than 2 mL, transfer sample to a microcentrifuge tube and go to **step 8**.
7. If the volume of the sample is greater than 2 mL, transfer sample to a 15 mL Falcon tube. Spin at 3,220 × *g* for 15 min. Remove all but 1 mL supernatant. Resuspend the pellet in the 1 mL and transfer to a microcentrifuge tube.
8. Spin at 21,130 × *g* for 3 min. Remove all but 100 μL supernatant. Resuspend the pellet in the 100 μL.
9. Add 900 μL PBS.
10. Repeat **steps 8** and **9** until the antibiotic concentration is below the MIC. Resuspend the pellet in the remaining 100 μL PBS, resulting in a concentrated sample, and then serially dilute 10 μL of this cell suspension into 90 μL PBS.
11. Plate serial dilutions of the concentrated samples on LB agar plates.
12. In order to increase the limit of detection, plate the remaining 80 μL of the concentrated samples onto another agar plate.
13. Incubate plates at 37 °C for 16 h and count the CFUs by taking into account the concentration factor.
14. Repeat **steps 1–13** for unstained cells (control of RSG staining) and un-induced cells (control of FP expression) (*see* **Note 22**).

4 Notes

1. The number of test tubes depends on the duration of treatment. For each time point, one test tube is used. We have found that 5 h of treatment results in biphasic killing of *E. coli* growing in LB [4]. We reiterate that one must ensure that the

duration of antibiotic treatment is long enough to measure CFUs within the second regimen of a biphasic kill curve.

2. Agar plates should be dried 1–2 days at room temperature to ensure that 10 μL spots do not run together when plated.
3. Treat samples with a concentration of antibiotic that is many-fold higher than the minimum inhibitory concentration (MIC) of the strain. The MIC of the strain may be determined by a broth dilution method [30] or an agar method [31]. We have determined the MIC of our strains to be ~0.075–0.15 μg/mL OFL and 1.5–3 μg/mL AMP. Our antibiotic treatment concentrations for persister assays are 5 μg/mL OFL or 200 μg/mL AMP.
4. It is optimal to have a volume of exactly 100 μL, not simply an approximation. Therefore, we recommend measuring the amount of liquid with the pipet tip, and adjusting the volume.
5. We generally count spots containing 10–100 CFUs [32].
6. Note that since we use sterile-filtered PBS as a sheath fluid in FACS, sorted samples are suspended in PBS, and antibiotic treatments are done in a mixture of PBS and 2× LB medium. We have found that treatment in the PBS/2× LB mixture results in persister fractions comparable to those of samples treated in 1× LB for exponential phase cultures (OD_{600} ~ 0.1), and therefore, our preliminary experiments were done using 1× LB. However, one may wish to perform the preliminary experiments in Subheading 3.2.1 by treating in a PBS/2× LB mixture, so that the conditions more accurately represent those that are used with FACS.
7. A sample of sheath fluid can be taken from the sheath fluid stream directly above the waste catcher on the front of the instrument and placed into culture medium for incubation to confirm the cleanliness of the system.
8. We perform sorting with a FACSVantage SE w/DiVa (BD Biosciences, San Jose, CA) with a 70 μm nozzle at 16 psi and the following settings: frequency 32.3, amplitude 27.5, phase 10, drop delay 14.75. Purity precision sort mode is used. All system settings are unique to each FACS instrument and sort setup should be optimized and tested for your specific system prior to conducting all sort experiments.
9. FSC and SSC are measurements taken from the amount of laser light scattered from the interrogating laser beam as each particle (cell, debris, or aggregates of cells) passes through. FSC is affected more by the cross-sectional area and refractive index of the cell, whereas SSC is related to the granularity or internal complexity of a cell [24]. Using log scale for FSC and SSC is helpful when looking at small particles such as bacteria.

10. One may also wish to create one or more doublet discrimination plots. Doublets (two cells stuck together) and/or aggregates of cells can be a confounding factor in FACS. Pulse processing analysis allows one to reduce the likelihood of doublets/clumps in subsequent analysis plots by gating on discrimination plots (FSC-W vs. FSC-A and/or SSC-W vs. SSC-A). Each particle passing through the laser beam creates a peak pulse in all activated detection parameters. The width (W) signal displays the duration of the peak pulse; the height (H) signal, the maximum light; and the area (A) signal, the total light detected. Since the *E. coli* samples we used had insignificant cell aggregation, we did not cover this section in detail. See reference [24] for specifics.
11. To minimize the electronic noise signal detected, set the SSC threshold value slightly above the minimum allowable value for your system and lower the FSC & SSC PMT voltage values until event rate falls below 100 events per second. In systems that allow dual threshold parameters one may also wish to activate the FSC threshold as well to better address the elimination of system noise from the analysis.
12. One may use 1 μm sized beads, which are similar in size to *E. coli*, rather than cells to adjust the PMT voltages and make sure that the sorter detects the signal from these events. In order to create the bead sample, dilute 5 μL Fluoresbrite Plain YG 1 μm beads or equivalent in 2 mL PBS. Filter bead suspension through a 35 μm mesh cell strainer to remove any aggregates.
13. Observe the events/second of the cells or beads alone. As one adjusts the FSC and SSC voltages, the event rate will spike (often to tens of thousands events/s) when noise is detected. Lower the voltage(s) until noise signal disappears and event rate decreases.
14. Samples that are too concentrated can cause difficulty in system setup and performance. If fluorescence signal drifts while running (moves from high to low to high again), remove sample and dilute.
15. Data files of all test and control samples should be recorded to generate flow diagrams. Once PMT voltage values are optimized using control samples, all test samples should be recorded using the same voltage values.
16. Sort into appropriate culture medium or simply collect droplets containing sorted cells into empty tubes. We sort at room temperature, but some sorters are equipped with temperature control options for both the sample and collection tubes if needed.
17. Transfer a small amount of each sorted fraction to a clean tube for reanalysis to avoid any risk of mixing sorted samples. Also

be advised that any electronic noise contribution from the system will lower the sort fraction purity values displayed. Compare sort check data to PBS only sample to draw conclusions as to the level of success obtained for each sorted fraction.

18. The FACS procedure might affect the culturability of the cells. Therefore, once sorting parameters (such as pressure and flow rate) have been optimized, the culturability of cells being sorted should be checked by plating a number of cells immediately after sorting. We identified that more than 80 % of the cells from exponentially growing cultures in LB sorted with FACS with the indicated parameters in **Note 8** can form CFUs.
19. Under our conditions, adding 2×-concentrated LB to the cell samples sorted into PBS does not change persister fractions from samples treated in 1×-LB.
20. If the cells are sorted into a large volume of PBS, one may wish to remove the excessive PBS by centrifugation.
21. As an internal consistency check, we calculate the Recovery (R), which is the frequency of persisters in the total population as calculated from the segregated quantiles. If the entire cell population is divided into four different quantiles (A, B, C, D), the recovery is calculated as follows:

$$R = p_A f_A + p_B f_B + p_C f_C + p_D f_D$$

where p_A is the proportion of the total population in the A quantile and f_A is the frequency of persisters in the A quantile (note that $p_A + p_B + p_C + p_D = 1$). The R should equal the frequency of persisters obtained from a non-segregated sample.

22. We have used a two-tailed t-test to perform a pairwise comparison of the persister fractions that result from the sort quantiles [10]. We have already confirmed that the CFU measurements performed for persister assays were normally distributed by using a larger sample data set and the Anderson–Darling and Shapiro–Wilk tests [16].

Acknowledgements

This work was supported by the Department of the Army under award number W81XWH-12-2-0138 and the National Institute of Allergy and Infectious Diseases of the National Institutes of Health under award number R21AI105342. The content is solely the responsibility of the authors and does not necessarily represent the official views of the funding agencies.

References

1. Amato SM, Fazen CH, Henry TC et al (2014) The role of metabolism in bacterial persistence. Front Microbiol 5:70
2. Kint CI, Verstraeten N, Fauvart M et al (2012) New-found fundamentals of bacterial persistence. Trends Microbiol 20 (12):577–585
3. Balaban NQ, Merrin J, Chait R et al (2004) Bacterial persistence as a phenotypic switch. Science 305(5690):1622–1625
4. Lewis K (2010) Persister cells. In: Gottesman S, Harwood CS (eds) Annual review of microbiology, vol 64. Annual Reviews, Palo Alto, pp 357–372
5. Lewis K (2007) Persister cells, dormancy and infectious disease. Nat Rev Microbiol 5 (1):48–56
6. Fauvart M, De Groote VN, Michiels J (2011) Role of persister cells in chronic infections: clinical relevance and perspectives on anti-persister therapies. J Med Microbiol 60(Pt 6):699–709
7. Joers A, Kaldalu N, Tenson T (2010) The frequency of persisters in *Escherichia coli* reflects the kinetics of awakening from dormancy. J Bacteriol 192(13):3379–3384
8. Roostalu J, Jõers A, Luidalepp H et al (2008) Cell division in *Escherichia coli* cultures monitored at single cell resolution. BMC Microbiol 8:68
9. Orman MA, Brynildsen MP (2013) Establishment of a method to rapidly assay bacterial persister metabolism. Antimicrob Agents Chemother 57(9):4398–4409
10. Orman MA, Brynildsen MP (2013) Dormancy is not necessary or sufficient for bacterial persistence. Antimicrob Agents Chemother 57 (7):3230–3239
11. Wakamoto Y, Dhar N, Chait R et al (2013) Dynamic persistence of antibiotic-stressed mycobacteria. Science 339(6115):91–95
12. Oliver JD (2005) The viable but nonculturable state in bacteria. J Microbiol 43 Spec No:93–100
13. Keren I, Shah D, Spoering A et al (2004) Specialized persister cells and the mechanism of multidrug tolerance in Escherichia coli. J Bacteriol 186(24):8172–8180
14. Shah D, Zhang Z, Khodursky A et al (2006) Persisters: a distinct physiological state of E. coli. BMC Microbiol 6:53
15. Canas-Duarte SJ, Restrepo S, Pedraza JM (2014) Novel protocol for persister cells isolation. PLoS One 9(2):e88660
16. Amato SM, Orman MA, Brynildsen MP (2013) Metabolic control of persister formation in *Escherichia coli*. Mol Cell 50 (4):475–487
17. Vega NM, Allison KR, Khalil AS et al (2012) Signaling-mediated bacterial persister formation. Nat Chem Biol 8(5):431–433
18. Allison KR, Brynildsen MP, Collins JJ (2011) Heterogeneous bacterial persisters and engineering approaches to eliminate them. Curr Opin Microbiol 14(5):593–598
19. Keren I, Kaldalu N, Spoering A et al (2004) Persister cells and tolerance to antimicrobials. FEMS Microbiol Let 230(1):13–18
20. Kalyuzhnaya MG, Lidstrom ME, Chistoserdova L (2008) Real-time detection of actively metabolizing microbes by redox sensing as applied to methylotroph populations in Lake Washington. ISME J 2(7):696–706
21. Ullrich S, Karrasch B, Hoppe HG et al (1996) Toxic effects on bacterial metabolism of the redox dye 5-cyano-2,3-ditolyl tetrazolium chloride. Appl Environ Microbiol 62 (12):4587–4593
22. Gray DR, Yue S, Chueng CY et al (2005) Bacterial vitality detected by a novel fluorogenic redox dye using flow cytometry. Abstr Gen Meet Am Soc Microbiol 105:331
23. Arnold LW, Lannigan J (2010) Practical issues in high-speed cell sorting. Curr Protoc Cytom Chapter 1, Unit 1.24.1-30
24. Givan A (2001) Flow cytometry: first principles, 2nd edn. Wiley-Liss, New York
25. Shapiro H (2003) Practical flow cytometry: fourth edition. Wiley-Liss, New York
26. Ormerod M (2000) Flow cytometry: a practical approach. Oxford University Press, New York
27. Holmes KL, Fontes B, Hogarth P et al (2014) International Society for the Advancement of Cytometry cell sorter biosafety standards. Cytom A 85(5):434–453
28. Schmid I, Nicholson JK, Giorgi JV et al (1997) Biosafety guidelines for sorting of unfixed cells. Cytometry 28(2):99–117
29. Schmid I, Lambert C, Ambrozak D et al (2007) International Society for Analytical Cytology biosafety standard for sorting of unfixed cells. Cytom A 71(6):414–437

30. Ericsson HM, Sherris JC (1971) Antibiotic sensitivity testing. Report of an international collaborative study. Acta Pathol Microbiol Scand B Microbiol Immunol 217(Suppl 217):1+
31. Andrews JM (2001) Determination of minimum inhibitory concentrations. J Antimicrob Chemother 48(Suppl 1):5–16
32. Kohanski MA, Dwyer DJ, Hayete B et al (2007) A common mechanism of cellular death induced by bactericidal antibiotics. Cell 130(5):797–810
33. Baba T, Ara T, Hasegawa M et al (2006) Construction of Escherichia coli K-12 in-frame, single-gene knockout mutants: the Keio collection. Mol Syst Biol 2(2006):0008

Chapter 9

Single-Cell Detection and Collection of Persister Bacteria in a Directly Accessible Femtoliter Droplet Array

Ryota Iino, Shouichi Sakakihara, Yoshimi Matsumoto, and Kunihiko Nishino

Abstract

A directly accessible femtoliter droplet array as a platform for single-cell detection and collection of persister bacteria is described. Device microfabrication, femtoliter droplet array formation and concomitant enclosure of single cells, long-term culture and observation of single cells in droplets, and collection of identified persisters from single droplets are described in detail.

Keywords: Microfabrication, Microdevice, Microdroplet array, Single-cell analysis, Drug tolerance, Persister, *Pseudomonas aeruginosa*, Optical microscopy, Micropipette

1 Introduction

Persisters, which constitute a small proportion (typically less than 1 %) of bacterial populations, are naturally insensitive (tolerant) to multiple antibiotics despite having the same genotype as the sensitive majority [1–5]. Single-cell analysis of bacteria using microfabricated devices allows for the identification of very rare cells with properties that differ from those of the majority [6], and has contributed to the understanding of fundamentals of bacterial persistence [7, 8]. However, most microdevices used are based on microfluidic channels and valves, or microdroplets generated in a microfluidic channel. The closed nature of these systems makes the recovery and subsequent use of cells from the device difficult.

Here, we describe the single-cell detection and collection of persisters in a directly accessible femtoliter droplet array [9–11]. Our method allows for individual bacterial cells to be enclosed and isolated, cultured in droplets for the long term, and finally allows for persisters to be collected and identified. Preparation of the hydrophilic-in-hydrophobic micropatterned glass substrate, assembly of the microdevice, formation of the femtoliter droplet array

Jan Michiels and Maarten Fauvart (eds.), *Bacterial Persistence: Methods and Protocols*, Methods in Molecular Biology, vol. 1333, DOI 10.1007/978-1-4939-2854-5_9,

concomitant with enclosure of single cells of *Pseudomonas aeruginosa* in each droplet, cell culture and microscopic observation in droplets, and collection of the identified persisters from single droplets using a micropipette are described.

2 Materials

2.1 Microdevice Components

1. Electron beam resist (ZEP520A, ZEON).
2. Electron beam resist thinner (ZEP-A, ZEON).
3. Chromium mask blanks (2.5 in. in diameter, Clean Surface Technology Co.).
4. Spin coater (MS-A100, Mikasa).
5. Electron beam lithography system (JSM 6390, JEOL and SPG 724, Sanyu Electron).
6. Electron beam resist developer (ZED-N50, ZEON).
7. Electron beam resist rinse (ZMD-B, ZEON).
8. Chromium etchant (Kanto Chemical).
9. Electron beam resist remover (ZDMAC, ZEON).
10. Microscope coverslips (30 mm in diameter, ~0.17 mm in thickness).
11. Fluorinated polymer CYTOP (9 wt%, type M, Asahi Glass).
12. Photoresist (AZ P4903, AZ Electronic Materials) (*see* **Note 1**).
13. Photoresist developer (AZ 300MIF developer, AZ Electronic Materials).
14. Mask aligner (ES410s, SAN-EI ELECTRIC).
15. Reactive ion etching instrument (RIE-10NR, Samco).
16. Disposable plastic Petri dish (35 mm in diameter).
17. Drill press (~20 mm in diameter).
18. Epoxy adhesive (Araldite AR-R30, NICHIBAN).
19. Knife (K-35, HOZAN).
20. Bath-type sonicator.

2.2 Cells, Cell Enclosure, Cell Culture and Antibiotics Treatment Components

1. *Pseudomonas aeruginosa* strain PAO1.
2. Trypticase soy broth.
3. Carbenicillin, disodium salt.
4. Fluorinated oil (Fluorinert FC40, SIGMA-ALDRICH) (*see* **Note 2**).
5. Air displacement pipette.

2.3 Cell Collection Components

1. Inverted microscope.
2. Micromanipulator (MNM-21, Narishige).
3. Capillary (75 μL, Drummond Scientific).
4. Puller (Model PC10, Narishige).
5. Microforge (MF900, Narishige).
6. Pressure controller (Femtojet, Eppendorf).

3 Methods

3.1 Microfabrication and Construction of the Device

Carry out all procedures in a yellow clean room (Fig. 1).

3.1.1 Micropatterned Photomask Preparation

1. Dilute the electron beam resist 1.4-fold (w/w) with a thinner (*see* **Note 3**). Place the diluted electron beam resist on chromium mask blanks and spincoat it with a spin-coater using the following program:

   Slope 5 s.

   500 rpm 5 s.

   Slope 8 s.

   3500 rpm 60 s.

   Slope 5 s.

   End.
2. Bake at 180 °C for 3 min.

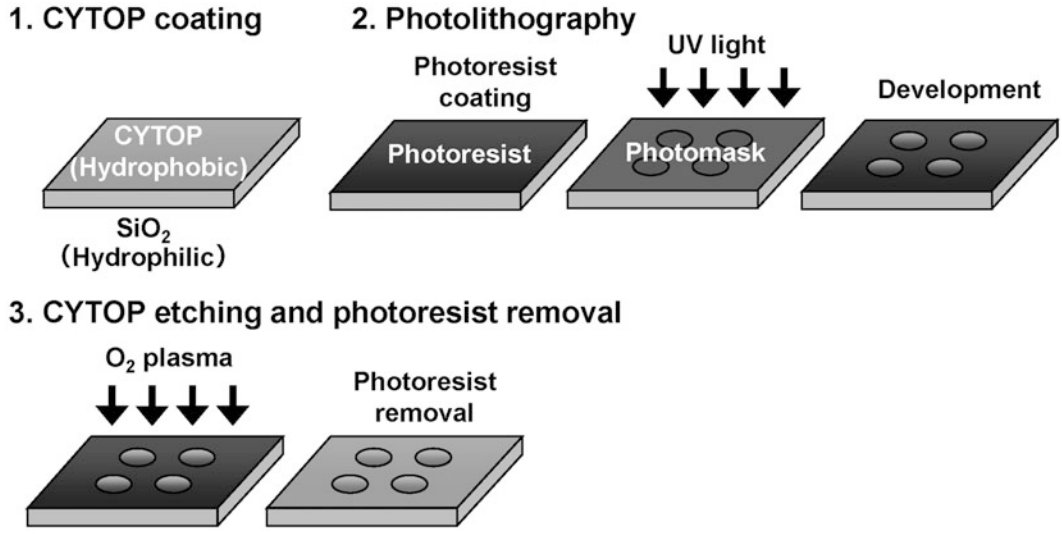

Fig. 1 Schematics showing the procedure of microfabrication

3. Place the resist-coated chromium mask blanks in the electron beam lithography system and carry out lithography under the following conditions:

   Dose: 72 μC/cm^2.

   Voltage: 30 keV.

   Current: 1000 pA.
4. Immerse the chromium mask blanks in electron beam resist developer for 1 min.
5. Rinse well with electron beam resist rinse and then isopropyl alcohol, and dry with a blower.
6. Wet-etch the surface with the chromium etchant (*see* **Note 4**).
7. Remove the electron beam resist using a remover.

3.1.2 CYTOP Coating

1. Wash the microscope coverslips with ethanol and ultrapure water for 5 min each using a bath-type sonicator. Dip the coverslips in 10 N KOH and leave overnight at room temperature. Wash well with ultrapure water, dry on a heated plate at 180 °C, and cool to room temperature.
2. Place 75 μL of CYTOP on the coverslip, and spincoat using the following program:

   Slope 2 s.

   500 rpm 5 s.

   Slope 8 s.

   2000 rpm 30 s (*see* **Note 5**).

   Slope 5 s.

   End.
3. Pre-bake at 80 °C for 30 min (*see* **Note 6**).
4. Bake at 180 °C for 1 h.

3.1.3 Photolithography

1. Place the photoresist (~10 mm in diameter) at the center of the CYTOP-coated glass (*see* **Note 7**). Spincoat using the following program:

   Slope 2 s.

   500 rpm 5 s.

   Slope 8 s.

   4000 rpm 30 s.

   4500 rpm 1 s (*see* **Note 8**).

   Slope 5 s.

   End.
2. Bake at 55 °C for 3 min.
3. Bake at 110 °C for 5 min.

4. Tightly contact the photomask with the substrate using the mask aligner, and irradiate with UV light for 35 s (*see* **Note 9**).
5. Immerse in developer for 6 min (*see* **Note 10**).
6. Rinse well with ultrapure water.

3.1.4 CYTOP Etching by Oxygen Plasma and Photoresist Removal

1. Place the photoresist-patterned coverslips into a reactive ion etching instrument, and dry-etch the CYTOP film with O_2 plasma using the following conditions:

   O_2: 50 sccm (standard cc/min).

   Pressure: 10 Pa.

   Power: 50 W.

   Time: 30 min.
2. Rinse the etched coverslips three times with acetone for 1 min each using a bath-type sonicator (*see* **Note 11**).
3. Rinse the etched coverslips with isopropyl alcohol once, and dry with a blower.

3.1.5 Device Assembly

1. Punch a hole in the bottom of the disposable plastic Petri dish using a drill press. Thoroughly remove burr with a knife, and wash with ultrapure water and ethanol for 5 min each in a bath-type sonicator. Dry at room temperature.
2. Coat the edge of the hole with the epoxy adhesive from the bottom of the Petri dish, and completely cover the hole with the hydrophilic-in-hydrophobic micropatterned coverslip (*see* **Note 12**). The coverslip should be orientated such that the CYTOP-coated surface is in contact with the epoxy adhesive.
3. Allow the Petri dish and the coverslip to completely adhere to one another overnight (Fig. 2).

3.2 Bacterial Cell Preparation and Antibiotic Treatment

1. Grow *Pseudomonas aeruginosa* PAO1 to late exponential phase (optical density at 600 nm [OD_{600}] ~1.0) in trypticase soy broth in a test tube at 37 °C.
2. Add carbenicillin (final concentration 5 mg/mL, ~100 times higher than the minimal inhibitory concentration) to the bacterial suspension (*see* **Note 13**), and incubate further for 3 h at 37 °C.
3. Collect the cells, wash them in fresh medium, and resuspend them in fresh medium (OD_{600} 0.2–0.6).

3.3 Formation of Femtoliter Droplet Array and Enclosure of Single Bacterial Cells (Fig. 3)

1. Completely cover the micropatterned coverslip in the device with the bacterial suspension prepared as described in Subheading 3.2. The volume of the bacterial suspension on the micropatterned coverslip must be as low as possible (*see* **Note 14**).

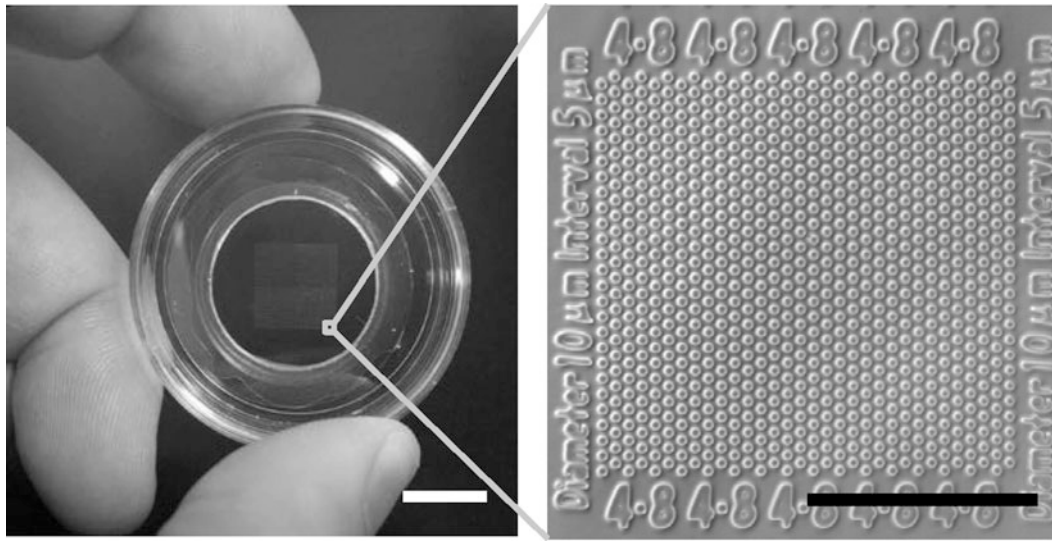

Fig. 2 (*Left*) Image of the assembled device. Scale bar, 10 mm. (*Right*) Microscopic image of the hydrophilic-in-hydrophobic micropatterned surface. Micropatterns are grouped into islands using numbers. This facilitates the identification of individual droplets and the cells enclosed in each droplet. Scale bar, 200 μm

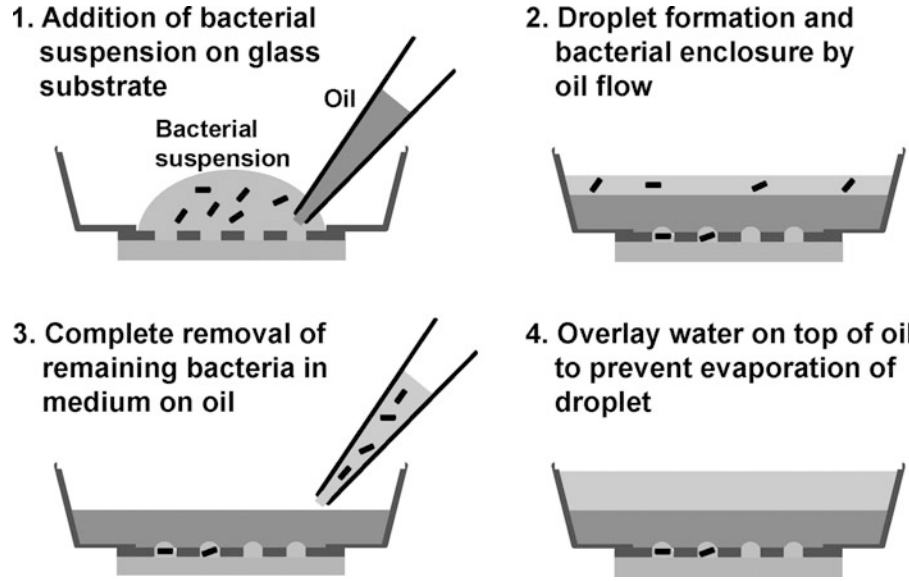

Fig. 3 Procedure of droplet formation and cell enclosure

2. Using an air displacement pipette, introduce 1 mL fluorinated oil into the culture medium near the glass surface. The hydrophilic SiO_2 glass surfaces will retain the medium and the bacteria, while the hydrophobic surfaces are replaced with oil. As a result, femtoliter droplets (3×10^5 droplets per 1 cm^2 for a 10 μm diameter droplet) containing zero, one, or more bacteria will form (*see* **Note 15**).

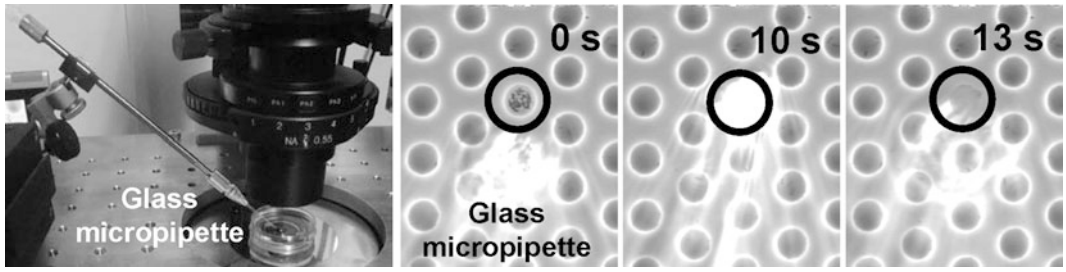

Fig. 4 (*Left*) Image of the micropipette used for droplet collection. (*Right*) Sequential images of droplet collection

3. Remove excess medium on the oil (the density of the fluorinated oil used exceeds that of water) and place ethanol on top of the oil layer. Repeat this procedure several times (*see* **Note 16**). Overlay ultrapure water on top of the oil layer to prevent evaporation of the droplet. Incubate the device at 37 °C for the required amount of time.

3.4 Collection of the Persister with Micropipette (Fig. 4)

1. Prepare a glass micropipette (inside aperture ~10 μm) from a capillary using a puller and a microforge.
2. Identify droplets containing bacteria by phase-contrast or bright-field optical microscopy.
3. Identify persister cells as those undergoing multiple cell divisions in a droplet using optical microscopy.
4. Collect the persister cells with a glass micropipette under an optical microscope. Fill the micropipette with medium, set the pressure to a positive value (several tens of hPa) (*see* **Note 17**), immerse the micropipette into the water layer on the oil and then into the oil layer approaching the droplet containing persister cells. When the micropipette is close to the droplet, reduce the pressure to zero and allow the tip of the glass micropipette to make contact with the droplet. The droplet will spontaneously be drawn into the glass micropipette by capillary force.
5. Dip the glass micropipette into the medium in the test tube and culture the collected cells at 37 °C.

4 Notes

1. Photolithography must be carried out with a high viscosity photoresist, as the CYTOP-coated surface has very low friction and thus cannot be fully covered with a low-viscosity photoresist.

2. For the formation of femtoliter droplet arrays and for subsequent procedures, fluorinated oil with a density higher than that of water is favored.
3. Dilution of electron beam resist with thinner results in a thinner coat, which allows for shorter processing times in electron beam lithography.
4. Chromium can be wet-etched with an aqueous solution of ceric ammonium nitrate; however, the use of commercially available chromium etchant, which contains surfactants, is beneficial because the electron beam resist is generally hydrophobic and thus makes wet-etching with aqueous solutions difficult.
5. This procedure results in a CYTOP coat of ~1-μm thickness. However, if the speed used during the spincoat process is increased, a thinner coat will be formed.
6. The solvent used in the CYTOP solution has a boiling point of 180 °C. A pre-bake step at 80 °C results in slow evaporation of the solvent from the surface, and facilitates the formation of a uniform CYTOP layer.
7. Because the CYTOP-coated surface has very low friction, the placement of the photoresist at the center of the coverslip is important for uniform coating.
8. This process (spincoating at 4500 rpm, 1 s) is important for the removal of excess photoresist that has remained at the edge of the CYTOP-coated glass.
9. Repetition of this procedure will result in contamination of the photomask with photoresist, which will hinder the formation of the required tight contact with the substrate. If the procedure needs to be repeated, remove the photoresist on the photomask using gauze containing acetone, or wash the photomask in acetone using a bath-type sonicator.
10. The time required for development will vary depending on the temperature and the concentration of the developer. Completion of the developing process can be ascertained by observation under an optical microscope equipped with a yellow filter.
11. This procedure will remove photoresist. When photoresist is completely removed, the surface will repel acetone.
12. If the hole is not completely covered with epoxy adhesive and the coverslip, the culture medium will leak from the bottom of the Petri dish in subsequent experiments.
13. Other antibiotics beside carbenicillin can be used.
14. Typically, 100–200 μL bacterial suspension is required. This low volume will make subsequent processes, including replacement of the medium on the surface of the substrate with oil, much easier.

15. Enclosure of the cells in the droplets is stochastic and is dependent on the cell density of the bacterial suspension. At an OD_{600} of 0.6, approximately 20–30 % of the 10 μm droplets contain single cells. Increasing the droplet diameter to 20 or 30 μm increases the proportion of droplets containing multiple cells, but not that of droplets containing single cells. Therefore, we use 10 μm droplets, because the total number of droplets formed in a single device can be significantly increased.
16. This procedure is important for the complete removal of living cells from the medium on top of the oil layer. If living cells remain, they may grow on top of the oil layer and contaminate the subsequent collection process.
17. At this pressure, medium slowly flows out from the glass micropipette into the water layer, preventing contamination. On the other hand, flow spontaneously stops in the oil layer due to the difference in the surface tensions of the water and the oil.

References

1. Lewis K (2010) Persister cells. Annu Rev Microbiol 64:357–372
2. Allison KR, Brynildsen MP, Collins JJ (2011) Heterogeneous bacterial persisters and engineering approaches to eliminate them. Curr Opin Microbiol 14:593–598
3. Balaban NQ (2011) Persistence: mechanisms for triggering and enhancing phenotypic variability. Curr Opin Genet Dev 21:768–775
4. Gerdes K, Maisonneuve E (2012) Bacterial persistence and toxin-antitoxin loci. Annu Rev Microbiol 66:103–123
5. Kint CI, Verstraeten N, Fauvart M, Michiels J (2012) New-found fundamentals of bacterial persistence. Trends Microbiol 20: 577–585
6. Weibel DB, Diluzio WR, Whitesides GM (2007) Microfabrication meets microbiology. Nat Rev Microbiol 5:209–218
7. Balaban NQ, Merrin J, Chait R, Kowalik L, Leibler S (2004) Bacterial persistence as a phenotypic switch. Science 305: 1622–1625
8. Wakamoto Y, Dhar N, Chait R, Schneider K, Signorino-Gelo F, Leibler S, McKinney JD (2013) Dynamic persistence of antibiotic-stressed mycobacteria. Science 339:91–95
9. Sakakihara S, Araki S, Iino R, Noji H (2010) A single-molecule enzymatic assay in a directly accessible femtoliter droplet array. Lab Chip 10:3355–3362
10. Iino R, Hayama K, Amezawa H, Sakakihara S, Kim SH, Matsumono Y, Nishino K, Yamaguchi A, Noji H (2012) A single-cell drug efflux assay in bacteria by using a directly accessible femtoliter droplet array. Lab Chip 12:3923–3929
11. Iino R, Matsumoto Y, Nishino K, Yamaguchi A, Noji H (2013) Design of a large-scale femtoliter droplet array for single-cell analysis of drug-tolerant and drug-resistant bacteria. Front Microbiol 4:300

Part IV

Identification of Persister Mutants and Genes

Chapter 10

A Whole-Cell-Based High-Throughput Screening Method to Identify Molecules Targeting *Pseudomonas aeruginosa* Persister Cells

Veerle Liebens, Valerie Defraine, and Maarten Fauvart

Abstract

Despite its clinical relevance and the fact that the phenomenon of persistence was discovered in the 1940s, little is known about the mechanisms behind persister cell formation. Research in this field has mainly focused on the model organism *Escherichia coli* and few genetic determinants of persistence have been described in other bacterial species, impairing the development of target-based strategies to combat these antibiotic-tolerant cells. In this chapter we describe a top-down large-scale screening method capable of specifically identifying small molecule compounds that, in combination with conventional antibiotics, significantly reduce the persister fraction in *Pseudomonas aeruginosa*. The method is readily adaptable for other species. Further characterization and analysis of the mode of action of the identified compounds can provide additional insight into the mechanisms behind persister formation and can guide the development of future anti-persister therapies.

Keywords: High-throughput screening, *Pseudomonas aeruginosa*, Small molecules, Combination therapy, Growth kinetics

1 Introduction

Pseudomonas aeruginosa is a gram-negative opportunistic pathogen that causes deadly infections in cystic fibrosis (CF) patients. Although several bacterial species colonize the CF lung, *P. aeruginosa* is the dominant species present in this environment [1]. Most of these infections become chronic, continuously damaging the lung and ultimately leading to respiratory failure [2]. When comparing *P. aeruginosa* isolates from the onset and late stages of chronic and clonal infections in the CF lung, a 100-fold increase in persister cells was observed, providing evidence for a causal relationship between the presence of persister cells and the recalcitrant nature of these infections [3]. Furthermore, *P. aeruginosa* is one of the leading causes of healthcare-associated infections,

Jan Michiels and Maarten Fauvart (eds.), *Bacterial Persistence: Methods and Protocols*,
Methods in Molecular Biology, vol. 1333, DOI 10.1007/978-1-4939-2854-5_10,

responsible for 8.9 % of all nosocomial infections in Europe. Isolates are most frequently found in infections of the lower respiratory tract, surgical sites, and urinary tract [4]. Many of these infections are associated with biofilm formation on catheters and implants [5] greatly contributing to treatment failure. Recently, the NIH estimated that up to 80 % of all bacterial infections is biofilm-associated [6]. One of the major explanations for biofilm tolerance is the presence of persister cells [7]. Due to the protection against the host immune system provided by the extracellular matrix, these cells are capable of repopulating the biofilm once the antibiotic pressure subsides. In addition, persisters provide a reservoir of viable cells within the host, increasing the chance of acquiring additional resistance mechanisms by horizontal gene transfer or mutation and thereby contributing to the development of multidrug-resistant strains [8]. Since the pharmaceutical pipeline contains few new antibiotics active against *P. aeruginosa* [9, 10], treatment of infections caused by multidrug-resistant strains becomes challenging. Therefore, targeting persisters will not only facilitate the clearing of biofilm-associated infections or infections present in the CF lung, but also prevent development of resistance.

Screening of single gene knockout libraries, both in *P. aeruginosa* [11] and *E. coli* [12, 13], did not result in the identification of mutants lacking persister cells, indicating redundancy in mechanisms of persister formation. Additionally, it seems that different bacterial species may use different mechanisms to form these tolerant cells. For example, a major mechanism of persister formation in *E. coli*, a model system for persistence, involves toxin–antitoxin (TA) modules [14, 15]. However, the involvement of TA modules in *P. aeruginosa* persistence has not yet been reported. The mechanism of persister formation in *P. aeruginosa* is largely unknown and only a few genetic determinants have been linked to persistence (as reviewed in [16]). Taken together, development of a rational *P. aeruginosa* anti-persister strategy is very challenging.

So far, a limited number of anti-persister compounds acting on *P. aeruginosa* have been reported. The molecule 3-[4-(4-methoxyphenyl)piperazin-1-yl]piperidin-4-yl biphenyl-4-carboxylate (C10), identified in a screening of a small chemical library, reverts persisters cells to antibiotic-sensitive cells [17]. Additionally, a synthetic quorum-sensing inhibitor (Z)-4-bromo-5-(bromomethylene)-3-methylfuran-2(5H)-one (BF8) has been described to revert multidrug tolerance in wild type [18] and mucoid [19] *P. aeruginosa* strains. More recently, a molecule was identified that specifically targets the quorum sensing regulator MvfR [20]. This regulator controls among others the production of the small volatile molecule 2-aminoacetophenon (2-AA), which was shown to increase the number of antibiotic-tolerant cells of *P. aeruginosa* by decreasing the transcription of genes involved in the translational capacity of the cell [21].

Here, we describe a screening method that was successfully used to identify small compounds that, in combination with an conventional antibiotic, specifically target *P. aeruginosa* persister cells in stationary phase cultures. A similar procedure has been used to screen a mutant library for mutants that display an altered persistence phenotype [11]. First of all, we describe how this procedure was optimized for identification of anti-persister molecules, followed by a detailed overview of the screening procedure itself.

2 Materials

1. Tryptic Soy Broth (TSB): 30 g Tryptic Soy Broth, 1000 mL distilled water. Autoclave and store at room temperature.
2. 1:20 diluted Tryptic Soy Broth (1:20 TSB): 1.5 g Tryptic Soy Broth, 1000 mL distilled water. Autoclave and store at room temperature.
3. Tryptic Soy Broth (TSB) agar: 30 g Tryptic Soy Broth, 15 g agar, distilled water to a final volume of 1000 mL. Autoclave and pour into Petri dishes. Store plates at 4 °C before use.
4. Magnesium sulfate solution ($MgSO_4$, 10 mM): 2.46 g $MgSO_4 \cdot 7H_2O$, distilled water to a final volume of 1000 mL. Autoclave and store at room temperature.
5. Antibiotic stock solution. Antibiotics targeting stationary phase cells of *P. aeruginosa* are for example fluoroquinolones. For ofloxacin, a stock solution of 10 mg/mL was prepared by weighing 10 mg of ofloxacin powder stored at 4 °C and adding sterile ultrapure water (resistivity of 18.2 MΩ/cm at 25 °C) to a final volume of 1 mL. A few drops of HCl were added to increase solubility.
6. Small-molecule library (<500 g/mol) provided in 96-well format as a dry film.
7. Sterile glass test tubes and Erlenmeyer flasks of 50 mL.
8. Sterile Bioscreen honeycomb plates.
9. Breathable membranes for sealing 96-well plates.
10. Polystyrene 96-well plates, flat bottom, and polystyrene lid.
11. Bioscreen C MBR (Oy Growth Curves Ab Ltd).
12. Incubator at 37 °C, fitted with trays for test tubes and microplates.

3 Methods

3.1 Optimization

1. Determine the minimal inhibitory concentration (MIC) of the antibiotic that will be used in the screening against *P. aeruginosa* grown in 1:20 TSB. Grow *P. aeruginosa* PA14

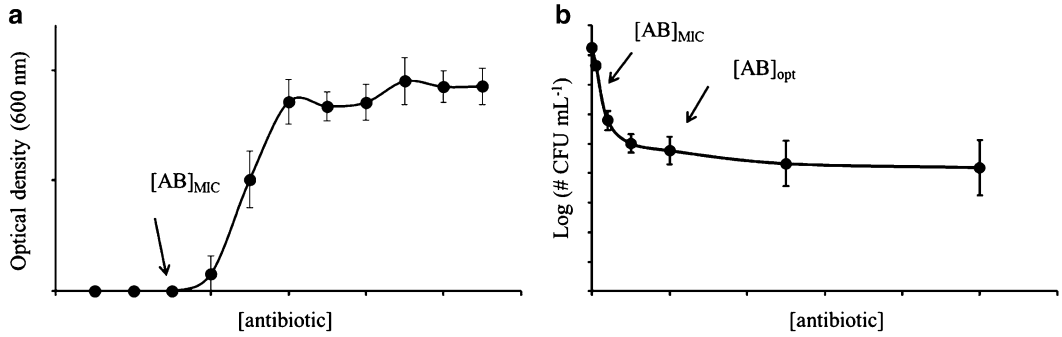

Fig. 1 Optimization of screening conditions. (**a**) The susceptibility of growing cells to the chosen antibiotic was determined by exposing them to a range of antibiotic concentrations. Effect on growth was evaluated by measurement of OD_{600} and determination of the MIC value as the lowest concentration that completely inhibits bacterial growth. (**b**) Stationary phase cells were treated for 5 h with different concentrations of ofloxacin, up to 10–50 times the determined $[AB]_{MIC}$-value, prior to viable cell counts by plating. Each experiment was repeated independently at least three times, data points correspond to the mean. Error bars represent standard error of the mean (SEM)

precultures overnight at 37 °C while shaking at 200 rpm in a rotary shaker. Measure the OD_{625} and adjust to 0.1 in 1 mL $MgSO_4$ (10 mM) to obtain the McFarland standard of 10^8 cells/mL. Dilute this culture 200-fold in 1:20 TSB to obtain an inoculum of 5×10^5 cells/mL. Prepare a twofold dilution series of antibiotic by adding 150 μL of twice the desired final concentration of antibiotics to 150 μL of inoculum, followed by serial dilution in inoculum. After 24 h of growth, measure the OD_{600}. The lowest antibiotic concentration that completely inhibits bacterial growth is considered the MIC (Fig. 1a, indicated by $[AB]_{MIC}$). Repeat this experiment three times independently.

2. Determine the conditions to obtain a stable persister fraction in stationary phase cultures after treatment with the antibiotic. Inoculate *P. aeruginosa* in 1:20 TSB and grow overnight until stationary phase. Next, dilute the preculture 100-fold in a 50 mL sterile flask containing 1:20 TSB and grow for 48 h. Distribute the stationary phase culture into the wells of a 96-well microplate (*see* **Note 1**) and treat the cells with different concentrations of the antibiotic (*see* **Note 2**) in a final volume of 200 μL. Fill the remaining wells with sterile water or culture medium (*see* **Note 3**). Seal the 96-well plate with a breathable membrane and close by putting a lid on top. After 5 h incubation at 37 °C, shaking at 200 rpm, transfer the treated cultures to Eppendorf tubes and wash the cells of each sample in 10 mM $MgSO_4$ (centrifuge in a microfuge at 3300 × *g*, 5 min, 4 °C). Prepare a tenfold dilution series in 10 mM $MgSO_4$ and plate on TSB agar growth medium. Incubate these plates statically at

37 °C and determine the number of colony forming units (CFU) after 24 and 48 h (*see* **Note 4**). Repeat this experiment independently three times. An optimal condition is reached when a further increase in antibiotic concentration does not lead to a further reduction of the number of surviving cells (Fig. 1b, indicated by $[AB]_{opt}$).

3. Determine the time needed to carry out 1 run. Inoculate *P. aeruginosa* in 1:20 TSB and grow overnight until stationary phase. Dilute the preculture 100-fold in 50 mL of 1:20 TSB and grow for 48 h. Next, distribute the stationary phase cells into the wells of a 96-well microtiter plate (*see* **Note 3**) and add antibiotics to a final concentration $[AB]_{opt}$, as determined in **step 2**, in total volumes of 200 μL. After 5 h treatment, dilute the samples in undiluted TSB by carrying out consecutive dilutions steps (*see* **Note 5**). The choice of dilution factor depends on the $[AB]_{MIC}$ and $[AB]_{opt}$ values determined in **steps 1** and **2**, respectively. For the treatment of a *P. aeruginosa* PA14 culture with 10 μg/mL of ofloxacin, a 100-fold dilution factor was chosen. Transfer the diluted samples to a Bioscreen plate and incubate in the preheated Bioscreen C MBR device to monitor the growth kinetics over time. Use the following settings: 37 °C, OD_{600} measurement every 15 min during 24 h and continuous shaking between measurements at "medium" intensity. When the run is finished, check each well visually for precipitation (*see* **Note 6**). Ideally, late exponential phase is reached within 24 h of measurement, which allows to carry out a new run daily.
4. Determination of correlation between number of surviving cells and optical density values. Dilute a preculture of *P. aeruginosa* cells grown in 1:20 TSB 100-fold and incubate for 48 h. Treat an aliquot of the cells with $[AB]_{opt}$ or sterile water for 5 h in a microplate. Next, make a tenfold dilution series of each sample and divide each sample into 2. Plate out the first sample on TSB agar growth medium in order to determine the number of CFU present in each sample. Dilute the second sample x-fold (as chosen in **step 3**) in fresh 1× TSB growth medium and monitor growth kinetics for 24 h by using the Bioscreen C MBR. Check for a correlation between the two datasets. In our case, a linear relationship was observed between the time needed to reach an OD_{600} of 0.6 and the logarithmic value of the number of CFU present in a sample (Fig. 2).
5. Check the susceptibility of *P. aeruginosa* cells toward the solvent you will use to dissolve the compounds. This is done by performing a MIC measurement as described in **step 1**, replacing the antibiotic by the solvent of choice. Incubate the prepared start inoculum of 5×10^5 cells/mL in the presence of a twofold dilution series of solvent. After 24 h of growth,

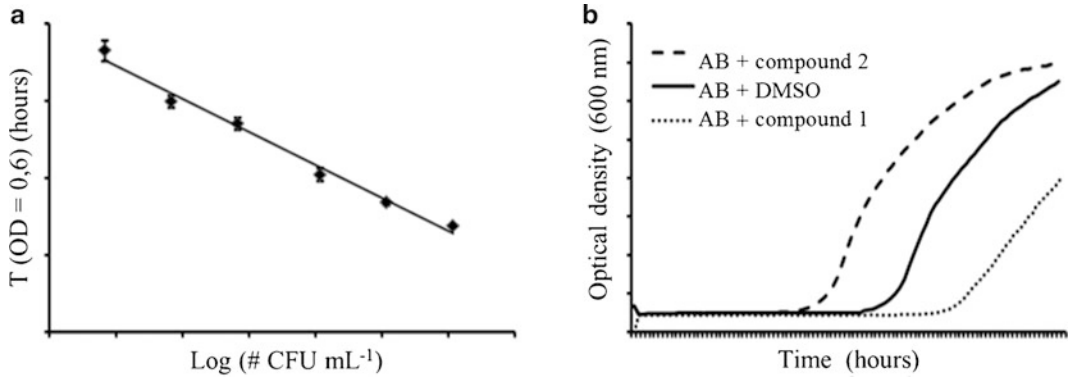

Fig. 2 Selection method of promising anti-persister compounds. (**a**) Linear relationship between the number of cells incubated in the automated plate reader and the duration of the lag phase of the resulting growth curves, represented by the time needed to achieve an OD_{600} of 0.6. (**b**) Representative growth curves of cells diluted after 5 h treatment with a combination of antibiotic (AB) and compound 1 (*dotted curve*), compound 2 (*dashed curve*) or DMSO (*solid curve*). Compound 1 decreases and compound 2 increases the number of cells in combination with antibiotic as compared to monotherapy

measure the OD_{600}. Determine the lowest concentration at which the solvent acts growth inhibitory. The concentration of solvent used to dissolve the compounds must always be lower than the determined growth inhibitory concentration. Repeat this experiment three times independently.

3.2 Screening

We use a small-molecule library (<500 g/mol) in 96-well format as a dry film. Just before use, components are dissolved in 100 % DMSO after which they are stored in closed bags under N_2 atmosphere at room temperature (short-term storage) or −20 °C (long-term storage) in a dark environment.

1. Inoculate *P. aeruginosa* PA14 in 1:20 TSB and incubate overnight at 37 °C.
2. The next day, dilute the bacterial cells 100-fold into a sterile flask containing 50 mL 1:20 TSB and grow for 48 h.
3. To ensure compliance between the different optimization tests and the actual screening, all antibiotic treatments of stationary phase cells are to be carried out in microplates.
4. Add $[AB]_{opt}$, mix and distribute this culture immediately over the wells of a 96-well plate. Add a different compound to each well such that a final volume of 200 μL per well is reached. Seal with a breathable membrane and close the plate by putting the lid on top. Incubate the 96-well plate for 5 h at 37 °C.
5. After 5 h of treatment, remove the lid and breathable membrane and dilute each sample as determined in **step 3** of

Subheading 3.1 into rich TSB growth medium using a Bioscreen plate as the final recipient. Incubate these plates into the preheated Bioscreen C MBR device using the settings as described in **step 3** of Subheading 3.1.

6. After 24 h of measurement, remove the plates and check visually for precipitation in each well (*see* **Note 6**). Analyze the data for each 96-well plate separately. Plot the growth curves for each well and calculate the time needed to reach an optical density of 0.6, which is a measure for the number of CFUs present in the sample after treatment. Check for normality of these data and select positive hits by identifying the outliers ($P < 0.05$) under the given normal distribution.
7. Confirm the effect of the selected small molecules by a plate counting experiment. Repeat **steps 1–3** and include a treatment with solvent and the combination of $[AB]_{opt}$ and solvent. Next, wash the cells in an isovolume of 10 mM $MgSO_4$. Make a tenfold dilution series in 10 mM $MgSO_4$ and plate an aliquot on solidified TSB medium. Count the number of CFU after 24 and 48 h (*see* **Note 4**).

4 Notes

1. In order to avoid differences in test results due to different treatment conditions, all optimization tests are carried out in a total volume of 200 μL in 96-well plates, unless otherwise stated.
2. The concentrations of antibiotic tested are chosen based on $[AB]_{MIC}$ determined in **step 1**. Be sure to include concentrations that are 10–50 times higher than $[AB]_{MIC}$ in order to visualize the biphasic killing pattern that is representative of the presence of persister cells in the population (Fig. 1).
3. Adding growth medium to the surrounding wells prevents evaporation of liquid from the samples, especially for longer treatment durations.
4. Depending on the antibiotic used, cells stressed with high concentrations of the bactericidal agent will take longer to resume growth and consequently need more time to produce countable CFUs.
5. By carrying out consecutive dilution steps, reproducibility is increased by reducing the pipetting error. Be sure that the culture is sufficiently diluted to exclude effects from remaining antibiotic used in the treatment.
6. Precipitation of bacterial cells due to the action of the compound can affect a correct measurement of the optical density.

References

1. Zhao J, Schloss PD, Kalikin LM, Carmody LA, Foster BK, Petrosino JF, Cavalcoli JD, VanDevanter DR, Murray S, Li JZ, Young VB, LiPuma JJ (2012) Decade-long bacterial community dynamics in cystic fibrosis airways. Proc Natl Acad Sci U S A 109(15):5809–5814. doi:10.1073/pnas.1120577109
2. Folkesson A, Jelsbak L, Yang L, Johansen HK, Ciofu O, Hoiby N, Molin S (2012) Adaptation of *Pseudomonas aeruginosa* to the cystic fibrosis airway: an evolutionary perspective. Nat Rev Microbiol 10(12):841–851. doi:10.1038/nrmicro2907
3. Mulcahy LR, Burns JL, Lory S, Lewis K (2010) Emergence of *Pseudomonas aeruginosa* strains producing high levels of persister cells in patients with cystic fibrosis. J Bacteriol 192 (23):6191–6199. doi:10.1128/JB.01651-09
4. ECDC (2013) Point prevalence survey of healthcare-associated infections and antimicrobial use in European acute care hospitals. European Centre for Disease Prevention and Control, Stockholm
5. Mulcahy LR, Isabella VM, Lewis K (2013) *Pseudomonas aeruginosa* biofilms in disease. Microb Ecol 68(1):1–12. doi:10.1007/s00248-013-0297-x
6. Romling U, Balsalobre C (2012) Biofilm infections, their resilience to therapy and innovative treatment strategies. J Intern Med 272 (6):541–561. doi:10.1111/joim.12004
7. Lewis K (2008) Multidrug tolerance of biofilms and persister cells. Curr Top Microbiol Immunol 322:107–131
8. Cohen NR, Lobritz MA, Collins JJ (2013) Microbial persistence and the road to drug resistance. Cell Host Microbe 13(6):632–642. doi:10.1016/j.chom.2013.05.009
9. Bassetti M, Ginocchio F, Mikulska M (2011) New treatment options against gram-negative organisms. Crit Care 15(2):215. doi:10.1186/cc9997
10. Pendleton JN, Gorman SP, Gilmore BF (2013) Clinical relevance of the ESKAPE pathogens. Expert Rev Anti Infect Ther 11(3):297–308. doi:10.1586/eri.13.12
11. De Groote VN, Verstraeten N, Fauvart M, Kint CI, Verbeeck AM, Beullens S, Cornelis P, Michiels J (2009) Novel persistence genes in Pseudomonas aeruginosa identified by high-throughput screening. FEMS Microbiol Lett 297(1):73–79. doi:10.1111/j.1574-6968.2009.01657.x
12. Hu Y, Coates AR (2005) Transposon mutagenesis identifies genes which control antimicrobial drug tolerance in stationary-phase Escherichia coli. FEMS Microbiol Lett 243(1):117–124. doi:10.1016/j.femsle.2004.11.049
13. Hansen S, Lewis K, Vulic M (2008) Role of global regulators and nucleotide metabolism in antibiotic tolerance in *Escherichia coli*. Antimicrob Agents Chemother 52(8):2718–2726. doi:10.1128/aac.00144-08
14. Maisonneuve E, Shakespeare LJ, Jorgensen MG, Gerdes K (2011) Bacterial persistence by RNA endonucleases. Proc Natl Acad Sci U S A 108(32):13206–13211. doi:10.1073/pnas.1100186108
15. Maisonneuve E, Castro-Camargo M, Gerdes K (2013) (p)ppGpp controls bacterial persistence by stochastic induction of toxin-antitoxin activity. Cell 154(5):1140–1150. doi:10.1016/j.cell.2013.07.048
16. Fauvart M, De Groote VN, Michiels J (2011) Role of persister cells in chronic infections: clinical relevance and perspectives on anti-persister therapies. J Med Microbiol 60 (Pt 6):699–709. doi:10.1099/jmm.0.030932-0
17. Kim JS, Heo P, Yang TJ, Lee KS, Cho DH, Kim BT, Suh JH, Lim HJ, Shin D, Kim SK, Kweon DH (2011) Selective killing of bacterial persisters by a single chemical compound without affecting normal antibiotic-sensitive cells. Antimicrob Agents Chemother 55(11):5380–5383. doi:10.1128/AAC.00708-11
18. Pan J, Bahar AA, Syed H, Ren D (2012) Reverting antibiotic tolerance of *Pseudomonas aeruginosa* PAO1 persister cells by (Z)-4-bromo-5-(bromomethylene)-3-methylfuran-2 (5H)-one. PLoS One 7(9):e45778. doi:10.1371/journal.pone.0045778
19. Pan J, Song F, Ren D (2013) Controlling persister cells of *Pseudomonas aeruginosa* PDO300 by (Z)-4-bromo-5-(bromomethylene)-3-methylfuran-2 (5H)-one. Bioorg Med Chem Lett 23(16): 4648–4651. doi:10.1016/j.bmcl.2013.06.011
20. Starkey M, Lepine F, Maura D, Bandyopadhaya A, Lesic B, He J, Kitao T, Righi V, Milot S, Tzika A, Rahme L (2014) Identification of anti-virulence compounds that disrupt quorum-sensing regulated acute and persistent pathogenicity. PLoS Pathog 10(8):e1004321, doi:10.1371/journal.ppat.1004321
21. Que YA, Hazan R, Strobel B, Maura D, He J, Kesarwani M, Panopoulos P, Tsurumi A, Giddey M, Wilhelmy J, Mindrinos MN, Rahme LG (2013) A quorum sensing small volatile molecule promotes antibiotic tolerance in bacteria. PLoS One 8(12):e80140, doi:10.1371/journal.pone.0080140

Chapter 11

Functional Analysis of the Role of Toxin–Antitoxin (TA) Loci in Bacterial Persistence

Aaron T. Butt and Richard W. Titball

Abstract

We have developed a method to analyze the functionality of putative TA loci by expressing them in *Escherichia coli*. Here, we describe the procedure for cloning recombinant TA genes into inducible plasmids and expressing these in *E. coli*. Following expression, toxicity, resuscitation of growth, and changes in persister cell formation are assayed. This can confirm whether predicted TA loci are active in *E. coli* and whether expression can affect persister cell formation.

Keywords: Toxin–antitoxin, Persistence, Inducible expression, *E. coli*, Antibiotic

1 Introduction

Toxin–antitoxin (TA) systems are found in many bacterial species and typically consist of a gene pair coding for a toxin and antitoxin gene. The toxins can typically bind and inhibit the function of a cellular target causing inhibition of bacterial growth [1]. The antitoxin gene codes for either a protein or an RNA molecule that inhibits the activity of the toxin under normal cellular conditions. One role for TA systems is in the formation of bacterial persister cells [2]. Bacterial persisters are a sub-population of cells that can tolerate and survive antibiotic or stress treatment, whereas the majority of the population is killed [3]. Expression of TA toxins can increase the population of tolerant persister cells [4, 5]. An increase in persistence has been best demonstrated in *E. coli* following expression of a variety of toxins. One of the first examples of this was ampicillin treatment of *E. coli* cultures expressing the TA toxin HipA from an arabinose-driven pBAD promoter [6]. Other toxins such as RelE, TisB and HicA have also been tested using similar methodology, expressing the toxin from an inducible promoter and then treating with antibiotic [4, 5, 7]. The method we have developed permits testing on the functionality of putative

Jan Michiels and Maarten Fauvart (eds.), *Bacterial Persistence: Methods and Protocols*,
Methods in Molecular Biology, vol. 1333, DOI 10.1007/978-1-4939-2854-5_11,

or predicted TA systems though expression in *E. coli*. Predicted TA systems native to the *E. coli* host or from other bacteria, such as *Burkholderia pseudomallei*, can be expressed in *E. coli* MG1655 [4, 8]. The method requires cloning of putative toxin and antitoxin genes into separate compatible and inducible plasmids and firstly assaying for growth arrest/reduction in culturability following expression of the toxin and resuscitation/restoration of growth following expression of the antitoxin. Following assessment of these phenotypes, the methodology can be implemented to assay for the effect of TA expression on the persistence of *E. coli* following treatment with various antibiotics. Failure of *E. coli* to express cloned recombinant genes and differences between toxin target(s) in the native host compared to target(s) in *E. coli* are potential limitations of this technique. However, in using *E. coli* as a host, a safe and high throughput method has been developed to screen a variety of predicted TA systems from a range of bacteria for functionality. This method can be used to down select TA gene candidates for further phenotypic study in the native host or for structural studies.

2 Materials

1. *E. coli* MG1655 strain (F^-, $lambda^-$, rph-1).
2. Expression plasmids: e.g. pBAD/his and pME6032.
3. Antibiotics for plasmid selection: 100 mg/ml ampicillin and 15 mg/ml tetracycline. Weigh the appropriate amount of antibiotic, dissolve in distilled water and filter sterilize.
4. PCR reagents for gene amplification.
5. Restriction enzymes for cloning.
6. LB medium: weigh 5 g Bacto-tryptone, 2.5 g yeast extract, 5 g NaCl and dissolve in 500 ml water. Autoclave for sterilization.
7. LB agar: weigh 5 g Bacto-tryptone, 2.5 g yeast extract, 5 g NaCl, 7.5 g agar and dissolve in 500 ml water. Autoclave for sterilization.
8. Arabinose 20 % stock solution: dissolve 20 g of arabinose in water and filter sterilize.
9. Glucose 20 % stock solution: dissolve 20 g of glucose in water and filter sterilize.
10. Isopropyl β-D-1-thiogalactopyranoside (IPTG) solution: 1 M IPTG in water.
11. Tubes and flasks: universal tubes, 200 ml Conical flasks.
12. 96-Well and 24-well plates.
13. Cuvettes: 1 cm diameter.

14. 1.5 ml Eppendorf tubes.
15. Spectrophotometer set for measurement at 590 nm.
16. Centrifuge(s) capable of speeds of 3000 × *g* for universal tubes and 13,000 × *g* for 1.5 ml Eppendorf tubes.

3 Methods

3.1 Cloning into Expression Vectors

1. Select specific primers to amplify the putative toxin and antitoxin genes of choice. PCR amplify the putative toxin or antitoxin genes using genomic DNA as a template and specific primers containing appropriate restriction sites.
2. Clone the toxin gene into an inducible expression plasmid such as the pBAD/his vector using appropriate restriction sites (Fig. 1a) (*see* **Note 1**).
3. Clone the antitoxin gene into a different inducible expression plasmid such as the pME6032 vector using appropriate restriction sites within the multiple cloning sites (Fig. 1b), (*see* **Note 2**).

3.2 Toxicity Assay

The following protocols assume the use of the pBAD/his and pME6032 plasmids. If other plasmids are used, change the antibiotics for plasmid selection and sugar inducers/repressors as appropriate.

1. Inoculate 5 ml of LB broth containing 100 μg/ml ampicillin with *E. coli* harboring pBAD with cloned toxin gene and incubate at 37 °C, while shaking at 200 rpm on a rotating platform for 16 h.

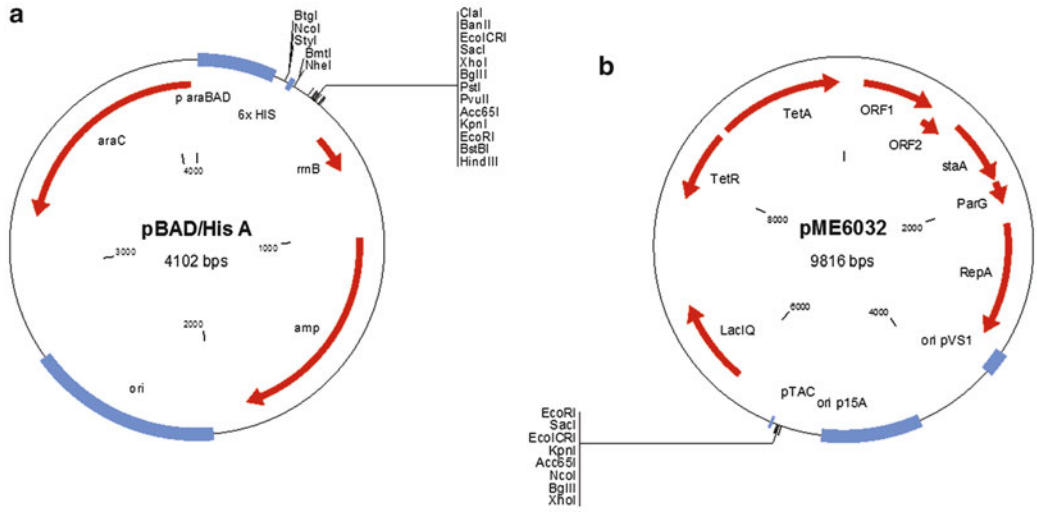

Fig. 1 Expression plasmid maps. Key features such as antibiotic resistance genes, multiple cloning sites, and origins of replication are shown for pBAD/his (**a**) and pME6032 (**b**)

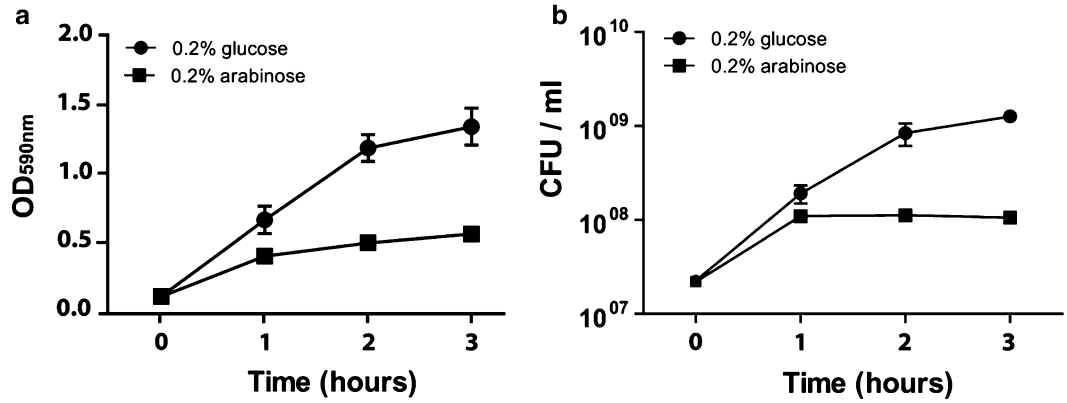

Fig. 2 Effect of toxin expression from the pBAD/his vector on *E. coli* growth. 0.2 % glucose or arabinose was used to repress or induce expression of the toxin, respectively. (**a**) Growth measured by optical density. (**b**) Growth measured by CFU counts. Reproduced from [8] with permission

2. Dilute the culture 1:100 in 40 ml of fresh LB in a 200 ml conical flask supplemented with 100 μg/ml ampicillin. Grow cultures at 37 °C, 200 rpm until reaching an OD_{590}nm of ~0.1 (*see* **Note 3**).
3. Aliquot 2 × 10 ml of culture into universal tubes and supplement with either 0.2 % (w/v) glucose or 0.2 % (w/v) arabinose to repress or induce expression from the pBAD promoter respectively. Incubate cultures at 37 °C while shaking at 200 rpm.
4. At hourly intervals, remove 1 ml of culture (or 100 μl and mix with 900 μl LB for a 1:10 dilution) and add to a cuvette to record the OD_{590}nm using a spectrophotometer.
5. In parallel, remove 10 μl of culture and set up a serial dilution in a 96-well plate containing LB. Carry out a dilution range from 10^{-1} to 10^{-6}. Spot plate the dilution range onto LB plates containing 100 μg/ml ampicillin and incubate plates statically at 37 °C until colonies are visible for enumeration (Fig. 2).

3.3 Co-expression Assay

1. Inoculate 5 ml of LB broth containing 100 μg/ml ampicillin, 15 μg/ml tetracycline with *E. coli* harboring pBAD/toxin gene and pME6032/antitoxin gene and incubate at 37 °C while shaking at 200 rpm for 16 h.
2. Dilute the culture 1:100 in 50 ml of fresh LB in a 200 ml conical flask supplemented with 100 μg/ml ampicillin, 15 μg/ml tetracycline. Grow cultures at 37 °C while shaking at 200 rpm until reaching an OD_{590}nm of ~0.1.
3. Aliquot 4 × 10 ml of culture into universal tubes and supplement with either 0.2 % (w/v) glucose or 0.2 % (w/v) glucose, 25 mM IPTG or 0.2 % (w/v) arabinose or 0.2 % arabinose, 25 mM IPTG to repress or induce expression from the pBAD and pME6032 promoters. Incubate cultures at 37 °C while shaking at 200 rpm.

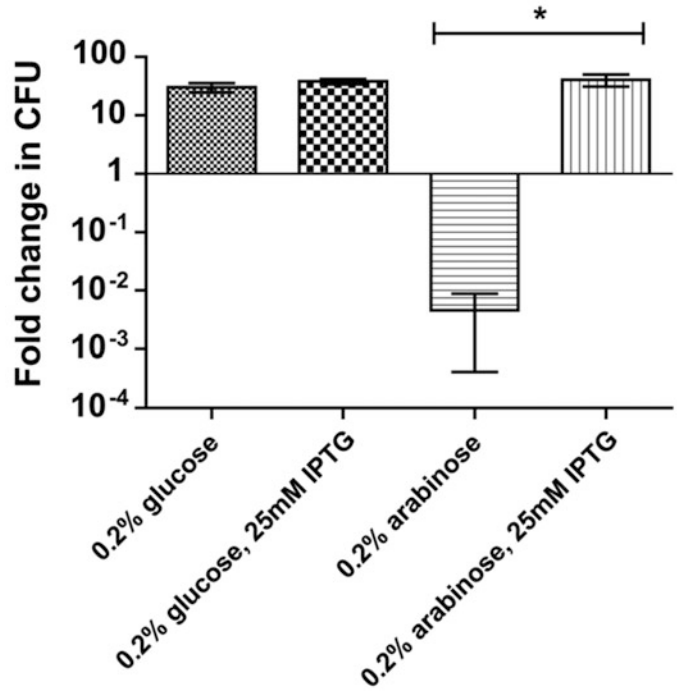

Fig. 3 Co-expression of toxin and antitoxin from different inducible promoters in *E. coli* and the change in the number of culturable cells. 0.2 % glucose or 0.2 % arabinose was used to repress or induce expression of the plasmid-cloned toxin, respectively. 25 mM IPTG was used to induce expression of the plasmid-cloned antitoxin. Reproduced from [8] with permission

4. At hourly intervals, remove 1 ml of culture (or 100 μl and mix with 900 μl LB for 1:10 dilution) and add to a cuvette to record the OD_{590}nm using a spectrophotometer.
5. In parallel, remove 10 μl of culture and set up a serial dilution in a 96-well plate containing LB. Carry out a dilution range from 10^{-1} to 10^{-6}. Spot plate the dilution range onto LB plates containing 100 μg/ml ampicillin, 15 μg/ml tetracycline and incubate plates statically at 37 °C until colonies are visible for enumeration (Fig. 3).

3.4 Resuscitation Assay

1. Inoculate 5 ml of LB broth containing 100 μg/ml ampicillin, 15 μg/ml tetracycline with *E. coli* harboring pBAD/toxin gene and pME6032/antitoxin gene and incubate at 37 °C while shaking at 200 rpm for 16 h.
2. Dilute the culture 1:100 in 60 ml of fresh LB in a 200 ml conical flask supplemented with 100 μg/ml ampicillin, 15 μg/ml tetracycline. Grow cultures at 37 °C while shaking at 200 rpm until reaching an OD_{590}nm of ~0.1.

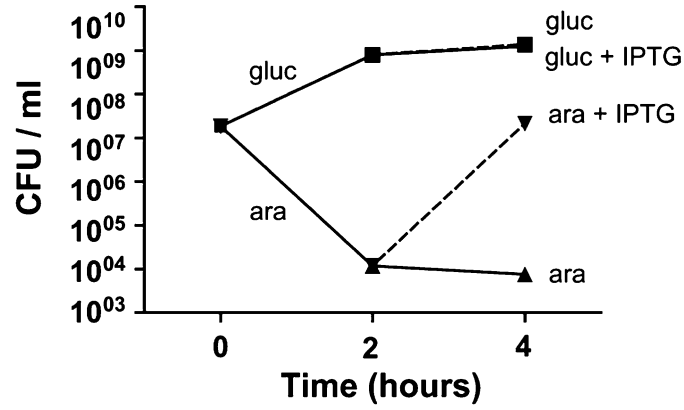

Fig. 4 Resuscitation of growth by antitoxin expression. 0.2 % glucose or 0.2 % arabinose was used to repress or induce expression of the plasmid-cloned toxin, respectively. Two hours later, 25 mM IPTG was used to induce expression of the plasmid-cloned antitoxin before plating for enumeration. Reproduced from [8] with permission

3. Aliquot 2 × 25 ml of culture into 200 ml conical flasks and supplement with either 0.2 % (w/v) glucose or 0.2 % (w/v) arabinose to repress or induce expression from the pBAD promoter respectively. Incubate cultures at 37 °C while shaking at 200 rpm for 2 h (T2).
4. Aliquot 2 × 10 ml of each culture into universal tubes and supplement one with 25 mM IPTG to induce antitoxin expression from the pME6032 promoter. Incubate cultures at 37 °C, 200 rpm for a further 2 h (T4) (*see* **Note 4**).
5. At hours T0, T2 and T4 remove 1 ml of culture (or 100 μl and mix with 900 μl LB for 1:10 dilution) and add to a cuvette to record the OD_{590}nm using a spectrophotometer. In parallel, remove 10 μl of culture and set up a serial dilution in a 96-well plate containing LB. Carry out a dilution range from 10^{-1} to 10^{-6}. Spot plate the dilution range onto LB plates containing 100 μg/ml ampicillin, 15 μg/ml tetracycline and incubate plates statically at 37 °C until colonies are visible for enumeration (Fig. 4).

3.5 Persister Assay

1. Inoculate 5 ml of LB broth containing 100 μg/ml ampicillin, 15 μg/ml tetracycline with *E. coli* harboring pBAD/toxin gene and pME6032/antitoxin gene and incubate at 37 °C while shaking at 200 rpm for 16 h.
2. Dilute the culture 1:100 in 30 ml of fresh LB in a 200 ml conical flask supplemented with 100 μg/ml ampicillin, 15 μg/ml tetracycline. Grow cultures at 37 °C while shaking at 200 rpm until reaching an OD_{590}nm of ~0.1.

3. Aliquot 2 × 10 ml of culture into universal tubes and supplement with either 0.2 % (w/v) glucose or 0.2 % (w/v) arabinose to repress or induce expression from the pBAD promoter respectively. Incubate cultures at 37 °C while shaking at 200 rpm for 3 h.
4. Standardize cultures to 2 × 10^8 CFU/ml (OD_{590}nm 0.5) in a 5 ml volume and add 500 μl aliquots to a 24-well plate.
5. Add 500 μl of LB antibiotic stock at 200× minimum inhibitory concentration (MIC) to each of the wells. This gives 10^8 CFU/ml and 100× MIC antibiotic per well (*see* **Note 5**).
6. Add 10 μl of standardized culture from **step 4** to a 96-well plate containing LB for serial dilution. Carry out a dilution range from 10^{-1} to 10^{-6}. Spot plate the dilution range onto LB plates containing 100 μg/ml ampicillin, 15 μg/ml tetracycle, 1 mM IPTG and incubate plates statically at 37 °C until colonies are visible for enumeration (*see* **Note 6**).
7. Incubate the 24-well persister assay plate statically at 37 °C for 24 h.
8. Remove cultures from the 24-well plate and add to 1.5 ml Eppendorf tubes.
9. Centrifuge the tubes for 7 min at maximal speed in a microcentrifuge.
10. Remove the supernatant and then resuspend the pellet in fresh LB broth.
11. Make serial dilutions of the cultures in LB broth using a dilution range of 10^0–10^{-4} in a 96-well plate. Spot plate the dilution range onto LB plates containing 100 μg/ml ampicillin, 15 μg/ml tetracycle, 1 mM IPTG and incubate plates statically at 37 °C until colonies are visible for enumeration.
12. Persister frequency is determined as CFU post antibiotic treatment divided by CFU pre antibiotic treatment (*see* **Note 7**) (Fig. 5).

4 Notes

1. If using the pBAD/his vector, clone into the *Nco*I sites and *Eco*RI/*Hind*III sites to create a non-his tagged construct or *Sac*I and *Eco*RI/*Hind*III to create a his-tagged construct. The N-terminal his-tag, although useful for protein purification and Western blotting, may interfere with the function of the toxin or shield the antitoxin binding site. It is advisable to make both a his-tagged and non-his-tagged version of the toxin for phenotypic analysis.

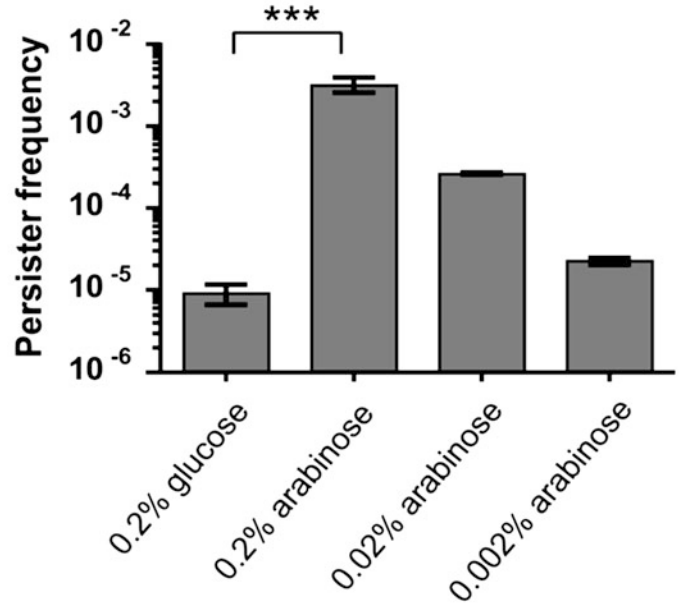

Fig. 5 Persister cell frequency following 24-h treatment of *E. coli* cultures with 100× MIC of ciprofloxacin. Toxin expression was repressed with 0.2 % glucose or induced with a range of arabinose concentrations for 3 h before ciprofloxacin treatment. Reproduced from [4] with permission

2. Both inducible expression plasmids need to be in different incompatibility groups, as it is not possible to maintain two different plasmids which use the same mechanism for replication in a single cell. The plasmids described in this manuscript fall into the pMB1 group (pBAD/his) and p15A group (pME6032). Both plasmids have a similar copy number per cell.
3. If cultures of *E. coli* harboring pBAD with a cloned toxin are growing slower than a control *E. coli* harboring empty pBAD, add 0.2 % glucose to the media to prevent leaky expression from the pBAD promoter. Cultures should be harvested and resuspended in fresh media prior to adding 0.2 % arabinose if glucose is added during the initial growth step.
4. If addition of IPTG, to induce expression of the antitoxin from pME6032, fails to resuscitate growth of toxin-induced cultures, a wash step should be added to the protocol. Prior to the addition of IPTG, harvest the cells by centrifugation at 3000 × *g* for 10 min. Remove the supernatant and resuspend the pellet in the same volume of fresh LB. Add IPTG and fresh antibiotic.
5. Some antibiotic stocks, such as ceftazidime, need to be made fresh every time as they are susceptible to degradation and will not work properly after prolonged storage.

6. 1 mM IPTG is included in the plates to induce antitoxin expression from the pME6032 promoter. This is to re-awaken/resuscitate any non-culturable/dormant cells induced by toxin expression. This is to achieve a more accurate measure of the total number of viable cells. If the total cell numbers are lower than expected the IPTG concentration should be increased.
7. Time 0 counts should be divided by 2, since only half of the standardized culture is added to the persister assay.

References

1. Yamaguchi Y, Inouye M (2011) Regulation of growth and death in *Escherichia coli* by toxin-antitoxin systems. Nat Rev Microbiol 9:779–790
2. Gerdes K, Maisonneuve E (2012) Bacterial persistence and toxin-antitoxin Loci. Annu Rev Microbiol 66:103–123
3. Lewis K (2010) Persister cells. Annu Rev Microbiol 64:357–372
4. Butt A, Higman VA, Williams C et al (2014) The HicA toxin from *Burkholderia pseudomalle*i has a role in persister cell formation. Biochem J 459:333–334
5. Dörr T, Vulić M, Lewis K (2010) Ciprofloxacin causes persister formation by inducing the TisB toxin in *Escherichia coli*. PLoS Biol 8, e1000317
6. Korch S, Hill T (2006) Ectopic overexpression of wild-type and mutant *hipA* genes in *Escherichia coli*: effects on macromolecular synthesis and persister formation. J Bacteriol 188:3826–3836
7. Keren I, Kaldalu N, Spoering A, Lewis K (2004) Persister cells and tolerance to antimicrobials. FEMS Microbiol Lett 230:13–18
8. Butt A, Muller C, Harmer N, Titball RW (2013) Identification of type II toxin-antitoxin modules in *Burkholderia pseudomallei*. FEMS Microbiol Lett 338:86–94

Chapter 12

Experimental Evolution of *Escherichia coli* Persister Levels Using Cyclic Antibiotic Treatments

Bram Van den Bergh*, Joran E. Michiels*, and Jan Michiels

Abstract

Persister cells are difficult to study owing to their transient nature and their usually small number in bacterial populations. In the past, numerous attempts have been made to elucidate persistence mechanisms. However, because of the challenges involved in studying persisters and the clear redundancy in mechanisms underlying their generation, our knowledge of molecular pathways to persistence remains incomplete. Here, we describe how to use experimental evolution with cyclic antibiotic treatments to generate mutants with an increased persister level in stationary phase, ranging from the initial ancestral level up to 100 %. This method will help to unravel molecular pathways to persistence, and opens up a myriad of new possibilities in persister research, such as the convenient study of nearly pure persister cultures and the possibility to investigate the role of time and environmental aspects in the evolution of persistence.

Keywords: Experimental evolution, Persister mutants, Adaptation, Cyclic treatments, *Escherichia coli*, Bet–hedging, Aminoglycosides

1 Introduction

Persistence is a bet–hedging strategy that allows microbial populations to avoid eradication by otherwise lethal antibiotic treatments through the formation of antibiotic tolerant variants (usually 0.0001-0.1 % of the total population) as a first line of defense [1, 2]. Persisters do not divide during antibiotic treatment and can only resume growth after reverting to the antibiotic-sensitive non-persister phenotype when the antibiotic concentration has dropped, distinguishing them from resistant cells [3]. As such they can avoid clinical detection while causing therapy failure and the resurgence of infection, especially given their presence in biofilms where they are shielded from immune components [4].

*Authors contributed equally.

Jan Michiels and Maarten Fauvart (eds.), *Bacterial Persistence: Methods and Protocols*, Methods in Molecular Biology, vol. 1333, DOI 10.1007/978-1-4939-2854-5_12,

Several groups have searched for persistence genes and mechanisms using classical approaches like screening mutant libraries [5–13], overexpression libraries [14, 15], and transcriptome studies on isolated populations enriched for persisters [16–19]. Although progress has been made and several genes and mechanisms have been reported recently [20, 21], many questions remain [22]. The usefulness of genetic screens is inherently limited for the study of complex traits such as persistence, and the rare and transient character of the persister phenotype makes transcriptomic analysis impossible without cumbersome enrichment protocols.

We propose experimental evolution as an alternative approach to study persistence for the following reasons. First, experimental evolution is a powerful tool for studying complex, redundant phenotypes [23]. Second, there is no bias in the type of mutations that can be found (e.g. gain-of-function mutations and mutations in regulatory domains or essential genes) [24]. Third, it has already been shown that persister levels are evolvable, both in vivo [25, 26] and in vitro [27]. Here, we demonstrate a method to evolve *Escherichia coli* populations and generate mutants producing a range of persister levels up to 100 % in stationary phase.

2 Materials

Prepare all solutions and media using deionized water and store at room temperature unless stated otherwise. Use *E. coli* strains carrying unique markers as ancestor. For example, we use *E. coli* BW25993 carrying different fluorescent markers [28] (*see* **Note 1**). Always follow safety instructions when handling hazardous goods or equipment. When disposing waste, please follow local regulations and make sure biological waste is sterilized properly in advance.

2.1 General Material

1. Antibiotic stock solution: amikacin 50 mg/ml (*see* **Note 2**). Weigh 50 mg of amikacin powder stored at 4 °C and add sterile ultrapure water (resistivity of 18.2 MΩ/cm at 25 °C) to a final volume of 1 ml. Filter sterilize (0.22 μm) and store aliquots immediately at −20 °C (*see* **Note 3**).
2. Mueller Hinton Broth (MHB): follow the instructions of the supplier of premixed MHB powder (*see* **Note 4**).
3. Lysogeny Broth (LB) agar: weigh 10 g tryptone, 10 g NaCl, 5 g yeast extract and 15 g agar and add water to a final volume of 1 l before autoclaving. Keep the sterile broth on at 50–60 °C for maximum 2 days before pouring. Store plates at 4 °C for up to 1 month before use.
4. Magnesium sulfate solution ($MgSO_4$, 10 mM): weigh 2.46 g of $MgSO_4 \cdot 7H_2O$ and add water to a final volume of 1 l before autoclaving.

5. Sterile glass test tubes and Erlenmeyer flasks of 250 ml (*see* **Note 5**).
6. Sterile plastic tubes of 15 and 50 ml, suitable for centrifugation.
7. Microcentrifuge capable of 4000 × *g*.
8. Centrifuge for 50 ml tubes capable of 4000 × *g*.
9. Incubator at 37 °C, fitted with trays for test tubes, microplates and Erlenmeyer flasks, capable of shaking at 200 rpm (*see* **Note 6**).
10. Spiral plater and automated colony counter or alternatively, sterile glass beads for manual plating and counting.

2.2 Determination of Antibiotic-Related Characteristics of Ancestral Strain

1. MHB agar plates containing different antibiotic concentrations: add 15 g of agar to 1 l of MHB before autoclaving. Keep the sterile broth on at 50–60 °C for maximum 2 days before pouring. Mix the sterile broth with amounts of antibiotic stock solution to reach the desired concentrations before pouring. Store MHB plates containing antibiotics at 4 °C for up to 1 week before use [29].
2. Sterile 96-well microplate with lid and breathable sterile adhesive seals.
3. 96-well OD_{595nm} reader.

2.3 Evolution Experiment

1. Micropipette tips with filters.
2. Disposable gloves.
3. Disinfection ethanol 70 % (v/v): mix 30 parts of water with 70 parts of denatured ethanol.
4. Cryoprotectant: glycerol 50 % (v/v): mix 50 parts of water with 50 parts of glycerol.
5. Polypropylene tubes suitable for −80 °C preservation (cryotube).
6. Fluorescence microscope (*see* **Note 7**).

3 Methods

Perform all handlings at room temperature and work under sterile conditions. Incubation is carried out at 37 °C, shaking at 200 rpm for liquid cultures. Centrifugation steps are performed at 4000 × *g*.

3.1 Characterization of Antibiotic-Related Characteristics of Ancestral Strain

The minimum inhibitory concentration (MIC), the minimum bactericidal concentration (MBC), the mutant prevention concentration (MPC) and the antibiotic concentration and treatment duration needed to reach the persister plateau must be determined for the ancestor before the start of the evolution experiment, and for evolved populations and/or clones afterwards (*see* **Notes 8** and **9**). Subheadings 3.1.1 and 3.1.2 are adaptations from previously described methods [30–32].

3.1.1 MIC and MBC Determination

1. Inoculate the ancestral strain (*see* **Notes 1** and **9**) in a test tube containing 5 ml of MHB and incubate overnight.
2. Adjust the optical density of the overnight culture at 595 nm (OD_{595nm}) to 0.5 by centrifugation in a microcentrifuge (5 min) and resuspending and diluting in MHB.
3. Dilute the OD_{595nm}-adjusted suspension 1/100 in 40 ml MHB and mix well. Add antibiotic to 10 ml of this inoculum to a final concentration of two times the highest concentration that you want to assess (*see* **Note 10**).
4. Add 150 μl of the remaining 30 ml of bacterial inoculum from **step 3** to the wells of a sterile microplate. Use three rows as technical replicates per antibiotic per clone and leave column 12 blank. Make also an appropriate tenfold serial dilution series in $MgSO_4$ solution (10 mM) of the remaining inoculum and plate out on LB agar. Count colonies after overnight incubation to determine the CFU per ml.
5. Add 150 μl of MHB to column 12 as negative control.
6. Make a twofold serial dilution series of the antibiotic: add 150 μl of the inoculum with antibiotic to the wells of column 1, mix, and transfer 150 μl to the next column and repeat for each column until column 10. Mix column 10 and remove 150 μl. Leave column 11 without antibiotics as a positive control. Cover the microplate with a breathable seal and plastic lid, and incubate for 16–20 h.
7. Measure the OD_{595nm} for each well in a multireader. Verify the positive and negative controls for adequate microbial growth and medium sterility. The MIC is the lowest concentration inhibiting visible growth.
8. Make appropriate tenfold serial dilutions in $MgSO_4$ (10 mM) of the wells containing antibiotic above the MIC (thus showing no visible growth) and plate out on LB agar. Count colonies after overnight incubation to determine the CFU per ml and compare with CFU per ml of the inoculum determined in **step 4**. The MBC is the lowest concentration capable of killing 99.9 % of cells.

3.1.2 MPC Determination

1. Inoculate the ancestral strain (*see* **Notes 1** and **9**) in a test tube containing 5 ml of MHB and incubate overnight.
2. Dilute the overnight culture 1/100 in a flask containing 100 ml of MHB and incubate overnight.
3. Concentrate the overnight culture tenfold: centrifuge 50 ml of the overnight culture (25 min), discard the supernatant and resuspend the cell pellet in 5 ml of $MgSO_4$ solution (10 mM).
4. Plate out $>10^{10}$ cells on MHB plates containing a twofold serial dilution range of antibiotic (*see* **Note 10**). We use five

plates per antibiotic concentration and plate out 200 μl of the cell suspension prepared in **step 3** on each plate. Incubate for 48 h to allow detection of colonies arising from resistant mutants.

5. The MPC is the lowest concentration inhibiting growth of resistant mutants.

3.1.3 Construction of Killing Curves in Function of Antibiotic Concentration and Treatment Duration to Determine the Persister Plateau

1. Inoculate the ancestral strain (*see* **Notes 1** and **9**) in a test tube containing 5 ml of MHB and incubate overnight.
2. Dilute the overnight culture 1/100 in a flask containing 100 ml of MHB and incubate overnight.
3. Transfer samples of 1 ml of the overnight culture to test tubes and incubate in the presence of a range of antibiotic concentrations for 5 h. Alternatively, samples can be treated with a fixed antibiotic concentration for various treatment durations to determine killing curves in function of time (*see* **Note 10**).
4. Make an appropriate tenfold serial dilution series of the overnight culture in $MgSO_4$ solution (10 mM) and plate out on LB agar. Count colonies after overnight incubation to determine the initial cell number.
5. After antibiotic treatment, spin the samples down in a microcentrifuge (5 min), wash once with $MgSO_4$ solution (10 mM) to remove the antibiotic, make appropriate tenfold serial dilutions in $MgSO_4$ solution (10 mM) and plate out on LB agar plates. Count colonies after 48 h of incubation to determine the number of surviving cells (*see* **Note 11**).
6. Plot the number of surviving cells in function of antibiotic concentration or treatment duration to determine the conditions needed to reach the persister plateau (*see* **Note 8**) (Fig. 1).

3.2 Evolution Experiment

Since evolution experiments often require many days of continuous lab work and many factors can confound the outcome of the experiment (e.g. contaminations, timing of growth and treatment periods, accidental events like power breakdown or glassware breakage and chance resulting in genetic drift), we want to stress the importance of material preparations, thoughtful experimental set-up and careful handling of evolving populations (*see* **Notes 3–5, 7, 9** and **12–19**) to improve replicability and increase work efficiency.

To start the evolution experiment:

1. Inoculate separate single colonies in test tubes containing 5 ml of MHB and incubate overnight. One colony is used as the founder of each population (*see* **Notes 12** and **13**).
2. Dilute the overnight cultures 1/100 in flasks containing 100 ml of MHB and incubate overnight (*see* **Note 14**).

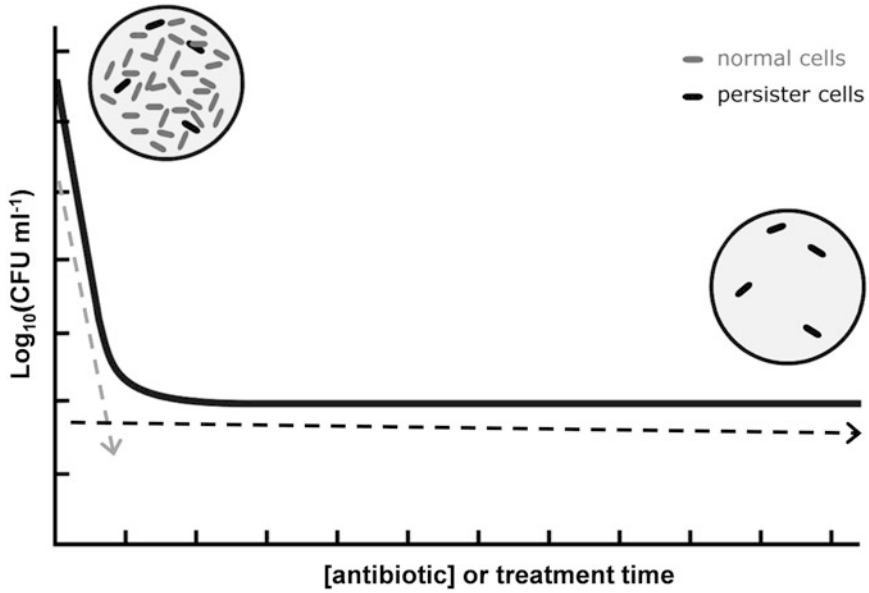

Fig. 1 Killing curve in function of treatment duration or antibiotic concentration reveals a persister plateau. Initially, the number of surviving cells decreases rapidly with increasing antibiotic concentration or treatment duration. However, at a certain point a plateau is reached where a further increase in concentration or treatment duration only slightly increases killing. At this point, all normal cells are killed, and only highly tolerant persister cells remain. This biphasic pattern is a result of the initial fast killing of normal cells (*gray*) and the increased survival of persisters (black) at longer treatment times or higher antibiotic concentrations. Antibiotic concentration and treatment time should be chosen to fall within the range sufficient to reach the persister plateau and ideally in a range where the surviving fraction is minimally influenced by small experimental fluctuations. Reproduced and adapted with permission from [20]

3. Depending on the desired treatment frequency, days with treatment should be alternated with days without treatment (*see* **Note 15**). If the overnight culture (resulting from **steps 2**, **6** or **8**) needs to be treated, continue with **step 4**. If not, move on to **step 8**. In case you want to end the experiment, proceed to **step 9** (*see* **Note 16**).

   On days with treatment:

4. Make appropriate tenfold serial dilutions of the overnight cultures in $MgSO_4$ (10 mM), plate out on LB agar and incubate overnight to determine the total CFU per ml.
5. Treat a 2 ml sample (2× 1 ml) of each overnight culture with antibiotic. Use a concentration and treatment duration according to the results obtained in Subheading 3.1 (*see* **Note 8**).
6. After antibiotic treatment, spin down the samples in a microcentrifuge (5 min) and wash three times with $MgSO_4$ solution (10 mM) to remove the antibiotic. Dilute each sample 1/100 in flasks containing 100 ml of MHB and incubate overnight to

start another cycle of growth (*see* **Note 14**). Make appropriate tenfold serial dilutions of the remaining of the washed samples in $MgSO_4$ solution (10 mM), plate out on LB agar and incubate for 48 h to determine CFU per ml of surviving cells (*see* **Note 11**). The ratio of CFU per ml of surviving cells to CFU per ml of total cells is defined as the persister fraction and should be monitored at regular time intervals throughout the experiment.

7. Irrespective of the desired treatment frequency, pellet 50 ml of the overnight cultures resulting from **step 6** by centrifugation (25 min). Resuspend the pellet in $MgSO_4$ solution (10 mM) to a final volume of 1 ml, add 1 ml of glycerol (50 %, v/v) and store immediately at −80 °C (*see* **Note 16**). Go to **step 3**.

   On days without treatment:

8. Dilute the overnight cultures from **step 6** or **step 8** 1/1,000,000 in flasks containing 100 ml of MHB and incubate overnight to start another cycle of growth (*see* **Notes 14** and **17**). Go to **step 3**.

   To end or interrupt the experiment (*see* **Note 16**):

9. Check every population for contaminations. We use different fluorescent markers to check for possible contamination using fluorescence microscopy (*see* **Notes 1** and **18**).
10. Cryopreserve the overnight cultures as described in **step 7**.
11. Plate out the overnight cultures as described in **step 4**.
12. Isolate clonal endpoints: pick single colonies and use these to inoculate test tubes containing 5 ml of MHB (*see* **Note 19**). Incubate overnight.
13. Cryopreserve the clones at −80 °C: mix 1 ml of overnight culture with 1 ml of glycerol (50 %, v/v).
14. Analyze the antibiotic-related characteristics of the clones and/or the populations according to Subheading 3.1 (*see* **Notes 8** and **9**).

4 Notes

1. We have used numerous *E. coli* lab strains with different genetic backgrounds but also pathogenic strains and even other species (e.g. *Salmonella* Typhimurium) to evolve high persister levels. Ideally, the selected strain should allow detection of (cross)-contamination (e.g. different fluorescent markers, auxotrophic markers), especially in initial experiments. Any extra information (e.g. genomic sequence) can also be taken into account when choosing an ancestral strain. Evidently, the strain should be sensitive to the used antibiotic.

2. We have confirmed our method with other aminoglycosides (kanamycin, tobramycin, and gentamicin). The concentration of the stock solution may be adapted in function of the desired final concentration. When shifting from formulation (e.g. hydrate, sulfates) or supplier, take into account the possible potency difference to achieve similar concentrations.
3. When using antibiotic stock solutions over a long time period (e.g. during a long-term evolution experiment), minimize freeze–thaw cycles of aliquots and renew antibiotic stocks frequently to avoid attenuation of antibiotic efficacy. Amikacin should not be stored for longer than 1 month at −20 °C [29]. Therefore, adjust the amount of antibiotic stock solution and volume of the aliquots to the expected needs.
4. Using premixed MHB formulas may enhance reproducibility. Since company formulas may differ, it is recommended to stick to one supplier and manage MHB stocks well to tackle accidental events in advance (e.g. problems with deliveries or differences between batches). Alternatively, MHB can be prepared using 2 g/l beef Extract powder, 17.5 g/l acid digest of casein, and 1.5 g/l starch. In some cases (depending on the organism and antibiotic of interest [30]) Ca^{2+} and Mg^{2+} content of MHB needs to be adjusted to final concentrations of 20–25 mg/l and 10–12.5 mg/l, respectively. Transfer MHB to other recipients (test tubes, Erlenmeyer flasks) before autoclaving and under continuous mixing or after gentle heating to dissolve it completely. When preparing MHB medium for the evolution experiment itself, please reserve sufficient MHB powder of the same batch for the entire experiment, never store the medium after autoclaving for longer than a week, store at room temperature and away from light and never autoclave twice.
5. Make sure to provide at least three times the number of populations in Erlenmeyer flasks when starting an evolution experiment. Depending on the turnover of your institution's glassware cleaning and the length of the experiment, four or five times the number of populations in flasks may be required.
6. For comparison between parallel evolutionary lines and to compare between independent phenotyping experiments, it is best stick to one incubator or use incubators with identical properties (e.g. shaking amplitude). In our case, 200 rpm equals to 0.11 g.
7. Depending on the unique markers present in the ancestral *E. coli* strains, other means may be needed to check for contamination.
8. These parameters need to be determined at least in biological triplicate. We recommend the antibiotic concentration in the evolution experiment to be at least ten times as high as the MIC

and MBC values, and well above the MPC. The antibiotic concentration and treatment duration also need to be sufficiently high to reach the persister plateau. In our case, antibiotic treatments using amikacin concentrations of minimum 50 μg/ml and maximum 400 μg/ml for 5 h were successfully used in the evolutionary set-up. After the evolution experiment, Subheading 3.1 can be used to assess evolution of genuine persistence, i.e. increased survival with no accompanying changes in MIC value, and to assess evolution of the other antibiotic-related characteristics.

9. If using evolved populations, it is best to limit the amount of growth cycles to reduce further evolution and change in population compositions. Therefore, for populations, Subheading 3.1 could be performed during the evolution experiment. Alternatively and more practically, frozen stocks can also be used as starting point. We advise to thaw these stocks completely and dilute them 1/100 in MHB medium to allow for one overnight growth cycle to stationary phase to obtain sufficient starting material for Subheading 3.1.
10. MIC, MBC, MPC and concentration and treatment durations needed to reach a persister plateau can vary between different species and even between *E. coli* strains. If no prior information is available, we advise starting with a broad range and/or few concentrations. In order to determine the concentrations and treatment durations needed to reach a persister plateau, we always start with optimizing the antibiotic concentration using a fixed and practical treatment time (e.g. 5 h, which leaves enough time to complete growth to stationary phase during a total cycle of 24 h). Subsequently, the persister plateau should be verified in function of time.
11. Since persister cells have longer lag times than normal cells [2, 27], we incubate for 48 h instead of 24 h when plating out after treatment to ensure colony formation of most persister cells.
12. Founding each population from a different colony can prevent compromised results due to the influence of random mutations that might be present in some initial clones. We also advise to replica plate these colonies at the start of the experiment on LB agar and cryopreserve part of the first overnight cultures from **step 1** at −80 °C, e.g. by mixing 1 ml of culture with 1 ml of glycerol (50 %, v/v) to be able to track back particular observations to the founding colony. Depending on the objective of the experiment, the number of replicate populations can be increased or decreased. For example, for a try-out experiment or when the goal is to obtain a high persister mutant for practical reasons in a follow-up study, 1–3 replicates might suffice.

In other cases, for example when the goal is to follow evolution over longer timescales or to study the dynamics of the evolutionary process, it is advised to increase the number of replicate populations to reduce the effect of chance and increase the study's resolution. However, keep in mind that each increase in number of replicates also implies increased work load, materials, and infrastructure demands. If high numbers of replicates are nevertheless necessary, good preparation becomes especially essential (*see* Subheading 2).

13. If you have access to isogenic tagged strains (*see* **Note 1**), we encourage to use them as founders for each population, especially in initial experiments. If you have more populations than uniquely marked strains, we suggest to alternately handle populations with contrasting markers. In this way, cross-contamination may be identified more easily. To limit contamination of any kind, we advise to wear gloves, disinfect gloves and materials between handling different populations, use micropipette tips with filters when handling evolving populations and exclusively use freshly autoclaved solutions of glycerol (50 %, v/v) and $MgSO_4$ solution (10 mM). Never open two flasks or recipients containing evolving populations at the same time.
14. To avoid accidental events that might result in the premature ending of the experiment, we advise storing stationary phase cultures on days with and without treatment at 4 °C as backup until populations have reached the next stationary phase.
15. Although treatment frequency is generally expressed as "once every x days", identical treatment frequencies can be obtained in different ways. For example, when the treatment frequency is once every 8 days, the set-up can start with a treatment followed by 7 dilution steps, start with 7 dilution steps and end with a treatment, or any situation in between. For uniformity, we always start with a treatment step followed by dilution steps in any given setup. On days without treatment, persister levels can still be assayed if necessary, analogous to **steps 4–6** but without inoculating the next cycle of evolution with persister cells.
16. At the last day of the evolution experiment, we once again assay persister levels by repeating **steps 4–6** and freeze the resulting overnight culture like in **step 7**. In this way, the evolution experiment can always be restarted if necessary. Although we advise to perform the experiment without interruption, this allows to pause the experiment if needed. It is possible and sometimes advisable to store samples at −80 °C more frequently as backup and cryopreserved evolution library.

As a minimum, we advise to cryopreserve overnight cultures after every treatment cycle. In this way, if you need to start over, the populations can be inoculated from completely thawed cryopreserved backups with a dilution factor similar to **step 8**. Furthermore, the populations then have at least one growth cycle to adjust from −80 °C conditions before treatment starts. In case the treatment frequency is once every day, persister cells at the end of the experiment (*see* **Note 14**), or at intermediate points, can be cryopreserved at −80 °C after removal of the antibiotic as in **step 6**.

17. On days without treatment, we dilute samples 1/1,000,000 to mimic the bottleneck populations experience on treatment days. Depending on the initial persister level (in our case 10^{-3}-10^{-4}), we advise to adjust this dilution factor. However, keep in mind that strong bottlenecks increase the effect of genetic drift, especially when initial persister levels are low. Furthermore, when using lower treatment frequencies, the selection pressure is not as strong, increasing the influence of drift [33].
18. We advise to check for contamination also at intermediate points during the experiment and definitely when storing samples to pause the experiment. Since the presence of a small number of non-fluorescent cells within a whole population might be difficult to observe, repeat the contamination check on the randomly selected clones.
19. The number of clonal endpoints to isolate from each population is somewhat arbitrary, but again depends on the goal of the experiment. If treatment frequency is low, we would recommend to pick at least five clones per population since variability within populations and between replicate populations might be high. If treatment frequency is high, the number of clones (and the number of replicate populations to isolate clones from) may be decreased.

Acknowledgements

The authors are fellows of the Research Foundation—Flanders (FWO) and the Agency for Innovation by Science and Technology (IWT). The research was further supported by grants from the KU Leuven Research Council (PF/10/010; IDO/09/010) and the IAP-BELSPO initiative.

References

1. Cohen NR, Lobritz MA, Collins JJ (2013) Microbial persistence and the road to drug resistance. Cell Host Microbe 13:632–642
2. Balaban NQ, Merrin J, Chait R et al (2004) Bacterial persistence as a phenotypic switch. Science 305:1622–1625
3. Lewis K (2010) Persister cells. Annu Rev Microbiol 64:357–372
4. Fauvart M, De Groote VN, Michiels J (2011) Role of persister cells in chronic infections: clinical relevance and perspectives on anti-persister therapies. J Med Microbiol 60:699–709
5. Manuel J, Zhanel GG, de Kievit T (2010) Cadaverine suppresses persistence to carboxy-penicillins in *Pseudomonas aeruginosa* PAO1. Antimicrob Agents Chemother 54:5173–5179
6. Li Y, Zhang Y (2007) PhoU is a persistence switch involved in persister formation and tolerance to multiple antibiotics and stresses in *Escherichia coli*. Antimicrob Agents Chemother 51:2092–2099
7. Girgis HS, Harris K, Tavazoie S (2012) Large mutational target size for rapid emergence of bacterial persistence. Proc Natl Acad Sci U S A 109:12740–12745
8. De Groote VN, Verstraeten N, Fauvart M et al (2009) Novel persistence genes in *Pseudomonas aeruginosa* identified by high-throughput screening. FEMS Microbiol Lett 297:73–79
9. Leung V, Levesque CM, Lévesque CM (2012) A stress-inducible quorum-sensing peptide mediates the formation of persister cells with noninherited multidrug tolerance. J Bacteriol 194:2265–2274
10. Hu Y, Coates ARM (2005) Transposon mutagenesis identifies genes which control antimicrobial drug tolerance in stationary-phase *Escherichia coli*. FEMS Microbiol Lett 243:117–124
11. Dhar N, McKinney JD (2010) *Mycobacterium tuberculosis* persistence mutants identified by screening in isoniazid-treated mice. Proc Natl Acad Sci USA 107:12275–12280
12. Ma C, Sim S, Shi W et al (2010) Energy production genes *sucB* and *ubiF* are involved in persister survival and tolerance to multiple antibiotics and stresses in *Escherichia coli*. FEMS Microbiol Lett 303:33–40
13. Hansen S, Lewis K, Vulić M (2008) Role of global regulators and nucleotide metabolism in antibiotic tolerance in *Escherichia coli*. Antimicrob Agents Chemother 52:2718–2726
14. Spoering AL, Vulic M, Lewis K et al (2006) GlpD and PlsB participate in persister cell formation in *Escherichia coli*. J Bacteriol 188: 5136–5144
15. Germain E, Castro-Roa D, Zenkin N et al (2013) Molecular mechanism of bacterial persistence by HipA. Mol Cell 52:248–254
16. Shah D, Zhang Z, Khodursky A et al (2006) Persisters: a distinct physiological state of *E. coli*. BMC Microbiol 6:53
17. Keren I, Minami S, Rubin E et al (2011) Characterization and transcriptome analysis of *Mycobacterium tuberculosis* persisters. MBio 2: e00100–e00111
18. Keren I, Shah D, Spoering A et al (2004) Specialized persister cells and the mechanism of multidrug tolerance in *Escherichia coli*. J Bacteriol 186:8172–8180
19. Van Acker H, Sass A, Bazzini S et al (2013) Biofilm-grown *Burkholderia cepacia* complex cells survive antibiotic treatment by avoiding production of reactive oxygen species. PLoS One 8:e58943
20. Kint CI, Verstraeten N, Fauvart M et al (2012) New-found fundamentals of bacterial persistence. Trends Microbiol 20:577–585
21. Amato SM, Fazen CH, Henry TC et al (2014) The role of metabolism in bacterial persistence. Front Microbiol 5:70
22. Balaban NQ, Gerdes K, Lewis K et al (2013) A problem of persistence: still more questions than answers? Nat Rev Microbiol 11:587–591
23. Blaby IK, Lyons BJ, Wroclawska-Hughes E et al (2012) Experimental evolution of a facultative thermophile from a mesophilic ancestor. Appl Environ Microbiol 78:144–155
24. Barrick JE, Yu DS, Yoon SH et al (2009) Genome evolution and adaptation in a long-term experiment with *Escherichia coli*. Nature 461:1243–1247
25. Lafleur MD, Qi Q, Lewis K (2010) Patients with long-term oral carriage harbor high-persister mutants of *Candida albicans*. Antimicrob Agents Chemother 54:39–44
26. Mulcahy LR, Burns JL, Lory S et al (2010) Emergence of *Pseudomonas aeruginosa* strains producing high levels of persister cells in patients with cystic fibrosis. J Bacteriol 192:6191–6199
27. Fridman O, Goldberg A, Ronin I et al (2014) Optimization of lag time underlies antibiotic tolerance in evolved bacterial populations. Nature 513:418–421

28. Yu J, Xiao J, Ren X et al (2006) Probing gene expression in live cells, one protein molecule at a time. Science 311:1600–1603
29. Andrews JM (2001) Determination of minimum inhibitory concentrations. J Antimicrob Chemother 48(Suppl 1):5–16
30. Wiegand I, Hilpert K, Hancock REW (2008) Agar and broth dilution methods to determine the minimal inhibitory concentration (MIC) of antimicrobial substances. Nat Protoc 3:163–175
31. Liebens V, Defraine V, Van der Leyden A et al (2014) A putative de-N-acetylase of the PIG-L superfamily affects fluoroquinolone tolerance in *Pseudomonas aeruginosa*. Pathog Dis 71:39–54
32. Drlica K (2003) The mutant selection window and antimicrobial resistance. J Antimicrob Chemother 52:11–17
33. Barrick JE, Lenski RE (2013) Genome dynamics during experimental evolution. Nat Rev Genet 14:827–839

Part V

Cellular and Animal Model Systems for Studying Persistence

Chapter 13

In Vitro Models for the Study of the Intracellular Activity of Antibiotics

Julien M. Buyck*, Sandrine Lemaire*, Cristina Seral, Ahalieyah Anantharajah, Frédéric Peyrusson, Paul M. Tulkens, and Françoise Van Bambeke

Abstract

Intracellular bacteria are poorly responsive to antibiotic treatment. Pharmacological studies are thus needed to determine which antibiotics are most potent or effective against intracellular bacteria as well as to explore the reasons for poor bacterial responsiveness. An in vitro pharmacodynamic model is described, consisting of (1) phagocytosis of pre-opsonized bacteria by eukaryotic cells; (2) elimination of non-internalized bacteria with gentamicin; (3) incubation of infected cells with antibiotics; and (4) determination of surviving bacteria by viable cell counting and normalization of the counts based on sample protein content.

Keywords: Intracellular infection, Gentamicin, Antibiotic, Phagocytosis, Opsonization, Pharmacodynamics, Efficacy, Relative potency

1 Introduction

Intracellular survival of bacteria is now recognized as a major factor associated with dissemination, persistence, and/or recurrence of infections [1–5]. When residing inside eukaryotic cells, bacteria are indeed protected from the host humoral immune defenses and often adopt a dormant lifestyle less responsive to antibiotic action. Moreover, in order to exert their activity against intracellular bacteria, antibiotics have to gain access to the infected compartment within the cells and to express their activity in this specific environment [6, 7]. For these reasons, intracellular activity of antibiotics is unpredictable based on the simple evaluation of their

*Both authors contributed equally to this work.

J.M. Buyck: Focal Area Infection Biology, Biozentrum, University of Basel, Basel, Switzerland
C. Seral: Department of Microbiology, Hospital Clínico Universitario Lozano Blesa, Zaragoza, Spain

Jan Michiels and Maarten Fauvart (eds.), *Bacterial Persistence: Methods and Protocols*,
Methods in Molecular Biology, vol. 1333, DOI 10.1007/978-1-4939-2854-5_13,

activity against extracellular bacteria in broth and of their accumulation within eukaryotic cells. Appropriate models need to be developed for the correct assessment of the capacity of antibiotics to act upon intracellular bacteria.

We present here an in vitro model which allows studying the pharmacodynamics of antibiotics against intracellular bacteria. This model is highly flexible, being adaptable to several bacterial species or strains [8–11] as well as to many cell types [9, 12, 13]. It has been used to compare the activity of commercially available antibiotics [11, 14] and of molecules in preclinical or clinical development (most of which are now registered or in the late phases in clinical trials; [9, 12, 15–19]), with the aim of predicting their potential interest for the treatment of persistent infections. In the case of *Staphylococcus aureus* infections, it has been validated versus animal models of intracellular infection [20, 21].

2 Materials

2.1 Equipment

1. Laminar flow hood: Work is performed in a laminar flow hood in a room with biosafety level adapted to the pathogenicity of the microorganism under investigation [22].
2. CO_2 incubator.
3. Bacteriology incubator.
4. Hemocytometer.
5. Spectrophotometer.

2.2 Reagents

1. Culture medium adapted for eukaryotic cell line used: usually RPMI-1640 or DMEM, supplemented with 10 % fetal calf serum.
2. Cation-adjusted Mueller-Hinton broth (CA-MHB) and tryptic soy agar plates (TSA) (or any other specific media more adapted to the bacterial species investigated).
3. Sterile distilled water.
4. Sterile phosphate buffer saline (PBS): 8 g NaCl, 0.2 g KCl, 1.44 g Na_2HPO_4, 0.24 g KH_2PO_4, 1 L distilled water. Adjust to pH 7.4.
5. Human serum from healthy volunteers (for bacterial opsonization).
6. Gentamicin stock solution (40 mg/mL).
7. Stock solution of the antibiotic under study.
8. Reagents (*see* **Note 1**) or kit (several kits are commercially available) for protein assay according to the Folin-Ciocalteu method, also referred to as Lowry's method [23].
9. Reagents (*see* **Note 2**) or kit for cell viability assay (trypan blue exclusion assay [24] or release of the cytosolic enzyme lactate dehydrogenase [25], for example).

3 Methods

The method described is illustrated in Fig. 1.

3.1 Preparation of Bacterial Suspension and of Media

1. The day before the experiment, prepare an overnight bacterial culture in 15 mL of MHB (37 °C; agitation) to obtain a stationary-phase culture.
2. Unfreeze human serum.
3. Prewarm culture medium, sterile water, and PBS at 37 °C.

3.2 Opsonization of Bacteria

Opsonization is a process by which bacteria are marked by opsonins, which are serum proteins (like antibodies) bridging bacteria to the cell surface in order to favor phagocytosis (*see* **Note 3**).

1. Centrifuge the overnight culture to pellet bacteria (7 min at 3200 × *g*).
2. Resuspend in 1 mL of human serum; dilute with 9 mL of eukaryotic cell culture medium (not supplemented with fetal calf serum in this case, since human serum [final concentration 10 %] is present). Do not vortex.
3. Incubate for 30–60 min at 37 °C under gentle agitation (130 rpm) [11, 26].

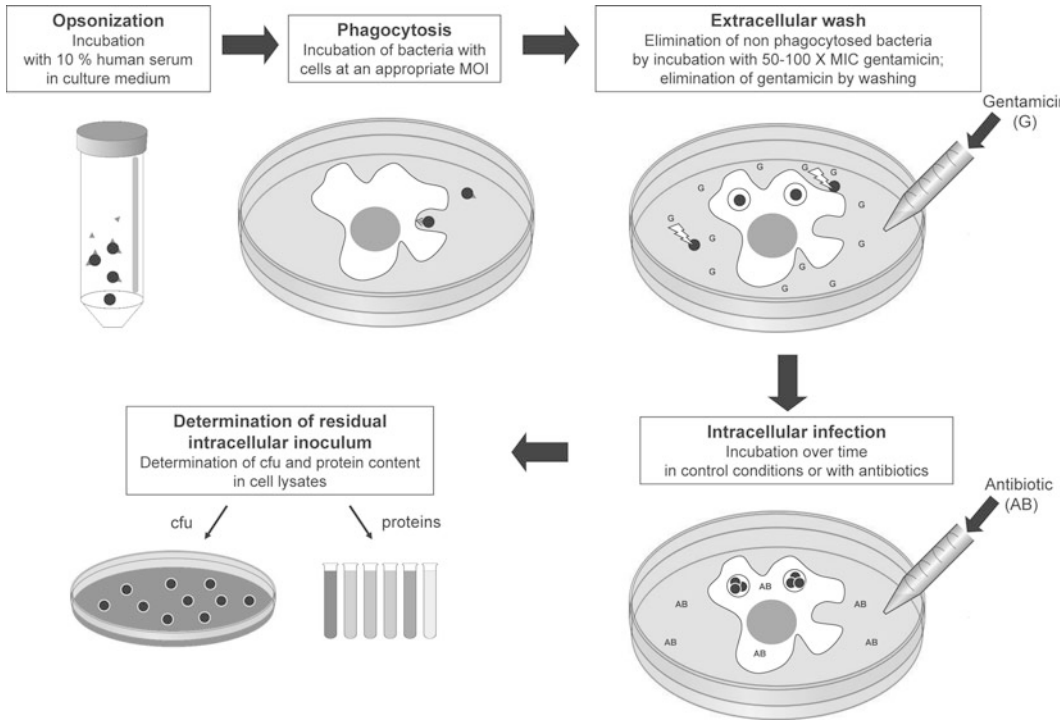

Fig. 1 In vitro model for the assessment of intracellular activity of antibiotics

3.3 Preparation of Eukaryotic Cells and Bacteria for Infection

1. If using eukaryotic cells in suspension, count them (for example using a hemocytometer) in order to obtain a density of 500,000–750,000 cells/mL (*see* **Note 4**).
2. If using adherent cells, plate them in multi-well plates. They should have reached 80 % confluence at the time of the experiment. Prepare extra wells to be used for cell counting at the time of the infection.
3. Centrifuge opsonized bacteria for 7 min at 3200 × *g* and remove supernatant. Resuspend the pellet in 2 mL of PBS or culture medium; and calculate the bacterial concentration, based on a calibration curve establishing the correlation between colony-forming unit (cfu) counts and OD_{620nm} or on the turbidity of the bacterial suspension [McFarland].

3.4 Phagocytosis

This step is critical, in the sense that it is specific for each bacterial strain or species [8, 11, 14, 27] and for the cell type to use for infection [9, 12, 13, 15] and should be adapted by the experimenter (*see* Fig. 2). The objective is to obtain after phagocytosis

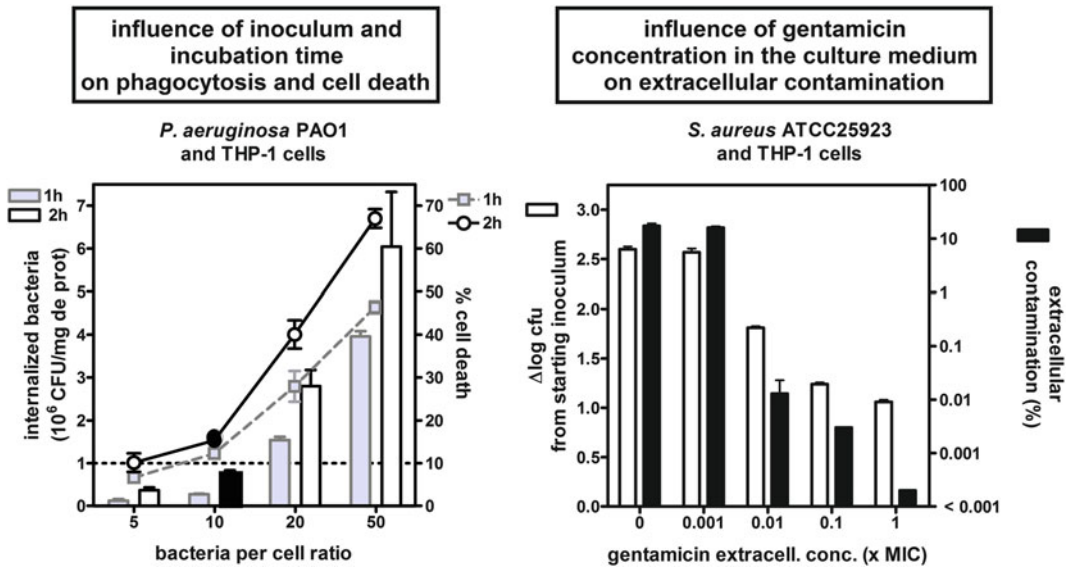

Fig. 2 Setting up a model of intracellular infection. *Left:* determination of the optimal bacterial inoculum and phagocytosis time, as exemplified for *P. aeruginosa* PAO1 (adapted from [11]). Cells were incubated for 1 or 2 h with PAO1 at increasing bacteria-to-cell ratios (*left axis*). The percentage of mortality of THP-1 cells was assessed at the end of the phagocytosis period (*right axis*). Data for 1 h: *gray* symbols and bars; data for 2 h: *open* symbols and bars; the *back* bar and *black* dot correspond to the conditions considered as optimal for this model (*dotted line*: 10^6 cfu/mg protein with <10 % cell toxicity). *Right:* Determination of the optimal concentration of gentamicin to add to culture medium of controls during incubation to avoid extracellular contamination, as exemplified for *S. aureus* ATCC25923 (adapted from [14]). Change in intracellular inoculum (log scale) after 24 h of incubation of infected cells in the presence of increasing concentrations of gentamicin (expressed in multiples of the MIC (*left axis*) percentage of contamination of the extracellular medium in these conditions as assessed by the counting of colonies after plating of pooled culture fluids and washing media (*right axis*; limit of detection: 0.001 %)

an intracellular inoculum that is high enough to allow detecting intracellular bacteria in sufficient numbers but low enough to avoid killing the host cells (typically 10^6 cfu/mg cell protein). The general principle of this part of the protocol is explained hereafter.

1. Phagocytosis: Add bacterial suspension to cell suspension or to adherent cells in order to obtain the desired multiplicity of infection (MOI; number of bacteria/cell); when setting up the model, use in parallel different MOI (typically 1:1; 5:1; 10:1; 20:1; 50:1). Incubate at 37 °C in a CO_2 incubator for appropriate times; when setting up the model, compare different incubation times (typically 0.5, 1, 2 h).
2. Eliminate non-phagocytized bacteria either by centrifugation (cells in suspension; 7 min; 340 g) or by elimination of the medium (adherent cells).
3. Re-incubate infected cells during 45–60 min (37 °C; CO_2 incubator) in cell culture medium (without serum) containing gentamicin at high concentration (typically 50–100 times the MIC for the bacterial strain used [11, 14]) in order to eliminate non-phagocytized bacteria that may adhere to the cell surface (*see* **Note 5**).
4. Wash three times with PBS at room temperature to eliminate bacterial debris and gentamicin.
5. Collect infected cells in 1 mL of sterile water in order to lyse them and allow for release of phagocytized bacteria.
6. Prepare logarithmic dilutions of the cell lysates in PBS and plate 50 µL on TSA or any other appropriate agar plate; proceed to colony counting after 24-h incubation.
7. In parallel, determine protein content of the cell lysates by the Folin-Ciocalteu method [23], using a commercial kit or the method described in **Note 1**.
8. Express the data as cfu/mg of cell protein and select for further experiments the conditions for which you obtain approx. 10^6 cfu/mg cell protein (*see* **Note 6**).

3.5 Intracellular Growth

1. Re-incubate the infected cells in cell culture medium supplemented with 10 % fetal calf serum. For control conditions, add gentamicin at a concentration close to the MIC (as measured in the culture medium used for the experiment) to avoid extracellular growth (*see* Fig. 2) and, in case of cell killing, the multiplication of released bacteria into the medium [14]. For experimental conditions, add the antibiotic you wish to test at the appropriate concentration in the culture medium (*see* **Notes 7** and **8**).

2. At the end of the incubation period, wash the cells three times in PBS and collect them in sterile distilled water as explained above. Proceed to plating, cfu counting, and protein assay.

3.6 Assessment of Antibiotic Intracellular Activity

The model described here allows to monitor antibiotic activity against intracellular bacteria over time or as a function of the extracellular concentration of the antibiotic [11, 14].

1. Considering time effects, bacterial growth is often delayed inside the cells (lag phase of a few hours), so that bacterial killing by antibiotics occurs slower than in broth.
2. Considering concentration effects, performing experiments with broad ranges of extracellular concentrations (from sub-MIC values to many times the MIC) allows obtaining full concentration-response curves for fitting with sigmoid regressions (*see* Fig. 3).
3. Using the corresponding Hill's equation, key pharmacological descriptors of activity can be calculated.

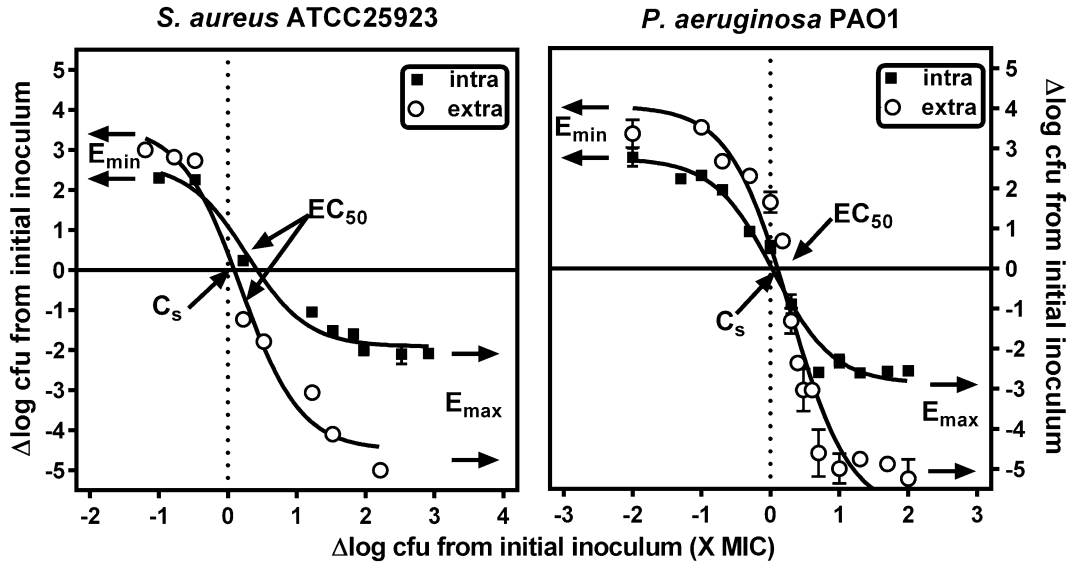

Fig. 3 Concentration-effect relationship for the extracellular and intracellular activity of antibiotics, exemplified for moxifloxacin against *S. aureus* and *P. aeruginosa*. Comparison of the activity of moxifloxacin after 24-h incubation with moxifloxacin in broth (extracellular activity; *open* symbols) or in infected THP-1 cells (*closed* symbols). The ordinate shows the change in the number of cfu per mL (extracellular) or per mg cell protein (intracellular) compared to the post-phagocytosis inoculum (horizontal line at 0). The abscissa shows the antibiotic concentration expressed as the $\log_{10}$ of its MIC in broth. The *dotted line* shows the MIC value. Data are used to fit Hill equations (slope factor = 1) and derive the pertinent key pharmacodynamic parameters, namely (1) E_{min} (change in cfu for an infinitely low antibiotic concentration); (2) E_{max} (relative efficacy; maximal reduction in inoculum as extrapolated for an infinitely large concentration, in $\log_{10}$ cfu units compared to the original inoculum); (3) EC_{50} (relative potency; concentration causing a reduction of the inoculum halfway between E_{min} and E_{max}; C_s (static concentration; concentration resulting in no apparent bacterial growth). Constructed based on data presented in [10, 11]

- The relative minimal efficacy [E_{min}; in $\log_{10}$ cfu units], i.e., the increase in the number of cfu for an infinitely low antibiotic concentration compared to the original post-phagocytosis inoculum.
- The relative maximal efficacy [E_{max}; in $\log_{10}$ cfu units], i.e., the decrease in the number of cfu for an infinitely large concentration of antibiotic.
- The relative potency [EC_{50}; in mg/L or in multiples of MIC], i.e., the concentration of antibiotic yielding a response half-way between E_{min} and E_{max}.
- The static concentration [C_s; in mg/L or in multiple of MIC], i.e., the concentration of antibiotic resulting in no apparent bacterial growth compared to the original inoculum [10].

4. Two major observations have been made with this type of model (*see* Fig. 3).
   - First, the static concentration against intracellular bacteria (i.e., the antibiotic concentration preventing bacterial growth) is in most cases close to the MIC, suggesting that the potency of the drug is not directly correlated with its accumulation inside the cells, possibly because of poor intracellular bioavailability.
   - Second, the antibiotic maximal efficacy is in most cases much lower against intracellular bacteria than against extracellular bacteria, suggesting poor bacterial responsiveness to antibiotic action in the intracellular environment. The molecular reasons for this loss of maximal efficacy inside the cells remain to be established.

4 Notes

1. Protein assay can be performed without any commercial kit, using the protocol described by Lowry [23]. Reagents required are Biuret reagent (extemporaneous mixture of 100 mL 2 % Na_2CO_3, 1 mL 2 % potassium sodium tartrate, 1 mL 1 % $CuSO_4 \cdot 5H_2O$), 2 N Folin-Ciocalteu reagent (diluted to 1 N), 1 N NaOH, and a standard (100 μg/mL bovine albumin). In brief, 0.5 mL of cell lysate (or dilution thereof), blank (medium in which cells were collected), water (solvent of standard), or standard are incubated during 30–120 min with 0.5 mL 1 N NaOH, after which 5 mL of Biuret reagent is added and incubation is continued for 10–20 min. 0.5 mL of 1 N Folin reagent is then added to each tube and absorbance is read at 660 nm after 30 min of incubation (the last step needs to be done tube by tube and with a timer;

incubation time should be strictly the same for each tube). The concentration of proteins in the sample is then calculated as ({[OD_{sample} − OD_{blank}/$OD_{standard}$ − DO_{water}]} × 100 µg/mL [standard concentration] × dilution factor).

2. Viability can be easily assessed using trypan blue exclusion test (vital colorant excluded from viable cells). To this effect, 100 µL of cell suspension are diluted by 900 µL of trypan blue reagent, incubated during 10 min at 37 °C, after which the proportion of dead cells (colored in blue) is determined by cell counting using a hemocytometer. An alternative method consists in measuring the release of lactate deshydrogenase, a cytosolic enzyme, in the supernate of cell culture, which occurs upon permeabilization of the cell membrane. Lactate deshydrogenase (LDH) viability kits are commercialized. The assay can also been performed using the method of Vassault [25], which measures the consumption of NADH upon reduction of pyruvate in lactate by LDH.

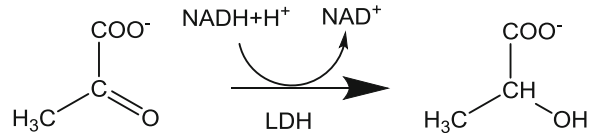

In brief, 50 µL of culture medium or 10 µL of cell lysate are mixed with 2.5 mL of 0.244 mM NADH solution in Tris buffer (81.3 mM Tris/203.3 mM NaCl). 500 µL of 9.76 mM natrium pyruvate (prepared in the same buffer) are added and NADH consumption is followed by measuring optical density at 339 nm immediately and then every minute during 5 min. Cell mortality is evaluated by the ratio between LDH activity in the supernate (estimated by [OD_{0min} − $OD_{5\ min}$] /µL of medium × total volume of the culture medium) and the total activity in the culture (sum of total activity in supernate and total activity in cell lysate estimated as ([OD_{0min} − $OD_{5\ min}$] /µL of medium × total volume of cell lysate).

3. When using obligatory or facultative intracellular organisms which are specifically adapted to use the serum complement to increase phagocytosis, opsonization causes massive infection of the cells [28]. Pre-opsonization is therefore not systematically required [27] and, alternatively, culture medium could be supplemented with decomplemented serum or calf serum (heated for 30 min at 56 °C; [29]) to reduce phagocytosis in order to reach post-phagocytosis inocula compatible with maintenance of cell viability for 24 h.

4. The number of eukaryotic cells to use depends on the virulence of the bacterial strain. For cytotoxic bacterial strains or species, use a higher eukaryotic cell number in order to keep enough cells after phagocytosis, as some killing may occur during this step [11].

5. A limitation of this assay is that the strain has to be susceptible to gentamicin. This antibiotic is selected for the elimination of non-phagocytozed bacteria because it is rapidly bactericidal while at the same time entering only very slowly inside eukaryotic cells. It is therefore important to test for the susceptibility of the bacterial strain to gentamicin (MIC determination) before starting the experiment. Use of lysostaphin as a lytic agent for extracellular bacteria is also proposed in the literature but we showed that it enters inside the cells and may thus affect intracellular viability [26].
6. Depending on the virulence of the strain and its capacity to multiply intracellularly, it is important to check in parallel for the viability of the cells at the end of the phagocytosis period as well as at the end of the experiment. To this effect, a viability assay (trypan blue exclusion assay; lactate dehydrogenase release assay) should be run in parallel as described in **Note 2** and the post-phagocytosis inoculum should be selected so as to guarantee cell viability.
7. Antibiotics or antibacterial agents (or even their solvent if not soluble in water) may also be toxic to eukaryotic cells. Again, it is important to check for cell viability in the presence of the tested agent for correct interpretation of the data. Massive cell death induced by the antibacterial agent can trigger bacterial release into the culture medium and therefore lead to the evaluation of the activity of the tested agent against extracellular bacteria rather than against intracellular bacteria [30].
8. For highly bactericidal antibiotics, check that the amount of carried-over antibiotic does not impair bacterial growth on the plates [26]. This can be done by comparing the number of cfu on plates from lysates pre-exposed or not to 12.5 mg/L charcoal (adsorbing residual antibiotic) during 10 min [16].

Acknowledgments

Intracellular infection models have been developed thanks to the financial support of the Belgian *Fonds National de la Recherche Scientifique*, the Interuniversity Attraction Poles initiated by the Belgian Science Policy Office, and the Brussels and Walloon Regions.

References

1. Anderson GG, Martin SM, Hultgren SJ (2004) Host subversion by formation of intracellular bacterial communities in the urinary tract. Microbes Infect 6:1094–1101
2. Cossart P, Sansonetti PJ (2004) Bacterial invasion: the paradigms of enteroinvasive pathogens. Science 304:242–248

3. Garzoni C, Kelley WL (2011) Return of the Trojan horse: intracellular phenotype switching and immune evasion by Staphylococcus aureus. EMBO Mol Med 3:115–117
4. Mehlitz A, Rudel T (2013) Modulation of host signaling and cellular responses by Chlamydia. Cell Commun Signal 11:90
5. Rohde M, Chhatwal GS (2013) Adherence and invasion of streptococci to eukaryotic cells and their role in disease pathogenesis. Curr Top Microbiol Immunol 368:83–110
6. Carryn S, Chanteux H, Seral C et al (2003) Intracellular pharmacodynamics of antibiotics. Infect Dis Clin North Am 17:615–634
7. Van Bambeke F, Barcia-Macay M, Lemaire S et al (2006) Cellular pharmacodynamics and pharmacokinetics of antibiotics: current views and perspectives. Curr Opin Drug Discov Devel 9:218–230
8. Garcia LG, Lemaire S, Kahl BC et al (2012) Influence of the protein kinase C activator phorbol myristate acetate on the intracellular activity of antibiotics against hemin- and menadione-auxotrophic small-colony variant mutants of Staphylococcus aureus and their wild-type parental strain in human THP-1 cells. Antimicrob Agents Chemother 56:6166–6174
9. Lemaire S, Kosowska-Shick K, Appelbaum PC et al (2010) Cellular pharmacodynamics of the novel biaryloxazolidinone radezolid: studies with infected phagocytic and nonphagocytic cells, using Staphylococcus aureus, Staphylococcus epidermidis, Listeria monocytogenes, and Legionella pneumophila. Antimicrob Agents Chemother 54:2549–2559
10. Lemaire S, Kosowska-Shick K, Appelbaum PC et al (2011) Activity of moxifloxacin against intracellular community-acquired methicillin-resistant Staphylococcus aureus: comparison with clindamycin, linezolid and co-trimoxazole and attempt at defining an intracellular susceptibility breakpoint. J Antimicrob Chemother 66:596–607
11. Buyck JM, Tulkens PM, Van Bambeke F (2013) Pharmacodynamic evaluation of the intracellular activity of antibiotics towards Pseudomonas aeruginosa PAO1 in a model of THP-1 human monocytes. Antimicrob Agents Chemother 57:2310–2318
12. Lemaire S, Glupczynski Y, Duval V et al (2009) Activities of ceftobiprole and other cephalosporins against extracellular and intracellular (THP-1 macrophages and keratinocytes) forms of methicillin-susceptible and methicillin-resistant Staphylococcus aureus. Antimicrob Agents Chemother 53:2289–2297
13. Lemaire S, Olivier A, Van Bambeke F et al (2008) Restoration of susceptibility of intracellular methicillin-resistant Staphylococcus aureus to beta-lactams: comparison of strains, cells, and antibiotics. Antimicrob Agents Chemother 52:2797–2805
14. Barcia-Macay M, Seral C, Mingeot-Leclercq MP et al (2006) Pharmacodynamic evaluation of the intracellular activities of antibiotics against Staphylococcus aureus in a model of THP-1 macrophages. Antimicrob Agents Chemother 50:841–851
15. Lemaire S, Van Bambeke F, Appelbaum PC et al (2009) Cellular pharmacokinetics and intracellular activity of torezolid (TR-700): studies with human macrophage (THP-1) and endothelial (HUVEC) cell lines. J Antimicrob Chemother 64:1035–1043
16. Lemaire S, Tulkens PM, Van Bambeke F (2011) Contrasting effects of acidic pH on the extracellular and intracellular activities of the anti-gram-positive fluoroquinolones moxifloxacin and delafloxacin against Staphylococcus aureus. Antimicrob Agents Chemother 55:649–658
17. Barcia-Macay M, Lemaire S, Mingeot-Leclercq MP et al (2006) Evaluation of the extracellular and intracellular activities (human THP-1 macrophages) of telavancin versus vancomycin against methicillin-susceptible, methicillin-resistant, vancomycin-intermediate and vancomycin-resistant Staphylococcus aureus. J Antimicrob Chemother 58:1177–1184
18. Lemaire S, Van Bambeke F, Tulkens PM (2009) Cellular accumulation and pharmacodynamic evaluation of the intracellular activity of CEM-101, a novel fluoroketolide, against Staphylococcus aureus, Listeria monocytogenes, and Legionella pneumophila in human THP-1 macrophages. Antimicrob Agents Chemother 53:3734–3743
19. Melard A, Garcia LG, Das D et al (2013) Activity of ceftaroline against extracellular (broth) and intracellular (THP-1 monocytes) forms of methicillin-resistant Staphylococcus aureus: comparison with vancomycin, linezolid and daptomycin. J Antimicrob Chemother 68:648–658
20. Sandberg A, Jensen KS, Baudoux P et al (2010) Intra- and extracellular activities of dicloxacillin against Staphylococcus aureus in vivo and in vitro. Antimicrob Agents Chemother 54:2391–2400
21. Sandberg A, Jensen KS, Baudoux P et al (2010) Intra- and extracellular activity of linezolid against Staphylococcus aureus in vivo and in vitro. J Antimicrob Chemother 65:962–973

22. Centers for Disease Control and Prevention (2009) In: Chosewood LC, Wilson DE (eds) Biosafety in Microbiological and Biomedical Laboratories, 5th edn. U.S. Department of Health and Human Services, Bethesda, MA, pp 1–415
23. Lowry OH, Rosebrough AL, Farr AL et al (1951) Protein measurement with the Folin phenol reagent. J Biol Chem 193:265–275
24. Strober W (2001) Trypan blue exclusion test of cell viability. Curr Protoc Immunol Appendix 3, Appendix
25. Vassault A (1987) Lactate dehydrogenase. In: Bergemeyer HU (eds) Methods in enzymatic analysis. VHC Publishers, Veinheim, Federal Republic of Germany, III: Enzyme I oxydoreductases, transferases, pp 118–126
26. Seral C, Van Bambeke F, Tulkens PM (2003) Quantitative analysis of gentamicin, azithromycin, telithromycin, ciprofloxacin, moxifloxacin, and oritavancin (LY333328) activities against intracellular Staphylococcus aureus in mouse J774 macrophages. Antimicrob Agents Chemother 47:2283–2292
27. Seral C, Carryn S, Tulkens PM et al (2003) Influence of P-glycoprotein and MRP efflux pump inhibitors on the intracellular activity of azithromycin and ciprofloxacin in macrophages infected by Listeria monocytogenes or Staphylococcus aureus. J Antimicrob Chemother 51:1167–1173
28. Drevets DA, Campbell PA (1991) Roles of complement and complement receptor type 3 in phagocytosis of Listeria monocytogenes by inflammatory mouse peritoneal macrophages. Infect Immun 59:2645–2652
29. Carryn S, Van Bambeke F, Mingeot-Leclercq MP et al (2002) Comparative intracellular (THP-1 macrophage) and extracellular activities of beta-lactams, azithromycin, gentamicin, and fluoroquinolones against Listeria monocytogenes at clinically relevant concentrations. Antimicrob Agents Chemother 46:2095–2103
30. Lemaire S, Bogdanovitch T, Chavez-Bueno S et al (2006) Bactericidal activity of ceragenin CSA-13 against intracellular MSSA, hospital-acquired (HA) and Community-acquired (CA) MRSA, and VISA in THP-1 macrophages: relation to cellular toxicity ? 46th Interscience Conference on Antimicrobial Agents and Chemotherapy, San Francisco, CA, A-0633

Chapter 14

A Murine Model for *Escherichia coli* Urinary Tract Infection

Thomas J. Hannan and David A. Hunstad

Abstract

Urinary tract infections (UTI) are among the most common bacterial infections of humans. The mouse provides an excellent and tractable model system for cystitis and pyelonephritis caused by *Escherichia coli* and other uropathogens. Using a well-established model of experimental cystitis in which the bladders of female mice are infected via transurethral catheterization, the molecular details of the pathogenesis of bacterial cystitis have been substantially illuminated in the last decade. Uropathogenic *E. coli* attach to bladder epithelium (both in human and mouse) via adhesive type 1 pili, establish a replicative niche within epithelial cell cytoplasm, and form intracellular bacterial communities that are protected from antibiotic effects and immune clearance. The use of different inbred and mutant mouse strains offers the opportunity to study outcomes of infection, including resolution, formation of quiescent intracellular bacterial reservoirs, chronic bacterial cystitis, and recurrent infections. Urine, bladder, and kidney tissues can be analyzed by bacterial culture, histology, immunohistochemistry, immunofluorescent and confocal microscopy, electron microscopy, and flow cytometry, while a broad array of soluble markers (e.g., cytokines) can also be profiled in serum, urine, and tissue homogenates by ELISA, Western blotting, multiplex bead array, and other approaches. This model promises to afford continued opportunity for discovery of pathogenic mechanisms and evaluation of therapeutic and preventive strategies for acute, chronic, and recurrent UTI.

Key words Urinary tract infection, Cystitis, *Escherichia coli*, Intracellular bacterial community, Bacterial persistence

1 Introduction

The human urinary tract is among the most common sites of bacterial infection. Uncomplicated urinary tract infections (UTIs) in the USA result in >10 million medical visits and nearly $4 billion in medical expenditures annually [1]. Predisposing factors for UTI include structural and urodynamic abnormalities, pregnancy [2], diabetes [3], bladder catheterization [4], prostate enlargement [1], HIV infection [5], and sexual activity [6, 7]. Notably, most outpatient UTIs occur in otherwise healthy women with no identifiable risk factors. Indeed, 50 % of women will experience a UTI during their lifetimes, and up to 25 % will suffer recurrence of infection within 6 months following treatment of initial UTI [8].

Jan Michiels and Maarten Fauvart (eds.), *Bacterial Persistence: Methods and Protocols*, Methods in Molecular Biology, vol. 1333, DOI 10.1007/978-1-4939-2854-5_14,

Two-thirds of these recurrences are attributable to the initial strain recovered from a given patient [8, 9].

Uropathogenic *Escherichia coli* (UPEC) cause the bulk of all diagnosed UTIs [8] and are the leading cause of both community-acquired and healthcare-associated UTIs. UPEC wield distinct virulence determinants to cause disease in the bladder (cystitis) and in the kidney (pyelonephritis). Pyelonephritis is distinguished clinically from cystitis by the presence of flank pain, fever, nausea, and vomiting. It follows that a proportion of patients diagnosed with cystitis may also have bacterial colonization of the kidney(s) that does not elicit the overt symptoms typically associated with pyelonephritis. Because no routine clinical testing clearly defines which urinary tissues are involved in an infection, classification of tissue tropism for each clinical isolate relies on patient symptom histories. As a result, it can be difficult to ascertain specific bacterial virulence traits that associate only with cystitis or pyelonephritis.

In the last 1–2 decades much has been learned about the initiation, progression, and resolution of mammalian UTIs using the murine model which will be described herein. In short, female mice of various backgrounds (with varying susceptibility to the establishment of UTI) can be temporarily anesthetized and UPEC (or other uropathogenic species) can be delivered to the bladder by means of catheterization. Following the procedure, which in experienced hands requires only 2–3 min per mouse, animals can be monitored clinically and by collection of blood and urine. Mice are sacrificed at designated time points following infection, and the body fluids (blood and urine) and organs (kidneys and bladder) are harvested and can be processed for numerous cellular and soluble analyses (e.g., bacterial loads, tissue microscopy and histology, leukocyte populations, tissue and serum cytokines).

The mouse represents a desirable model system for mammalian UTI, as the bladder structure and cellular composition mimic those found in the human bladder. As in human disease, bacterial attachment to the bladder epithelium is mediated by a heteropolymeric bacterial surface fiber known as the type 1 pilus [10], while a related organelle (the P pilus) can promote UPEC binding to globoseries glycolipids on the kidney epithelial surface [11]. Recent work in this UTI model has demonstrated that UPEC not only bind, but also invade superficial bladder epithelial cells [12–27] and kidney epithelial cells [28, 29]. Invasion into bladder epithelial cells during cystitis has also been observed with other common uropathogens, including *Staphylococcus saprophyticus* [30], *Klebsiella pneumoniae* [31], and *Salmonella enterica* [22]. This process entails the uptake of UPEC into Rab27b-positive fusiform vesicles, which are normally shuttled into and out of the apical membrane to regulate bladder surface area during the accumulation of urine. As a further result of this vesicle traffic, a proportion of internalized bacteria are

returned to the luminal space via exocytosis [22, 23]. A minority of internalized UPEC then gain unrestricted access to the cytoplasm and grow exponentially in coccoid form, forming clonal, biofilm-like intracellular bacterial communities (IBCs) that can contain up to 10^5 organisms and cause superficial epithelial cells to protrude into the bladder lumen [18]. Arriving phagocytes (largely neutrophils) hone to infected cells but cannot access the replicating bacteria within [32]. Subsequently, bacteria at the IBC periphery regain a bacillary shape or even a phagocytosis-resistant filamentous form [32–34], exit the infected cell, and proceed to infect naïve epithelial cells or to leave the host via micturition. Meanwhile, infected epithelial cells may undergo apoptosis and also be eliminated in the urine [35–38]. Overall, the IBC niche provides UPEC with a protected haven for replication in the face of a burgeoning soluble and cellular inflammatory response. Underscoring the importance of this stage in the establishment of bacterial cystitis, UPEC also employs multiple strategies to dampen initial neutrophil recruitment (see below), allowing a window of opportunity for epithelial invasion and establishment of the intracellular niche. IBC formation might also serve to select subpopulations of introduced UPEC that possess characteristics optimized for intracellular life, subversion of immune effectors, and intraepithelial persistence (see below). Finally, the relevance of the murine IBC cascade to human cystitis is corroborated by the identification of filamentous UPEC (and other Gram-negative uropathogens) and exfoliated, IBC-bearing uroepithelial cells in the urine of patients with UTI [39, 40].

The catheterization model of murine UTI has also been used extensively to characterize the inflammatory response to UPEC arriving in the bladder and kidneys, and to elucidate mechanisms by which UPEC manipulates host responses (reviewed in [41]). To summarize here, UPEC components, including lipopolysaccharide and pili, ligate Toll-like receptors (primarily TLR4) on host epithelium and resident leukocytes [42], stimulating NF-κB and other signaling pathways, eliciting the local secretion of inflammatory cytokines (e.g., IL-1, IL-6, IL-8) [43, 44], and drawing neutrophils to the infected tissues. These findings in mice correlate with genetic polymorphisms in TLR4 and IL-8 receptors that have been demonstrated in selected human populations with repetitive UTI [45–49]. On the bacterial side, UPEC has been demonstrated to downregulate the production of pro-inflammatory cytokines by uroepithelial cells [50–54], deliver leukotoxins [55, 56], and attenuate the trafficking of neutrophils across the uroepithelium [57–59]. These studies represent only a fraction of published work that demonstrates the broad utility of the murine UTI model in dissecting the host-pathogen conversation during bacterial cystitis and pyelonephritis.

Finally, recent advances have revealed multiple phenotypes of UPEC persistence within the bladder. In C57BL/6 mice, bladder infection following inoculation via catheter resolves in nearly all animals within 2 weeks of infection, leaving behind a quiescent intracellular reservoir of UPEC [19] that manifests as small nests of 4–8 organisms visible in Lamp1-positive vesicles within bladder epithelial cells [60]. These bacteria resist clearance by systemically administered antibiotics, appear not to attract immune attention, and reemerge periodically in the murine host to yield recurrent bacteriuria [61]. More recent studies in C3H mice demonstrate a "bimodal" phenotype in which some animals resolve acute infection, while others develop chronic, high-titer cystitis with ongoing cellular inflammation. This model has already yielded novel, translatable insights into host immunologic determinants of the outcome of acute infection and propensity for recurrence [62, 63], as will be addressed further in the methods outlined below.

2 Materials

1. Luria-Bertani (LB) broth: Dissolve 10 g tryptone, 5 g yeast extract, and 10 g NaCl in 1 L deionized (dI) water, and autoclave for 30 min at 121 °C.
2. LB agar plates: Add 16 g agar powder to 1 L LB medium. Autoclave 30 min at 121 °C and allow the medium to cool to 50–60 °C. Pour approximately 25 mL LB agar into 100 × 15 mm plastic petri dishes.
3. Phosphate-buffered saline (PBS): 800 mL of distilled water, 8 g of NaCl, 0.2 g of KCl, 1.44 g of Na_2HPO_4, 0.24 g of KH_2PO_4, adjust the pH to 7.4 with HCl, add distilled water to a total volume of 1 L.
4. Dulbecco's PBS for tissue culture: 2.7 mM KCl, 1.5 mM KH_2PO_4, 137.9 mM NaCl, 8.1 mM $Na_2HPO_4{\cdot}7H_2O$.
5. Triton X solution: 0.01 % (v/w) Triton X-100 in PBS.
6. Sterile lubricating jelly.
7. Ethanol 70 %: 70 % (v/v) ethanol (denatured).
8. Paraformaldehyde 20 % (w/v) solution: Electron microscopy grade.
9. Neutral-buffered formalin solution 10 % (w/v).
10. ProLong Gold antifade reagent.
11. Isoflurane.
12. Mobile rodent anesthesia induction system: Respirator including an isoflurane vaporizer with reservoir, a nose cone and/or induction chamber, and waste anesthetic gas-scavenging canisters.

13. Intramedic non-radiopaque polyethylene tubing, PE10 [inner diameter 0.28 mm (0.011 in.), outer diameter 0.61 mm (0.024 in.)].
14. 30-Gauge hypodermic needles, 1/2 in.
15. 1 mL tuberculin Slip-Tip syringe.
16. Rotor-stator tissue homogenizer with 0.7 mm × 95 mm sawtooth generator probe, or FastPrep24 bead beater with 2 mL screw-top tubes and 5 mm stainless steel beads.
17. SYLGARD 184 silicone elastomer kit.
18. 6-Well polystyrene flat-bottom culture plates.
19. 96-Well polystyrene round-bottom microplates.
20. Sterile microcentrifuge tubes.
21. 5 mL Falcon polycarbonate tubes.
22. Minutien pins, 0.2 mm base diameter.
23. Fisherbrand TRUFLOW tissue and biopsy cassettes.
24. X-gal solution: 25 mg/mL X-gal (5-bromo-4-chloro-3-indolyl-β-D-galactoside) in dimethylformamide.
25. LacZ wash buffer: 2 mM $MgCl_2$, 0.01 % sodium deoxycholate, 0.02 % Nonidet-P40 (Roche) in PBS, pH 7.4.
26. LacZ stain: Mix 9.5 mL LacZ wash buffer with 0.4 mL 25 mg/mL X-gal (final concentration 1 mg/mL) and 0.1 mL combined stock solution of 100 mM potassium ferrocyanide and 100 mM potassium ferricyanide (final concentration 1 mM each).
27. Digestion buffer: 1 mg/mL collagenase D or IV plus 100 μg/mL DNase I in PBS.
28. Confocal and/or epifluorescent microscopes.

3 Methods

3.1 Preparing the Bacterial Inoculum

1. Inoculate 20 mL Luria-Bertani (LB) broth with a single colony of UPEC or from a frozen bacterial stock (*see* **Note 1**). Grow statically for 18–24 h at 37 °C.
2. Subculture 20 μL of overnight culture into 20 mL fresh LB broth and grow statically for 18 h at 37 °C.
3. Centrifuge culture at room temperature for 10 min at 3000 × *g*, discard supernatant and resuspend pellet in 10 mL sterile PBS.
4. Normalize OD_{600} of a 1:10 dilution of the washed culture to 0.35 (for 1 cm path length). For the UPEC strain UTI89 grown under the above conditions, this corresponds to a titer

of 1–2 × 10^7 colony-forming units (CFU) per 50 μL inoculum (*see* **Note 2**).

5. Verify titer inoculum by plating serial dilutions using the spotting method (*see* Subheading 3.2).

3.2 Bacterial Enumeration Using the Spotting Method

1. Use sterile, round-bottom clear polystyrene 96-well plate (Corning 3788).
2. Fill rows A-F with 180 μL sterile PBS per well, where each column allows for serial dilution of a single sample.
3. Add 20 μL of the inoculum to the top row (row A) to make a 1:10 dilution and mix by gently pipetting up and down; Discard pipette tips.
4. Aspirate 20 μL from row A and add to row B to make another 1:10 dilution. Mix by gently pipetting. Discard tips.
5. Repeat **step 4**, aspirating from row B to row C, etc., until row F contains sample diluted 1:10^6 in PBS.
6. Using a repeating multichannel pipettor, aspirate 10 μL of each row for a single column and spot onto an LB agar plate, with or without antibiotic. Repeat four additional times so that a column is spotted five times on a single plate, 50 μL (5 × 10 μL) total per dilution.
7. Allow plates to dry face up, then invert, and incubate overnight at 37 °C (*see* **Note 3**).
8. Count colonies for the row (dilution) that contains a total of 15–150 CFU and calculate the overall titer.
9. Urine and bladder or kidney tissue homogenates can be titered in a similar fashion (*see* **Note 4**).

3.3 Preparing Urinary Catheters

1. Urinary catheters are best prepared in a sterile laminar flow hood equipped with an ultraviolet lamp (such as that used for tissue culture), and all working surfaces, gloves, and instruments should be sprayed with 70 % ethanol.
2. With a sterile blade or scissors, cut a length of polyethylene tubing (PE-10) sufficient for the number of catheters being made.
3. Place a sterile 30-ga × ½-in. needle on a sterile 1 mL tuberculin syringe.
4. Pick up one end of the polyethylene tubing with forceps and gently slide it onto the needle up to the hub.
5. Cut the tubing approximately ½ in. from the needle tip, remove the catheter from the syringe, and place it in a sterile petri dish.

6. Repeat **steps 2–5** as required. A minimum of one catheter is needed per cage of five mice to be infected.
7. UV-irradiate catheters for at least 30 min to ensure sterility.
8. Replace and secure the lid of the petri dish and store catheters for future use.

3.4 Intravesical Inoculation of Mice with Bacteria

1. Draw up the bacterial inoculum (Subheading 3.2) into a tuberculin syringe with 10 μL gradations.
2. Place catheter on syringe and expel all air.
3. Trim catheter to 1–2 mm past the tip of the catheter needle, using fine scissors sterilized with 70 % ethanol or alcohol swabs.
4. Set syringe down, with catheter tip in sterile lubricating jelly.
5. Induce anesthesia in mice with 2–3 % isoflurane using a vaporizer and induction chamber; be careful not to overcrowd the chamber with mice (*see* **Note 5**).
6. Once mice are anesthetized, remove a mouse and place it supine on the working surface (absorbent pad or piece of Styrofoam covered with a clean paper towel) with the tail directed toward the technician; maintain anesthesia using a nose cone assembly connected to the vaporizer (*see* **Note 6**).
7. Place a finger on the caudal abdomen, locate the bladder, and apply pressure in a gentle rostral/caudal motion to empty the bladder of urine (*see* **Note 7**).
8. Place the lubricated catheter tip into the urethral opening, with the catheter and syringe oriented perpendicular to the table.
9. Advance the catheter about 0.5 cm or until resistance is encountered, and then rotate the syringe caudally in an arc 90° so that it is now parallel to the table and tail. The catheter should now be free to pass through the pelvis and into the urinary bladder (*see* **Note 8**).
10. Once the catheter is advanced to the hub of the needle, slowly inject the bladder with 50 μL of inoculum, delivering it in 10 μL increments over 10–15 s to allow the bladder to slowly expand (*see* **Note 9**).
11. Remove the syringe/catheter assembly and set aside with catheter tip in lubricating jelly.
12. Record mouse identification so that each individual can be tracked for longitudinal analyses. Use an ear punch or ear tags to identify co-housed mice. Replace the inoculated mouse back in its cage to recover.
13. Repeat **steps 6–12** for each mouse, changing catheters as needed (e.g., every 5 mice). If different bacterial strains or mutants are part of the same experiment, catheters should be changed between strains.

3.5 Longitudinal Urinalysis

1. For long-term infections in mice, the course of infection can be monitored longitudinally by collecting and analyzing their urine over time (*see* **Note 10**).
2. At each time point, grasp the mouse at the base of the tail and remove from the cage.
3. In one hand, set the mouse on the edge of the cage wire rack with the tail pointing toward the technician while keeping hold of the tail by the thumb and forefinger. In the other hand, hold an open, sterile, pre-labeled 1.5 mL microcentrifuge tube.
4. With the hand that is holding the mouse, use the remaining fingers to apply gentle pressure to the back of the mouse, so that the edge of the wire rack exerts pressure on the ventral suprapubic region of the mouse. Collect the urine in tube.
5. Bacterial enumeration of urines can be performed as explained in Subheading 3.2.
6. Urine white blood cell enumeration can be performed quantitatively using a manual hemacytometer (*see* **Note 11**).
7. An aliquot of urine can be centrifuged at $>12{,}000 \times g$ for 5 min and the supernatants stored at −20 °C or −80 °C for future immunological studies, such as urine cytokine and/or immunoglobulin quantification.

3.6 Antibiotic Treatment and Bacterial Challenge Studies

1. Mice with chronic cystitis (*see* **Note 12**) can be treated with antibiotics to eliminate infection by susceptible organisms at any time after experimental inoculation.
2. Add commonly available veterinary formulations of trimethoprim/sulfamethoxazole to the drinking water at concentrations of 270 and 54 μg/mL, respectively, for 3 or 10 days [61].
3. Antibiotic water should be changed at least every other day, as needed.
4. Monitor urines weekly for bacteriuria to ensure sterilization of urine (*see* **Note 13**).
5. Four weeks or more after initiation of antibiotic therapy, mice can be challenged with UPEC or other bacteria by intravesical inoculation, preferably using a bacterial strain that can be differentiated from the initial infecting strain by phenotypic selection (e.g., an antibiotic marker).

3.7 Tissue Harvesting

1. Humanely euthanize the mouse by CO_2 asphyxiation or cervical dislocation under anesthesia.
2. Place the mouse on the back and spray the ventral abdomen with 70 % ethanol.
3. Using blunt surgical scissors and fine forceps, pull up the skin of the caudal ventral abdomen with the forceps and make a small cut through the skin and peritoneum.

4. Once the peritoneal cavity is entered, use the scissors to make a V-shaped opening in the abdomen by cutting toward the ribs on either side of the body.
5. Manually pull the flap forward toward the nose (rostrally) to bluntly make the opening larger.
6. Remove bladder, kidneys, and other tissues desired for downstream analyses, e.g., tissue homogenization for bacterial enumeration and cytokine analysis (Subheading 3.8), flash freezing of bladder tissue in liquid nitrogen for transcriptomics and proteomics studies, generation of single-cell suspensions for flow cytometry (Subheading 3.9), or fixation of tissues for imaging (Subheading 3.10).

3.8 Tissue Homogenization

1. Place bladder tissue in 1 mL PBS (0.8 mL PBS for kidneys) in a 5 mL Falcon tube on ice and homogenize tissue using a rotor-stator homogenizer for about 40 s (*see* **Note 14**).
2. Take an aliquot of homogenate for bacterial enumeration, described in Subheading 3.2.
3. The remaining homogenate can be cleared by centrifugation at >12,000 × *g* for 5 min and the supernatants and cell pellets separated and frozen at −80 °C for cytokine analysis and Western blotting, respectively.

3.9 Bladder Single-Cell Suspensions for Flow Cytometry

1. Bisect bladder (if desired, rinse in PBS to remove cells and debris from lumen).
2. Digest bladder tissue for 60–90 min at 37 °C in 1 mL digestion buffer (1 mg/mL collagenase D or IV and 100 μg/mL DNase I (from 1000× stock) in PBS).
3. Pass digested tissue through a 40 μm cell strainer into a 50 mL conical tube on ice. Use the black (rubber) end of a sterile 1 mL syringe plunger to assist passage. From this point on, keep cells on ice.
4. Wash the filters twice in 1 mL PBS, and transfer the cell suspension to microcentrifuge tubes; centrifuge at 300 × *g* for 5 min. Remove supernatant carefully with gel-loading tips.
5. Wash cells twice by resuspending in 1 mL PBS, centrifuging at 300 × *g* for 5 min, and removing supernatants with gel-loading tips.
6. Cells can now be stained as required by the experiment (*see* **Note 15**).

3.10 Long-Term Fixation of Tissues for Imaging

1. Aseptically remove the tissue and place in choice of fixative (*see* Subheading 4 for types of fixation).
2. Wash fixed tissues three times in 70 % ethanol and store in 70 % ethanol in watertight container.

3. Place tissues in cassette and submit to histology services for paraffin embedding, sectioning, and hematoxylin and eosin staining (*see* **Note 16**).

3.11 LacZ Staining and Confocal Imaging of Bladder Whole-Mount tissue

1. Aseptically remove each bladder, bisect sharply, and pin out each hemisphere, lumen side up, on silicone elastomer surfaces in 6-well plates containing 1 mL sterile PBS, using two pairs of forceps to manipulate and stretch the bladder and to place pins (*see* **Note 17**).
2. Wash bladders lightly once with PBS.
3. Fix the bladders with 3 % paraformaldehyde in PBS at room temperature for 45–60 min with very gentle movement on a rotator (*see* **Note 18**). If visualizing the bladder by confocal microscopy, proceed with **step 4**; if only visualizing IBCs, skip to **step 9**.
4. Permeabilize the tissue with 0.01 % Triton X-100 in PBS for 10 min.
5. Stain bladders with a nuclear stain (e.g., Topro3, DAPI, or Syto 61) in 0.01 % Triton X-100 in PBS for 3–10 min.
6. Wash in fresh PBS three times for 5 min each.
7. Remove salt by washing in distilled H_2O for 5 min.
8. Mount on glass slide using ProLong Gold antifade reagent with a cover slip, and image using a confocal microscope. If proceeding to LacZ staining, bladders can be stored overnight in PBS at 4 °C.
9. Wash bladders with LacZ wash buffer, three times for 5 min each with gentle rotation.
10. Incubate in LacZ stain for 8–16 h at 30 °C in a light-shielded environment. Monitor staining at 4–6 h and continue stain incubation until punctate staining is visible (on positive control bladders infected with virulent UPEC at known time points). Overlong incubations will result in background staining of uroepithelial cells.
11. Wash in PBS three times for 5 min each.
12. Observe bladders on a dissecting scope and enumerate IBCs. It is advisable to save an image of each bladder half for quantifying IBCs and as a permanent data record.

4 Notes

1. For long-term studies involving urinalysis or challenge infections, the use of a chromosomally encoded antibiotic marker (e.g., conferring resistance to kanamycin or chloramphenicol)

is recommended to distinguish the infecting UPEC strain from contaminating flora of the skin and vagina and from the initial infecting strain during challenge infections. The use of spectinomycin-resistant strains can be problematic, as many spectinomycin-resistant bacteria reside in the vaginal flora. If spectinomycin is used for selection, the use of MacConkey agar containing spectinomycin may be necessary to eliminate contamination from spectinomycin-resistant vaginal flora. The presence of antibiotics may alter bacterial expression of virulence factors even if the strain is able to replicate. Therefore, in preparing the inoculum it is best to grow the bacteria without antibiotics during static growth in LB broth. However, antibiotic selection may be used when streaking on LB agar for single colonies from freezer stock.

2. For a tenfold higher inoculum (~10^8 CFU), apply the same dilution factor to undiluted washed culture. The relationship between culture absorbance (OD_{600}) and viable bacterial titer can vary with bacterial strain and culture/laboratory conditions and should not be assumed to be identical to those described in Subheading 3.1.
3. UPEC grow well on LB agar plates at both room temperature and 37 °C, so the time allowed for drying is not critical. However, this is not true for some other media. Therefore, the use of selective media agar plates to eliminate contamination from the skin and vaginal flora may require more strict culture conditions for bacterial enumeration. For example, UPEC grow poorly on MacConkey agar at room temperature and thus the plates must be dried quickly and placed into 37 °C promptly after plating or bacterial numbers may be underestimated.
4. For longitudinal urinalysis, because of the inherent imprecision in quantifying urine titers due to variability in urine collection, it may be advisable to spot only 10 μL per sample, to allow urines from 5 to 6 mice to be titered using a single plate, thus saving on materials. For tissue titers, PBS is typically not added to row A; instead, undiluted homogenates are placed in this row for serial dilution.
5. Anesthesia can be safely maintained with 2–3 % isoflurane for an extended period of time, provided that the oxygen flow rate is sufficient (this will vary with vaporizer circuit dead space and frequency of induction chamber opening). Alternatively, anesthesia can be induced one mouse at a time in a glass jar containing a steel tea ball that has been filled with cotton balls soaked with isoflurane. However, mice should be monitored very closely and removed immediately from the glass jar after induction (when the respiratory rate begins to decrease) to avoid accidental overdosing and death.

6. If a nose cone connected to a vaporizer is not available, a 50 mL conical tube containing isoflurane-soaked cotton balls packed into the bottom may be used. In this case, the concentration of isoflurane that the mouse is inhaling can be crudely adjusted by altering how deeply the head is positioned in the conical tube.
7. Emptying the bladder of urine prior to bacterial inoculation is a critical step in reducing variability during experimental infection.
8. If resistance is encountered when passing the catheter through the internal urethral sphincter, re-lubricate the catheter and try again. If still encountering resistance, arc the syringe from side to side while gently applying forward pressure. The catheter should pass easily into the bladder—it should never be forcibly passed into the bladder, as this may result in trauma to the lower urinary tract and perhaps death. If the catheter cannot be advanced within 30 s, the technician should stop and move on to the next mouse, coming back a little bit later to the mouse that is causing difficulty. When first learning intravesical inoculation technique, it is a good idea to do practice inoculations with a dye and then dissect out the bladder and urethra to examine for signs of trauma or puncture.
9. Excessive volume or too rapid instillation can lead to iatrogenic vesicoureteral reflux (VUR) in mice, causing the inoculum to be forced into the upper urinary tract. In host strains genetically resistant to VUR, the incidence of kidney infections increased as the volume of UPEC suspension instilled into the bladder exceeded 50 μL [64, 65]. In contrast, C3H and CBA mice are genetically susceptible to VUR, and kidney infection occurs in all mice at inocula of 10^7 and 10^8 CFU per 50 μL.
10. For long-term infections (2–4 weeks), it is sufficient to collect urines at days 1, 3, 7, 10, 14, and weekly thereafter. Persistent high-titer ($>10^4$ CFU/mL) bacteriuria at every time point over 4 weeks is a sensitive and specific indicator of ongoing bladder infection (i.e., chronic cystitis) [62].
11. Alternatively, semiquantitative urine neutrophil analysis can be performed by sedimenting a standard volume of urine (8 μL diluted in sterile PBS is a convenient volume, as 80 μL of 1:10 diluted urine is typically what remains in row A after plating on both LB and LB with an antibiotic for bacterial titers) onto glass slides using a cytocentrifuge (e.g., Wescor CytoPro 7620 at 440 × *g* for 6 min with high acceleration). Stain the slides using Hema-3, Diff-Quik or similar cytology stain, and score degree of pyuria based on cells with segmented nuclei (neutrophils) per high-power field (hpf; 400×) (0: <1/hpf; 1: 1–5/hpf; 2: 6–10/hpf; 3: 11–20/hpf; 4: 21–40/hpf; and 5: >40/hpf). Ghosts (degraded cells without distinct nuclei) are not counted.

12. Some mouse strains (e.g., C3H/HeN) are susceptible to chronic and recurrent infections. It has been demonstrated that the outcome of initial infection in naïve animals can alter their susceptibility to subsequent challenge infections [62]. To specify the outcome of infection, longitudinal urinalysis can be performed for 4 weeks as described in Subheading 3.5. High-titer persistent bacteriuria ($>10^4$ CFU/mL at every time point) is a strong predictor of chronic bacterial cystitis with UPEC, whereas having any time point with bacteriuria $<10^4$ CFU/mL is a strong predictor of resolution of bladder infection. PBS mock-inoculated mice are useful here to provide age-matched naïve controls for bacterial challenge.
13. Antibiotic therapy is generally successful in eliminating susceptible urinary tract infections, especially with antibiotics that concentrate in the urine, such as trimethoprim/sulfamethoxazole. However, some mouse strains are susceptible to abscess formation when the kidneys become infected, and treatment failures can result from poor antibiotic penetration of the abscess.
14. Alternatively, tissue can be homogenized by bead beating. Place tissue in a 2 mL screw-top tube (selected according to bead-beating equipment) containing 200 μL PBS and either one (for kidneys) or two (for bladder) 5 mm stainless steel beads. Homogenize tissue by pulsing twice for 60 s at 4.0 m/s and add 800 or 600 μL PBS to bladder and kidney homogenates, respectively, to reach a final volume of 1 mL.
15. This isolation protocol is optimized for immune cell recovery. Cells can be processed for surface marker and/or intracellular staining. For surface marker staining, it is preferable to stain unfixed cells and gate out dead cells using live/dead stains such as propidium iodide or 7-AAD to improve the quality of analysis. Dead cells predominantly represent non-immune cells and can nonspecifically stain with antibodies.
16. Extra unstained slides may be prepared for later immunofluorescence staining. QIRs can be quantified at >2 weeks post-infection by systematically analyzing by immunofluorescence serial sections through the bladder that have been stained with fluorescent antibodies to *E. coli* and Lamp-1 [60, 66]. A collection of 4–12 organisms within a Lamp-1-positive vesicle constitutes a QIR.
17. The use of fluorescent bacteria, particularly UPEC-expressing green fluorescent protein from a multicopy plasmid [67], greatly enhances the identification of UPEC by confocal microscopy in mounted bladder halves.
18. Alternatively, bladders can be fixed in glutaraldehyde for scanning or transmission electron microscopy, using protocols optimized for your imaging equipment or facility.

Acknowledgment

This work was supported by National Institutes of Health grants R01-DK080752, R01-DK082546, P50-DK064540, and U01-AI095542.

References

1. Litwin MS, Saigal CS, Yano EM, Avila C, Geschwind SA, Hanley JM, Joyce GF, Madison R, Pace J, Polich SM, Wang M (2005) Urologic Diseases in America Project: analytical methods and principal findings. J Urol 173 (3):933–937
2. Andriole VT, Patterson TF (1991) Epidemiology, natural history, and management of urinary tract infections in pregnancy. Med Clin North Am 75(2):359–373
3. Ronald A, Ludwig E (2001) Urinary tract infections in adults with diabetes. Int J Antimicrob Agents 17(4):287–292
4. Nicolle LE (2005) Catheter-related urinary tract infection. Drugs Aging 22(8):627–639
5. Flanigan TP, Hogan JW, Smith D, Schoenbaum E, Vlahov D, Schuman P, Mayer K (1999) Self-reported bacterial infections among women with or at risk for human immunodeficiency virus infection. Clin Infect Dis 29(3):608–612
6. Scholes D, Hooton TM, Roberts PL, Stapleton AE, Gupta K, Stamm WE (2000) Risk factors for recurrent urinary tract infection in young women. J Infect Dis 182(4):1177–1182
7. Eschenbach DA, Patton DL, Hooton TM, Meier AS, Stapleton A, Aura J, Agnew K (2001) Effects of vaginal intercourse with and without a condom on vaginal flora and vaginal epithelium. J Infect Dis 183(6):913–918
8. Foxman B (2003) Epidemiology of urinary tract infections: incidence, morbidity, and economic costs. Dis Mon 49(2):53–70
9. Brauner A, Jacobson SH, Kuhn I (1992) Urinary *Escherichia coli* causing recurrent infections: a prospective follow-up of biochemical phenotypes. Clin Nephrol 38(6):318–323
10. Zhou G, Mo WJ, Sebbel P, Min G, Neubert TA, Glockshuber R, Wu XR, Sun TT, Kong XP (2001) Uroplakin Ia is the urothelial receptor for uropathogenic *Escherichia coli*: evidence from in vitro FimH binding. J Cell Sci 114(Pt 22):4095–4103
11. Dodson KW, Jacob-Dubuisson F, Striker RT, Hultgren SJ (1993) Outer-membrane PapC molecular usher discriminately recognizes periplasmic chaperone-pilus subunit complexes. Proc Natl Acad Sci U S A 90(8):3670–3674
12. Song J, Bishop BL, Li G, Duncan MJ, Abraham SN (2007) TLR4-initiated and cAMP-mediated abrogation of bacterial invasion of the bladder. Cell Host Microbe 1(4):287–298
13. Wright KJ, Seed PC, Hultgren SJ (2007) Development of intracellular bacterial communities of uropathogenic *Escherichia coli* depends on type 1 pili. Cell Microbiol 9(9):2230–2241
14. Eto DS, Gordon HB, Dhakal BK, Jones TA, Mulvey MA (2008) Clathrin, AP-2, and the NPXY-binding subset of alternate endocytic adaptors facilitate FimH-mediated bacterial invasion of host cells. Cell Microbiol 10 (12):2553–2567
15. Schilling JD, Mulvey MA, Vincent CD, Lorenz RG, Hultgren SJ (2001) Bacterial invasion augments epithelial cytokine responses to *Escherichia coli* through a lipopolysaccharide-dependent mechanism. J Immunol 166 (2):1148–1155
16. Berry RE, Klumpp DJ, Schaeffer AJ (2009) Urothelial cultures support intracellular bacterial community formation by uropathogenic *Escherichia coli*. Infect Immun 77 (7):2762–2772
17. Martinez JJ, Mulvey MA, Schilling JD, Pinkner JS, Hultgren SJ (2000) Type 1 pilus-mediated bacterial invasion of bladder epithelial cells. EMBO J 19(12):2803–2812
18. Anderson GG, Palermo JJ, Schilling JD, Roth R, Heuser J, Hultgren SJ (2003) Intracellular bacterial biofilm-like pods in urinary tract infections. Science 301(5629):105–107
19. Mulvey MA, Schilling JD, Hultgren SJ (2001) Establishment of a persistent *Escherichia coli* reservoir during the acute phase of a bladder infection. Infect Immun 69(7):4572–4579
20. Eto DS, Jones TA, Sundsbak JL, Mulvey MA (2007) Integrin-mediated host cell invasion by type 1-piliated uropathogenic *Escherichia coli*. PLoS Pathog 3(7), e100
21. Duncan MJ, Li G, Shin JS, Carson JL, Abraham SN (2004) Bacterial penetration of bladder epithelium through lipid rafts. J Biol Chem 279(18):18944–18951
22. Bishop BL, Duncan MJ, Song J, Li G, Zaas D, Abraham SN (2007) Cyclic AMP-regulated exocytosis of *Escherichia coli* from infected

bladder epithelial cells. Nat Med 13 (5):625–630

23. Eto DS, Sundsbak JL, Mulvey MA (2006) Actin-gated intracellular growth and resurgence of uropathogenic *Escherichia coli*. Cell Microbiol 8(4):704–717
24. Martinez JJ, Hultgren SJ (2002) Requirement of Rho-family GTPases in the invasion of Type 1-piliated uropathogenic *Escherichia coli*. Cell Microbiol 4(1):19–28
25. Doye A, Mettouchi A, Bossis G, Clement R, Buisson-Touati C, Flatau G, Gagnoux L, Piechaczyk M, Boquet P, Lemichez E (2002) CNF1 exploits the ubiquitin-proteasome machinery to restrict Rho GTPase activation for bacterial host cell invasion. Cell 111 (4):553–564
26. Miyazaki J, Ba-Thein W, Kumao T, Obata Yasuoka M, Akaza H, Hayshi H (2002) Type 1, P and S fimbriae, and afimbrial adhesin I are not essential for uropathogenic *Escherichia coli* to adhere to and invade bladder epithelial cells. FEMS Immunol Med Microbiol 33 (1):23–26
27. Terada N, Ohno N, Saitoh S, Saitoh Y, Fujii Y, Kondo T, Katoh R, Chan C, Abraham SN, Ohno S (2009) Involvement of dynamin-2 in formation of discoid vesicles in urinary bladder umbrella cells. Cell Tissue Res 337(1):91–102
28. Chassin C, Vimont S, Cluzeaud F, Bens M, Goujon JM, Fernandez B, Hertig A, Rondeau E, Arlet G, Hornef MW, Vandewalle A (2008) TLR4 facilitates translocation of bacteria across renal collecting duct cells. J Am Soc Nephrol 19(12):2364–2374
29. Pichon C, Hechard C, du Merle L, Chaudray C, Bonne I, Guadagnini S, Vandewalle A, Le Bouguenec C (2009) Uropathogenic *Escherichia coli* AL511 requires flagellum to enter renal collecting duct cells. Cell Microbiol 11 (4):616–628
30. Szabados F, Kleine B, Anders A, Kaase M, Sakinc T, Schmitz I, Gatermann S (2008) *Staphylococcus saprophyticus* ATCC 15305 is internalized into human urinary bladder carcinoma cell line 5637. FEMS Microbiol Lett 285(2):163–169
31. Rosen DA, Pinkner JS, Jones JM, Walker JN, Clegg S, Hultgren SJ (2008) Utilization of an intracellular bacterial community pathway in *Klebsiella pneumoniae* urinary tract infection and the effects of FimK on type 1 pilus expression. Infect Immun 76(7):3337–3345
32. Justice SS, Hung C, Theriot JA, Fletcher DA, Anderson GG, Footer MJ, Hultgren SJ (2004) Differentiation and developmental pathways of uropathogenic *Escherichia coli* in urinary tract pathogenesis. Proc Natl Acad Sci U S A 101 (5):1333–1338
33. Horvath DJ Jr, Li B, Casper T, Partida-Sanchez S, Hunstad DA, Hultgren SJ, Justice SS (2011) Morphological plasticity promotes resistance to phagocyte killing of uropathogenic *Escherichia coli*. Microbes Infect 13(5):426–437
34. Justice SS, Hunstad DA, Seed PC, Hultgren SJ (2006) Filamentation by *Escherichia coli* subverts innate defenses during urinary tract infection. Proc Natl Acad Sci U S A 103 (52):19884–19889
35. Mulvey MA, Lopez-Boado YS, Wilson CL, Roth R, Parks WC, Heuser J, Hultgren SJ (1998) Induction and evasion of host defenses by type 1-piliated uropathogenic *Escherichia coli*. Science 282(5393):1494–1497
36. Thumbikat P, Berry RE, Zhou G, Billips BK, Yaggie RE, Zaichuk T, Sun TT, Schaeffer AJ, Klumpp DJ (2009) Bacteria-induced uroplakin signaling mediates bladder response to infection. PLoS Pathog 5(5), e1000415
37. Thumbikat P, Berry RE, Schaeffer AJ, Klumpp DJ (2009) Differentiation-induced uroplakin III expression promotes urothelial cell death in response to uropathogenic *E. coli*. Microbes Infect 11(1):57–65
38. Klumpp DJ, Rycyk MT, Chen MC, Thumbikat P, Sengupta S, Schaeffer AJ (2006) Uropathogenic *Escherichia coli* induces extrinsic and intrinsic cascades to initiate urothelial apoptosis. Infect Immun 74(9):5106–5113
39. Robino L, Scavone P, Araujo L, Algorta G, Zunino P, Vignoli R (2013) Detection of intracellular bacterial communities in a child with *Escherichia coli* recurrent urinary tract infections. Pathog Dis 68(3):78–81
40. Rosen DA, Hooton TM, Stamm WE, Humphrey PA, Hultgren SJ (2007) Detection of intracellular bacterial communities in human urinary tract infection. PLoS Med 4(12), e329
41. Hunstad DA, Justice SS (2010) Intracellular lifestyles and immune evasion strategies of uropathogenic *Escherichia coli*. Annu Rev Microbiol 64:203–221
42. Hagberg L, Hull R, Hull S, McGhee JR, Michalek SM, Svanborg Eden C (1984) Difference in susceptibility to gram-negative urinary tract infection between C3H/HeJ and C3H/HeN mice. Infect Immun 46(3):839–844
43. Hedges S, Anderson P, Lidin-Janson G, de Man P, Svanborg C (1991) Interleukin-6 response to deliberate colonization of the human urinary tract with gram-negative bacteria. Infect Immun 59(1):421–427

44. Samuelsson P, Hang L, Wullt B, Irjala H, Svanborg C (2004) Toll-like receptor 4 expression and cytokine responses in the human urinary tract mucosa. Infect Immun 72(6):3179–3186
45. Artifoni L, Negrisolo S, Montini G, Zucchetta P, Molinari PP, Cassar W, Destro R, Anglani F, Rigamonti W, Zacchello G, Murer L (2007) Interleukin-8 and CXCR1 receptor functional polymorphisms and susceptibility to acute pyelonephritis. J Urol 177(3):1102–1106
46. Lundstedt AC, Leijonhufvud I, Ragnarsdottir B, Karpman D, Andersson B, Svanborg C (2007) Inherited susceptibility to acute pyelonephritis: a family study of urinary tract infection. J Infect Dis 195(8):1227–1234
47. Lundstedt AC, McCarthy S, Gustafsson MC, Godaly G, Jodal U, Karpman D, Leijonhufvud I, Linden C, Martinell J, Ragnarsdottir B, Samuelsson M, Truedsson L, Andersson B, Svanborg C (2007) A genetic basis of susceptibility to acute pyelonephritis. PLoS One 2(9), e825
48. Ragnarsdottir B, Jonsson K, Urbano A, Gronberg-Hernandez J, Lutay N, Tammi M, Gustafsson M, Lundstedt AC, Leijonhufvud I, Karpman D, Wullt B, Truedsson L, Jodal U, Andersson B, Svanborg C (2010) Toll-like receptor 4 promoter polymorphisms: common TLR4 variants may protect against severe urinary tract infection. PLoS One 5(5), e10734
49. Svensson M, Irjala H, Svanborg C, Godaly G (2008) Effects of epithelial and neutrophil CXCR2 on innate immunity and resistance to kidney infection. Kidney Int 74(1):81–90
50. Billips BK, Forrestal SG, Rycyk MT, Johnson JR, Klumpp DJ, Schaeffer AJ (2007) Modulation of host innate immune response in the bladder by uropathogenic *Escherichia coli*. Infect Immun 75(11):5353–5360
51. Cirl C, Wieser A, Yadav M, Duerr S, Schubert S, Fischer H, Stappert D, Wantia N, Rodriguez N, Wagner H, Svanborg C, Miethke T (2008) Subversion of Toll-like receptor signaling by a unique family of bacterial Toll/interleukin-1 receptor domain-containing proteins. Nat Med 14(4):399–406
52. Hilbert DW, Pascal KE, Libby EK, Mordechai E, Adelson ME, Trama JP (2008) Uropathogenic *Escherichia coli* dominantly suppress the innate immune response of bladder epithelial cells by a lipopolysaccharide- and Toll-like receptor 4-independent pathway. Microbes Infect 10(2):114–121
53. Hunstad DA, Justice SS, Hung CS, Lauer SR, Hultgren SJ (2005) Suppression of bladder epithelial cytokine responses by uropathogenic *Escherichia coli*. Infect Immun 73 (7):3999–4006
54. Klumpp DJ, Weiser AC, Sengupta S, Forrestal SG, Batler RA, Schaeffer AJ (2001) Uropathogenic *Escherichia coli* potentiates type 1 pilus-induced apoptosis by suppressing NF-κB. Infect Immun 69(11):6689–6695
55. Davis JM, Carvalho HM, Rasmussen SB, O'Brien AD (2006) Cytotoxic necrotizing factor type 1 delivered by outer membrane vesicles of uropathogenic *Escherichia coli* attenuates polymorphonuclear leukocyte antimicrobial activity and chemotaxis. Infect Immun 74(8):4401–4408
56. Davis JM, Rasmussen SB, O'Brien AD (2005) Cytotoxic necrotizing factor type 1 production by uropathogenic *Escherichia coli* modulates polymorphonuclear leukocyte function. Infect Immun 73(9):5301–5310
57. Lau ME, Loughman JA, Hunstad DA (2012) YbcL of uropathogenic *Escherichia coli* suppresses transepithelial neutrophil migration. Infect Immun 80(12):4123–4132
58. Loughman JA, Hunstad DA (2011) Attenuation of human neutrophil migration and function by uropathogenic bacteria. Microbes Infect 13(6):555–565
59. Loughman JA, Hunstad DA (2012) Induction of indoleamine 2,3-dioxygenase by uropathogenic bacteria attenuates innate responses to epithelial infection. J Infect Dis 205 (12):1830–1839
60. Mysorekar IU, Hultgren SJ (2006) Mechanisms of uropathogenic *Escherichia coli* persistence and eradication from the urinary tract. Proc Natl Acad Sci U S A 103 (38):14170–14175
61. Schilling JD, Lorenz RG, Hultgren SJ (2002) Effect of trimethoprim-sulfamethoxazole on recurrent bacteriuria and bacterial persistence in mice infected with uropathogenic *Escherichia coli*. Infect Immun 70(12):7042–7049
62. Hannan TJ, Mysorekar IU, Hung CS, Isaacson-Schmid ML, Hultgren SJ (2010) Early severe inflammatory responses to uropathogenic *E. coli* predispose to chronic and recurrent urinary tract infection. PLoS Pathog 6(8), e1001042
63. Hannan TJ, Totsika M, Mansfield KJ, Moore KH, Schembri MA, Hultgren SJ (2012) Host-pathogen checkpoints and population bottlenecks in persistent and intracellular uropathogenic *Escherichia coli* bladder infection. FEMS Microbiol Rev 36(3):616–648
64. Hopkins WJ, Hall JA, Conway BP, Uehling DT (1995) Induction of urinary tract infection by intraurethral inoculation with *Escherichia coli*: refining the murine model. J Infect Dis 171 (2):462–465

65. Murawski IJ, Watt CL, Gupta IR (2011) Vesicoureteric reflux: using mouse models to understand a common congenital urinary tract defect. Pediatr Nephrol 26 (9):1513–1522
66. Wang C, Mendonsa GR, Symington JW, Zhang Q, Cadwell K, Virgin HW, Mysorekar IU (2012) Atg16L1 deficiency confers protection from uropathogenic *Escherichia coli* infection in vivo. Proc Natl Acad Sci U S A 109(27):11008–11013
67. Valdivia RH, Hromockyj AE, Monack D, Ramakrishnan L, Falkow S (1996) Applications for green fluorescent protein (GFP) in the study of host-pathogen interactions. Gene 173(1):47–52

Chapter 15

Analysis of Macrophage-Induced *Salmonella* Persisters

Robert A. Fisher, Angela M. Cheverton, and Sophie Helaine

Abstract

A small subpopulation of non-replicating, multidrug-tolerant bacteria is present within clonal populations of many bacterial species. Known as persisters, these bacteria are probably the cause of relapsing infections such as typhoid fever. Formation of non-growing *Salmonella* persisters is stimulated by macrophage phagocytosis. This chapter outlines methods to identify and study persisters resulting from interactions between bacterial pathogens and their hosts. We use their antibiotic tolerance for isolation and enumeration and developed a method to study the heterogeneity of growth within clonal populations through single-cell analysis.

Key words Persisters, *Salmonella*, Single-cell analysis, Macrophages, Bacterial pathogen, Fluorescence dilution

1 Introduction

Colony-forming units (CFU) are commonly used to measure intracellular bacterial proliferation; however CFU only provides a value for the average growth and killing of a population. It is now evident that bacterial replication is heterogeneous and that a small subpopulation of viable but non-replicating multidrug-tolerant bacteria is present within clonal populations. These cells are called persisters and are thought to be the cause of relapsing infections after the use of antibiotic therapy. Persisters have been observed in a number of medically important pathogens (e.g., *Salmonella, Pseudomonas, Staphylococcus, Streptococcus*, and pathogenic *Escherichia coli*). However the naturally infrequent occurrence of persisters in culture makes their characterization difficult.

Salmonella enterica serovar Typhi causes typhoid fever in humans, and is responsible for an estimated 21 million cases worldwide each year. Fifteen percent of people treated for typhoid fever experience a relapse in infection and 1–6 % of infected individuals become symptomless, chronic carriers and act as reservoirs for the pathogen, even after antibiotic treatment. *Salmonella enterica*

Jan Michiels and Maarten Fauvart (eds.), *Bacterial Persistence: Methods and Protocols*,
Methods in Molecular Biology, vol. 1333, DOI 10.1007/978-1-4939-2854-5_15,

serovar Typhimurium, though non-typhoidal in humans, causes a typhoid-like infection in mice and so is used frequently as a model for typhoid. Recently Helaine et al. demonstrated that internalization of *Salmonella* by macrophages produced a 100–1000-fold increase in the proportion of persisters when compared to those present in vitro [1, 2]. Fluorescence dilution is a method of single-cell analysis that allows to observe the heterogeneity of replication within clonal bacterial populations and to identify and isolate non-replicating bacteria.

This chapter outlines methods that we used to identify, enrich, and analyze *Salmonella* persisters induced as a result of uptake by macrophages.

2 Materials

2.1 Extraction and Growth of Bone Marrow Macrophages

1. Autoclave three sets of scissors and tweezers for dissection.
2. Bone marrow macrophage medium (BMM): Add 500 mL RPMI 1640 medium, 5 mL of a 100 mM Na pyruvate solution, 5 mL of a 200 mM glutamine solution, 5 mL of a 1 M HEPES solution, 50 mL heat-inactivated fetal calf serum (FCS), and 0.5 mL of a 0.05 M beta-mercaptoethanol solution to the funnel of a 500 mL Stericup vacuum filter unit (Millipore). Filter-sterilize and keep the medium in the Stericup receiver (Millipore) at 4 °C.
3. BMM + penicillin and streptomycin (BMM + P/S): Add 5 mL of a 10,000 U/mL penicillin/streptomycin solution to 500 mL of filtered BMM.
4. BMM + P/S + L929 cell conditioned medium: Add 100 mL of L929 cell conditioned medium to 900 mL of BMM + P/S.
5. 0.83 % NH_4Cl: Weigh 0.415 g of NH_4Cl and transfer to a 0.1 L graduated cylinder. Add tissue culture-grade water up to 50 mL and sterilize using a 0.2 μm syringe filter unit into a sterile 50 mL centrifuge tube. Keep at 4 °C for no more than 2–3 weeks.
6. 0.4 % Sterile trypan blue.
7. Sacrifice the animal just before proceeding to the extraction of bone marrow.

2.2 Infection of Bone Marrow Macrophages

1. Bacterial culture: Using a plastic sterile loop, seed one bacterial colony in 5 mL Luria Bertani (LB) medium in a 30 mL sterile plastic tube and incubate overnight at 37 °C in a shaking incubator.
2. Lysis solution: Dissolve 500 μL of Triton X-100 in 500 mL of sterile PBS and keep at 4 °C.

3. 100 mg/mL Gentamicin stock solution: Dissolve 0.5 g gentamicin sulfate salt in 5 mL dH_2O, and sterilize using a 0.2 μm syringe filter unit into sterile 1.5 mL microfuge tubes in aliquots of 1 mL. Store at −20 °C and thaw before use.

2.3 Transformation of Salmonella with FD Plasmid

1. 50 mg/mL Carbenicillin stock solution: Dissolve 0.5 g carbenicillin disodium salt in 10 mL dH_2O, and sterilize using a 0.2 μm syringe filter unit into sterile 1.5 mL microfuge tubes in aliquots of 1 mL. Store at −20 °C and thaw before use.
2. LB + carbenicillin$_{50}$ agar plates: Weigh out 8 g of Lennox L Broth Base (Invitrogen) and 6 g of bacteriological agar (Oxoid) into 400 mL dH_2O and autoclave at 121 °C for 15 min. Allow to cool before adding 400 μL of carbenicillin stock solution (50 mg/L final) to the agar, mix well, and pour into Petri dishes to set. Once set, leave dishes open for 30 min to dry near the flame or inside a microbiological safety cabinet. Store at 4 °C.
3. Dissolve 5 mL of >99.5 % glycerol in 45 mL of dH_2O in a 100 mL glass bottle and sterilize by autoclaving. Pour 50 mL of dH_2O in a 100 mL glass bottle and sterilize by autoclaving.
4. FD plasmid preparation: Using a plastic sterile loop, seed one bacterial colony of *E. coli* strain containing FD plasmid in 5 mL LB medium supplemented with 5 μL of carbenicillin stock solution in a 30 mL sterile plastic tube and incubate overnight at 37 °C in a shaking incubator. Purify plasmid using a miniprep kit.
5. Bacterial culture: Using a plastic sterile loop, seed one bacterial colony of the *S.* Typhimurium strain in 5 mL LB medium in a 30 mL sterile plastic tube and incubate overnight at 37 °C in a shaking incubator.

2.4 Fluorescence Dilution and Flow Cytometry

1. Arabinose stock solution 20 % (w/v): Dissolve 2 g arabinose in 10 mL dH_2O and sterilize using a 0.2 μm syringe filter unit. Store at room temperature.
2. 100 mg/mL Gentamicin stock solution: *See* Subheading 2.2, **item 3**.
3. MgMes pH 5.0 minimal medium: 5 mM KCl, 7.5 mM $(NH_4)_2SO_4$, 1 mM KH_2PO_4, 8 μM $MgCl_2$, 38 mM glycerol, 0.1 % (w/v) casamino acids, 0.5 mM K_2SO_4, 170 mM MES pH 5.0 in dH_2O. Add 1 mL of 1 M KCl, 3 mL of 500 mM $(NH_4)_2SO_4$, 2 mL of 100 mM KH_2PO_4, 1.6 mL of 1 M $MgCl_2$, 2 mL of 3.8 M glycerol, 2 mL of 10 % (w/v) casamino acids, 2 mL of 50 mM K_2SO_4, and 68 mL of 500 mM MES pH 5.0–118.4 mL of dH_2O to make a final volume of 200 mL to the funnel of a 500 mL Stericup vacuum filter unit (Millipore). Filter-sterilize and keep the medium in the Stericup receiver (Millipore) at room temperature.

4. BMM + gentamicin$_{100}$: Add 5 mL of gentamicin stock solution to 50 mL of filtered BMM.
5. BMM + gentamicin$_{20}$: Add 1 mL of gentamicin stock solution to 50 mL of filtered BMM.
6. Lysis solution: Dissolve 500 μL of Triton X-100 in 500 mL of sterile PBS and keep at 4 °C.
7. 3 % PFA solution: Add phosphate-buffered saline (PBS) tablet (Sigma) to 200 mL of dH_2O in a beaker and stir until dissolved. This yields 0.01 M phosphate buffer, 0.0027 M potassium chloride, and 0.137 M sodium chloride, pH 7.4, at 25 °C. Weigh out 6 g of paraformaldehyde (PFA) powder (use a safety mask) and add to PBS. Warm the mixture on a hotplate to a maximum of 60–65 °C in a chemical fume hood stirring constantly (place a thermometer in the solution to monitor the temperature). Once the solution has reached temperature (after approximately 30 min) and the PFA has dissolved completely—allow to cool, and then aliquot 12 mL into 15 mL centrifuge tubes. Store aliquots at −20 °C.
8. FACS tubes with cell strainer cap (Beckton Dickinson).
9. LSR Fortessa flow cytometer (Beckton Dickinson) using FACSDiva software (Beckton Dickinson).
10. FlowJo software (TreeStar, Inc.).

3 Methods

3.1 Extraction and Growth of Bone Marrow Macrophages

Work within a microbiological safety cabinet (MSC) to maintain sterility of the extracted cells.

1. Spray 70 % ethanol onto the mouse legs, and then gently dislocate knees and hips. Using scissors and tweezers kept in 70 % ethanol, cut the skin on the upper part of the leg and pull down towards the foot. Bend the ankle and cut it to remove the foot without cutting the tibia.
2. Change scissors and tweezers, hold the tibia with the tweezers, and cut away the muscles gently. Cut the joint and put both legs into 15 mL BMM + P/S in a sterile centrifuge tube, on ice (*see* **Note 1**).
3. Using tissue paper, separate the tibia from the femur, by pinching the knee and pulling gently by hand. Remove all the muscles with tissue paper by hand and put the bones in 10 mL BMM + P/S in a sterile centrifuge tube, on ice.
4. Fill a PD with 70 % ethanol and transfer the bones into 70 % ethanol for 2 min. During that time, add 20 mL cold BMM + P/S into another PD and 20 mL into the PD cover. Using a

new set of scissors and tweezers, place the bones in the cover. Prepare a 2 mL syringe with a 25G needle, and fill it with medium from the PD.

5. Holding the femur in the middle of the bone with the tweezers, let the scissors glide to the extremities of the bone until they reach the head of the bone on both sides to cut off both ends. For the tibia, cut the ends of the bone where the red pigmented zones stop.
6. Insert the needle from one side and flush the bone marrow out vigorously. Repeat it on the other side until the bone turns white.
7. Break up the clumps by drawing up and down with the syringe, and then place contents of the PD in a sterile 50 mL centrifuge tube. Wash the PD with 10 mL BMM + P/S, add to the same tube, and place on ice (*see* **Note 2**).
8. Centrifuge at 300 × *g* for 5 min at 4 °C. Aspirate off the supernatant and resuspend in 2 mL of cold 0.83 % NH_4Cl. Leave at room temperature for 3 min. Add 28 mL cold BMM + P/S to stop lysis of red blood cells.
9. Centrifuge at 300 × *g* for 5 min at 4 °C. Aspirate off the supernatant and resuspend cells thoroughly in 10 mL of cold BMM + P/S. Place a sterile cell strainer (100 μm) in a sterile 50 mL centrifuge tube and pipette cells through the strainer into the tube. Keep cells on ice.
10. Mix 10 μL of the cell suspension with 10 μL of 0.2 % trypan blue and count cell concentration using a hemocytometer (*see* **Note 3**).
11. Seed 2.5–3.0 × 10^6 cells/PD and add 8 mL of BMM + P/S + L929 cell conditioned medium. Incubate PD at 37 °C, 5 % CO_2 (*see* **Note 4**).
12. Two to three days later, gently add 10 mL/PD of BMM + P/S (+20 % L929 cell conditioned medium).
13. A week after the extraction, aspirate off the medium from PD and add 10 mL of ice-cold PBS. Leave at 4 °C for 10 min (*see* **Note 5**).
14. Pipette well to detach all cells while tilting the PD. Place into a sterile 50 mL centrifuge tube. Centrifuge at 300 × *g* for 5 min at 4 °C and resuspend cells in 10 mL BMM (*see* **Note 6**).
15. Count using a hemocytometer (*see* **Note 3**).
16. Seed as necessary for infection (1 × 10^6 cells in 2 mL of media per well in a 6-well plate).

3.2 Quantification of Macrophage-Induced Salmonella Persisters

1. Thaw mouse serum and pre-warm BMM at 37 °C. Opsonize bacteria prior to macrophage uptake by mixing 45 μL of overnight culture and 20 μL of mouse serum in 170 μL of BMM. Mix well and incubate at room temperature for 20 min (*see* **Note 7**), then add 600 μL more of warmed BMM, and mix by vortexing.
2. Add 30 μL of opsonized bacteria to each well of a 6-well plate (1×10^6 macrophages per well) to reach a multiplicity of infection (MOI) of 5–10. Centrifuge the plates at $100 \times g$ for 5 min at room temperature (this step counts as start of infection) and then incubate at 37 °C, 5 % CO_2.
3. After 30-min incubation, wash the macrophages three times with room-temperature sterile PBS to remove extracellular bacteria. Add 0.5 mL of PBS + Triton X-100 (0.1 % v/v) to each well to lyse macrophages and release the internalized bacteria. After 2–3 min, collect the lysis suspension in 2×1.5 mL microfuge tubes per plate.
4. Centrifuge at $14{,}000 \times g$ for 2 min and remove supernatant. Resuspend both bacterial pellets together in 1 mL of LB and add to 3 mL LB in a 30 mL sterile plastic tube. Mix by vortexing. Take 100 μL of the bacterial suspension in LB and make serial dilutions (100 μL in 900 μL of sterile PBS in 1.5 mL microfuge tubes). Plate out 100 μL of dilutions (10^{-2}, 10^{-3}, 10^{-4}, and 10^{-5}) on LB agar to enumerate bacteria (T_0 ex vivo).
5. In parallel to infection, add 5 μL of overnight culture of the same strain to 4 ml LB in a 30 mL sterile plastic tube. Mix by vortexing. Take 100 μL of the bacterial suspension in LB and make serial dilutions (100 μL in 900 μL of sterile PBS in 1.5 mL microfuge tubes). Plate out 100 μL of dilutions (10^{-2}, 10^{-3}, 10^{-4}, and 10^{-5}) on LB agar to enumerate bacteria (T_0 in vitro).
6. Add 4 μL of gentamicin stock solution to ex vivo and in vitro LB suspensions and incubate for 24 h at 37 °C in a shaking incubator.
7. After 24 h, remove 1 mL from each of the in vitro and ex vivo cultures, centrifuge at $14{,}000 \times g$ for 2 min, and resuspend in 1 mL PBS. Plate out 200 μL of the in vitro and ex vivo suspensions on LB agar and incubate at 37 °C overnight (T_{24}).
8. Count colonies on the plates for T_0 ex vivo and T_0 in vitro.
9. The next day, count colonies on the plates for T_{24} ex vivo and T_{24} in vitro.
10. Calculate the T_{24}/T_0 CFU ratio to work out the ratio of persisters in both populations.

3.3 Use of Fluorescence Dilution (FD) to Identify Non-replicating Intracellular Salmonella

3.3.1 Transformation of Salmonella with FD Plasmid

1. Add 50 μL of overnight culture of *S.* Typhimurium to 5 mL fresh LB medium and grow to exponential phase by incubating at 37 °C for 2.5 h in a shaking incubator (200 rpm).
2. Place the sterile 10 % glycerol- and dH_2O-containing bottles on ice. Place the bacterial subculture tube on ice for 10 min, then transfer in a sterile 15 mL centrifuge tube, and centrifuge at 8000 × *g* for 15 min at 4 °C.
3. After centrifugation, discard supernatant and resuspend the pellet in 1 mL ice-cold dH_2O.
4. Repeat centrifugation four more times, first resuspending again in 1 mL ice-cold dH_2O, then in 500 μL ice-cold dH_2O, then 500 μL ice-cold 10 % glycerol, and finally in 100 μL ice-cold 10 % glycerol.
5. Aliquot 50 μL of electro-competent bacteria in sterile 1.5 mL microfuge tubes and add 1 μL of pDiGc/pFCcGi mini-prep. Transfer the mix to a 2 mm gap electroporation cuvette (Molecular BioProducts, Fisher Scientific), then apply a charge (2.5 kV, 25 μF, 200 Ω using a Gene Pulser II (BioRad) and Pulse Controller Plus (BioRad) machine), and immediately place cells in 1 mL of SOC broth to shake at 37 °C for 1 h.
6. Centrifuge cells at full speed (1 min), resuspend in 100 μL of broth, plate out on LB + carbenicillin$_{50}$ agar plates, and incubate overnight at 37 °C.

3.3.2 Growth of Bacteria-Carrying FD Plasmids

The pDiGc or pFCcGi plasmids can be used for fluorescence dilution, which allows replicating and non-replicating bacteria to be distinguished by the level of red and green fluorescence respectively (*see* Fig. 1). From the pDiGc plasmid *gfp* is constitutively expressed and an arabinose-inducible promoter controls *dsRed* expression. From the pFCcGi plasmid *mCherry* is constitutively expressed while *gfp* expression is arabinose inducible. The *ampR* gene provides resistance to carbenicillin (or ampicillin), allowing for selection of bacteria carrying the plasmids. Inoculate a single colony of *Salmonella* containing pDiGc or pFCcGi in 5 mL of minimal medium (Mg-MES pH 5.0) supplemented with 5 μL of carbenicillin stock solution (50 mg/L final) and 50 μL of arabinose stock solution (0.2 % final) (*see* **Note 8**). Grow overnight in a shaking incubator at 37 °C (*see* **Note 9**).

3.3.3 Fluorescence Dilution of Salmonella in Macrophages

1. Thaw mouse serum and pre-warm BMM at 37 °C. Opsonize bacteria prior to macrophage uptake by adding 45 μL of overnight culture to 20 μL of mouse serum in 170 μL of BMM (pre-warmed to 37 °C). Mix well and incubate at room temperature for 20 min (*see* **Note 7**), then add 600 μL more of warmed BMM, and mix by vortexing.

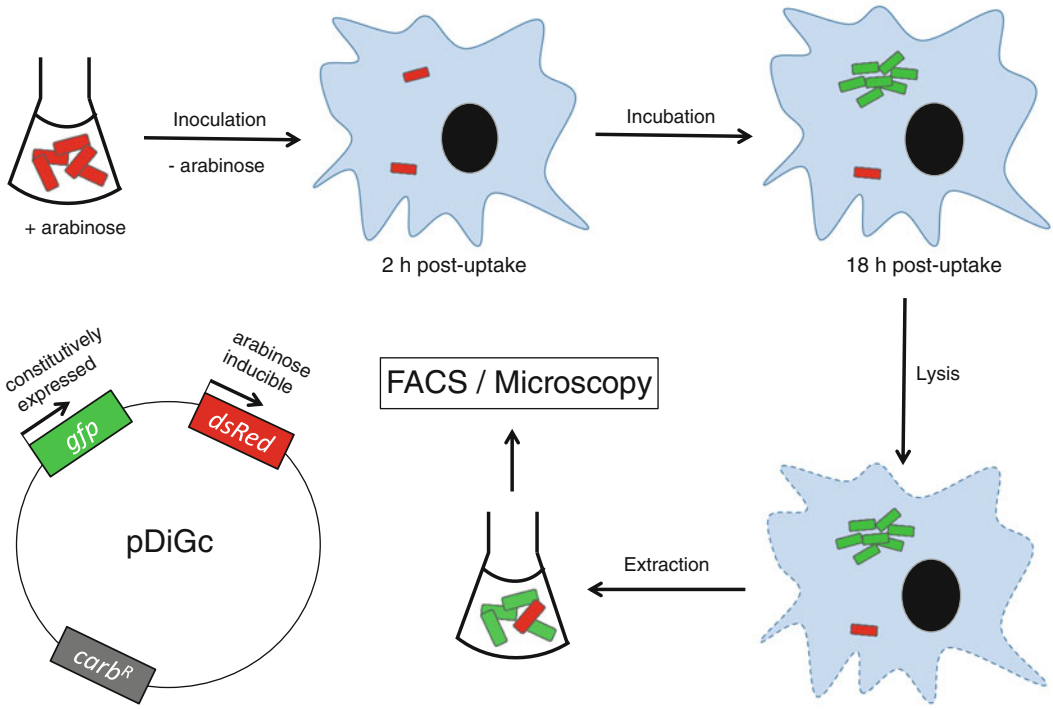

Fig. 1 Fluorescence dilution of *Salmonella* carrying the pDiGc plasmid during infection of bone marrow-derived macrophages. From the pDiGc plasmid *gfp* is constitutively expressed and an arabinose-inducible promoter controls *dsRed* expression. *Salmonella* containing the pDiGc plasmid are grown overnight in the presence of arabinose to induce *red* fluorescence. The bacteria are then inoculated onto the macrophages to be phagocytosed in the absence of DsRed inducer; therefore the expression of *dsRed* is shut down and any subsequent intracellular division will lead to halving of the preformed pool of DsRed in the two daughter cells. 18 h post-uptake, the macrophages are lysed to release the intracellular bacteria. Dilution of the *red* fluorescence signal is an indicator of bacterial replication and can be used to differentiate the two subpopulations of replicating and non-replicating bacteria by flow cytometry or microscopy

2. Add 300 µL of opsonized bacteria to each well of a 6-well plate (1×10^6 cells macrophages per well; 4 wells per different bacterial strain) to reach an MOI of approximately 10. Centrifuge plates at 100 × *g* for 5 min at room temperature (this step counts as start of infection) and then incubate at 37 °C, 5 % CO_2.
3. After 30-min incubation, wash the macrophages three times with room-temperature sterile PBS before adding to each well 2 mL of BMM + gentamicin$_{100}$ and incubate again at 37 °C, 5 % CO_2, to kill extracellular bacteria.
4. After 1-h incubation, wash three times with room-temperature sterile PBS and add 2 mL of BMM + gentamicin$_{20}$ to inhibit growth of any bacteria in the extracellular medium during infection (*see* **Note 10**).
5. At 2 h post-uptake, wash the macrophages in two of the four wells per strain (two technical replicates) three times with

room-temperature sterile PBS and add 1 mL of PBS + Triton X-100 (0.1 % v/v) to each well to lyse the macrophages. After 2–3 min, collect the lysis suspension in two 1.5 mL microfuge tubes.

6. Centrifuge the suspension at 14,000 × *g* for 2 min and remove the supernatant, resuspend the cells in 500 μL PBS 3 % PFA and incubate at room temperature. After 10 min of incubation centrifuge sample at 14,000 × *g* for 2 min and resuspend in 500 mL PBS. Store at 4 °C before carrying out FACS analysis.
7. At 18 h post-uptake, repeat **steps 5** and **6** with the two remaining wells (two technical replicates).
8. When ready to analyze the samples using the flow cytometer, add the 500 mL fixed-cell suspensions to FACS tubes through the cell strainer cap (to remove any macrophage-cell debris that may clog the flow cytometer).
9. Analyze the samples using a flow cytometer (*see* **Note 11**). A minimum of 30,000 bacterial events are acquired.

3.3.4 FACS Analysis

Data can be analyzed using FlowJo Software (TreeStar, Inc.). Our gating strategy with pDiGc-carrying *Salmonella* is illustrated in Fig. 2. The analyzed events are plotted as SSC on the *y*-axis and FSC on the *x*-axis. After gating for the nominal bacterial size and internal complexity using the forward and side scatter, plot the red fluorescent signal (561–610/20 nm) on the *y*-axis against the green fluorescent signal (488–530/30 nm) on the *x*-axis (*see* Fig. 2). Gate on the green-positive events to discriminate bacteria from cellular debris. The dilution of the red fluorescent signal is a readout of bacterial replication and non-replicating bacteria retain high red fluorescence levels equivalent to those displayed by the population 2 h after uptake, before any intracellular replication takes place.

4 Notes

1. A short pause (up to 1 h) can be taken after this step if necessary.
2. A short pause (up to 1 h) can be taken after this step if necessary.
3. Do not count the blue (dead) cells or the red (smaller, round dark border) cells.
4. We use Sterilin Petri dishes (PD) for optimal adhesion of the cells.
5. The cold temperature aides in detaching the macrophages from the PD—for ease, we place the PD in the fridge for this step of the procedure.

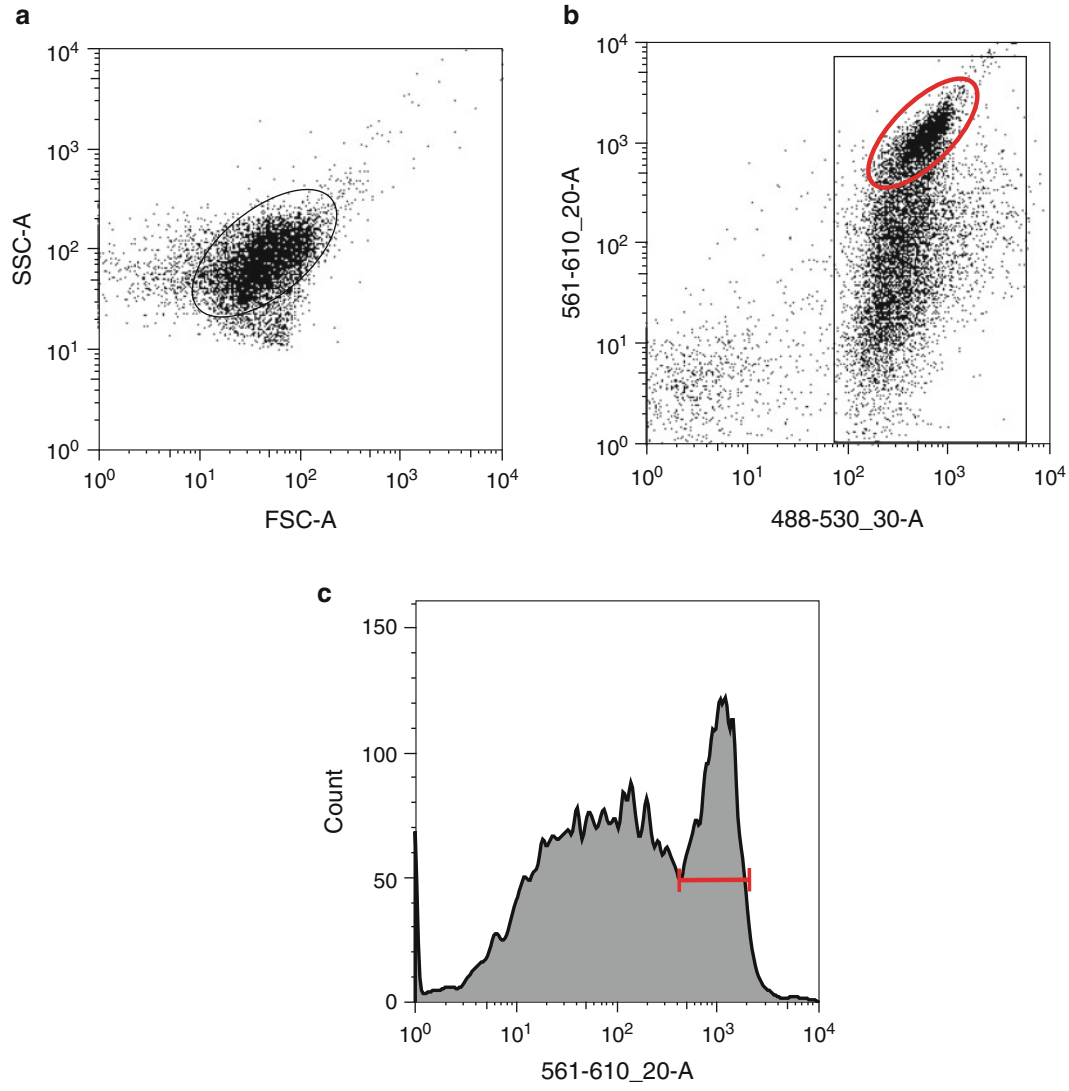

Fig. 2 FACS analysis of fluorescence dilution in pDiGc-carrying *Salmonella* released from macrophages. (**a**) Representative flow cytometry FSC/SSC dot plot of a sample containing *Salmonella* released from macrophages after an 18-h infection, where each point represents an individual event being analyzed. A gate is drawn around events that are typical of size and granularity of *Salmonella* (ellipse). (**b**) Events gated in A are then plotted with their *green* fluorescent signal (488–530/30 nm) on the *x*-axis against their *red* fluorescent signal (561–610/20 nm) on the *y*-axis. Bacteria can be identified and gated for as particles displaying *green* fluorescence (rectangle). Bacteria that retain high *red* fluorescence levels are non-replicating bacteria (*red* ellipse). (**c**) *Red* fluorescence levels of events gated in B can be displayed as histograms. Non-replicating bacteria retain high *red* fluorescence levels (*red* bar)

6. If the macrophages are to be used for bacterial infection, it is important to use BMM (without P/S) at this step, so that antibiotics do not affect subsequent experiments.
7. When infecting with different bacterial strains of *Salmonella*, measure OD_{600} of each overnight culture and adjust volumes to aim for similar bacterial concentrations.
8. Minimal medium is used as the bacteria produce a higher level of fluorescence per cell than if grown in rich medium.
9. Do not let the overnight culture grow for too long at 37 °C (i.e., do not leave in the incubator throughout the next day) as it may affect fluorescence levels.
10. Do not leave the BMM + $gentamicin_{100}$ for longer than 1 h as with time gentamicin permeates the macrophages and may kill intracellular bacteria.
11. We use a LSRFortessa flow cytometer (Beckton Dickinson) where GFP levels are measured using the 488 nm excitation laser and 530/30 filter, and mCherry and DsRed levels are analyzed using the 561 nm excitation laser and 610/20 filters. Results are acquired using the FACSDiva software (Beckton Dickinson).

References

1. Helaine S, Cheverton AM, Watson KG, Faure LM, Matthews SA, Holden DW (2014) Internalization of Salmonella by macrophages induces formation of nonreplicating persisters. Science 343 (6167):204–208. doi:10.1126/science.1244705
2. Helaine S, Thompson JA, Watson KG, Liu M, Boyle C, Holden DW (2010) Dynamics of intracellular bacterial replication at the single cell level. Proc Natl Acad Sci U S A 107(8):3746–3751. doi:10.1073/pnas.1000041107

Chapter 16

Population Dynamics Analysis of Ciprofloxacin-Persistent *S.* Typhimurium Cells in a Mouse Model for *Salmonella* Diarrhea

Patrick Kaiser, Roland R. Regoes, and Wolf-Dietrich Hardt

Abstract

In vivo, antibiotics are often surprisingly inefficient at eliminating bacterial pathogens. In the case of ciprofloxacin therapy in a *Salmonella enterica* subspecies 1 serovar Typhimurium (*S.* Typhimurium, *S.* Tm) mouse infection model, this has been traced to tolerant bacterial cells surviving in lymph node monocytes (i.e., classical dendritic cells). To analyze the growth characteristics of these persisters, we have developed a population dynamics approach using mixtures of wild-type isogenic tagged strains (WITS) and a computational model. Here, we are providing a detailed description of the inoculum, the infection experiments, the computational analysis of the WITS data, and a computer simulation for assessing the quality of the growth parameters of the persistent *S.* Typhimurium cells. This approach is generic. It may be adapted to any organ infected and to any bacterial pathogen, provided that tools exist for generating, retrieving, and quantifying isogenic tagged strains.

Key words Persistence, Population dynamics, Mouse model, *Salmonella* Typhimurium, Ciprofloxacin

1 Introduction

Classical infection biology has focused on endpoints, such as final bacterial burden or death, to assess the efficiency and severity of an infectious process and the efficiency of antibiotic therapy. This approach however neglects the population biological aspects of host colonization which can be of great importance to understand the spatial and temporal events leading to a successful infection, slow in vivo performance of antibiotics, and/or incomplete elimination of the pathogen. Pathogen loads within an organ are a product of immigration, replication, and clearance, three parameters which cannot be distinguished using endpoint analysis and which may change dynamically during the standoff between the pathogen and the host. To assess these dynamic aspects, one needs to devise suitable methods.

Jan Michiels and Maarten Fauvart (eds.), *Bacterial Persistence: Methods and Protocols*,
Methods in Molecular Biology, vol. 1333, DOI 10.1007/978-1-4939-2854-5_16,

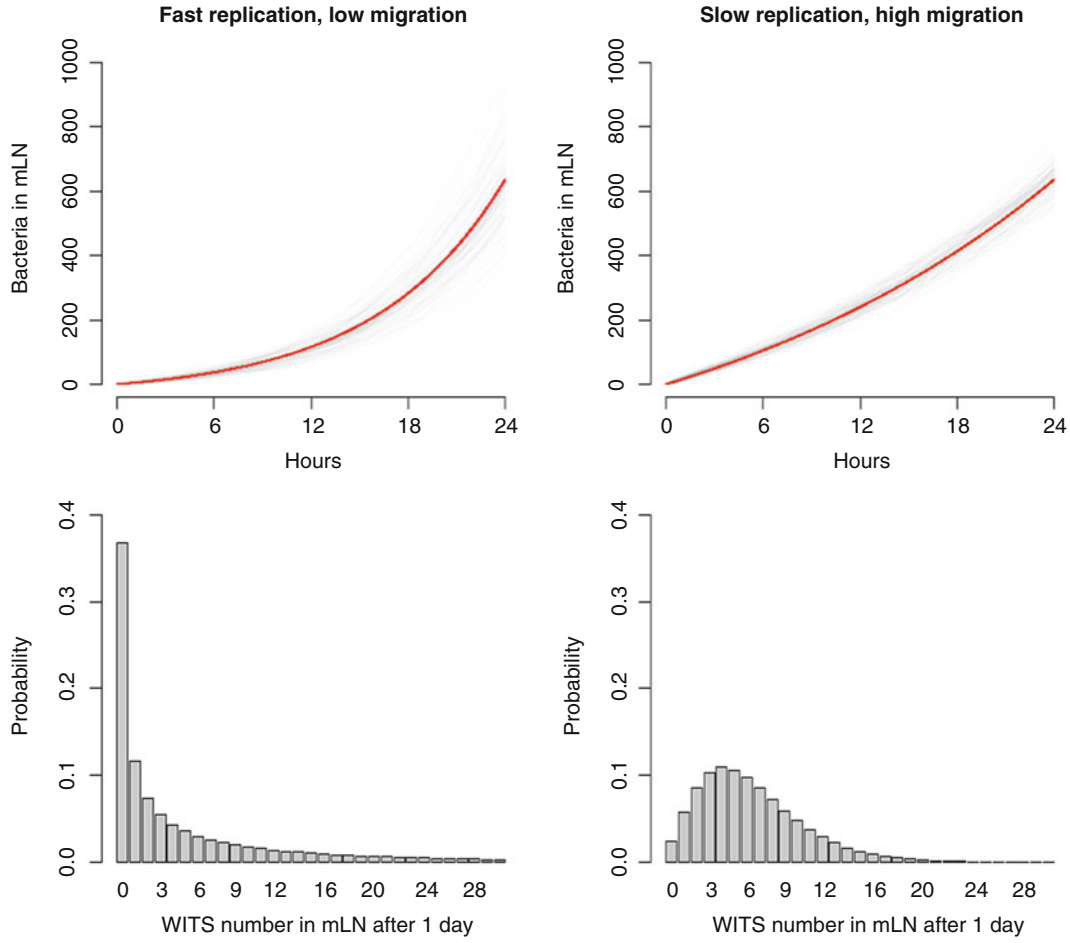

Fig. 1 Infection dynamics leading to equivalent outcomes (e.g., pathogen loads at 24 h post-infection; *upper panels*) can be resolved using isogenic "barcoded" strains (WITS; adapted from [5], Fig. 1). Please note the striking difference between the two bottom plots, depicting data from the analysis of WITS subpopulations

Tracking the fate of subpopulations offers one approach to resolve temporal and spatial aspects of an infection process ([1], Fig. 1). In addition to giving a more defined insight into the initiation of infection, this approach can help understanding later phases of infection, in which pathogens persist over long periods of time without being cleared by the host immune system, and the effect of medical interventions. Moreover, it allows analysis of the features of persistent bacteria that can remain in the host tissues even after prolonged antibiotic therapy [2].

In this chapter, we would like to describe "hands on" how differential tagging of a bacterial pathogen population and mathematical modeling allows the estimation of parameters of the colonization dynamics, which cannot be determined by classical endpoint analysis. The ability to follow changes in the structure of the pathogen population forms the basis of the population dynamic

modeling. Shifts in population structure can be followed by inserting short unique stretches of DNA (together with an antibiotic resistance marker) into a noncoding region of the bacterial chromosome, which can later be detected using real-time quantitative PCR and unique primers complementary to the inserted DNA tag. Shifts in tag abundance between two time points can then be used to estimate the parameters governing the population dynamics.

The protocol described will use *Salmonella enterica* serovar Typhimurium (*S.* Typhimurium) as a model pathogen, but can easily be adapted to any other bacterial pathogen which is genetically accessible. Specifically, we describe how lymph node colonization and the pathogen's population dynamics were analyzed in the streptomycin mouse model for *Salmonella* diarrhea ([3, 4]) before and during treatment with the broad-spectrum fluoroquinolone antibiotic ciprofloxacin [2]. The lymph node colonization before ciprofloxacin treatment establishes the composition of the *S.* Typhimurium population at the beginning of the therapy [5]. This is an important input for subsequent analysis of the growth parameters of persistent *S.* Typhimurium cells in the mesenteric lymph node during the course of antibiotic treatment. We first describe the infection experiment and then explain how the experimental data is analyzed computationally.

2 Materials

1. RT-qPCR primers are listed in Table 1.
2. WITS strains (*S.*Tm^{WITS}): These are wild-type *S.* Typhimurium SL1344 strains carrying a unique 40-nucleotide-long sequence and a kanamycin resistance cassette in the chromosome [5, 6]. Due to their co-localization, the WITS tags and the kanamycin resistance gene cassette can easily be transduced by P22 phage transduction [7] into any *S.* Typhimurium mutant strain background of interest.

Table 1
RT-qPCR primers used in this chapter

WITS1	acgacaccactccacaccta
WITS2	acccgcaataccaacaactc
WITS11	atcccacacactcgatctca
WITS13	gctaaagacacccctcactca
WITS17	tcaccagcccacccccctca
WITS19	gcactatccagccccataac
WITS21	acaaccaccgatcactctcc
ydgA (common reverse primer)	ggctgtccgcaatgggtc

Sequences are oriented 5′ to 3′

3. Mice: The infection experiments are performed in "specified pathogen-free" C57BL/6 mice. However, the streptomycin mouse model can also be performed in any other mouse line, i.e., Balb/c, 129SvEv, and DBA [8, 9] or in knockout mice of interest.
4. Antibiotics: 0.5 g/ml streptomycin. Streptomycin is dissolved in water and filter-sterilized. To generate ciprofloxacin solutions, ciproxine 500 is dissolved in water, and filter-sterilized, and the concentration is determined by UV spectrometry ($A271\ nm = 30{,}614\ l \times mol^{-1} \times cm^{-1}$). 50 mg/ml kanamycin is dissolved in water and filter-sterilized.
5. LB medium: Dissolve 10 g tryptone, 5 g yeast extract, and 10 g NaCl (0.3 M) in 1 l deionized (dI) water, and autoclave for 30 min at 121 °C.
6. LB medium 0.3 M NaCl: LB medium containing 17.5 g NaCl.
7. LB agar plates: Dissolve 15 g agar powder in 1 l LB medium and autoclave for 30 min at 121 °C. Allow the medium to cool down to 50–60 °C and add antibiotics. Pour approximately 30 ml LB agar into each petri dish.
8. MacConkey agar plates: Suspend a measured amount of powder (as specified by the supplier) in 1 l of distilled water and autoclave for 30 min at 121 °C. Allow the medium to cool down to 50–60 °C and add antibiotics. Pour approximately 30 ml LB agar into each petri dish.
9. Phosphate-buffered saline (PBS): 800 ml of distilled water, 8 g of NaCl, 0.2 g of KCl, 1.44 g of Na_2HPO_4, 0.24 g of KH_2PO_4, adjust the pH to 7.4 with HCl, add distilled water to a total volume of 1 l.
10. PBS containing 0.5 % BSA and 0.5 % Tergitol: Add 0.5 g BSA and 0.5 g Tergitol to 100 ml of PBS.
11. DNA purification kit.
12. Equipment for growing the bacteria: 37 °C bacterial incubator with rotating wheel, sterile test tubes, LB agar plates with or without 50 μg/ml kanamycin, Potter homogenizer (15 ml), pipettes, and equipment for plating.
13. Computational analysis: Computer running the R environment for statistical computing that can be downloaded at http://www.r-project.org. This website also hosts documentation about how to install and use R. The methods to analyze the data from the infection experiments are implemented in an R-package `kaiser14pb` published as supplementary material in [2] (Text S1, Protocol S1). For instructions regarding how to install and use the package `kaiser14pb` see below. The package also contains the data set presented in [2].

3 Methods

3.1 Generating a Mixed Inoculum

1. Prepare overnight cultures in LB containing 0.3 M NaCl (one for each *S.*Tm^{WITS} strain containing 50 μg/ml kanamycin and one for the *S.*Tm^{untagged} strain containing 50 μg/ml streptomycin) and incubate aerobically for 12 h at 37 °C on a rotating wheel (45 rpm).
2. For each overnight culture prepare a 1:20 dilution in LB containing 0.3 M NaCl (without antibiotics) and incubate aerobically for 4 h at 37 °C on a rotating wheel (45 rpm). After 4 h, the cultures have reached an OD_{600} of approximately 0.7.
3. Mix 143 μl of each *S.*Tm^{WITS} subculture in a 1.5 ml Eppendorf tube to prepare the $WITS_{mix}$. Spin down $WITS_{mix}$ and 1 ml of *S.*Tm^{untagged} subculture in a microfuge (11,000 G, 5 min, 4 °C). Resuspend pellets in 750 μl PBS and dilute the $WITS_{mix}$ with *S.*Tm^{untagged} as needed to generate the inoculum containing approximately 5×10^7 colony-forming units (cfu) in 70 μl PBS (assume that $OD_{600} = 1$ corresponds to 2×10^9 cfu per ml) (*see* **Note 1**).
4. To verify the composition of the inoculum, an aliquot of the inoculum mix is inoculated into an LB overnight culture containing 50 μg/ml kanamycin to enrich for *S.*Tm^{WITS}. Another two aliquots are plated on two MacConkey agar plates containing either streptomycin (50 μg/ml) or kanamycin (50 μg/ml) to determine the total cfu (*S.*Tm^{untagged} + *S.*Tm^{WITS}) and the total population size of *S.*Tm^{WITS}. Plates and the enrichment culture are incubated for 24 h at 37 °C.

3.2 Mouse Infection and Sample Preparation

1. Mice are infected using the standard streptomycin pretreatment protocol [3]. In brief, mice are deprived of food and water for 4 h and treated with a single dose of streptomycin (25 mg in water; by gavage). Afterwards, food and water are provided ad libitum. Twenty hours after streptomycin treatment, mice are again deprived of food and water for 4 h. Then, they are infected with approx. 5×10^7 cfu *S.*Tm (by gavage). Water is given ad libitum immediately upon infection and food is returned 4 h later. To study antibiotic persistence, mice are orally treated with 62 mg/kg ciprofloxacin (*see* **Note 2**) twice per day (every 12 h). Treatment started generally at day 1 post-infection and was continued for 2–8 days post-infection [2, 10].
2. To end the experiment, mice are sacrificed and organs are aseptically removed and homogenized in 500 μl PBS (0.5 % BSA, 0.5 % Tergitol) using a Potter homogenizer. Half of the lysate is inoculated into an LB overnight culture containing 50 μg/ml kanamycin to enrich for *S.*Tm^{WITS}, and the rest is

plated on MacConkey agar plates containing either streptomycin (50 μg/ml) or kanamycin (50 μg/ml) to determine the total cfu (*S*.Tm^{untagged} + *S*.Tm^{WITS}) and the total population size of *S*.Tm^{WITS}. Plates and the enrichment culture are incubated for 24 h at 37 °C (*see* **Note 3**).

3.3 Quantification of Tag Abundance

1. *rtqPCR*. Chromosomal DNA from whole enrichment cultures can be isolated using any standard method. We used the Qiagen DNA Mini Kit and directly used the DNA for rtqPCR. Each reaction contains 5 μl DNA (~500 ng). For each sample seven reactions using the seven WITS primers (and the common *ydgA* reverse primer) are run according to the following protocol (compare [6]):

   94 °C 10 min
   94 °C 15 s ←┐
   61 °C 30 s 40×
   72 °C 20 s ──┘

2. *Relative abundance to absolute numbers*. For each reaction, a standard curve using defined amounts of DNA isolated from a pure culture of a specific *S*.Tm^{WITS} is generated. These standard curves are used to quantify copy numbers of each WITS tag in every sample. The copy numbers are then used to determine the relative abundance of each tag within the sample.

   To determine the absolute number of bacteria carrying a specific WITS tag in a given sample, the total population size (determined by plating on kanamycin-containing plates) is multiplied by the relative abundance at which the specific tag is present in the rtqPCR reaction (compare [2]).

3.4 Computational Analysis

3.4.1 Installing the R-Package Kaiser14pb

The R-package can be downloaded from http://www.plosbiology.org/article/fetchSingleRepresentation.action?uri=info:doi/10.1371/journal.pbio.1001793.s017. Save the package as `kaiser14pb.tgz` on your local hard drive.

The package `kaiser14pb` relies on another R-package, `GillespieSSA` (http://CRAN.R-project.org/package=GillespieSSA), which has to be installed first. To do that, R and execute

```
> install.packages("GillespieSSA")
```

Now the package `kaiser14pb` can be installed:

```
> install.packages("<path_to_the_file>kaiser14pb.tgz",
+                  repos=NULL, type="source")
```

Load the installed package by executing

```
> library("kaiser14pb")
```

An overview of the function in the package `kaiser14pb` is given in the online manual page:

```
> ?kaiser14pb
```

The derivation of the likelihood functions in this package is described in [5] and [2]. The likelihoods are based on a stochastic birth-death model with immigration.

3.4.2 Estimating Migration, Replication, and Clearance Rates

To illustrate how one can fit the birth-death-immigration model to data, we use the data set `kaiser14pb.data` included in the package. The first lines of the data set can be viewed by executing

```
> head(kaiser14pb.data)
  day mouse.type mouse salmonella.strain total WITS.dilution WITS number
1   1         wt    21             SB300   950   0.007142857    1      0
2   1         wt    21             SB300   950   0.007142857    2     32
3   1         wt    21             SB300   950   0.007142857   11      1
4   1         wt    21             SB300   950   0.007142857   13      0
5   1         wt    21             SB300   950   0.007142857   17      2
6   1         wt    21             SB300   950   0.007142857   19      0
```

The two most important columns are `number`, which contains the population size of each WITS, and `day`, which states the time point after inoculation (in days) when the WITS population size was determined (*see* **Note 4**).

To estimate the immigration rate during the first day of infection one can use the convenience function `fit.function.c0`:

```
> fit.function.c0(data = subset(kaiser14pb.data,
+                               mouse.type=="wt" & day==1))[c("pars","ll")]
$pars
       r       muG
2.819520  2.127068

$ll
[1] -269.4307
```

This function assumes that the clearance rate $c = 0$, and hence the estimate of the replication rate `r` has to be interpreted as a net replication rate (i.e., the difference between replication and clearance). The estimated parameter `muG` represents the immigration rate of a single WITS (in our case the rate of pathogen travel into the gut draining cecal lymph node, one of the mesenteric lymph nodes) and has to be divided by the frequency of this WITS to obtain the immigration rate of the entire *S.* Tm population from the gut to the lymph node. For the particular estimate of `muG` above, we obtain an immigration rate of 298 cells per day for the entire population.

For the subsequent stages of infection (i.e., during ciprofloxacin treatment), one can use the convenience function `fit.function.muG0`:

```
> fit.function.muG0(data = subset(kaiser14pb.data,
+                                 mouse.type=="wt+Cipro" & day==3),
+                   pgf = pgf.treat.d3, output.sd=FALSE)[c("pars","ll")]
$pars
       r        c
4.586701  5.042901

$ll
[1] -125.4199
> fit.function.muG0(data = subset(kaiser14pb.data,
+                                 mouse.type=="wt+Cipro" & day==5),
+                   pgf = pgf.treat.d5, output.sd=FALSE) [c("pars","ll")]
$pars
       r        c
1.881296  2.497735

$ll
[1] -31.29975
> fit.function.muG0(data = subset(kaiser14pb.data,
+                                 mouse.type=="wt+Cipro" & day==10),
+                   pgf = pgf.treat.d10, output.sd=FALSE)[c("pars","ll")]
$pars
       r        c
3.757764e-01  2.430427e-07

$ll
[1] -59.94681
```

This function assumes that the immigration rate $\mu = 0$. This is reasonable, as the gut lumen, the key reservoir for "new" bacteria traveling towards the lymph node, is cleared within a few hours after the onset of ciprofloxacin treatment [2].

3.4.3 Estimating Colonization Parameters from Your Own WITS Infection Data (Before Onset of Antibiotic Therapy)

To analyze your own data, first format them as a data frame in R with at least two columns, called `day` and `number`. These columns should contain the time after inoculation in days, and the population size of each WITS recovered at that time from the lymph node, respectively. For example, your data could comprise the population sizes of seven WITS in three mice sampled at day 1 after inoculation, and could look like this:

```
> your.data <-
+   data.frame(day=1,
+              number=c(0, 4, 7,  3, 7, 3,  5,
+                       0, 9, 0, 12, 0, 3, 23,
+                       0, 4, 11, 0, 3, 0, 11))
```

To estimate the parameters that characterize the early colonization dynamics, you can simply apply `fit.function.c0` on your data:

```
> fit.function.c0(data=your.data)
$pars
       r       muG
2.212298  1.359794

$sd
     sd.r     sd.muG
0.3954401  0.3251824

$ll
[1] -56.05399

$convergence
[1] 0

$fit.message
NULL
```

If the `convergence` is `0`, the likelihood maximization converged and the estimates are reliable. In this case `sd` provides the standard deviations of the estimates for `r` and `muG`. If, however, the function yields something other than `0` as `convergence`, you need to use the basal likelihood functions and maximize them using the function `optim` (*see* **Note 5**).

You can compare the observations with the model predictions (Fig. 2, analogously to Fig. 3b in [5]), by plotting cumulative distribution functions:

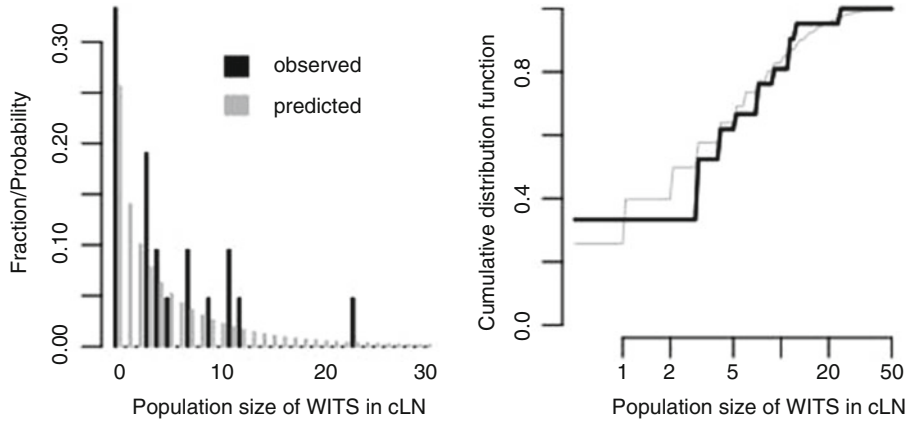

Fig. 2 Comparison of experimental data with modeled data, as described in [5], Fig. 3b

```
> par(mfrow=c(1,2), pty="s") -> op
> your.MLEs <- fit.function.c0(data=your.data)$pars
> pk.pred <-
+     sapply(0:100,
+            function(x) {
+               exp(pk.log(parms=c(r=your.MLEs[["r"]],
+                                  muG=your.MLEs[["muG"]],
+                                  c=0),
+                          dataline=data.frame(number=x,day=1))$ll)})
> pk.obs <-
+     sapply(0:100,
+            function(x) {
+               sum(your.data$number==x)/length(your.data$number)})
> ind <- 0:30
> barplot(rbind(pk.obs[ind+1], pk.pred[ind+1]),
+         names.arg = c(0,rep(NA,9),10,rep(NA,9),20,rep(NA,9),30),
+         xlab="Population size of WITS in cLN",
+         ylab="Fraction/Probability",
+         beside=T,space=c(0.9,1.4),
+         border=c(1, "gray"), col=c(1, "gray"),
+         legend.text=c("observed", "predicted"),
+         args.legend=list(bty="n", border=c(1, "gray")))
> plot(c(0.5,50),c(0,1),
+      xlim=c(0.5,50), ylim=c(0,1),
+      type="n", log="x", axes=FALSE,
+      xlab="Population size of WITS in cLN",
+      ylab="Cumulative distribution function")
> axis(1, at=c(1,2,5,10,20,50));axis(2)
> curve(stepfun(0:100, c(0,cumsum(pk.pred)))(x),
+       lwd=1, col="gray", lty=1, add=TRUE)
> curve(ecdf(your.data$number)(x),
+       lwd=2, col=1, add=TRUE)
> par(op); rm(op)
```

The above code uses the function `pk.log` that calculates the probability of having a certain population size of WITS in the lymph node at a given time after infection.

3.4.4 Estimating Population Dynamics of Persistent S.Tm Cells During Antibiotic Treatment of the Infected Host

The estimation of the immigration and net replication rate before treatment assumed that the cecal lymph node does not contain any *Salmonella* initially. To obtain estimates of the population dynamical parameters during treatment, we need to factor in the size of the population size in the cecal lymph node at the start of the treatment (day 1 after inoculation).

Mathematically, the predicted distribution of WITS population sizes is captured in the probability generating functions. These are used in the likelihood functions for the parameter estimation. To estimate colonization parameters from data obtained at day 3 after inoculation, the probability generating function `pgf.treat.d3` is used. This probability generating function is based on that for the distribution of WITS population sizes 1 day after inoculation, `pgf.salmonella`.

To fit data you obtained under treatment requires to define your own probability generating functions that replace `pgf.treat.d3`, `pgf.treat.d5`, and `pgf.treat.d10`:

```
> your.MLEs <- fit.function.c0(data=your.data)$pars
> your.pgf.treat.d3 <- function(parms, t = 3, s) {
+   t <- t - 1
+   with(as.list(parms), {
+     s0 <- ((r * s - c) * exp(c * t - r * t) - c * s + c)/
+       ((r * s - c) * exp(c * t - r * t) - r * s + r)
+     pgf.salmonella(parms = c(r = your.MLEs[["r"]],
+                              c = 0,
+                              muG = your.MLEs[["muG"]]),
+                    t = 1, s0)
+   })
+ }
```

In the newly defined probability generating function `your.pgf.treat.d3`, the estimates in `kaiser14pb.MLEs` are replaced by your own estimates stored in `your.MLEs`. This can be seen by comparing the definitions of `your.pgf.treat.d3` to those of `pgf.treat.d3`:

```
> pgf.treat.d3
function (parms = c(r = 3, c = 3.5, muG = 0), t = 3, s)
{
     t <- t - 1
     with(as.list(parms), {
          s0 <- ((r * s - c) * exp(c * t - r * t) - c * s + c)/((r *
            s - c) * exp(c * t - r * t) - r * s + r)
          pgf.salmonella(parms = c(r = kaiser14pb.MLEs[kaiser14pb.MLEs$data
set == "SB300", "r"], c = 0, muG = kaiser14pb.MLEs[kaiser14pb.MLEs$data
set == "SB300", "muW"]), t = 1, s0)
    })
}
<environment: namespace:kaiser14pb>
```

To analyze data obtained under treatment we can apply `fit.function.muG0` using `your.pgf.treat.d3`. Assume for example that you determined the population size of WITS in the lymph node 3 days after inoculation, and that treatment was started at day 1. These data may look like the following data frame:

```
> your.data.treat <-
+   data.frame(day=3,
+              number=c(0, 0, 0, 6, 14, 0, 0,
+                       0, 18, 0, 21, 0, 0, 46,
+                       0, 0, 22, 0, 0, 0, 25))
```

Now apply `fit.function.muG0` using `your.pgf.treat.d3` as the `pgf`:

```
> fit.function.muG0(data = your.data.treat,
+                   pgf = your.pgf.treat.d3,
+                   output.sd=FALSE)[c("pars","ll")]
$pars
        r         c
4.916529  4.731710

$ll
[1] -41.80708
```

If your sampling times are not the same as in [2], the functions `pgf.treat.d3`, `pgf.treat.d5`, and `pgf.treat.d10` need to be rewritten to accommodate the alternative sampling schedule. For example, if treatment started at day 1.5, not 1, after inoculation, the first line in the definition of `pgf.treat.d3` should be `t <- t - 1.5` instead of `t <- t - 1`, and `pgf.salmonella` needs to be evaluated at `t = 1.5`, not at `t = 1`.

3.4.5 Simulating the Colonization Dynamics of the Entire Population

Once you obtained estimates for initial immigration and net replication rates, as well as subsequent replication and clearance rates, you can simulate the process using the function `sim.treat`. With the estimates for `kaiser14pb.data` we get

```
> sim.treat(parms.d1=c(r=2.82,c=0.00,mu=298),
+           parms.d3=c(r=4.59,c=5.04,mu= 0),
+           parms.d5=c(r=1.88,c=2.50,mu= 0),
+           parms.d10=c(r=0.38,c=0.00,mu= 0),
+           output.data=FALSE)
  d1  d3  d5  d10
1696 663 195 1292
```

This function is a convenience function that uses a more basic function `bdi.sim` that generates a realization of the stochastic birth-death-immigration process using a Gillespie algorithm. This function relies on the package `GillespieSSA`. Since this simulates a stochastic process, the output will be different for every realization. Also note that we use the immigration rate of the entire *S.*Tm population, 298 per day, as input into this function.

To produce a plot such as the one shown in (Fig. 3, Fig. 4b in [2]), run a few simulations, and plot them as in this example:

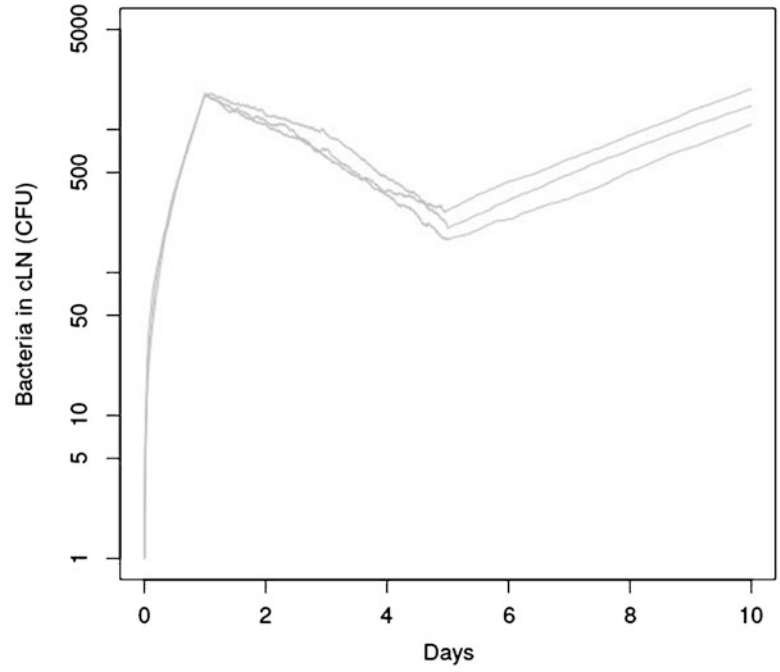

Fig. 3 Simulation of lymph node colonization. The output can be compared to lymph node pathogen loads analyzed in the infection experiments (adapted from [2], Fig. 4b)

```
> few <- 3
> plot(c(0,10), c(1,5000),
+      xlab="Days", ylab="Bacteria in cLN (CFU)",
+      type="n", log="y")
> for(run in 1:few){
+     st <- sim.treat(parms.d1 = c(r=2.82, c=0.00, mu=298),
+                     parms.d3 = c(r=4.59, c=5.04, mu= 0),
+                     parms.d5 = c(r=1.88, c=2.50, mu= 0),
+                     parms.d10= c(r=0.38, c=0.00, mu= 0),
+                     output.data=TRUE)
+     lines(st$t[-1], st$M[-1], col="grey")
+ }
```

By comparing this plot to the number of colony-forming units, you can assess the quality of the parameters determined in Subheading 3.4, **steps 3** and **4** (*see* **Notes 6** and **7**).

4 Notes

1. For mouse lymph node colonization, dilutions of 1:10–1:50 have proven to yield useful data. This ratio may have to be adapted to the infection experiment of interest, aiming at "losing" some but not all of the WITS in the majority of mice.
2. Ciprofloxacin is dissolved in water, filter-sterilized, and stored in aliquots at −20 °C. Avoid refreezing; ciprofloxacin will precipitate if kept at 4 °C for longer periods of time.
3. In non-treated mice, the cecal lymph node harbored approximately 1000 bacteria at days 1–2 and about 10,000 bacteria at days 3 and 4 post-infection. In ciprofloxacin-treated mice, we typically observe that about 10–20 % of the lymph node *S.* Typhimurium population survives the antibiotic treatment.
4. Please note that in our experiments, the mice were infected for 1 day without ciprofloxacin treatment. The ciprofloxacin treatment was started on day 1 post-infection. Therefore "day 1" denotes the state just before the onset of the antibiotic therapy.
5. The most likely reason for a convergence failure is bad starting values for optimization.
6. Please note that the estimation of the population dynamical parameters (muG, r) does not use the total cfu data obtained in the experiments. Therefore, the simulation of the population dynamics provides a valuable method for verification.
7. In addition to the population dynamics analysis described here, the use of WITS for infection experiments has practical merits. In particular, the number of different data points obtained

from a single experimental animal increases linearly with the number of different WITS used in the inoculum. This can help identifying bottlenecks in infection processes and provides a convenient means for analyzing "noisy" data sets, i.e., infection processes with significant animal-to-animal variation in the total organ loads. We have found this particularly useful in the case of competitive infection experiments which compare the fitness of a mutant *S.* Typhimurium strain and its isogenic wild-type parental strain within the same animal.

Acknowledgments

We are grateful to Emma Slack for critical reading of the manuscript. W.D.H. and P.K. were supported by grants from the Swiss National Science Foundation (310030-132997/1 and 310030-153074 to W. D.H.), in part by a Sinergia grant to W.D.H. from the SNF (CRSII3_136286) and in part from the ETH research foundation to W.D.H. (ETH-33 12-2). R.R. was supported by a grant from the Swiss National Science Foundation (315230-130855).

References

1. Mastroeni P, Grant A, Restif O, Maskell D (2009) A dynamic view of the spread and intracellular distribution of Salmonella enterica. Nat Rev Microbiol 7:73–80
2. Kaiser P, Regoes RR, Dolowschiak T, Wotzka SY, Lengefeld J et al (2014) Cecum lymph node dendritic cells harbor slow-growing bacteria phenotypically tolerant to antibiotic treatment. PLoS Biol 12, e1001793
3. Barthel M, Hapfelmeier S, Quintanilla-Martinez L, Kremer M, Rohde M et al (2003) Pretreatment of mice with streptomycin provides a Salmonella enterica serovar Typhimurium colitis model that allows analysis of both pathogen and host. Infect Immun 71:2839–2858
4. Kaiser P, Diard M, Stecher B, Hardt WD (2012) The streptomycin mouse model for Salmonella diarrhea: functional analysis of the microbiota, the pathogen's virulence factors, and the host's mucosal immune response. Immunol Rev 245:56–83
5. Kaiser P, Slack E, Grant AJ, Hardt WD, Regoes RR (2013) Lymph node colonization dynamics after oral *Salmonella* Typhimurium infection in mice. PLoS Pathog 9:1–12
6. Grant AJ, Restif O, McKinley TJ, Sheppard M, Maskell DJ et al (2008) Modelling within-host spatiotemporal dynamics of invasive bacterial disease. PLoS Biol 6, e74
7. Schmieger H (1972) Phage P22-mutants with increased or decreased transduction abilities. Mol Gen Genet 119:75–88
8. Hapfelmeier S, Stecher B, Barthel M, Kremer M, Muller AJ et al (2005) The Salmonella pathogenicity island (SPI)-2 and SPI-1 type III secretion systems allow Salmonella serovar typhimurium to trigger colitis via MyD88-dependent and MyD88-independent mechanisms. J Immunol 174:1675–1685
9. Stecher B, Paesold G, Barthel M, Kremer M, Jantsch J et al (2006) Chronic Salmonella enterica serovar Typhimurium-induced colitis and cholangitis in streptomycin-pretreated Nramp1 +/+ mice. Infect Immun 74:5047–5057
10. Endt K, Maier L, Kappeli R, Barthel M, Misselwitz B et al (2012) Peroral ciprofloxacin therapy impairs the generation of a protective immune response in a mouse model for Salmonella enterica serovar Typhimurium diarrhea, while parenteral ceftriaxone therapy does not. Antimicrob Agents Chemother 56:2295–2304

Part VI

Mathematical Modeling of Persistence

Chapter 17

Computational Methods to Model Persistence

Alexandra Vandervelde, Remy Loris, Jan Danckaert, and Lendert Gelens

Abstract

Bacterial persister cells are dormant cells, tolerant to multiple antibiotics, that are involved in several chronic infections. Toxin–antitoxin modules play a significant role in the generation of such persister cells. Toxin–antitoxin modules are small genetic elements, omnipresent in the genomes of bacteria, which code for an intracellular toxin and its neutralizing antitoxin. In the past decade, mathematical modeling has become an important tool to study the regulation of toxin–antitoxin modules and their relation to the emergence of persister cells. Here, we provide an overview of several numerical methods to simulate toxin–antitoxin modules. We cover both deterministic modeling using ordinary differential equations and stochastic modeling using stochastic differential equations and the Gillespie method. Several characteristics of toxin–antitoxin modules such as protein production and degradation, negative autoregulation through DNA binding, toxin–antitoxin complex formation and conditional cooperativity are gradually integrated in these models. Finally, by including growth rate modulation, we link toxin–antitoxin module expression to the generation of persister cells.

Key words Modeling, Toxin–antitoxin, Persister, ODE, Stochastic, Gillespie

1 Introduction

Biological systems are typically very complex and their functioning is often not fully understood. Traditionally, biologists have used qualitative methods to understand these systems. However, as the behavior of biological systems is often non-intuitive, mathematical models can be a valuable tool to study their characteristics quantitatively. Such models have successfully been used to study the eukaryotic cell cycle [1, 2], the heart [3], and transmission of infectious diseases [4], just to name a few examples. Recently, several groups have applied mathematical modeling to investigate persistence [5–15]. Bacterial persister cells are subpopulations of rare, slow-growing cells exhibiting multidrug tolerance even though the rest of the population is susceptible to the applied antibiotics [16]. Persisters have been found to play a role in several human diseases, for example cystic fibrosis, tuberculosis, and candidiasis [17].

Jan Michiels and Maarten Fauvart (eds.), *Bacterial Persistence: Methods and Protocols*,
Methods in Molecular Biology, vol. 1333, DOI 10.1007/978-1-4939-2854-5_17,

Different molecular pathways leading to the formation of a persister cell have been proposed (reviewed in [18]). One such pathway involves a hierarchical cascade, including increased concentrations of ppGpp (the signaling nucleotide regulating the stringent response), PolyP (inorganic polyphosphate), protease Lon and activation of toxin–antitoxin modules [19]. In an alternative mechanism, persister cells are formed due to elevated free toxin levels, caused by the dynamics of toxin–antitoxin module expression [9]. The latter mechanism has extensively been translated to mathematical models [10–15], and such models will be the topic of this chapter.

As mentioned above, several important routes towards persister generation involve the activity of toxin–antitoxin modules. Toxin–antitoxin modules are small genetic elements, omnipresent in the genomes of bacteria and archaea [20]. Most toxin–antitoxin modules code for two components: a toxic protein that is able to inhibit cell growth and an antitoxin that can antagonize this toxic activity. Five types of toxin–antitoxin modules have currently been described, depending on the nature of the antitoxin and the mode of neutralization. In type I toxin–antitoxin modules, the antitoxin is an antisense RNA, which negatively regulates toxin translation [21]. Both the antitoxin and the toxin are proteins in type II toxin–antitoxin modules, and neutralization occurs through the formation of a non-toxic toxin–antitoxin complex [22–25]. Type III toxin–antitoxin modules consist of a toxic protein and an RNA antitoxin like type I modules, yet in this case, binding of the antitoxin to the toxin ensures the neutralization instead of gene expression regulation [26]. In type IV toxin–antitoxin modules, toxin and antitoxin are proteins as in type II, however, the antitoxin interacts directly with the toxin target to protect it from the toxin's activity, instead of interacting with the toxin. Finally, in type V toxin–antitoxin modules, the antitoxin is again a protein, which antagonizes the toxin by specifically cleaving its mRNA [27].

Currently, all mathematical modeling papers focus on archetypical two-component type II toxin–antitoxin modules, for which the link with persistence is best established [28–30]. Such toxin–antitoxin modules are polycistronic operons in which the gene for the toxin is preceded by the gene for the antitoxin. Exceptions to this genetic make-up exist, as operons with an inverted genetic organization [31, 32] and three-component type II toxin–antitoxin modules [33] have been discovered. In typical type II toxin–antitoxin modules, the toxin is either a monomer, like RelE and HipA [34, 35], or a homodimer, like CcdB and MazF [36, 37]. The antitoxin is typically a dimer with a DNA-binding domain and an intrinsically disordered toxin-binding domain. Therefore, the antitoxin has a shorter in vivo lifetime than the toxin as it is vulnerable to degradation by cellular proteases. Type II toxin–antitoxin modules are further regulated at the transcriptional level by the antitoxin and the non-toxic complexes.

For many type II toxin–antitoxin modules like *phd/doc*, *ccdAB*, and *relBE*, this regulation involves conditional cooperativity [38–40]. In this mechanism, the antitoxin alone has a low affinity for its binding site on the operator DNA. At low intracellular toxin:antitoxin ratios, the toxin acts as a corepressor for the antitoxin by forming a toxin–antitoxin complex with a higher affinity for the DNA. At high toxin:antitoxin ratios, however, transcription and translation of the toxin–antitoxin module has to resume to maintain a viable toxin:antitoxin ratio. In this case, the toxin functions as a derepressor for the antitoxin, often by forming a second, non-repressing type of toxin–antitoxin complex [38, 41]. Even within type II toxin–antitoxin modules, conditional cooperativity is not universal. For example, the MqsR toxin of the *mqsRA* toxin–antitoxin module destabilizes the binding of antitoxin MqsA to DNA [42], only functioning as a derepressor in the autoregulation. Finally, the number of binding sites for the antitoxin on the operator varies depending on the toxin–antitoxin module, from two in the *phd/doc* and *relBE* operon to eight in the *ccdAB* operon [40, 43, 44].

In this work, we will present an overview of numerical methods to describe toxin–antitoxin modules and persistence. First, we will distinguish between deterministic and stochastic modeling approaches. Toxin–antitoxin dynamics involve biochemical processes such as transcription and translation, which are intrinsically noisy due to the low copy number of DNA and mRNA [45–47]. Moreover, as the intracellular free toxin levels are generally very low, limited to a few proteins, stochastic effects are likely to play an important role specifically in toxin–antitoxin modules. Therefore, next to the deterministic modeling approach involving Ordinary Differential Equations (ODEs), we will introduce two stochastic numerical methods incorporating unavoidable noise and randomness, being Stochastic Differential Equations (SDEs) and the Gillespie algorithm. We will start by illustrating these numerical methods using a very simple system, including only protein production and degradation, then, we will step by step introduce the characteristics of toxin–antitoxin modules in these models. As a first characteristic, we will include the negative transcriptional regulation due to DNA binding in this system. Then, we will explicitly model the production of toxin and antitoxin separately and describe the formation of toxin–antitoxin complexes. As a next step, we include conditional cooperativity in the autoregulation of the operon. Finally, we will consider how toxin–antitoxin modules affect the whole cell, as the presence of free toxins can slow down cell growth by interfering with the basic metabolism. Including such growth rate modulation leads to interesting behavior at the level of the cell as well as on the population level. Depending on the model and parameters, two different populations can emerge, one growing normally, and one with a severely

Table 1
Model parameters for the bacteriophage P1 *phd/doc* toxin–antitoxin module [14]

Parameter	Meaning	Value	Units
ζ_U	Unbound mRNA transcription rate	0.116086	s^{-1}
ζ_B	Bound mRNA transcription rate	0	s^{-1}
ρ_A	Antitoxin translation rate	$0.137\ \zeta_U/d_m$	s^{-1}
ρ_T	Toxin translation rate	$0.053\ \zeta_U/d_m$	s^{-1}
V	Volume *E. coli* cell	3.612e+8	m^3
d_m	mRNA decay rate	0.00203	s^{-1}
$d_c = d_T = d_{AT} = d_{TAT}$	Decay rate due to cell cycle dilution	2.8881e−4	s^{-1}
d_A	Antitoxin decay rate	$4 \cdot d_c$	s^{-1}
α_C	Binding of antitoxin and toxin	8.79e+6	$M^{-1}s^{-1}$
θ_C	Unbinding of antitoxin and toxin	5.3e−5	s^{-1}
α_{AT}	Binding of complex (AT) to binding site on the operator	9625	$M^{-1}s^{-1}$
θ_{AT}	Unbinding of complex (AT) from a binding site on the operator	0.0028875	s^{-1}

decreased cellular growth rate, the persister cells. We describe how a two-state model can be used to model populations in which cells can switch from a normal, growing stage to a persister stage and back. Throughout this chapter, we will use a parameter set based on experimental data for the bacteriophage P1 *phd/doc* toxin–antitoxin module (Table 1), as introduced in ref. [14].

2 Numerical Methods

In this section, we will introduce ODEs as a means to model TA systems in a deterministic manner, and we will introduce two stochastic numerical methods, being SDEs and the Gillespie algorithm. We illustrate these different methods using a toy model, based on the simplest approximation for a toxin–antitoxin module. We assume that the toxin–antitoxin complex AT is produced as a single entity.

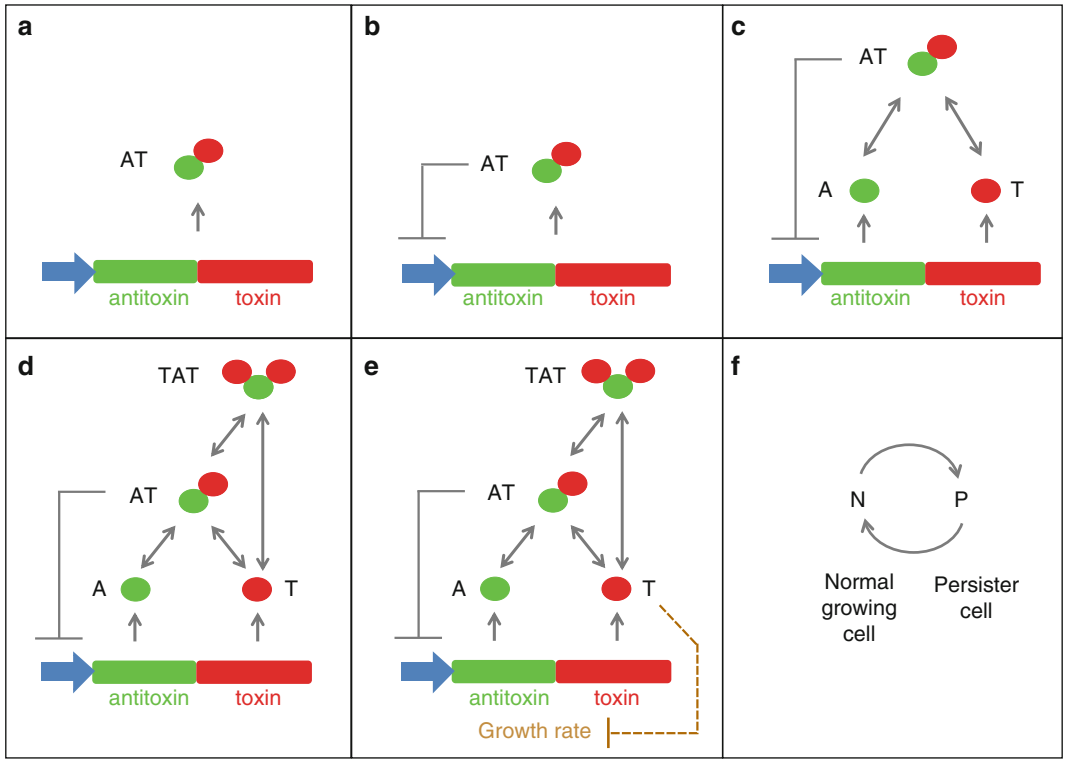

Fig. 1 Overview of the different toxin–antitoxin module topologies modeled in this chapter. (**a**) Direct production of toxin–antitoxin complex AT. (**b**) Direct production of complex AT and negative feedback through DNA binding. (**c**) Production of antitoxin A and toxin T, complex formation and negative feedback through DNA binding. (**d**) Regulation of toxin–antitoxin modules including conditional cooperativity. (**e**) Regulation of toxin–antitoxin modules including conditional cooperativity and growth rate modulation. (**f**) Modeling populations of normal cells and persister cells. Due to its susceptibility for degradation by cellular proteases, the antitoxin A has a shorter in vivo lifetime than the toxin T and complex AT and TAT, which decay with a rate corresponding to dilution due to cell division (Table 1)

This would be a good description for a hypothetical toxin–antitoxin module in which the antitoxin A and the toxin T are translated at equal rates, complex formation quickly reaches an equilibrium and the complex does not bind to the DNA operator site. As such, we obtain a genetic circuit consisting of AT being produced and degraded at a rate corresponding to dilution due to cell division. In the sketch shown in Fig. 1a, we illustrate this simple system. The genes on the DNA are transcribed into mRNA which in turn is translated into the corresponding complex AT. Throughout this paper we will neglect the intermediate step of mRNA production and assume that it happens fast enough such that it can be modeled as a modified translation rate of the protein itself. This model is not intended to provide an accurate description of TA systems, but is merely constructed to introduce the numerical methods and it will serve as a basis to construct more adequate toxin–antitoxin models in subsequent sections.

2.1 Deterministic Modeling Using ODEs

The toy system in Fig. 1a can be modeled in a deterministic way by using a single ODE. A differential equation is a mathematical equation which involves an unknown function, here AT, and its derivatives. In an ODE, the unknown function (the dependent variable AT) depends only on a single independent variable, in our case, time t [48]. The following ODE describes the time evolution of the number of AT complexes:

$$\frac{dAT(t)}{dt} = \rho_{AT} - d_{AT}AT(t), \tag{1}$$

The first term on the right-hand side, ρ_{AT}, is the average rate at which the complex AT is created through the process of transcription and translation from the DNA template. The second term on the right-hand side, $d_{AT}AT(t)$, models the average degradation rate of AT complexes and depends linearly on the amount of complex $AT(t)$ in the system at that time.

In order to numerically solve an ODE with a given initial value for the variables (here: AT), various methods have been developed. Such a numerical method typically uses the value of the variables at time t_0, called the initial condition, to make a prediction of those variables at a later time $t_0 + \delta t$, where δt is a chosen discrete time step. The simplest of such explicit methods is the Euler method [49], which is a first-order method, meaning that the error at a given time is proportional to the step size δt. Assume that we try to model the time evolution of a single protein X described by the following general ODE:

$$\frac{dX(t)}{dt} = F(t, X(t)), \tag{2}$$

where $F(t, X(t))$ is a function of time t and $X(t)$, with as initial condition $X(t = t_0) = X_0$. In order to use the Euler method to numerically solve this ODE, we first choose a discrete time step δt, which needs to be small enough to be numerically stable and to be able to capture the relevant dynamics of the ODE. The Euler method now makes a first prediction for time $t_1 = t_0 + \delta t$ after which $X(t_1)$ is used for the next prediction. In general, the value of X at time $t_{n+1} = t_n + \delta t$ is given by

$$X(t_{n+1}) = X(t_n) + \delta t F(t_n, X(t_n)) \tag{3}$$

For our system under study, Eq. 1, this numerical Euler method gives $AT(t_{n+1}) = AT(t_n) + \delta t(\rho_{AT} - d_{AT}AT(t_n))$. This method can easily be generalized to a system of multiple ODEs. As mentioned the Euler method is only a first-order method, which makes it more prone to numerical instabilities and errors. To overcome these drawbacks, this Euler method is often used as a basis to construct

more complicated and accurate methods. Here we will only introduce the Euler–Heun method [49], a quite robust second-order method which we will use throughout this paper. When using the Euler–Heun method, one first calculates an intermediate value $X^*(t_{n+1})$ after which this value and $X(t_n)$ are used to make an improved prediction of the actual value $X(t_{n+1})$. For the general ODE system, Eq. 2, this is done as follows:

$$X^*(t_{n+1}) = X(t_n) + \delta t F(t_n, X(t_n)) \tag{4}$$

$$X(t_{n+1}) = X(t_n) + \frac{\delta t}{2}(F(t_n, X(t_n)) + F(t_{n+1}, X^*(t_{n+1}))) \tag{5}$$

In Fig. 2a, we show the time evolution of the complex AT using the Euler–Heun method with $\delta t = 10^{-2}$ s and $AT(t_0) = 0$. The creation rate ρ_{AT} is chosen to be equal to the toxin creation rate ρ_T, given in Table 1. This is a good approximation if the complex formation between the antitoxin A and the toxin T is constantly near equilibrium, and if there is more A present in the system than T. The degradation rate $d_{AT} = d_c = \ln(2)/(40 \cdot 60\ \text{s})$ is assumed to be solely due to dilution caused by cell division every 40 min, *see* also Table 1. An example of a simple MATLAB code to numerically solve Eq. 1 can be found in Appendix 1. One can see in Fig. 2a that the number of complexes AT increases monotonically to a fixed level AT_{SS}. After the initial transient behavior, the properties of the system no longer change in time ($AT = AT_{SS}$), which is called a steady state solution. AT_{SS} can easily be calculated analytically from Eq. 1 by setting $\frac{dAT(t)}{dt} = 0$, yielding

$$AT_{SS} = \frac{\rho_{AT}}{d_{AT}}. \tag{6}$$

2.2 Stochastic Modeling Using SDEs

In the previous section, we introduced how to numerically solve an ODE equation using either a first-order Euler method or a second-order Euler–Heun method. This approach allows to model how the protein number evolves in time in a deterministic way. In other words, as long as one uses the same initial condition, every numerical simulation will provide you with exactly the same outcome for the time evolution of the protein level. In reality, however, most biological processes are to a certain extent stochastic. In toxin–antitoxin systems, noise may originate from the transcription and translation processes [45–47] and from the interactions of the free toxins, because they are generally present in very small amounts but have an important impact on the growth rate of the cell.

One way to introduce noise into the system is to use a SDE [50, 51], which is a differential equation in which one or more of the terms describes a stochastic process. In this work, we will limit ourselves to consider random white Gaussian noise. The SDE with white Gaussian noise that we use is the following:

$$\frac{dX(t)}{dt} = F(t, X(t)) + \eta(t), \tag{7}$$

similar as Eq. 2, where the extra last term is often called a Langevin noise term and $\eta(t)$ is the actual noisy process. Each sample of $\eta(t)$ has a normal distribution with zero mean, such that the signal is Gaussian white noise. The uncorrelated zero-mean stochastic term $\eta(t)$ is thus described by the correlation term $\langle \eta(t+\tau)\eta(t)\rangle = D\delta(\tau)$ where D is a constant diffusion noise strength. As we consider D to be a constant, the system is said to be subject to additive noise. In the case of multiplicative noise, extra care must be taken to solve the SDE [50, 51].

In order to solve the SDE, we use a similar Euler–Heun method, now adjusted to include the Langevin noise term:

$$X^*(t_{n+1}) = X(t_n) + \delta t F(t_n, X(t_n)) + \sqrt{D\delta t}\, r, \tag{8}$$

$$\begin{aligned} X(t_{n+1}) = X(t_n) + \frac{\delta t}{2}\left(F(t_n, X(t_n)) + F(t_{n+1}, X^*(t_{n+1}))\right) \\ + \frac{1}{2}\sqrt{D\delta t}\, r, \end{aligned} \tag{9}$$

where r is a random number taken from the standard normal distribution with standard deviation equal to 1. The presence of the time step δt under the square root in front of the noise term calls for an explanation. The analytical derivation is a bit technical, and for that we refer the reader to the specialized literature [51, 52]. Intuitively, it can be understood that, as one, e.g., decreases the time step, one should also rescale (decrease) the strength of the noise, if not, one would be injecting the same amount of noise in a shorter time interval which corresponds to an effectively higher noise level.

In Fig. 2b, we show the time evolution of the level of complex AT using the Euler–Heun method to solve the following SDE, corresponding to ODE Eq. 1

$$\frac{dAT(t)}{dt} = \rho_{AT} - d_{AT} AT(t) + \eta(t), \tag{10}$$

with $\delta t = 10^{-2}$ s, $\mathrm{AT}(t_0) = 0$ and $D = 25$. One can see that the result is essentially the same as the deterministic evolution (Fig. 2a) with a small noisy ripple superimposed on it.

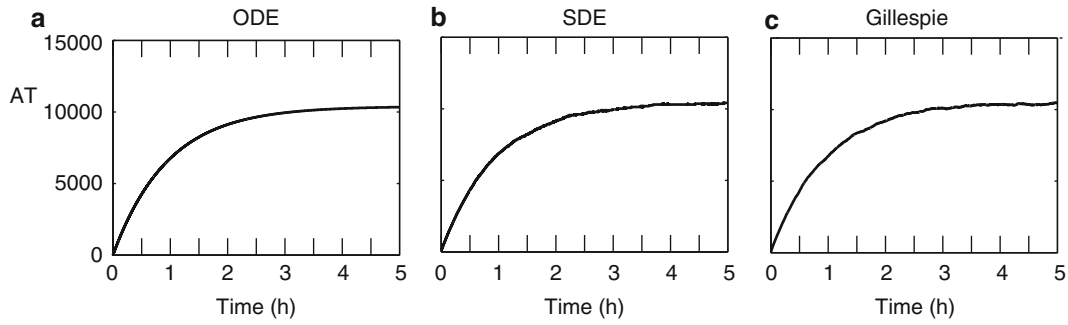

Fig. 2 Time evolution of the level of complex AT for a hypothetical toxin–antitoxin model describing direct production of complex AT (Fig. 1a). The system given by Eq. 1 was simulated for 5 h. The graphs show the results for a single cell. (**a**) Numerical simulation of the ODE using the Euler–Heun method. (**b**) Numerical simulation of the SDE given by Eq. 10 using the Euler–Heun method, $D = 25$. (**c**) Numerical simulation of stochastic equations using the Gillespie algorithm. Parameters are given in Table 1, with $\rho_{AT} = \rho_T$ and $d_{AT} = d_c$

2.3 Stochastic Modeling Using the Discrete Gillespie Method

The previous two methods, ODE and SDE, are both continuous methods that average out many discrete biochemical reactions. Therefore, these differential equations, both deterministic and stochastic, heavily rely on bulk reactions requiring many interactions. In contrast, the Gillespie algorithm allows for a more accurate discrete and stochastic simulation of a system involving biochemical reactions [53]. This approach is especially necessary when few molecules are present in the system. In the Gillespie method every single reaction is explicitly simulated. The algorithm is based on the random occurrence of collisions of molecules with a certain probability. Only collisions between two molecules are considered as the probability of three molecules colliding is very low.

We will illustrate the Gillespie algorithm with the simple system described deterministically by the ODE Eq. 1. Instead of a differential equation we now consider explicitly every possible reaction and the probability per unit time that a specific reaction occurs. This probability of each reaction i is also called a propensity p_i. In our simple example, there are two reactions that can occur, AT can be degraded (1) and created (2):

$$(1) \quad AT \quad \rightarrow \emptyset, \tag{11}$$

$$(2) \quad \emptyset \quad \rightarrow AT, \tag{12}$$

with corresponding propensities:

$$(1) \quad p_1 = d_{AT} AT, \tag{13}$$

$$(2) \quad p_2 = \rho_{AT}. \tag{14}$$

The Gillespie algorithm consists of four steps that are iterated:

1. *Computation of the random time step:* the probability that any reaction occurs is the sum of the propensities

$$p_0 = \sum_i p_i,$$

with i the number of each reaction. Randomly choose the time of the next event, δt, out of the exponential distribution $p_0 \exp[-p_0 t]$ as follows:

$$\delta t = \frac{1}{p_0} \ln\left(\frac{1}{r_1}\right),$$

with r_1 a uniform random number between 0 and 1.

2. *Selection of a random reaction:* consider the simple system of two reactions. The probability that the next reaction to occur is reaction (1) is p_1/p_0, and likewise for reaction (2) the probability is p_2/p_0. In general, reaction i will occur with probability p_i/p_0. The reaction is randomly selected from this distribution of probabilities. In practice this is done by picking a second uniform random number r_2 between 0 and 1. The selected reaction K is then found by looking for the value of K for which the following inequality is satisfied:

$$\sum_{i=1}^{K-1} p_i < r_2 \, p_0 \leq \sum_{i=1}^{K} p_i. \tag{15}$$

3. *Update the populations based on the reaction chosen:* In our example, if reaction (1) was chosen, we decrease the number of AT complexes by one, while if reaction (2) was chosen, we increase the number of AT complexes by one.
4. *Update the current time:* the time t in the simulation is updated to time $t + \delta t$.

An example of a simple MATLAB code to numerically solve Eq. 1 using the Gillespie algorithm above can be found in Appendix 2. Figure 2c shows the time evolution of the complex AT as obtained by using the Gillespie method. The same initial condition is used. Notice that there is no need to define a fixed time step δt as it is randomly chosen based on the propensities. As the steady-state solution AT_{SS} of the system equation is quite high, it is no surprise that the deterministic ODE, the SDE, and the Gillespie method all give approximately the same result in this case.

3 Negative Feedback Through DNA Binding

In this section, we allow the complex AT to bind to its own operator DNA, as shown in Fig. 1b. When AT is bound to the DNA, no transcription can take place and the production of AT is halted. This provides a negative feedback control system: when little AT is present in the system, the probability to bind to the DNA is low, and more AT is produced; in the presence of lots of AT, DNA binding is more likely and AT production stops. Assuming there is only one site on the operator DNA for AT to bind to, one can see that this is a very discrete on/off process. Either AT is produced at the fastest rate possible (no AT bound) or the production rate is zero (AT bound). This already illustrates that when choosing a numerical method to solve this system, the discrete Gillespie method is most appropriate. However, using an ODE or SDE description has the advantage of simplicity and allows for certain analytical derivations. ODEs have been used to describe DNA binding effects in toxin–antitoxin systems in various works [8, 10–12]. When using an ODE or SDE, the discrete process of DNA binding is approximated by including a negative feedback term in the growth rate as follows:

$$\frac{dAT(t)}{dt} = \frac{\rho_{AT}}{1 + \frac{AT(t)^n}{K^n}} - d_{AT}AT(t) + \eta(t), \tag{16}$$

with $K = \theta_{AT}/\alpha_{AT}$ where $\theta_{AT}(\alpha_{AT})$ are the unbinding (binding) rates of AT from a binding site on the DNA operator site. The relevant parameters used can be found in Table 1. The results of including such negative feedback regulation in the ODE and SDE model are shown in Fig. 3a, b. The top panels depict the fraction D_F of the time that the operator site on the DNA is free (unbound). In comparison, without DNA binding (*see* Fig. 2), this fraction D_F would always be 1. As the operator site on the DNA is on average bound by AT for 90 % of the time, it is no surprise that the steady state level of AT is decreased to approximately 1000, which is about 10 % of the level without DNA binding events. The difference between the ODE and SDE description is still minor, although the noisy fluctuations around the steady state level are already more pronounced in Fig. 3b.

When using the Gillespie algorithm, every individual DNA binding/unbinding event is implemented explicitly. The set of reactions in this case becomes:

$$(1) \quad AT \quad \rightarrow \emptyset, \tag{17}$$

$$(2) \quad D_F \quad \rightarrow AT, \tag{18}$$

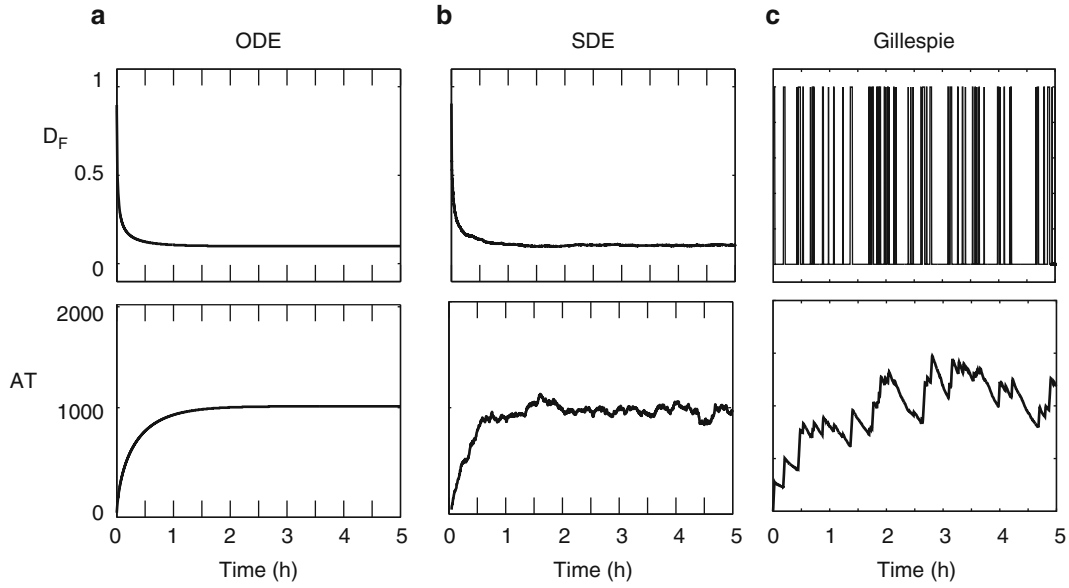

Fig. 3 Time evolution of the fraction D_F of time that the operator site on the DNA is unbound and the level of complex AT for a hypothetical toxin–antitoxin model describing direct production of complex AT and negative feedback through DNA binding (Fig. 1b). The systems given by Eq. 16 were simulated for 5 h. The graphs show the results for a single cell. (**a**) Numerical simulation of the ODE using the Euler–Heun method, $D = 0$. (**b**) Numerical simulation of the SDE using the Euler–Heun method, $D = 25$. (**c**) Numerical simulation of stochastic equations using the Gillespie algorithm. Parameters are given in Table 1

$$(3) \quad \text{Free operator DNA}(D_F = 1) + AT \rightarrow \text{Bound operator DNA}(D_F = 0), \tag{19}$$

$$(4) \quad \text{Bound operator DNA}(D_F = 0) \rightarrow \text{Free operator DNA}(D_F = 1) + AT, \tag{20}$$

with corresponding propensities:

$$(1) \quad p_1 = d_{AT} AT, \tag{21}$$

$$(2) \quad p_2 = \rho_{AT} D_F. \tag{22}$$

$$(3) \quad p_3 = \alpha_{AT} D_F AT. \tag{23}$$

$$(4) \quad p_4 = \theta_{AT}(1 - D_F). \tag{24}$$

In Fig. 3c the results obtained from the Gillespie algorithm are shown. The top panel clearly shows the discrete binding (unbinding)

events, which are accompanied by spikes in the production (degradation) of AT, which can be seen in the bottom panel. Such "bursty" dynamical behavior is typical for the evolution of mRNA levels in the presence of transcription factors that can bind to the DNA operator site [46, 47, 54, 55].

4 Sequestration of Toxin by Antitoxin

In the previous section, the complex AT was formed directly, while repressing its own production by binding to its own operator. In this section, AT is not created in a direct way. We rather introduce the antitoxin A and the toxin T that can bind to form the complex AT, which can still bind to the operator DNA (Fig. 1c). When it does so, it represses the transcription and translation of antitoxin and toxin, and therefore also indirectly its own production. We assume that the antitoxin alone is unable to bind to the operator. The relevant parameters for the antitoxin and toxin production and degradation are given in Table 1. These parameters are based on experimental measurements for the *phd/doc* TA system [14]. While antitoxin A is produced two to three times faster than the toxin protein T, it is also degraded four times faster. Faster creation and degradation rates for antitoxin than toxin are typical in toxin–antitoxin systems and have been shown to be essential for its operation [22]. The ODE and SDE description of this system is given as follows:

$$\frac{dA(t)}{dt} = \frac{\rho_A}{1 + \frac{AT(t)^n}{K^n}} - \alpha_C A(t)T(t) + \theta_C AT(t) - d_A A(t) + \eta(t), \tag{25}$$

$$\frac{dT(t)}{dt} = \frac{\rho_T}{1 + \frac{AT(t)^n}{K^n}} - \alpha_C A(t)T(t) + \theta_C AT(t) - d_T T(t) + \eta(t), \tag{26}$$

$$\frac{dAT(t)}{dt} = \alpha_C A(t)T(t) - \theta_C AT(t) - d_{AT} AT(t), \tag{27}$$

where $K = \theta_{AT}/\alpha_{AT}$ is defined the same as before, and $\alpha_C(\theta_C)$ describe the binding (unbinding) rates of A and T into the complex AT. Notice that AT is no longer produced in a direct way, but only indirectly through the binding of A and T. Furthermore, the Langevin noise term is only added to the evolution equations for A and T, as those are the only proteins that are actively created and are most likely to fluctuate in a stochastic manner. As before, Fig. 4a, b show the simulation results for the system simulated using the ODE and SDE.

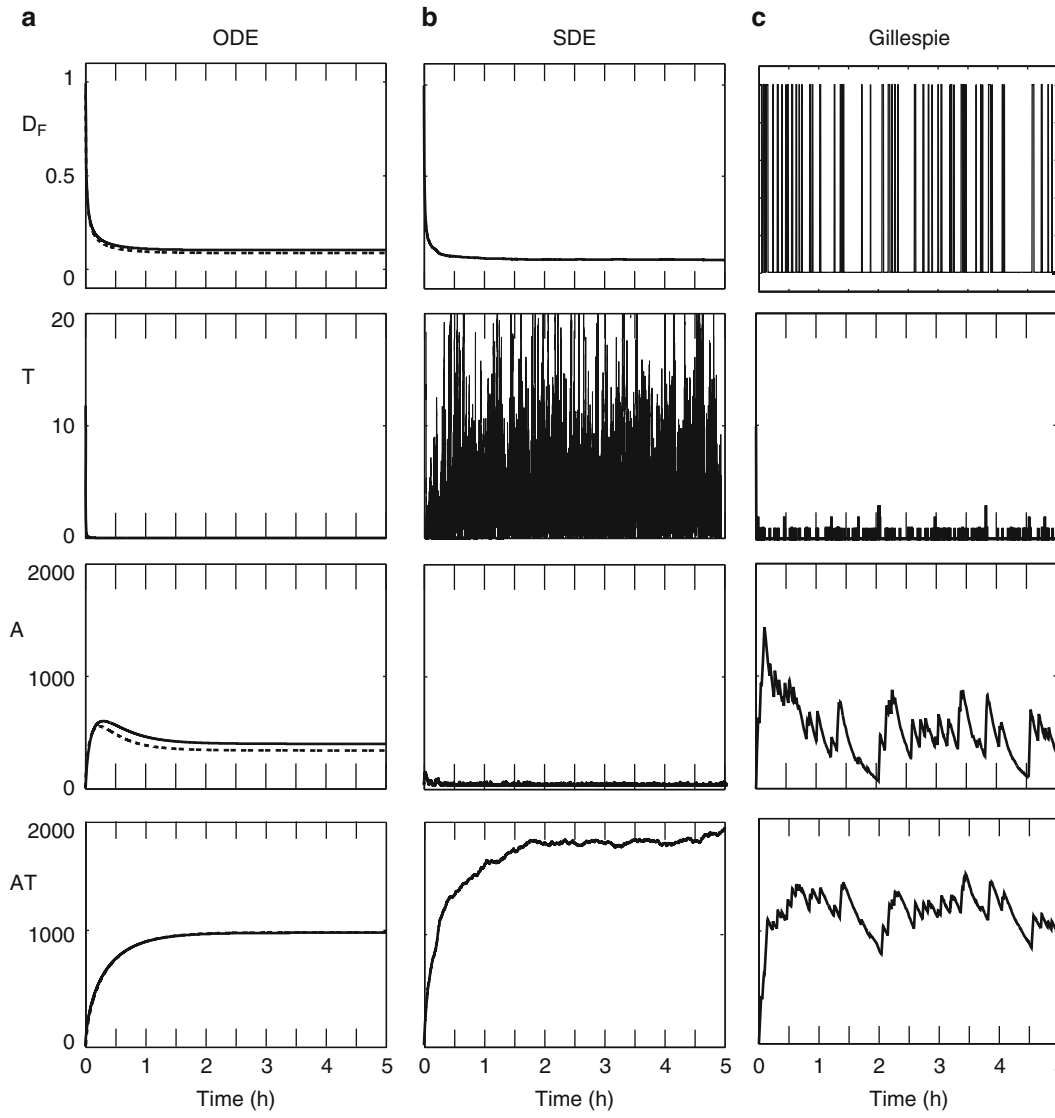

Fig. 4 Time evolution of the fraction D_F of time that the operator site on the DNA is unbound, the level of toxin T, antitoxin A and complex AT for a hypothetical toxin–antitoxin model describing production of antitoxin A and toxin T, complex formation and negative feedback through DNA binding (Fig. 1c). The systems given by Eqs. 25–27 were simulated for 5 h. The graphs show the results for a single cell. (**a**) Numerical simulation of the ODE using the Euler–Heun method, $D = 0$. The *dashed line* shows a simulation with the algebraic approximation (28). (**b**) Numerical simulation of the SDE using the Euler–Heun method, $D = 25$. (**c**) Numerical simulation of stochastic equations using the Gillespie algorithm. Parameters are given in Table 1

The results obtained by the ODE simulations are in fact very similar to the ones obtained through direct creation of AT (*see* Fig. 3a). This shows that the averaged response obtained by the deterministic ODE equations in (27) are adequately simplified by assuming that all toxins are quickly sequestered by the antitoxin A, forming the complex AT. This leads to a steady state value of

$T_{SS} \approx 0$ and the steady state value of AT is approximately the same as in Fig. 3a where we assumed it was created at the rate ρ_T.

A common approximation made in several papers is to assume that the process of complex formation through binding of A and T is constantly in equilibrium, *see*, e.g., [10, 12]. In this case, the amount of AT complexes in the system is determined by numerically simulating the evolution of antitoxin A and toxin T, after which one calculates AT at each discretization step using

$$AT(t) = \frac{A(t)T(t)}{K_C}, \tag{28}$$

which is thus solely determined by the ratio of the binding (unbinding) rates of A and T, $K_C = \theta_C/\alpha_C$. This approach is accurate for a wide range of binding (unbinding) rates of A and T. For instance, using the current parameter set (Table 1), the results of this approach are shown in Fig. 4a in the dashed lines. Apart from a minor difference in the level of antitoxin A, the approximation matches Eq. 27 which explicitly model the binding of A to T exceptionally well.

When introducing the Langevin noise terms, the results shown in Fig. 4b are quite different though. The toxin levels now fluctuate significantly and for these noise levels the antitoxin is no longer able to sequester all toxin, leading to larger toxin levels and low antitoxin levels. This shows that the effect of relatively small levels of noise can become significant due to the small numbers of toxin proteins. It also motivates the necessity to use the more correct discrete Gillespie algorithm to simulate stochastic effects.

The set of reactions used in the Gillespie algorithm are:

$$\begin{aligned}(1)\quad &\text{Free operator DNA}(D_F = 1) + AT \\ &\quad \rightarrow \text{Bound operator DNA}(D_F = 0),\end{aligned} \tag{29}$$

$$\begin{aligned}(2)\quad &\text{Bound operator DNA}(D_F = 0) \\ &\rightarrow \text{Free operator DNA}(D_F = 1) + AT,\end{aligned} \tag{30}$$

$$(3)\quad D_F \rightarrow A, \tag{31}$$

$$(4)\quad D_F \rightarrow T, \tag{32}$$

$$(5)\quad A \rightarrow \emptyset, \tag{33}$$

$$(6) \quad T \rightarrow \emptyset, \tag{34}$$

$$(7) \quad AT \rightarrow \emptyset, \tag{35}$$

$$(8) \quad A + T \rightarrow AT, \tag{36}$$

$$(9) \quad AT \rightarrow A + T, \tag{37}$$

with corresponding propensities:

$$(1) \quad p_1 = \alpha_{AT} D_F AT, \tag{38}$$

$$(2) \quad p_2 = \theta_{AT}(1 - D_F). \tag{39}$$

$$(3) \quad p_3 = \rho_A D_F, \tag{40}$$

$$(4) \quad p_4 = \rho_T D_F, \tag{41}$$

$$(5) \quad p_5 = d_A A, \tag{42}$$

$$(6) \quad p_6 = d_c T, \tag{43}$$

$$(7) \quad p_7 = d_c AT, \tag{44}$$

$$(8) \quad p_8 = \alpha_C A \cdot T, \tag{45}$$

$$(9) \quad p_9 = \theta_C AT, \tag{46}$$

The resulting time evolution obtained from the Gillespie method is shown in Fig. 4c. On average it gives a similar result as the results obtained from the ODE. However, the stochastic fluctuations in A and AT are considerably larger than with the SDE, while the toxin level remains at a stable low level. This shows that

the on/off toggling of the DNA transcription, only present in the Gillespie method, is essential to get the stochastic bursting behavior in the production of the various proteins.

Although we will further elaborate the model for the autoregulation of toxin–antitoxin modules in the next section, it should be noted that the model presented above can already be useful for toxin–antitoxin modules for which no indications of conditional cooperativity have been found, such as the *hipBA* operon [56]. Indeed, similar models have been published by Rotem et al., Koh and Dunlop and Feng et al. [9, 11, 15], often including the dimerization of the antitoxin HipB, repression by the antitoxin alone and growth rate modulation as explained below.

5 Conditional Cooperativity

Conditional cooperativity plays a pivotal role in the transcriptional regulation of many type II toxin–antitoxin modules [38, 40]. In this mechanism, the toxin acts as a corepressor for the DNA-binding antitoxin at low intracellular toxin:antitoxin ratios and as a derepressor at high toxin:antitoxin ratios. Here, we model conditional cooperativity solely via the binding of toxin T to the complex AT to form a secondary complex TAT which is unable to bind to the operator, as shown in Fig. 1d. In the presence of an excess of toxin T, this leads to a decrease in the level of AT, and consequently in a reduced repression through DNA binding. Direct derepression through toxins binding to AT complexes on the DNA itself is not included in this basic model.

A simplified view of conditional cooperativity can be obtained by only considering the binding (unbinding) events of A, T, AT, and TAT and neglecting active creation and degradation of these proteins and protein complexes. In Fig. 5a, we plot the amount of AT complexes in function of the total amount of toxin T_{tot} ($T_{\mathrm{tot}} = T + AT + 2 \cdot TAT$) present in the system, while keeping the total amount of antitoxin proteins A_{tot} ($A_{\mathrm{tot}} = A + AT + TAT$) fixed (e.g., $A_{\mathrm{tot}} = 1000$). We assume an immediate redistribution of toxin and antitoxin proteins among free antitoxin A, free toxin T, and complexes AT and TAT, based on the dissociation constants for the formation of complex AT from A and T and the formation of complex TAT from complex AT and T, which are chosen to be equal and are given by $K_C = \theta_C/\alpha_C$:

$$AT = \frac{A \cdot T}{K_C}, \tag{47}$$

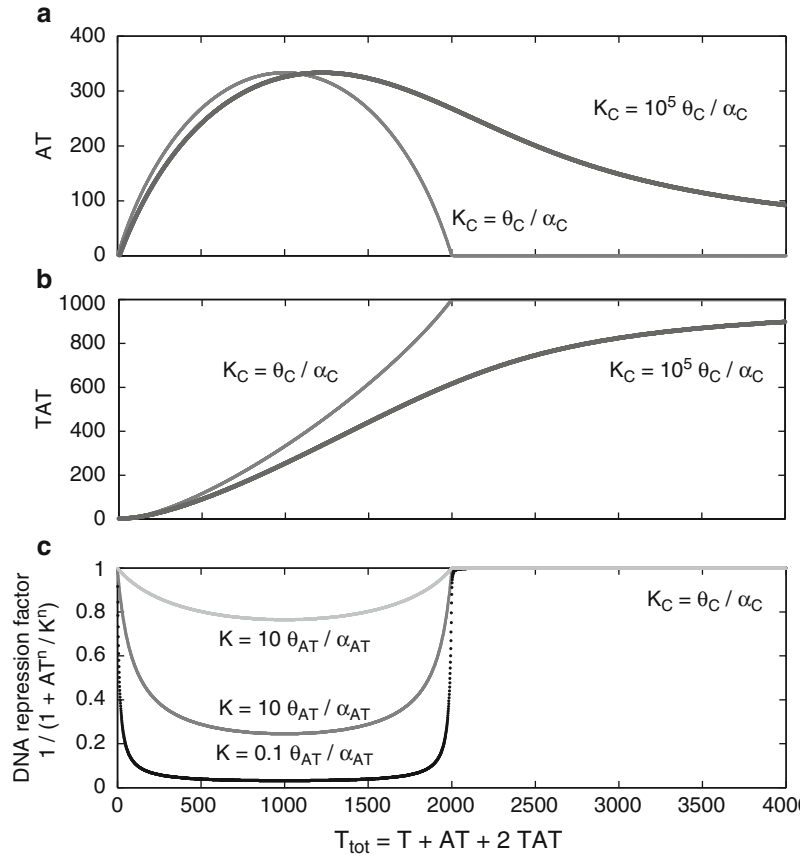

Fig. 5 Formation of complexes AT and TAT can lead to conditional cooperativity in a toxin–antitoxin system. Level of complex AT (**a**), complex TAT (**b**), and the DNA repression factor (**c**) as a function of the total toxin level T_{tot} for a fixed total antitoxin level $A_{tot} = 1000$, assuming immediate redistribution of free antitoxin, free toxin, complex AT, and complex TAT according to Eqs. 47 and 48. In panel (**a**) and (**b**), the *light gray line* represents physiological parameters, whereas the *dark gray line* represents a 10^5 times increased dissociation constant for the binding of toxin to antitoxin. In panel (**c**), the DNA repression factor is shown for three different values of the dissociation constant for the binding of complex AT to a binding site on the operator. Please note that the repression factor is defined so that it equals 1 when there is no repression and 0 when there is full repression. Parameters are given in Table 1

$$TAT = \frac{AT \cdot T}{K_C}, \tag{48}$$

Figure 5a, b shows that for values of $T_{tot} < 2A_{tot}$, the free toxins are efficiently sequestered in both complexes AT and TAT. As soon as the total amount of toxin T_{tot} exceeds twice the total amount of antitoxin A_{tot} present in the system (here $A_{tot} = 1000$),

AT complexes are removed from the system in favor of TAT complexes and free toxins. This transition is found to be a sharp one for physiological parameters, but can be smoothed out by greatly increasing the dissociation constant K_C, as shown in Fig. 5a, b. This transition has an immediate effect on the negative feedback through DNA repression, as the DNA repression factor was defined as $1/\left(1+\frac{AT(t)^n}{K^n}\right)$. As $AT \approx 0$ when $T_{\text{tot}} > 2A_{\text{tot}}$, no DNA repression takes place and all proteins can be transcribed and translated. However, when $T_{\text{tot}} < 2A_{\text{tot}}$ the AT complexes can bind to the DNA. The resulting repression is strong or weak, depending on the dissociation constant K for the binding of complex AT to a binding site on the operator. The stronger the DNA binding affinity, the stronger the resulting repression, as shown in Fig. 5c.

Although Fig. 5 provides insight into how conditional cooperativity can trigger a transition between two qualitatively different regions of operation (DNA repression vs. no DNA repression), the actual protein levels are dynamical variables that continuously influence each other in time. The ODE and SDE description of this system providing the time evolution of every protein level is given as follows:

$$\frac{dA(t)}{dt} = \frac{\rho_A}{1+\frac{AT(t)^n}{K^n}} - \alpha_C A(t)T(t) + \theta_C AT(t) - d_A A(t) + \eta(t), \tag{49}$$

$$\begin{aligned}\frac{dT(t)}{dt} = {} & \frac{\rho_T}{1+\frac{AT(t)^n}{K^n}} - \alpha_C A(t)T(t) + \theta_C AT(t) \\ & - \alpha_C AT(t)T(t) + \theta_C TAT(t) - d_T T(t) + \eta(t),\end{aligned} \tag{50}$$

$$\begin{aligned}\frac{dAT(t)}{dt} = {} & \alpha_C A(t)T(t) - \theta_C AT(t) - d_{AT} AT(t) \\ & + \theta_C TAT(t) - \alpha_C AT(t)T(t),\end{aligned} \tag{51}$$

$$\frac{dTAT(t)}{dt} = \alpha_C AT(t)T(t) - \theta_C TAT(t) - d_{TAT} TAT(t), \tag{52}$$

Notice that we again explicitly model all binding events and the approximation of Eqs. 47–48 is not used. Comparing Fig. 4a and Fig. 6a shows that the amount of free antitoxin A is approximately doubled and the amount of complex AT approximately halved

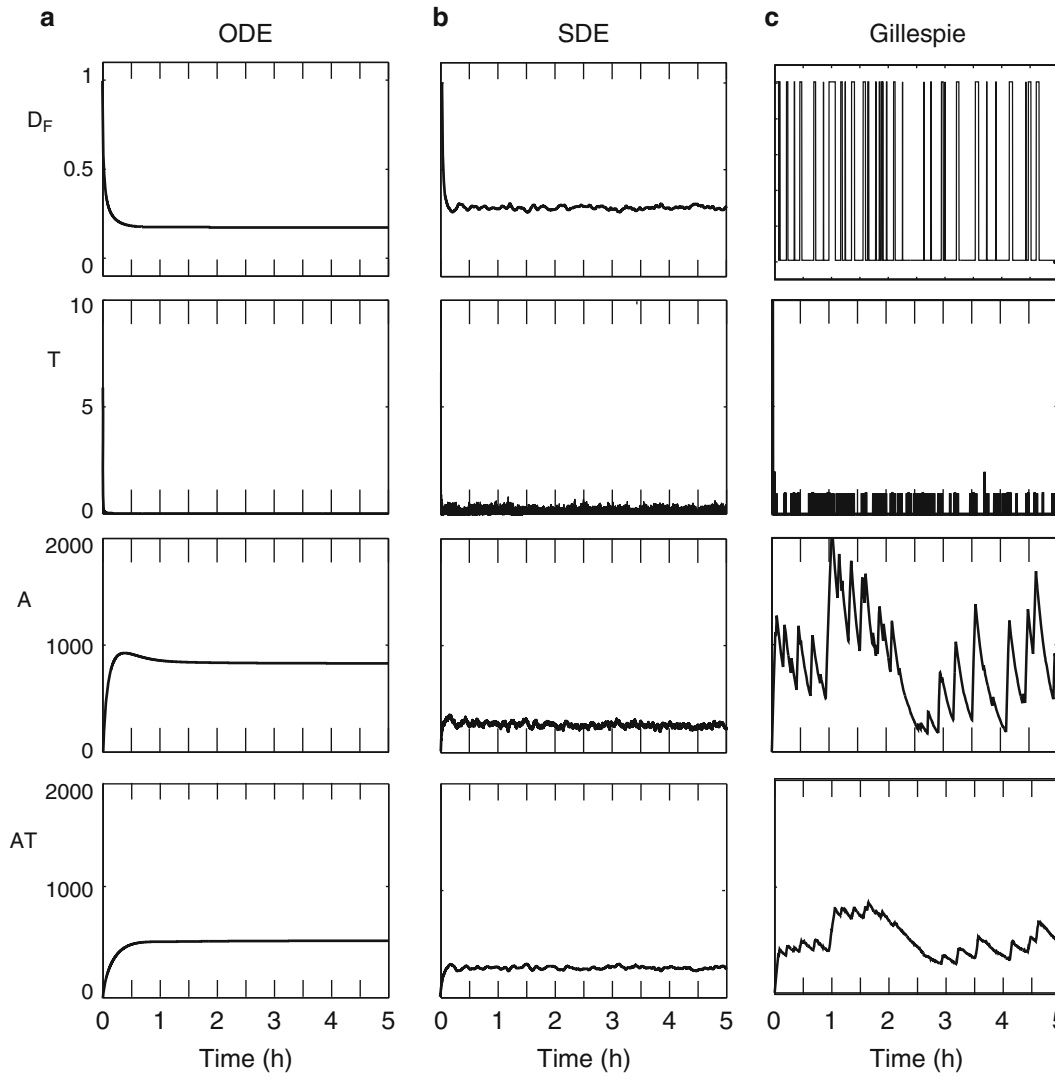

Fig. 6 Time evolution of the fraction D_F of time that the operator site on the DNA is unbound, the level of toxin T, antitoxin A and complex AT for a toxin–antitoxin model including conditional cooperativity (Fig. 1d). The systems given by Eqs. 49–52 were simulated for 5 h. The graphs show the results for a single cell. (**a**) Numerical simulation of the ODE using the Euler–Heun method, $D = 0$. (**b**) Numerical simulation of the SDE using the Euler–Heun method, $D = 25$. (**c**) Numerical simulation of stochastic equations using the Gillespie algorithm. Parameters are given in Table 1

when conditional cooperativity is included in the model. This is no surprise as AT complexes now help in sequestering toxins, and thus antitoxins have to do half the work in the presence of conditional cooperativity. Furthermore, including conditional cooperativity has a stabilizing effect in the presence of noise. Simulations using the

SDE become more robust, effectively decreasing the variation in the toxin level. Similarly as in Fig. 4b the average level of antitoxin A is decreased in the presence of moderate noise levels, due to the more frequent random production of toxins T that need to be sequestered into complexes.

The set of reactions used in the Gillespie algorithm are the same as before, with the addition of three extra reactions to account for the conditional cooperatively:

$$(10) \quad AT + T \rightarrow TAT, \tag{53}$$

$$(11) \quad TAT \rightarrow AT + T, \tag{54}$$

$$(12) \quad TAT \rightarrow \emptyset, \tag{55}$$

with corresponding propensities:

$$(10) \quad p_{10} = \alpha_C AT \cdot T, \tag{56}$$

$$(11) \quad p_{11} = \theta_C TAT, \tag{57}$$

$$(12) \quad p_{12} = d_c TAT, \tag{58}$$

Figure 6c shows similar results as before, but with larger variability of the free antitoxin level.

6 Growth Rate Modulation: Bistability and Metastability

Until now, we did not take into account that the toxin has an effect on the cellular metabolism. In reality, toxins can affect, e.g., translation, DNA replication, and the cell wall [57]. Therefore, the free toxin concentration will have an impact on the production rates of toxin and antitoxin, and more generally, by interfering with the global metabolism, on the cellular growth rate (Fig. 1e). We introduce a modulation factor,

$$\gamma_T = \frac{1}{1 + \frac{T(t)^{nn}}{KK^{nn}}},$$

with $KK = 1$ the threshold above which the toxin inhibits cell growth and $nn = 4$ the Hill factor. We assume that free toxin has

a symmetric effect on the production and degradation rates, reducing them with the same factor, while the degradation rate of the antitoxin remains the same.

The ODE and SDE description of this system is given as follows:

$$\frac{dA(t)}{dt} = \frac{\rho_A}{1 + \frac{AT(t)^n}{K^n}}\gamma_T - \alpha_C A(t)T(t) + \theta_C AT(t) - d_A A(t) + \eta(t), \tag{59}$$

$$\frac{dT(t)}{dt} = \frac{\rho_T}{1 + \frac{AT(t)^n}{K^n}}\gamma_T - \alpha_C A(t)T(t) + \theta_C AT(t) - \alpha_C AT(t)T(t) + \theta_C TAT(t) - d_T\gamma_T T(t) + \eta(t), \tag{60}$$

$$\frac{dAT(t)}{dt} = \alpha_C A(t)T(t) - \theta_C AT(t) - d_{AT}\gamma_T AT(t) + \theta_C TAT(t) - \alpha_C AT(t)T(t), \tag{61}$$

$$\frac{dTAT(t)}{dt} = \alpha_C AT(t)T(t) - \theta_C TAT(t) - d_{TAT}\gamma_T TAT(t), \tag{62}$$

The results are shown in Fig. 7a, b for an initial condition with a small excess of toxin: $A(t_0) = 1$ and $T(t_0) = 15$. In the deterministic case (ODE), the system finds itself initially in a situation where the toxin level is higher than the critical threshold KK above which cell growth is inhibited. The strength of this inhibition strongly depends on the Hill factor nn, which determines the sharpness of the transition from normal cell growth ($T < KK$) and reduced cell growth ($T > KK$). The increased level of initial toxin leads to a metastable state where one only slowly returns to low amounts of toxin and high amounts of antitoxin and complexes. In the end, the system is forced to return to the normal growth state due to the slow dilution of toxin in combination with the slow creation of antitoxin which sequesters the free toxins. A higher initial amount of toxin leads to an increasingly more slowly return to the controlled state. In the case for the SDE, the stochastic variations in protein level help to return more quickly to the controlled state.

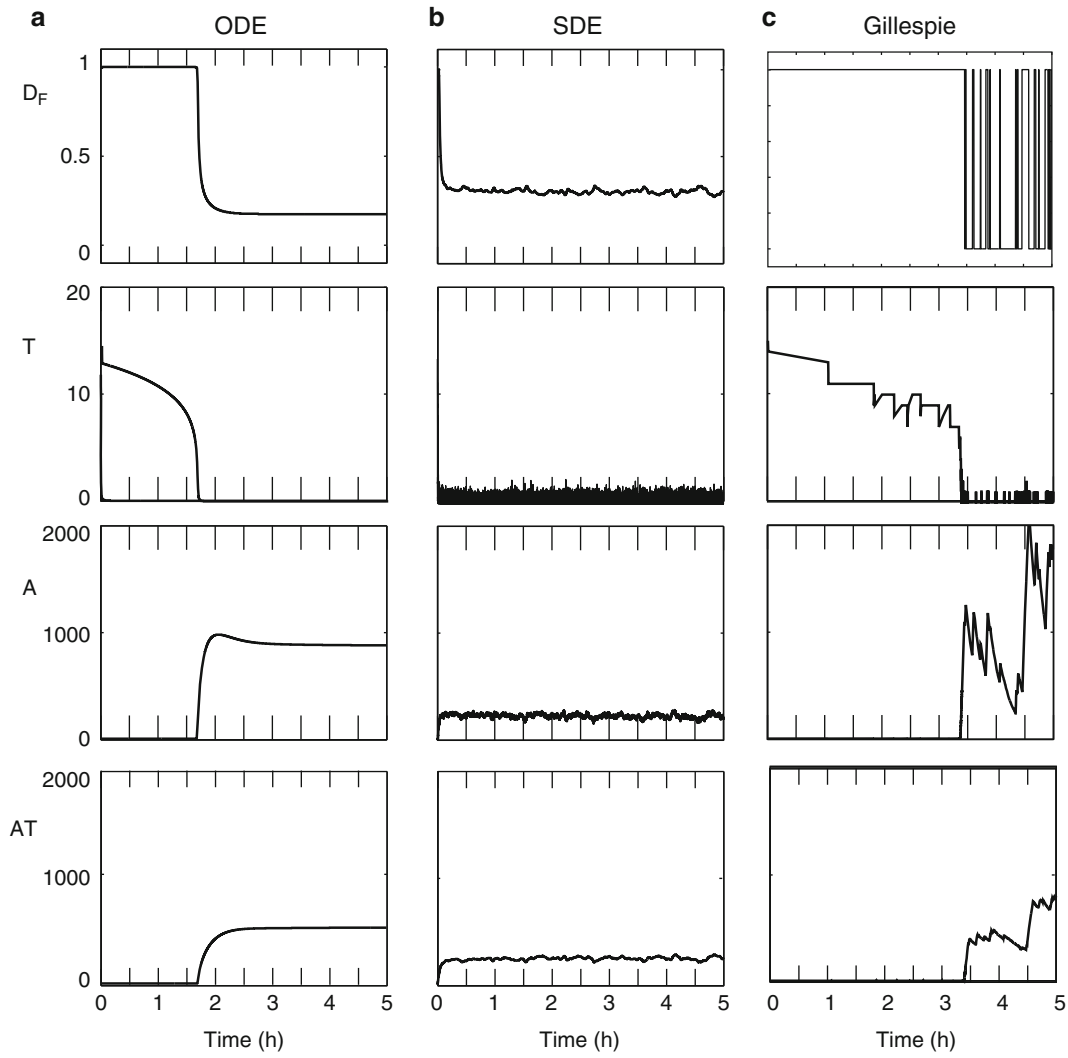

Fig. 7 Time evolution of the fraction D_F of time that the operator site on the DNA is unbound, the level of toxin T, antitoxin A and complex AT for a toxin–antitoxin model including conditional cooperativity and cell growth modulation (Fig. 1e). The systems given by Eqs. 59–62 were simulated for 5 h. The graphs show the results for a single cell. (**a**) Numerical simulation of the ODE using the Euler–Heun method, $D = 0$. (**b**) Numerical simulation of the SDE using the Euler–Heun method, $D = 25$. (**c**) Numerical simulation of stochastic equations using the Gillespie algorithm. Parameters are given in Table 1

The set of reactions used in the Gillespie algorithm remain the same, but the following propensities are adjusted to account for the growth rate modulation:

$$(3) \quad p_3 = \rho_A \gamma_T D_F, \tag{63}$$

$$(4) \quad p_4 = \rho_T \gamma_T D_F, \tag{64}$$

$$(6) \quad p_6 = d_c \gamma_T T, \tag{65}$$

$$(7) \quad p_7 = d_c \gamma_T AT, \tag{66}$$

$$(12) \quad p_{12} = d_c \gamma_T TAT, \tag{67}$$

Similar results were obtained for the Gillespie simulations (Fig. 7c). However, in the controlled state with low amounts of toxin, the stochastic variations of the antitoxin and complex levels are much larger than in the SDE approach.

These results indicate that noise can play an essential role in the formation of persister cells. Large stochastic excursions can drive the system above the threshold KK for growth inhibition. If these excursions are large enough, the growth rate can be reduced for potentially very long times. During this time the cell finds itself in a dormant state. In the end, however, the system relaxes back to the normally growing state, which is the only stable attractor. As shown in Fig. 7, noise can help to drive the system back to the stable growing state faster. Noise can thus work in both directions, stimulating the entry into a dormant state, and back to the normal state. Koh and Dunlop analyzed how various gene circuit architectures can give rise to more or less noise in the system and as such the frequency of persister cell creation might be influenced [11]. Furthermore, using the Gillespie algorithm, we showed that while the toxin level is generally controlled to be very low, noise could trigger very large pulses of free toxin [14]. This is illustrated in Fig. 8a, b. We analyzed the frequency of such rare extreme events in the absence of growth rate modulation, which is illustrated in Fig. 8a and shows that the probability of spikes in the toxin level becomes exponentially lower as their amplitude increases. When introducing growth rate modulation, these events were demonstrated to drive the cell into a metastable state of dormancy and returned back to normal growth conditions after a very long time (Fig. 8c).

For the parameter set used in this work, the system only admits one stable solution, the one in which cells grow normally and toxin levels are low and under control. Changing the initial conditions of the systems and/or adding noise can drive the system to a metastable state where it can reside for a potentially very long time, but eventually it returns to the normal growth conditions. No bistability has been found in the deterministic ODE system. Several authors have shown, however, that the presence of growth rate modulation can lead to bistability, where the normal state and the persister state are both stable [10, 12, 15]. In that case, noise can drive stochastic switches between both of these stable states.

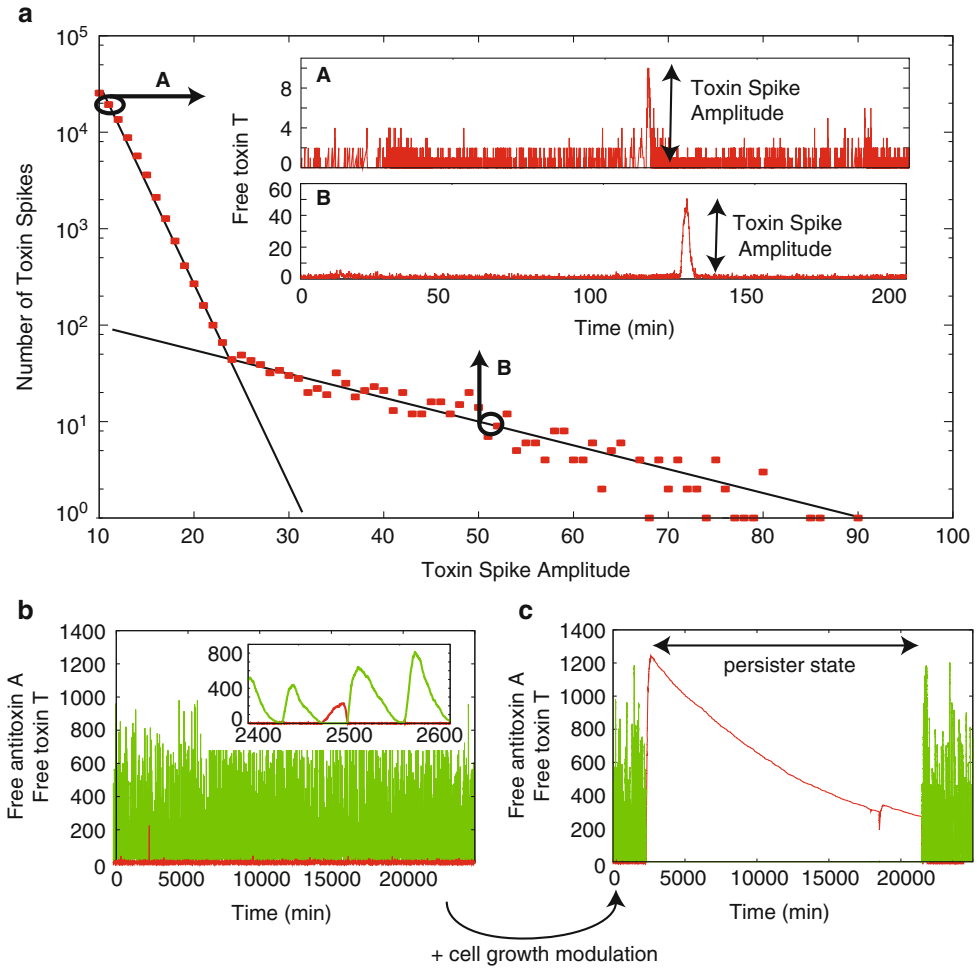

Fig. 8 Toxin–antitoxin module dynamics can cause large toxin spikes, providing a route to persister generation through growth rate suppression. (**a**) Number of toxin spikes in function of their amplitude. Two characteristic scaling laws (A) and (B) related to stochastic variation were found. (**b**) and (**c**) Level of free toxin (*red*) and antitoxin (*green*), respectively excluding (**b**) and including (**c**) toxic feedback effects. Figure adapted from [14]. For more details on model, parameter set and the presence of the two characteristic scaling laws in (**a**), *see* [14]

Cataudella et al. have shown how conditional cooperativity can help to mediate bistability between the normal state and the persister state [12]. In other works, such as [10, 15], bistability in the absence of conditional cooperativity was analyzed. However, no bistability has been observed in the absence of growth rate modulation, showing that this is an essential ingredient to achieve bistability.

7 Modeling Populations of Persister Cells

Previous sections focussed on modeling the dynamics of TA systems within a single cell. Such studies reveal potential mechanisms that can lead to elevated toxin levels driving a single cell into a dormant state, characterized by a much slower growth rate than normal cells. In reality, cells exist and grow within a larger population of cells. In order to understand how the single cell dynamics translates to the dynamics of whole cell populations, a simple two-state model can be used. One state is the normal (N) cell, while the other state is the persister (P) cell. Cells can actively switch from N to P and P to N (the switching rates are defined as a and b, respectively), while the growth rate of both states is given by μ_N and μ_P:

$$\frac{dN}{dt} = -aN + bP + \mu_N N \tag{68}$$

$$\frac{dP}{dt} = aN - bP + \mu_P P \tag{69}$$

This model was first introduced by Balaban et al. as a model for persisters created through normal growth (type II) [7]. The phenotypic switching rates a and b can be estimated from the underlying single cell dynamics and will depend on the system parameters, noise strength, and type of dynamics (e.g., bistability [58] vs. metastability [14]). In the presence of nutritional stress, cells tend to switch predominantly to the high toxin state and switch back much more rarely [14, 58]. This translates to $a > b$. While the cell spends most of its time in the persister state, the persister fraction of the overall cell population is only a minority. This is due to the fact that the normal cell population has a much larger individual cell growth rate with respect to the persisters. The persister fraction in the whole cell population is thus greatly determined by both phenotypic switching rates and the growth rates. Figure 9 shows an analysis of the dependence of the persister fraction on both switching rates a and b. One can clearly see that the switching rate to get into persistence strongly controls the persister fractions. In nutritional stress conditions, an increase in the switching rate a (N to P) thus immediately leads to an increased persister fraction. The return rate to normal cell growth (b) has little influence on the persister fraction, provided that it is slower than the growth rate μ_N.

The model for persisters generated through normal growth by Balaban et al. was further investigated by Kussell et al. Next to the deterministic approach, suitable for large bacterial populations, they also include stochastic simulations using the Gillespie algorithm,

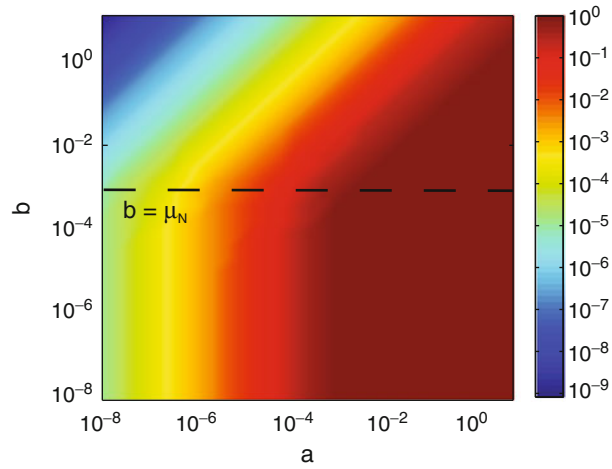

Fig. 9 Parameter scan showing the persister fraction in function of the switching rates *a* (from normal to persister cell) and *b* (from persister cell to normal cell). Parameters: $\mu_N = d_c$, $\mu_P = 0$

which better represents the behavior for small populations. This work shows that the optimal switching rate between normal cells and persisters depends more on the frequency of environmental changes than on the specific characteristics of each environment [6]. In 2007, Cogan published another model focusing on the dynamics of cell populations, yet incorporating toxin–antitoxin modules [8].

8 Discussion

When comparing different mathematical modeling papers on toxin–antitoxin modules and persisters, it becomes clear that different models can give different results, both depending on the system one is trying to simulate and on the assumptions that were made for a particular system. For example, for the *hipBA* operon, Koh and Dunlop concluded that the emergence of persistence is not caused by bistability [11], whereas Feng et al.—after inclusion of growth rate modulation—motivate that it is [15].

This indicates that model building is a crucial step when examining toxin–antitoxin modules and persister cells using numerical methods. Depending on the particular system one is modeling, the parameters and equations will differ from the ones presented here. Particular things that should be taken into account are the monomeric or multimeric state of the toxin and antitoxin, the toxin–antitoxin complexes that can be formed and the details of the transcriptional regulation. For the latter, one could consider, e.g., the amount of binding sites for the antitoxin on the DNA operator, the fact if the antitoxin alone can cause repression, and if conditional cooperativity has been found in the system.

As more and more details about the mechanisms regulating toxin–antitoxin modules are being elucidated experimentally, new interactions can of course be added to the models. For example, the explicit mode of action is known for several toxins, such as inhibition of translation by phosphorylation of elongation factor Tu (EF-Tu) for Doc [59] or ribosome-dependent degradation of mRNA for RelE [60]. The effect of the mode of action of the toxin on the toxin–antitoxin dynamics could be investigated by integrating the different toxic activities into a general model. Furthermore, for the *hipBA* operon, experimental results indicate that the autophosphorylation of toxin HipA plays a role in reverting from a persister to a growth phenotype. This behavior has not been included in *hipBA* models up to now.

Various models have been constructed to describe the single cell dynamics of type II TA systems [5, 9–15]. Although these models have often used different equations and different numerical methods (deterministic vs. stochastic), one general conclusion that can be drawn from these modeling efforts is that growth rate inhibition at higher toxin levels is an essential property to allow for persister cell creation. Without such growth rate dependence on the toxin level the system is found to be monostable with only minor short stochastic excursions to states with higher toxin levels. When including growth rate inhibition, two possible outcomes have been found that can lead to persister formation. Either the system is found to be metastable, where stochastic excursions can drive the system into a dormant state [14]. The system can reside in this state for a long transient time, but eventually returns to the stable solution of the system, corresponding to a low toxin level. The system has also been shown to allow for bistability [10, 12, 15]. This situation is fundamentally different from metastability as in the absence of noise there are two stable states (low and high toxin level). In the presence of noise, stochastic mode hopping between both these states can be found.

In this work, we did not consider the fact that one bacterium mostly contains many toxin–antitoxin modules. Fasani et al. did include this in their model and conclude that multiple toxin–antitoxin modules can be coupled to provide a strong hysteretic switch between the normal growing and the persister phenotype [13].

Apart from the actual model and its parameters, the outcome of simulations for toxin–antitoxin module dynamics depends heavily on whether randomness and noise are included. This was clearly illustrated in Fig. 4, where the level of the free toxin was close to zero when the ODE approach was used, but fluctuated heavily when relatively low levels of noise were added in the SDE approach. These fluctuations are greatly reduced when the Gillespie algorithm is used. This approach is more realistic because every reaction is simulated explicitly. As the gene regulation in toxin–antitoxin modules is a discrete process, where transcription and translation can

only take place when the operator is unbound, and as there are usually very few free toxin molecules in the cell, the Gillespie algorithm is the most appropriate method to simulate stochastic effects in this case. Although the ODE and SDE approach are less realistic than the Gillespie algorithm, they can be very useful because of their simplicity and the possibility to derive analytical solutions. Steady state solutions can be calculated in ODE systems and their stability can readily be analyzed using dynamical systems theory. In the case of the SDE, stationary probability distributions can be derived by solving the stationary Fokker–Planck equation corresponding to the SDE [51].

Acknowledgements

This research was supported by the Vlaams Interuniversitair Instituut voor Biotechnologie (VIB), by the Research Foundation - Flanders (FWO-Vlaanderen) for project support and individual support (A.V. and L.G.), by the Belgian American Educational Foundation (L.G.), and by the Onderzoeksraad of the Vrije Universiteit Brussel. The authors thank Lydia Hill, Abel Garcia-Pino, and Egon Geerardyn for fruitful discussions.

Appendix 1: Numerical Code to Solve an ODE/SDE

A simple matlab code to solve Eq. 10, with ($D \neq 0$) or without noise ($D = 0$), can be found here below:

```
function ODE_SDE

%% parameters
prodAT  = 0.0530 * 0.116086/0.00203;
degrAT  = 2.8881e-4;
D       = 25;
dt      = 0.01;     % [s] simulation time step
dt_save = 10;       % [s] plotting time step
t_end   = 5*60*60; % [s] final time

%% initialize system
AT       = 0;
t_saved  = [];
AT_saved = [];
count    = 0;

%% simulate the stochastic differential equation
for n = 0:((t_end)/dt)
    t = n * dt;

```

```
    %% Euler-Heun
    noise = sqrt(D) * sqrt(dt) * randn(); % sample from the
    noise

    AT_star = AT + dt * F(AT) + noise;
    AT      = AT + (dt/2)*(F(AT) + F(AT_star)) + noise/2;
    AT      = max(AT, 0); % force protein concentration to
              be positive

    %% Save data
       if (count == dt_save/dt)
       t_saved(end+1) = t;
       AT_saved(end+1) = AT;
       count = 0;
    end
    count = count + 1;

end

%% plot the results
figure;
plot(t_saved./3600, AT_saved, 'k');
xlabel('Time (h)')
ylabel('AT')

%% definition of the differential equation
    function dATdt = F(TA)
    dATdt = prodAT - degrAT*TA;
  end
end
```

Appendix 2: Numerical Code Using the Gillespie Algorithm

A simple matlab code to solve Eq. 1 using the stochastic Gillespie Algorithm can be found here below:

```
% Gillespie code
% There are 2 reactions and there is one species AT

%% Parameters
prodAT = 0.0530*0.116086/0.00203; % reaction 0 -> AT
degrAT = 2.8881e-4;               % reaction AT -> 0

%% Initialization
AT         = 0;       % [AT] initial concentration AT
t          = 0;       % [s] starting time
t_end      = 5*60*60; % [s] final time
t_saved    = [];      % [s] stored times
AT_saved   = [];

```

```
%% Simulation
while t <= t_end
  %% Update propensities
  p1 = degrAT * AT;
  p2 = prodAT;

  %% Computation of the random time step
  p0 = p1 + p2;
  r1 = rand();
  r2 = rand();
  dt = 1/p0 * log(1/r1); % [s] next time step

  %% Selection of random reaction
  %% Update the population based on selected reaction
  yr2 = r2 * p0;
  if yr2 <= p1
    % reaction 1
    AT = AT - 1;
  else
    % reaction 2
    AT = AT + 1;
  end

  %% Update the current time
  t = t + dt;

  %% Save population information
  t_saved(end+1) = t;
  AT_saved(end+1) = AT;

end

%% plot the results
figure;
plot(t_saved./3600, AT_saved, 'k');
xlabel('Time (h)')
ylabel('AT')
```

References

1. Pomerening JR, Sontag ED, Ferrell JE Jr (2003) Building a cell cycle oscillator: hysteresis and bistability in the activation of Cdc2. Nat Cell Biol 5(4):346–351
2. Novak B, Tyson JJ (1993) Numerical analysis of a comprehensive model of M-phase control in Xenopus oocyte extracts and intact embryos. J Cell Sci 106(Pt 4):1153–1168
3. Noble D (2004) Modeling the heart. Physiology (Bethesda) 19:191–197
4. Grassly NC, Fraser C (2008) Mathematical models of infectious disease transmission. Nat Rev Microbiol 6(6):477–487
5. Cataudella I, Trusina A, Sneppen K, Gerdes K, Mitarai N (2012) Conditional cooperativity in toxin-antitoxin regulation prevents random

toxin activation and promotes fast translational recovery. Nucleic Acids Res 40(14):6424–6434

6. Kussell E, Kishony R, Balaban NQ, Leibler S (2005) Bacterial persistence: a model of survival in changing environments. Genetics 169 (4):1807–1814
7. Balaban NQ, Merrin J, Chait R, Kowalik L, Leibler S (2004) Bacterial persistence as a phenotypic switch. Science 305(5690):1622–1625
8. Cogan NG (2007) Incorporating toxin hypothesis into a mathematical model of persister formation and dynamics. J Theor Biol 248(2):340–349
9. Rotem E, Loinger A, Ronin I, Levin-Reisman I, Gabay C, Shoresh N, Biham O, Balaban NQ (2010) Regulation of phenotypic variability by a threshold-based mechanism underlies bacterial persistence. Proc Natl Acad Sci USA 107 (28):12541–12546
10. Lou C, Li Z, Ouyang Q (2008) A molecular model for persister in E. coli. J Theor Biol 255 (2):205–209
11. Koh RS, Dunlop MJ (2012) Modeling suggests that gene circuit architecture controls phenotypic variability in a bacterial persistence network. BMC Syst Biol 6:47
12. Cataudella I, Sneppen K, Gerdes K, Mitarai N (2013) Conditional cooperativity of toxin - antitoxin regulation can mediate bistability between growth and dormancy. PLoS Comput Biol 9(8):e1003174
13. Fasani RA, Savageau MA (2013) Molecular mechanisms of multiple toxin-antitoxin systems are coordinated to govern the persister phenotype. Proc Natl Acad Sci USA 110(27): E2528–E2537
14. Gelens L, Hill L, Vandervelde A, Danckaert J, Loris R (2013) A general model for toxin-antitoxin module dynamics can explain persister cell formation in E. coli. PLoS Comput Biol 9(8):e1003190
15. Feng J, Kessler DA, Ben-Jacob E, Levine H (2014) Growth feedback as a basis for persister bistability. Proc Natl Acad Sci USA 111 (1):544–549
16. Lewis K (2010) Persister cells. Annu Rev Microbiol 64:357–372
17. Fauvart M, De Groote VN, Michiels J (2011) Role of persister cells in chronic infections: clinical relevance and perspectives on anti-persister therapies. J Med Microbiol 60(Pt 6):699–709
18. Maisonneuve E, Gerdes K (2014) Molecular mechanisms underlying bacterial persisters. Cell 157(3):539–548
19. Maisonneuve E, Castro-Camargo M, Gerdes K (2013) (p)ppGpp controls bacterial persistence by stochastic induction of toxin-antitoxin activity. Cell 154(5):1140–1150
20. Pandey DP, Gerdes K (2005) Toxin-antitoxin loci are highly abundant in free-living but lost from host-associated prokaryotes. Nucleic Acids Res 33(3):966–976
21. Fozo EM, Hemm MR, Storz G (2008) Small toxic proteins and the antisense RNAs that repress them. Microbiol Mol Biol Rev 72 (4):579–589
22. Gerdes K, Maisonneuve E (2012) Bacterial persistence and toxin-antitoxin loci. Annu Rev Microbiol 66:103–123
23. Buts L, Lah J, Dao-Thi MH, Wyns L, Loris R (2005) Toxin-antitoxin modules as bacterial metabolic stress managers. Trends Biochem Sci 30(12):672–679
24. Yamaguchi Y, Park JH, Inouye M (2011) Toxin-antitoxin systems in bacteria and archaea. Annu Rev Genet 45:61–79
25. Blower TR, Salmond GP, Luisi BF (2011) Balancing at survival's edge: the structure and adaptive benefits of prokaryotic toxin-antitoxin partners. Curr Opin Struct Biol 21 (1):109–118
26. Blower TR, Short FL, Rao F, Mizuguchi K, Pei XY, Fineran PC, Luisi BF, Salmond GP (2012) Identification and classification of bacterial Type III toxin-antitoxin systems encoded in chromosomal and plasmid genomes. Nucleic Acids Res 40(13):6158–6173
27. Wang X, Lord DM, Cheng HY, Osbourne DO, Hong SH, Sanchez-Torres V, Quiroga C, Zheng K, Herrmann T, Peti W, Benedik MJ, Page R, Wood TK (2012) A new type V toxin-antitoxin system where mRNA for toxin GhoT is cleaved by antitoxin GhoS. Nat Chem Biol 8 (10):855–861
28. Maisonneuve E, Shakespeare LJ, Jorgensen MG, Gerdes K (2011) Bacterial persistence by RNA endonucleases. Proc Natl Acad Sci USA 108(32):13206–13211
29. Helaine S, Cheverton AM, Watson KG, Faure LM, Matthews SA, Holden DW (2014) Internalization of Salmonella by macrophages induces formation of nonreplicating persisters. Science 343(6167):204–208
30. Tripathi A, Dewan PC, Barua B, Varadarajan R (2012) Additional role for the ccd operon of F-plasmid as a transmissible persistence factor. Proc Natl Acad Sci USA 109(31):12497–12502
31. Tian QB, Ohnishi M, Tabuchi A, Terawaki Y (1996) A new plasmid-encoded proteic killer

gene system: cloning, sequencing, and analyzing hig locus of plasmid Rts1. Biochem Biophys Res Commun 220(2):280–284

32. Yamaguchi Y, Park JH, Inouye M (2009) MqsR, a crucial regulator for quorum sensing and biofilm formation, is a GCU-specific mRNA interferase in Escherichia coli. J Biol Chem 284(42):28746–28753
33. Hallez R, Geeraerts D, Sterckx Y, Mine N, Loris R, Van Melderen L (2010) New toxins homologous to ParE belonging to three-component toxin-antitoxin systems in Escherichia coli O157:H7. Mol Microbiol 76 (3):719–732
34. Overgaard M, Borch J, Gerdes K (2009) RelB and RelE of Escherichia coli form a tight complex that represses transcription via the ribbon-helix-helix motif in RelB. J Mol Biol 394 (2):183–196
35. Schumacher MA, Piro KM, Xu W, Hansen S, Lewis K, Brennan RG (2009) Molecular mechanisms of HipA-mediated multidrug tolerance and its neutralization by HipB. Science 323(5912):396–401
36. Loris R, Dao-Thi MH, Bahassi EM, Van Melderen L, Poortmans F, Liddington R, Couturier M, Wyns L (1999) Crystal structure of CcdB, a topoisomerase poison from E. coli. J Mol Biol 285(4):1667–1677
37. Li GY, Zhang Y, Chan MC, Mal TK, Hoeflich KP, Inouye M, Ikura M (2006) Characterization of dual substrate binding sites in the homodimeric structure of Escherichia coli mRNA interferase MazF. J Mol Biol 357(1):139–150
38. Garcia-Pino A, Balasubramanian S, Wyns L, Gazit E, De Greve H, Magnuson RD, Charlier D, van Nuland NA, Loris R (2010) Allostery and intrinsic disorder mediate transcription regulation by conditional cooperativity. Cell 142 (1):101–111
39. Afif H, Allali N, Couturier M, Van Melderen L (2001) The ratio between CcdA and CcdB modulates the transcriptional repression of the ccd poison-antidote system. Mol Microbiol 41 (1):73–82
40. Overgaard M, Borch J, Jorgensen MG, Gerdes K (2008) Messenger RNA interferase RelE controls relBE transcription by conditional cooperativity. Mol Microbiol 69(4):841–857
41. De Jonge N, Garcia-Pino A, Buts L, Haesaerts S, Charlier D, Zangger K, Wyns L, De Greve H, Loris R (2009) Rejuvenation of CcdB-poisoned gyrase by an intrinsically disordered protein domain. Mol Cell 35(2):154–163
42. Brown BL, Lord DM, Grigoriu S, Peti W, Page R (2013) The Escherichia coli toxin MqsR destabilizes the transcriptional repression complex formed between the antitoxin MqsA and the mqsRA operon promoter. J Biol Chem 288(2):1286–1294
43. Magnuson R, Lehnherr H, Mukhopadhyay G, Yarmolinsky MB (1996) Autoregulation of the plasmid addiction operon of bacteriophage P1. J Biol Chem 271(31):18705–18710
44. Dao-Thi MH, Charlier D, Loris R, Maes D, Messens J, Wyns L, Backmann J (2002) Intricate interactions within the ccd plasmid addiction system. J Biol Chem 277 (5):3733–3742
45. McAdams HH, Arkin A (1999) It's a noisy business! Genetic regulation at the nanomolar scale. Trends Genet 15(2):65–69
46. Elowitz MB, Levine AJ, Siggia ED, Swain PS (2002) Stochastic gene expression in a single cell. Science 297(5584):1183–1186
47. Ozbudak EM, Thattai M, Kurtser I, Grossman AD, van Oudenaarden A (2002) Regulation of noise in the expression of a single gene. Nat Genet 31(1):69–73
48. Carrier GF (1968) Ordinary differential equations. A Blaisdell book in pure and applied mathematics. Blaisdell Pub. Co, Waltham, MA
49. Atkinson K, Han W, Stewart DE (2009) Numerical solution of ordinary differential equations. Pure and applied mathematics. Wiley, Hoboken, NJ
50. Coffey WT, Kalmykov YP, Waldron JT (2004) The Langevin equation. With applications to stochastic problems in physics, chemistry and electrical engineering. World Scientific series in contemporary chemical physics. World Scientific Publishing, Singapore
51. Gardiner CW (2004) Handbook of stochastic methods for physics, chemistry, and the natural sciences. Springer, Berlin
52. San Miguel M, Toral R (2000) Stochastic effects in physical systems. In: Instabilities and nonequilibrium structures VI. Springer, Netherlands, pp 35–127
53. Gillespie DT (1977) Exact stochastic simulation of coupled chemical reactions. J Phys Chem 81(25):2340–2361
54. Cai L, Friedman N, Xie XS (2006) Stochastic protein expression in individual cells at the single molecule level. Nature 440(7082): 358–362
55. McAdams HH, Arkin A (1997) Stochastic mechanisms in gene expression. Proc Natl Acad Sci USA 94(3):814–819
56. Loris R, Garcia-Pino A (2014) Disorder- and dynamics-based regulatory mechanisms in

toxin-antitoxin modules. Chem Rev 114 (13):6933–6947

57. Hayes F, Van Melderen L (2011) Toxins-antitoxins: diversity, evolution and function. Crit Rev Biochem Mol Biol 46(5):386–408
58. Nevozhay D, Adams RM, Van Itallie E, Bennett MR, Balazsi G (2012) Mapping the environmental fitness landscape of a synthetic gene circuit. PLoS Comput Biol 8(4):e1002480
59. Castro-Roa D, Garcia-Pino A, De Gieter S, van Nuland NA, Loris R, Zenkin N (2013) The Fic protein Doc uses an inverted substrate to phosphorylate and inactivate EF-Tu. Nat Chem Biol 9(12):811–817
60. Christensen SK, Gerdes K (2003) RelE toxins from bacteria and Archaea cleave mRNAs on translating ribosomes, which are rescued by tmRNA. Mol Microbiol 48(5):1389–1400

INDEX

Jan Michiels and Maarten Fauvart (eds.), *Bacterial Persistence: Methods and Protocols,*
Methods in Molecular Biology, vol. 1333, DOI 10.1007/978-1-4939-2854-5,

E

F

G

H

I

K

L

M

N

O

P

Q

R

S

T

U

V

W